May - August 1995
Volume I Number II

ISSN 0859 144X

THE ASEAN JOURNAL OF RADIOLOGY

Published by The Radiological Society and
the College of Radiologists of Thailand,
Bangkok, Thailand

Supported through an educational grant from

BRACCO
INTERNATIONAL

HDI™ 3000 Ultrasound System

"Best contrast resolution we've ever seen."

A. Thomas Stavros, MD
Medical Imaging of Colorado

"What impressed me the most is its ease of use and how quickly I felt comfortable at the controls. The system is designed to be intuitive to your needs as you scan."

Michael Grubb. RVT
Senior Vascular Technologist
The Cleveland Clinic Foundation

"The new HDI is very light and maneuverable, and much easier to push than any machine we've ever used."

Sheryl Weir, RDMS, RVT
Ultrasound Manager
Tampa General Hospital

"The resolution of Color Power Angio on the new HDI is a significant diagnostic advancement for ultrasound."

Beverly G. Coleman, MD
Professor of Radiology
Director of Ultrasound Imaging
Hospital of the University of Pennsylvania

The Next Major Step in Ultrasound Performance

Distributed By

บริษัท เมดิทอป จำกัด
MEDITOP CO., LTD.

334 ลาดพร้าว 71 บางกะปิ กรุงเทพฯ 10310
334 LADPRAO 71 BANGKAPI BANGKOK 10310
TEL. 9331133 (20 LINES) FAX: 9330811-2

May - August 1995
Volume I Number II

ISSN 0859 144X

THE ASEAN JOURNAL OF RADIOLOGY

Published by The Radiological Society and the College of Radiologists of Thailand, Bangkok, Thailand

Supported through an educational grant from

BRACCO INTERNATIONAL

1. The AAR Journal of Radiology publishes the papers on Radiological Sciences, such as research work, review articles, case reports, innovations in Medical Sciences related to all branches of Radiology, and letters to the editor. The aforementioned materials can be written in English only.

2. The authors have to submit 2 copies of the manuscript and a diskette: **to Prof. Dr. Kawee Tungsubutra**, 318 Kaweevej Hospital, Tarksin Road, Dhonburi, Bangkok 10600, Thailand.
or to the Associate Editors at the Radiological Society of Malaysia, Indonesia, Phillippine, Singapore and Brunei. The names and addresses of the Associate Editors in each country were published in the front page of this Journal.

3. The original copy to be submitted must be typed in a double space on one side of the page of 8″ × 11″ paper.

4. The format of the article must include:

   a. Title page and address of the author (s)

   b. Abstract

   c. Introduction (Background)

   d. Material and Method

   e. Results and discussion (Tables and Illustrations)

   f. Acknowledgement (it any)

   g. References (Follow the Vancouver style developed by ICMJE)

5. We will provide 25 copies of reprints for the author (s) who submit (s) and article for publication in the AAR Journal.

6. The illustrations and tables must be clearly prepared with legends in English as they are the art works to be reproduced.

7. The authors are responsible for the contents of the article as to its facts and findings.

8. Ethics.

Paper reporting studies which might be interpreated as human experimentation (e.g. controlled trials) should conform to the standards of the Declaration of Helsinki (see British Medical Journal 1964:2:177) and should indicate that approval that such studies may proceed has been granted by the local or hospital Ethics Committee.

When reporting experiments on animals indicate whether the institution's or the National Research Council's guide for, or any national law on, the care and use of laboratory animals was followed.

Message from Prof. Dr. Kawee Tungsubutra
Editor-in-Chief, The Asean Journal of Radiology

This is the second issue of the Asean Journal of Radiology. In this issue we have the articles from the Medical Schools of every region of the country from the North, the North-East, the South and the Central part of Thailand. In this Vol I. No II, we have improved the quality and the quantity of the articles in the Journal. We hope to have the articles from the other member countries and perhaps from other non-member countries as well.

With best wishes.

Kawee Tungsubutra

Prof. Dr. Kawee Tungsubutra

24 May 1995

THE ASEAN JOURNAL OF RADIOLOGY

Volume 1 Number II May-August 1995

CONTENTS

Volume 1 Number II May-August 1995

CONTENTS

AMBER: FOR CHEST, LARYNX AND ABDOMINAL RADIOGRAPHY

Patchrin PEKANAN [1], Chirote SUCHATO [2], Kamolpong OSATHAVANICHVONG [3].

ABSTRACT

Conventional radiography is limited by the small useful exposure range of radiographic film. The wide variation in absorption thickness of different parts of the body results in areas of under-and over exposure. An advanced multiple beam equalization system, **AMBER,** controls local exposure delivered to the film. The system has a row of 20 modulators in front of the x-ray tube, each able to change the height of the local slit beam during scanning. Changes are made in response to measurements from a linear detector array in front of the film cassette. This array consists of 20 individually functioning detectors coupled through electronic feedback loops to the 20 modulators. A scan is obtained in 0.8 second with a local exposure time of approximately 50 msec. **AMBER** results in radiographs with significantly improved exposure of the mediastinum without overexposure of the lungs. Originally, this system was aimed to use for the chest radiography, however, abdominal radiography and laryngeal radiography was used by us to illustrate the images produced by this machine.

Some tissues in the thoracic region are characterized by a relatively low absorption of x-rays (lung), whereas other tissues have a higher absorption (mediastinal, retrocardiac and subdiaphragmatic regions). This leads to great differences in the transmission of x-rays through the chest and to a necessary compromise between contrast and latitude of the film. In conventional radiography, these differences often exceed the dynamic range of the screen-film combination, even when commercially available wide-latitude films are used (1).

To overcome this problem, several solutions have been proposed. One of these solutions is a system based on a scanning multiple-beam equalization technique, advanced multiple-beam equalization radiography (AMBER)(2).

The **AMBER** unit was produced by Delft Instruments Medical Imaging, Delft, The Netherlands. It uses a horizontally oriented x-ray beam (slit technique) that scans the patient vertically. The fan shaped beam of radiation can be regarded as divided into 20 parallel segments, each covering approximately 1.3 square inches from a 1.6 X 0.8 square inch area. Each segment has its own modulator in front of the x-ray tube in a feedback loop with a corresponding detector. The detector array is located between the grid and the film cassette. When the image is obtained, the detector output signal is used to adjust the corresponding modulator to deliver the proper exposure to the part of the film covered by the detector. To reduce scatter, fore and aft slits and a grid are used. A standard x-ray tube is used, and a scanning time of 0.8 second can be achieved.

[1]Department of Radiology, Ramathibodi Hospital, Rama 6 Street, Bangkok 10400 Thailand.
[2]Urupong Medical Center, Thoeddamri Street, Bangkok 10300, Thailand.
[3]Medical software development project, Mahidol University, Pin-Klao-Kakornchaisri Street, Bangkok, Thailand.

The modulator, located with the fore slit in front of the x-ray tube, consists of 20 x-ray attenuation elements. Each element consists of an absorber on the tip of a piezoelectric actuator. Setting a voltage on the actuator causes the element to bend. Depending on the voltage, the absorber will more or less cover the fore slit collimator. When completely covering the fore slit, each absorber totally absorbs the local radiation. The voltage on the actuator is controlled with the measurements of the corresponding detector and feedback loop. During radiography, measurements of the detector will constantly cause the absorber to be set in different positions, thereby controlling the exposure to the section of film behind the detector. The height of the x-ray beam at the level of the detector is only slightly affected by different positions of the absorber. At a scanning time of 0.8 second, the local exposure time (50 msec) can therefore be calculated. Depending on the focus dimensions of the x-ray tube, the x-ray intensity distribution, the shape of the absorbers, and the size of the detectors, artifacts can appear on the image. Artifacts in the scanning direction can be caused by ineffective smoothing of the overlap area between two absorbers set at different positions.

The xenon detector is actually composed of 160 detector strips, in 20 segments of eight strips. Sampling of the detector is performed over an area of 1.6 X 0.6 inch to avoid cross talk between parallel detectors. Each detector measures the x-ray intensity after it has passed through the modulator as well as the patient. Since the detector chamber is in front of the film cassette, the material must be chosen so that no artifacts appear on the image.

This is achieved by using very thin electrodes that transmit more than 99.5% of the x-rays at 70 keV. This allows an extremely small contrast difference in respect to the wall material of the xenon detector. To keep patient x-ray exposure to a minimum, wall material with an absorption of less than 10% at 70 keV was chosen.

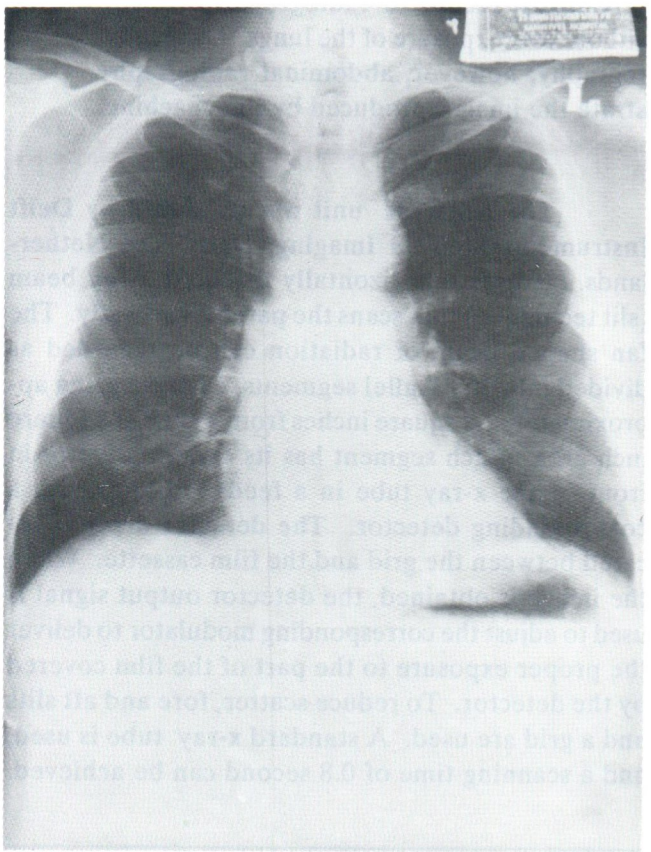

Fig. 1 a. Conventional chest film of the chest in P.A. view

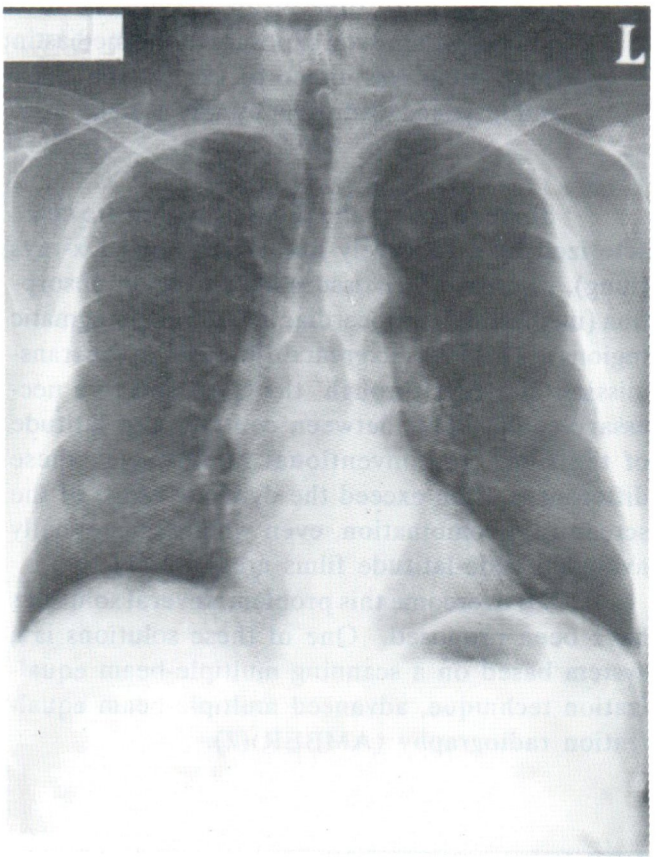

Fig. 1 b. Amber chest film of the same patient small nodule at RLL, clearly demonstrated even in rib-hidden

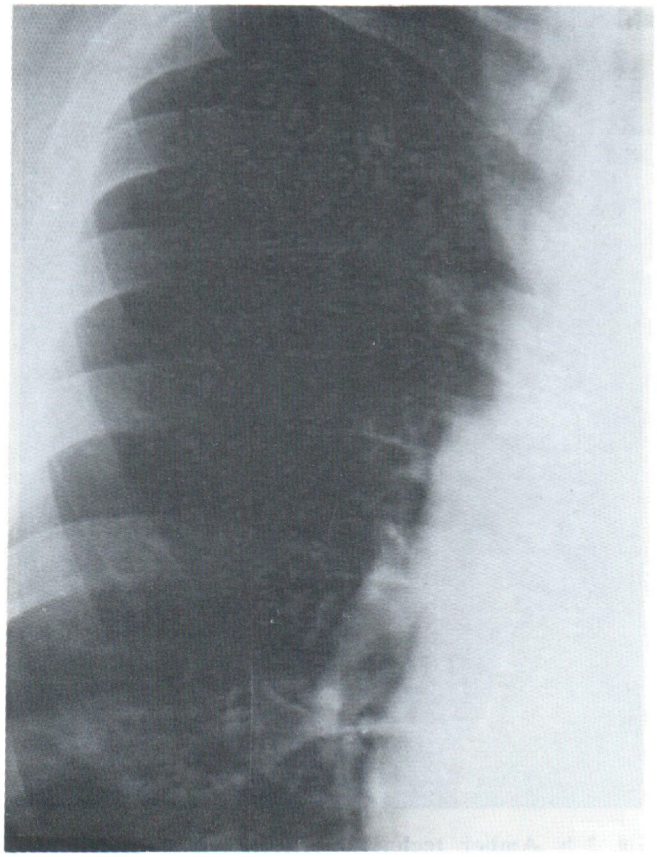

Fig 1 c. Conventional close up picture of right lower lobe

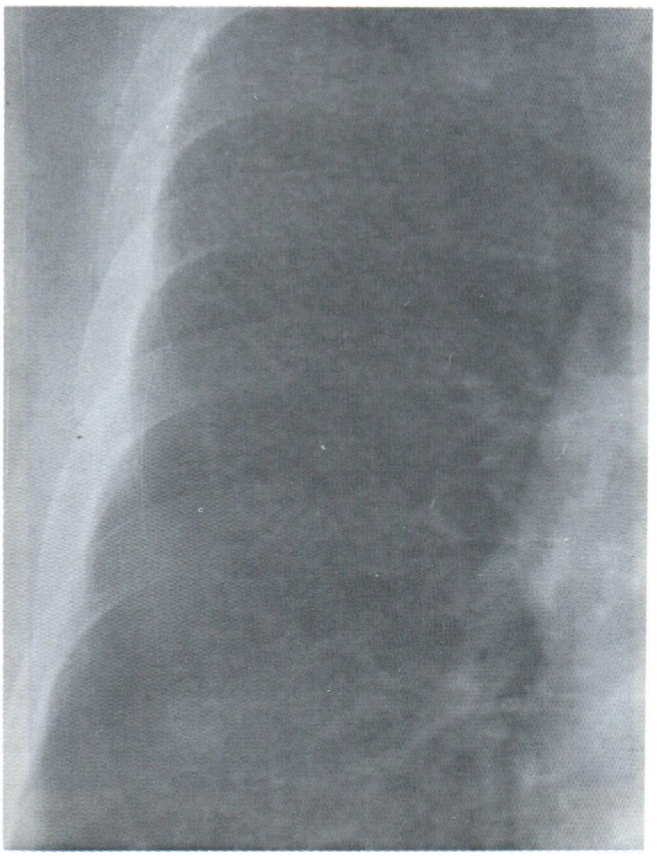

Fig 1d. Amber technique, close up picture of right lower lobe revealed the nodule more obviously

The detector signals are amplified electronically with 20 pre-and output amplifiers and one control amplifier. Only one control amplifier is needed because of the use of multiplex and demultiplex techniques. The microprocessor governing the control amplifier can be seen as the heart of the electronics. Different settings of both threshold value (above which the system starts to function) and control amplifier gain result in different control curves according to which the equalization takes place.(2)

Although **AMBER** has been described and used since 1988, the first machine was installed in Thailand in 1994 and is so far the only machine in the country. Images could be obtained only from the patient who could maintain the erect position. The main use is for chest radiography, however, the images of the upright abdomen and the larynx are also more informative than the conventional ones.

REFERENCES

1. Sorenson SA, Dobbins ST. Techniques for chest radiography. Proceedings of the Chest Imaging Conference, August 31-September 2, 1987. Madison: Medical Physics, 1987;1-15.
2. Vlasbloem H, Schultze Kool LJ. AMBER : a scanning multiple-beam equalization system for chest radiography. Radiology 1988;169:29-34.

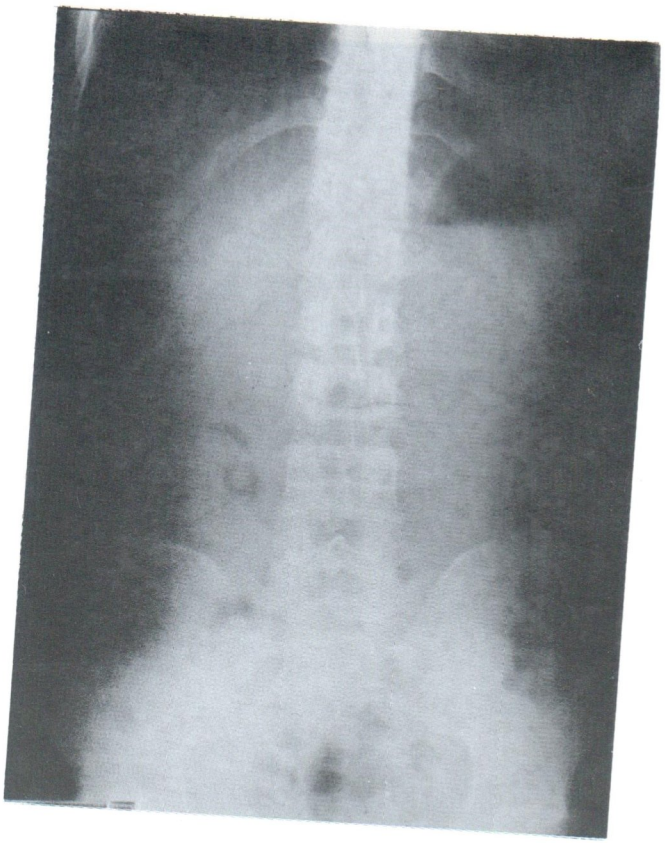

Fig. 2 a. Conventional technique of the upright abdomen.

Fig. 2 b. Amber technique of the upright abdomen. Better visualization of the spine and bowel loops. The lateral and central part of the abdomen is equally and beautifully seen.

Fig.3 a. Conventional technique of the neck in lateral view

Fig. 3 b. Amber technique of the neck in lateral view. Better visualization of the bony part, airway and soft part is shown.

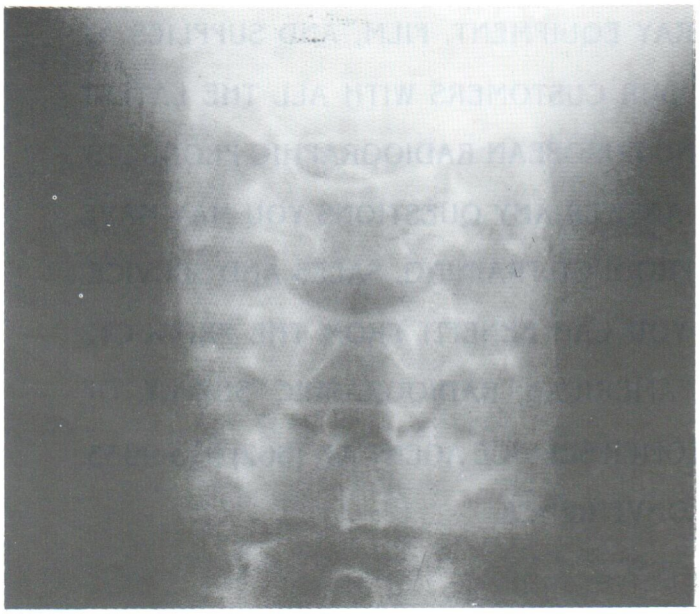

Fig. 3 c. Conventional technique of AP view of the neck.

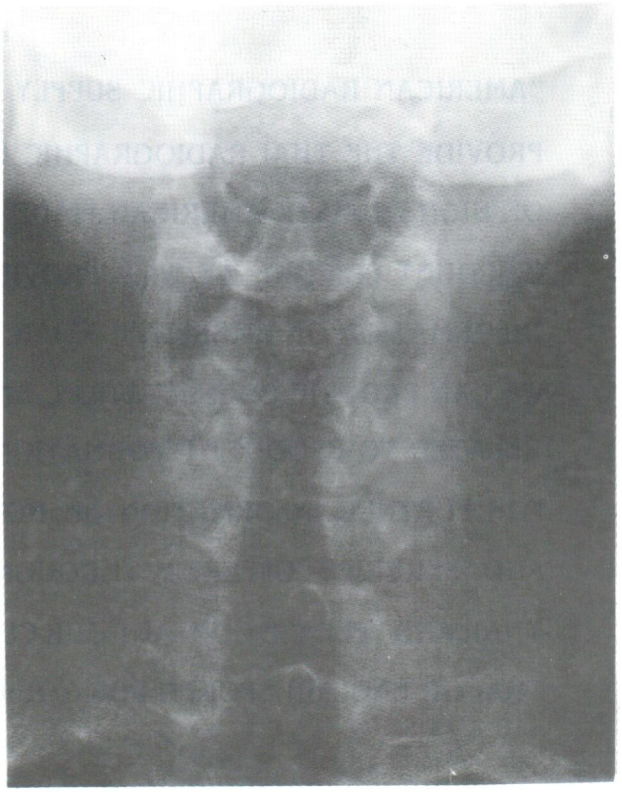

Fig. 3 d. Amber technique of AP view of the neck. Nicely visualization of the pharyngeal, laryngeal and tracheal airway, the surrounding soft tissue and the bony parts.

''AMERICAN RADIOGRAPHIC SUPPLY OF THAILAND''

IS PROUD TO ANNOUNCE THE GRAND OPENING OF OUR NEW BANGKOK OFFICE.

''AMERICAN RADIOGRAPHIC SUPPLY OF THAILAND'' HAS BEEN ESTABLISHED TO PROVIDE THE THAI RADIOGRAPHIC COMMUNITY WITH A ONE SOURCE SUPPLIER OF HIGH QUALITY AMERICAN MADE X-RAY EQUIPMENT, FILM, AND SUPPLIES AT DISCOUNT PRICING. WE WILL PROVIDE OUR CUSTOMERS WITH ALL THE LATEST INFORMATION ON AMERICAN, ASIAN, AND EUROPEAN RADIOGRAPHIC PRODUCTS. WE CAN PROVIDE CONSULTATION, AND ANSWER ANY QUESTIONS YOU MAY HAVE RELATED TO PRODUCT INFORMATION, PRODUCT TRAINING, SALES AND SERVICE. FOR FURTHER INFORMATION ON HOW YOU CAN BENEFIT FROM THE PRODUCTS AND SERVICES OFFERED THROUGH ''AMERICAN RADIOGRAPHIC SUPPLY OF THAILAND'' PLEASE CONTACT OUR CUSTOMER SERVICE AGENT AT; (662) 513-9933. THAI OR ENGLISH SPOKEN FOR YOUR CONVENIENCE.

บริษัท อเมริกัน เรดิโอกราฟฟิค ซัพพลาย จำกัด
AMERICAN RADIOGRAPHIC SUPPLY CO.,LTD.
103 SOI PHAHOLYOTHINGOLF, PHAHOLYOTHIN ROAD,
CHATUCHAK, BANGKOK 10900, THAILAND.
TEL: (662) 930-1211-2, 513-9933 FAX: 513-9933

A REPORTED CASE OF PULMONARY SPARGANOSIS : RADIOLOGICAL ASPECT AND REVIEW OF ARTICLES.

Jaturat KANPITTAYA,M.D.*, Watchara BOONSAWAD,M.D.**
Benjamas INTARAPOKA,M.D.**, Churairat KULARBKAEW,M.D.***
Smarn TESANA,M.Sc.****, Chertchai TANTISIRINTR,M.D.*****

ABSTRACT

Human sparganosis is a rare parasitic infestation caused by the migratory second stage larvae (plerocercoid) of the Pseudophyllidean cestode of genus Spirometra (Mueller, 1973). The first report of human sparganosis was made by Patrick Manson in a Chinese patient in 1882 (Beaver, 1984). The distribution of the cases was sporadically worldwide, but most commonly from East and Southeast Asia (Japan,China,Korea, Taiwan, Vietnam and Thailand). There were some reports from the Southern part of the United States and Europe (Mueller et al, 1975). Sparganosis was commonly reported to involve subcutaneous tissue, muscle, ocular and visceral organs including the central nervous system. Pulmonary involvement is extremely rare. A case of pulmonary sparganosis was presented with chronic hemoptysis and abnormal lung shadows. The diagnosis could not be made by radiological image and bronchoscopic examination.The patient received an antituberculous drug without response. Finally the diagnosis was confirmed by open lung biopsy which the plerocercoid larvae of sparganum was found.

INTRODUCTION

Sparganosis is an uncommon zoonotic disease caused by infection with Pseudophyllidean cestodes of the genus Spirometra. There are two types of the disease, namely nonproliferative and proliferative sparganosis.

Human infection occurs by one of the three routes:ingestion of freshwater cyclops which harbor an infective procercoid; ingestion of the plerocercoid directly from an intermediate animal hosts such as frogs or snakes ; or by percutaneous infection from crude poultices prepared from infected amphibians or reptiles. Once inside the host, larvae can migrate to various tissues, usually encysts in subcutaneous tissue, ocular involvement is not uncommon including the central nervous system. Pulmonary involvement is extremely rare. We report a case of pulmonary sparganosis which was misdiagnosed and treated as tuberculous infection consequently there was no improvement in the patient. Subsequently surgical open lung biopsy resulted in confirmation of the diagnosis.

CASE REPORT

A 37-year-old Thai man lived in Banpur district, Udonthani province (Northeastern part of Thailand). The patient presented with history of chronic cough, hemoptysis for about 3 months with low grade fever. He had a history of habitually consuming impure water but denied a history of having eaten raw or partially cooked meat. Seven years ago he contracted spinal tuberculosis and was treated for 1 year. Ten years

* Department of Radiology
** Department of Medicine
*** Department of Pathology
**** Department of Parasitology
***** Department of Surgery
Srinagarind Hospital, Khon Kaen, Thailand.

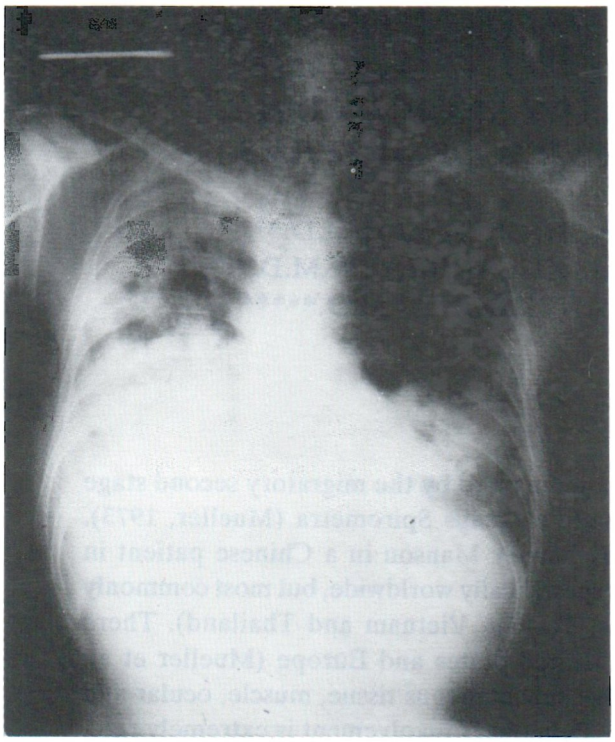

Fig. 1a PA chest film shows diffuse bilateral patchy alveolar infiltration with some cystic lesions within. More confluent lesions are noted on the right lung with bilateral pleural fluid.

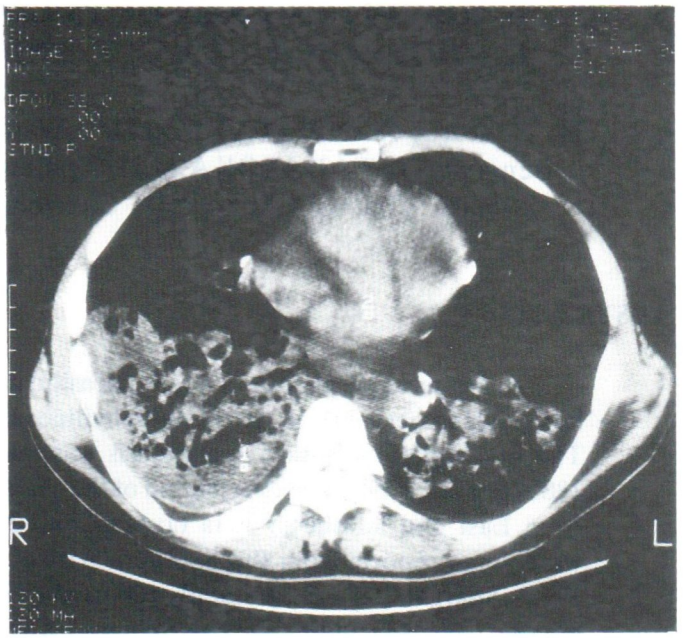

Fig. 1b

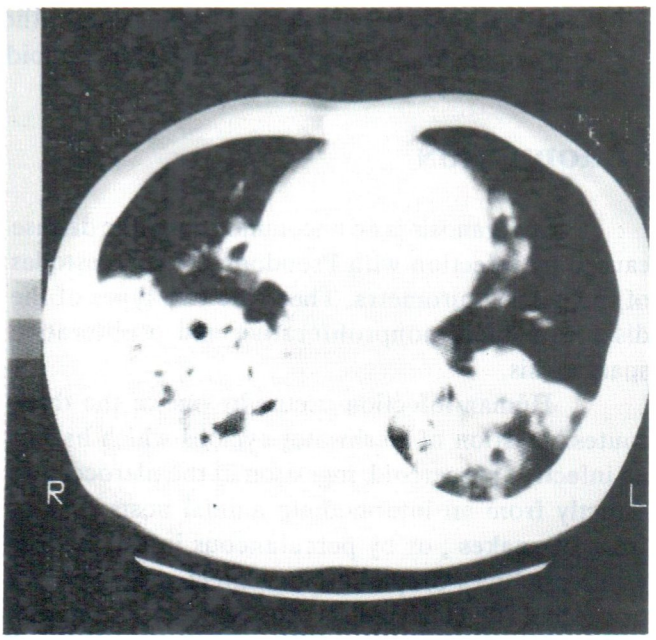

Fig. 1c

Fig. 1b, and 1c Computed tomography of the chest clarifies abnormal lung shadows as areas of consolidation with multiple thick wall cavitary lesions and tubular bronchiectatic changes.

ago he had an operation on the right kidney due to a renal stone. Physical examination revealed a middle aged man with mild thoracic kyphosis. Neither evidence of organomegaly nor lymphadenopathy was detected. Chest examination revealed fine crepitation in both lungs. Laboratory examination revealed a hematocrit of 36% and a white blood count of 11200/ mm^3 with a differential of polymorphonuclears 60%, lymphocytes 23%, monocytes 6% and eosinophils 10%. Pulmonary function showed a restrictive pattern.

Roentgen examination including chest x-ray revealed diffuse bilateral patchy alveolar infiltration more confluent on the right lung with some cystic cavitary lesions, suspected to be due to the pulmonary infection process.

Bronchoscopic examination revealed no endobronchial lesion and mild inflammation of the mucosa with contact bleeding. Cytologic examination revealed a negative AFB stain and unremarkable findings from bronchial biopsy.

The patient was treated for 2 months as having tuberculosis without improvement. He was lost to follow

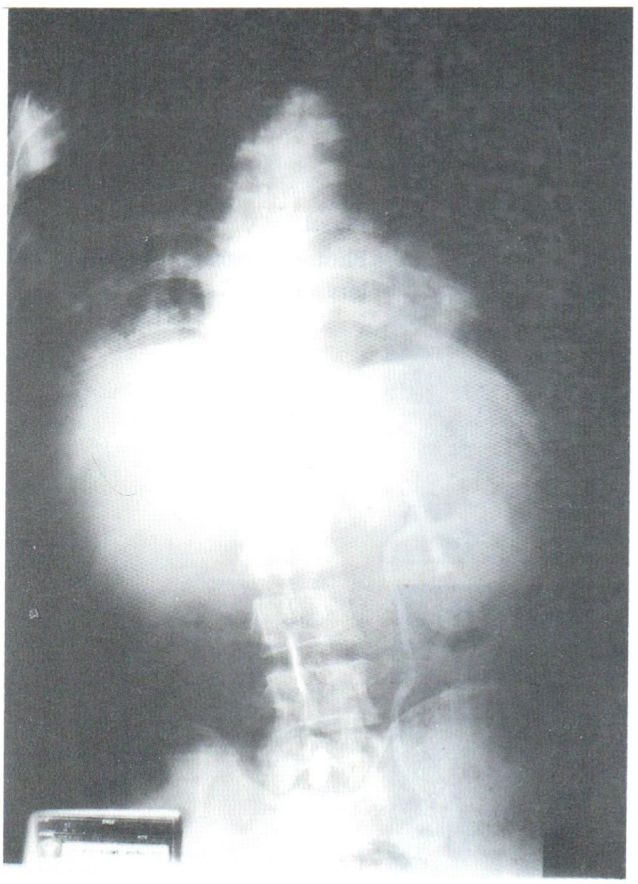

Fig. 2 Plain KUB following computed tomographic examination reveals excretion of contrast media only on the left kidney.

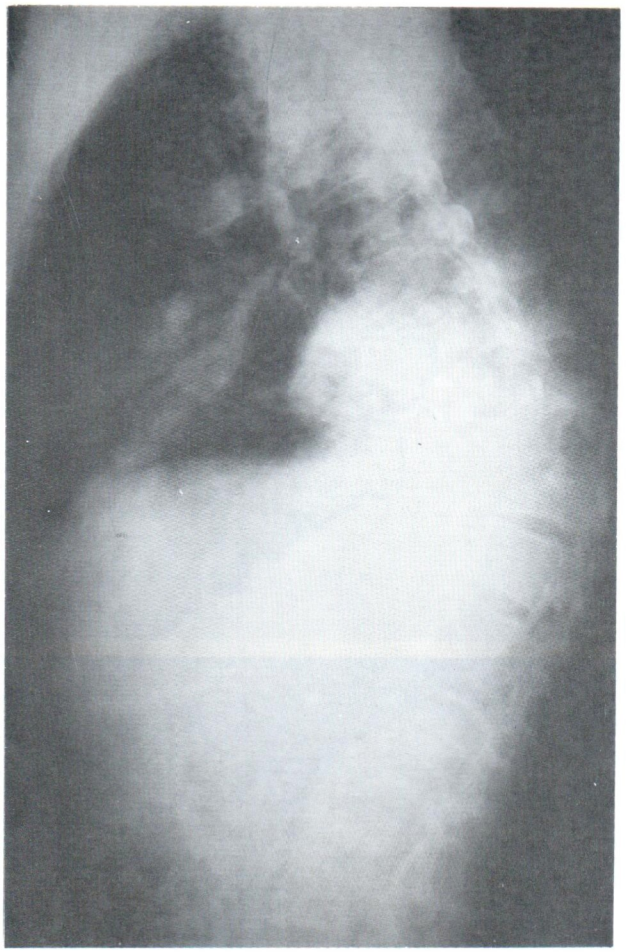

fig. 3 Lateral thoracic spine shows anterior wedging of T12 vertebral body.

up for 8 months and then came back again with clinical signs of chronic productive cough. A chest film still noted abnormal diffuse patchy alveolar shadows, which were well delineated on additional computed tomography. An area of lung consolidation with air bronchogram, multiple thick wall cavitary lesions right side and tubular bronchiectatic changes were also noted in both lower lungs with bilateral pleural effusion more on the right side. (fig 1a, 1b, 1c). The findings were suggestive of a pulmonary infection process. Plain film of the spine showed anterior wedging and collapse of T12 body with mild narrowing of intervertebral disc space of T11-12 level. We also noted expansile permeative destruction of the mid part of the posterior 11^{th} rib and upper cortical destruction of 12^{th} rib on the right side.

Repeated bronchoscopic examination was done which revealed mild inflammation of the mucosa but the cytologic examination was normal. He received a short course of antibiotics with minimal improvement of the symptoms. Finally open lung biopsy was carried out. Sections of the lung showed multiple foci of sparganum encyst in the lung tissue. The cystic space was lined by fibrous connective tissue, which was infiltrated by eosinophils,plasma cells and lymphocytes. Scattered macrophages contained hemosiderin pigment. Foci of a necrosed parasite with calcification were seen. Other areas of lung tissue showed atelectasis with hemorrhage. (fig 4,5)

The patient received Mebendazole 40 mg/kg/d and was followed up for about 5 months with minimal weight gain and slight improvement of clinical symptoms.

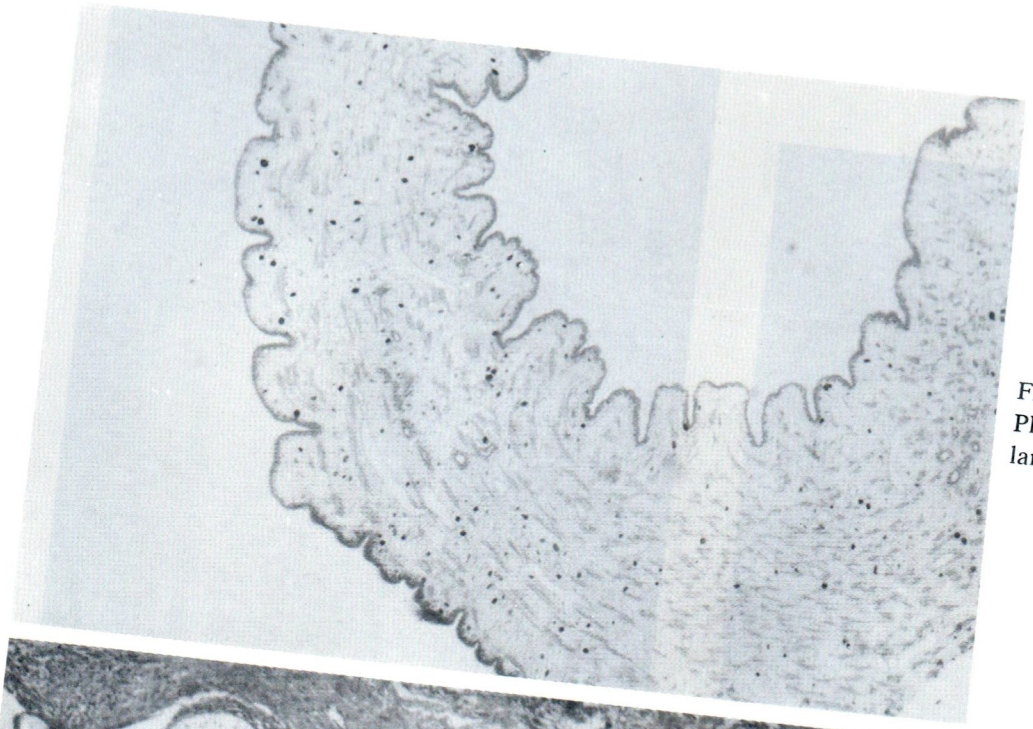

Fig. 4
Photomicrograph of sparganum larva (33x)

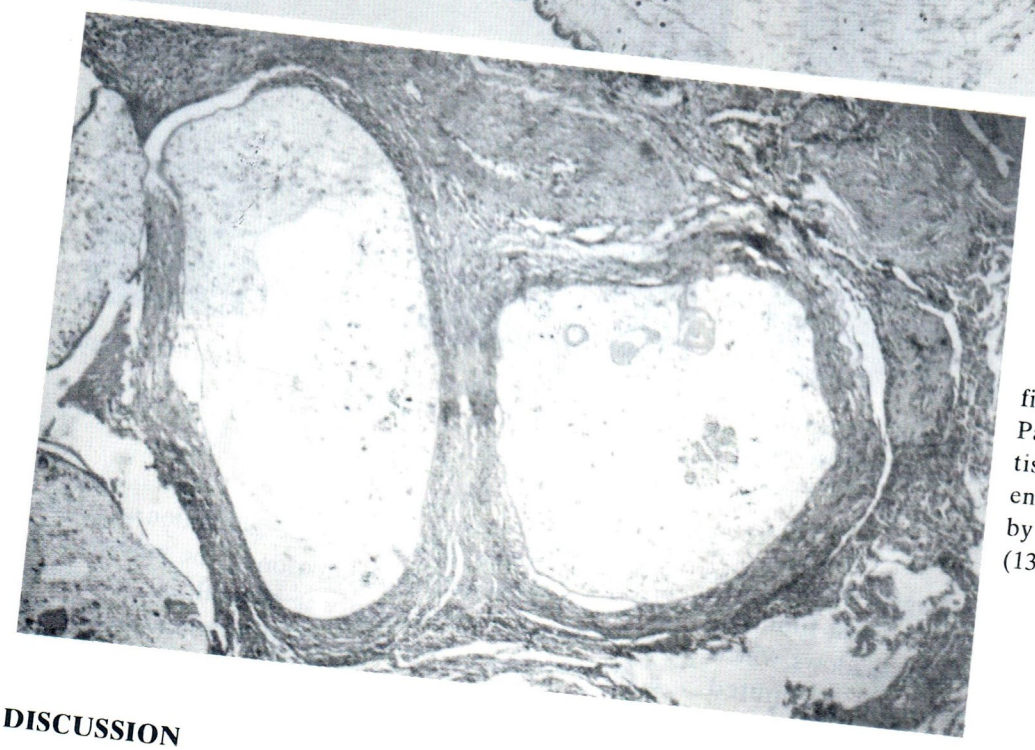

fig.5
Pathologic section of the lung tissue shows multiple foci of encysted sparganum surrounded by inflammatory cell reaction (13.2x)

DISCUSSION

Sparganosis is an uncommon parasitic infestation of man caused by larval tapeworms[2]. The eggs of the adult worms hatch in water and develop into larvae in Cyclops species, which are swallowed by intermediate hosts, such as frogs, snakes and lizards. Larvae develop and are finally ingested by the definitive host (dogs and cats). Humans become accidentally infected. Humans can be infected by three routes[12]. The first is by drinking unfiltered water contaminated with infected cyclops. The second is by ingestion of the second intermediate host such as raw or inadequately cooked flesh of snakes or frogs which contains living larvae (the most common source of human infection in Korea)[10]. The third route is by applying the flesh of an infected intermediate host to an open wound or sore eyes as "poultices", which is practised in China and Southeast Asian countries[1,3,6]. The infection route in this patient is unknown, but most likely, it is by drinking contaminated water.

When humans are infected by first or second

stage larvae, the larvae cannot develop into adult worms and will live in the tissues in the "sparganum" stage. Some authors believed that the larvae could live in the tissue for more than 20 years[4,5]. While living in the human hosts, the larvae can migrate, causing symptoms such as migratory swelling in subcutaneous tissue. They can lodge in tissue producing mass lesions or penetrate the gastrointestinal wall to migrate systemically. Pulmonary sparganosis is extremely rare[8]. The diagnosis in this patient can not be made preoperatively. The investigation showed eosinophilia, although serology and radiological evaluation is helpful, the definite diagnosis requires direct identification of the parasite from surgical specimens[5]. The characteristic pathologic findings of sparganosis is focal necrosis along the tortuous tract of migration. The track is surrounded by a zone of necrotic debries, lymphohistiocytic reaction and heavy eosinophilic infiltration are usually found. The inflammatory reaction often extends into surrounding tissue, particularly during the acute migration phase. Pulmonary pathology in this case can explain radiographic images retrospectively.

An aspect of prevention of this disease, should be the education of the community who live nearby in the endemic area about hygiene and public health especially in the field of sparganum life cycle.

ACKNOWLEDGEMENT

We are grateful to Mr.E.W. Renton for reviewing the manuscript.

REFERENCES

1. Ausayakhun S, Siriprasert V, Morakote N, et al. Ocular sparganosis in Thailand : case report. Southeast Asian J Trop Med Pulblic Health. 1993 ; 24: 603-606
2. Beaver PC, Jung RC and Cupp EW. Clinical Parasitology. 9th. ed. Lea&Febiger, Philadelphia. 1984; 825 pp.
3. Bedavanija A and Namatra B. Bilateral ocular sparganosis. J Med Assoc Thai. 1964; 47: 215-219
4. Chamadol W, Thanaphaisal C, Tangdumrongkul S, et al. Intracerebral hematoma caused by sparganum : a case report. J Med Assoc Thai. 1992; 75: 602-605
5. Holodniy M, Almenoff J, Loutit J, et al. Cerebral sparganosis : case report and review. Rev Infect Dis. 1991; 13 : 155-159
6. Kittiponghansa S, Tesana S and Ritch R. Ocular sparganosis: a cause of subconjunctival tumor and deafness. Trop Med Parasitol. 1988; 39 : 247-248
7. Kron MA, Guderian R, Guevara A, et al. Abdominal sparganosis in Ecuador: a case report. Am J Trop Med Hyg. 1991; 44 :146-150
8. Lin TP, Su IJ, Lu SC, et al. Pulmonary proliferating sparganosis : a case report. J Formosan Med Assoc. 1978; 77: 467-479
9. Moon WK,Chang KH, Cho SY,et al. Cerebral sparganosis :MR imaging versus CT features. Radiology. 1993;188: 751-757
10. NakamuraT, Hara M, Matsuoka M,et al.Human proliferative sparganosis: a new Japanese case. Am J Clin Pathol. 1990; 94: 224-228
11. OH SJ,Chi JE and Lee SE, Eosinophilic cystitis caused by vesical sparganosis : a case report. J Urol. 1993; 149: 581-583
12. Tansurat P. Human sparganosis in Thailand. J Med Assoc Thai. 1966; 49: 391-395
13. Torres JR, Noya OO, et al. Treatment of proliferative sparganosis with mebendazole and praziquantel. Trans R Soc Trop Med Hyg. 1981; 75: 846-847

B. GRIMM HEALTHCARE CO., LTD.

SIEMENS

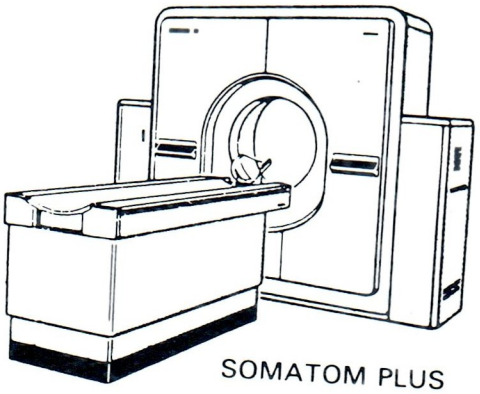

SOMATOM PLUS

*The Quantum Leap in CT
*Breaking Through The Boundaries of Conventional CT
*An Advances in Applications

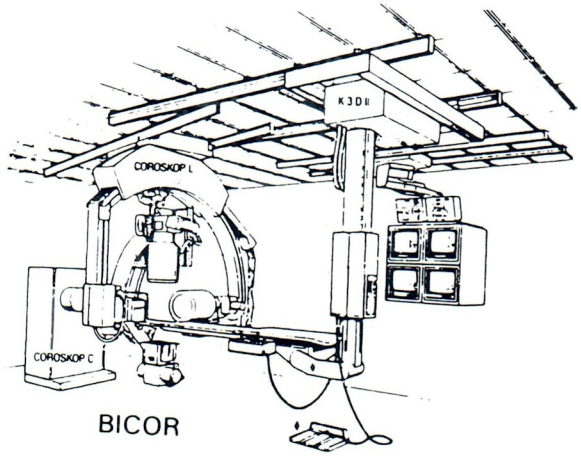

BICOR

The Superior System
for
Angio Cardiography
and
Angioplasty

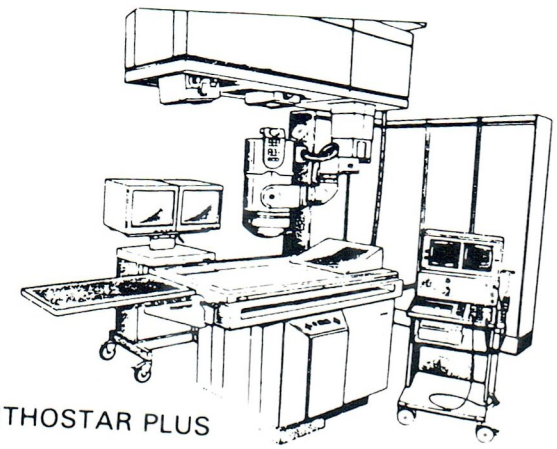

LITHOSTAR PLUS

The Universal Lithotripter for
all varieties of stone Therapy
in Urinary and Biliary treatment

1643/4 Phetburi Rd. Bangkok 10310 Tel. (02) 2524081, 2529131 GPO Box 66, Bangkok, Thailand. 10501 Cables THAIGRIMM Fax No. 2539867 Telex 82614 BGRIM TH

PULMONARY ACTINOMYCOSIS : PLAIN FILMS AND CT IMAGES

Patchrin PEKANAN[1,2] Supranee NIRAPATHPONGPORN[1,2]
Chirote SUCHATO[2] Prasit KIRATIKANOND[3]

ABSTRACT

A case report of pulmonary actinomycosis in a middle aged diabetic patient was presented. Plain chest film and CT scan of the lesion showed right lower lobe in location. The lesion presented as a mass lesion with small cavities and surrounding alveolar infiltration. The pleural space and bony parts were not involved due to partial treatment. Inadequate treatment showed worse progression. Needle aspiration was suggested for early diagnosis and treatment.

Key Words Pulmonary actinomycosis, plain film, CT scan

Actinomycosis is caused by members of the bacterial family Actinomycetaceae, of which the most important genus is Actinomyces. The orgnisms are nonmotile and nonspore-forming:branching filaments about 0.2 to 0.3 um. in diameter. They are anaerobic or microaerophilic. They are usually called sulfur granules because of their yellow color, although actual sulfur content is minimal (1,2). The organisms are normal inhabitants of human oropharynx. The disease is believed to be acquired by the spread of endogenous organisms from these sites, usually directly from the oropharynx into the lungs by aspiration or into the gastrointestinal tract by swallowing; spread occurs via the blood stream to distant tissues occasionally. Rare cases of exogenous transmission by human or animal bite or by other cutaneous trauma have been reported (3). Some cases result from extension of disease through the esphagus or diaphragm from primary sites in the gastrointestinal tract. The disease is of worldwide distribution and no age or race is immune; men are affected slightly more often than women, and there is no occupational predilection or seasonal variation (4).

Before the advent of antibiotics, actinomycosis was the most commonly diagnosed "fungus" disease of the lungs, presenting a fairly typical clinical picture of empyema and sinus tracts in the chest wall. This advanced stage is rarely seen now.

We report a case of pulmonary actinomycosis by plain film and CT images.

CASE REPORT

A 47 years-old female diabetic patient came to the hospital due to low grade fever and chronic cough. The sputum was white and the amount was not much. She was known to have "pneumonitis" for a year and was suggested by other doctors to have an operation due to this "pneumonitis problem". At the admission-time, she had low grade fever with measured temperature 38 degree celsius. Other physical examination was negative. Endoscope revealed no endobronchial lesion. Plain film of the chest (Fig.1) showed alveolar process at right lower lung zone with multiple cavities. CT scan of the thorax showed a mass-like lesion with small cavities

[1]Department of Radiology, Ramathibodi Hospital, Rama 6 Street, Bangkok 10400, Thailand.
[2]Department of Radiology, Samitivej Hospital, Sukhumvit 49, Bangkok 10110.
[3]Department of Medicine, Samitivej Hospital.

and surrounding alveolar process at right lower lobe (Fig.2). Aspiration of the lesion under CT scan guidance was performed, yielded foul smell pus. The pathology revealed fragment of blood clot containing many polymorphonuclear cells and clumps of actinomyces. Penicillin 12 m.u./ day was given to the patient with disappearance of the fever after 7 days and plain film (Fig. 3) showed partial clearing of the upper part of the lesion. The patient was discharged and was referred to receive further treatment with the doctor at her home-town. Two months later she came back with worse progression of the disease at the right lower lobe as shown in the figure 4.

DISCUSSION

The typical pattern in the acute variety of actinomycosis consists of airspace pneumonia, without recognizable segmental distribution, commonly in the periphery of the lung and with a predilection for the lower lobes (1). It is thus roentgenologically indistinguishable from acute pneumococcal pneumonia. Once the pneumonia has developed, the course of events depends largely upon whether antibiotic therapy is instituted. With appropriate therapy, most cases resolve without complications. If therapy is not instituted, a lung abscess may develop, and the infection may extend into the pleura (with consequent empyema) and into the chest wall, with osteomyelitis of the

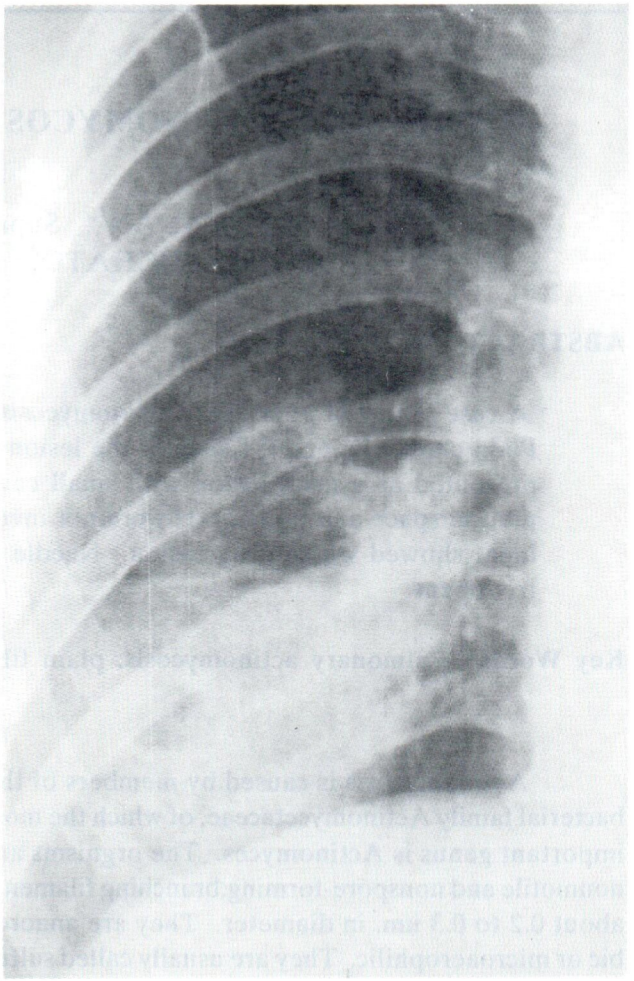

Fig. 1. P.A. view of the chest at right lower lobe showed thick wall cavitary lesions with fluffy border

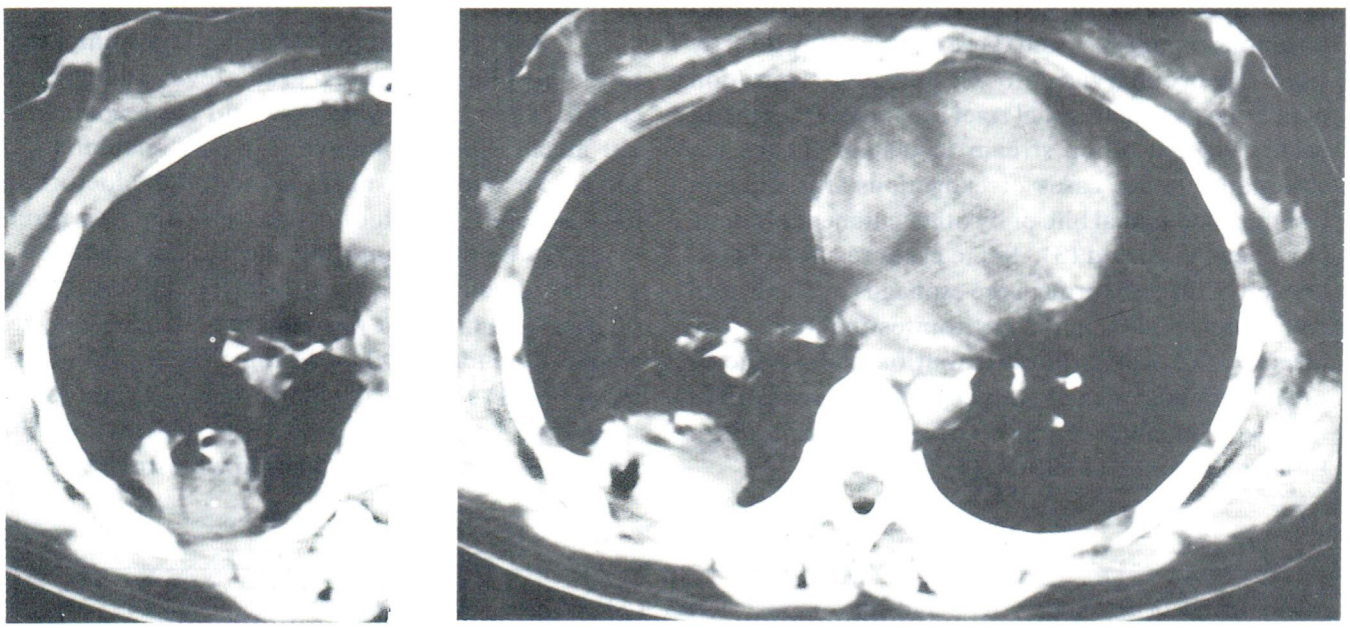

Fig. 2a. CT scan of the thorax at the lesion of right lower lobe, using mediastinal window showed a mass like lesion with small eccentric cavities.

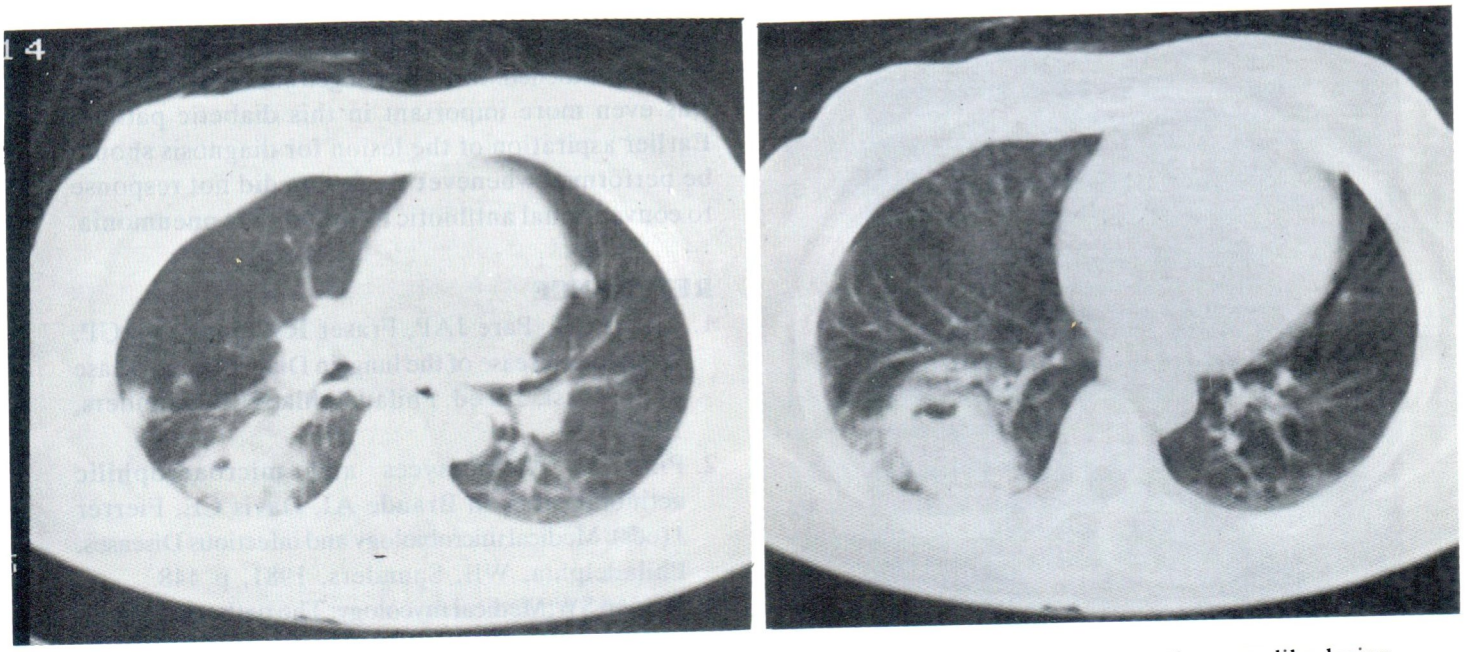

Fig. 2b. CT scan of the thorax, using lung window showed multiple small alveolar lesions near the mass like lesion.

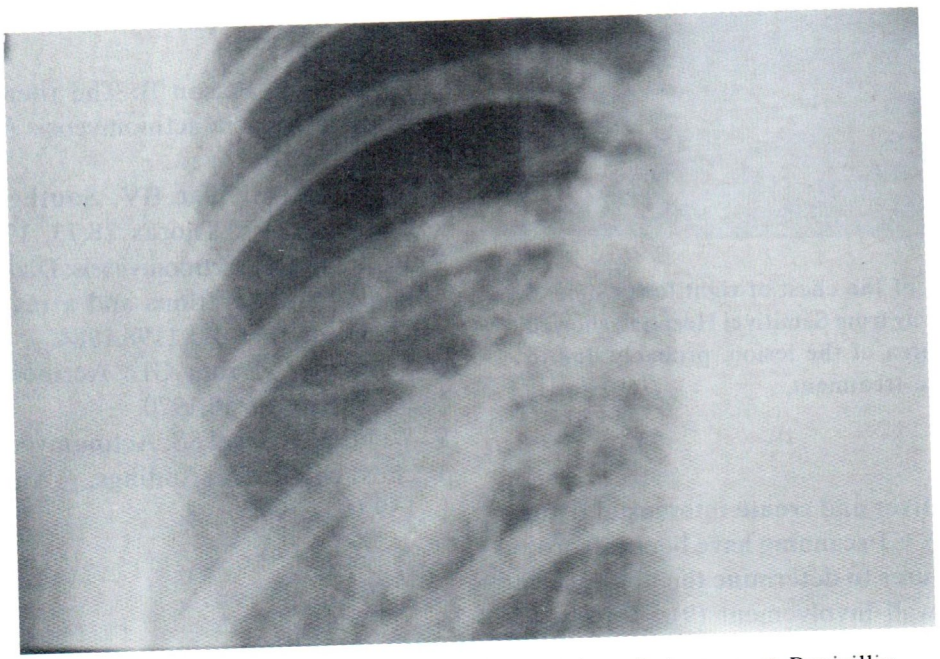

Fig. 3. Plain film of the chest at right lower lober, 7 days post Penicillin treatment, showed partial clearing at the superior part of the lesion.

ribs and abscess formation in these areas. In one serie of 15 cases (5), a mass lesion was the initial roentgenographic manifestation in six, cavitation was identified in six, pleural effusion in the form of either empyema or pleural thickening in 12 and chest wall involvement in nine. Like other anaerobic pulmonary infections that originate in oropharynx, actinomycosis frequently presents as a mass that simulates pulmonary carconoma (6). Since actinomycosis usually require prolonged antibiotic therapy, a pulmonary lesion may undergo initial remission following institution of therapy, only to exacerbate when therapy has been withdrawn too early (7). The disease may start in a lower lobe, penetrate through the dia-

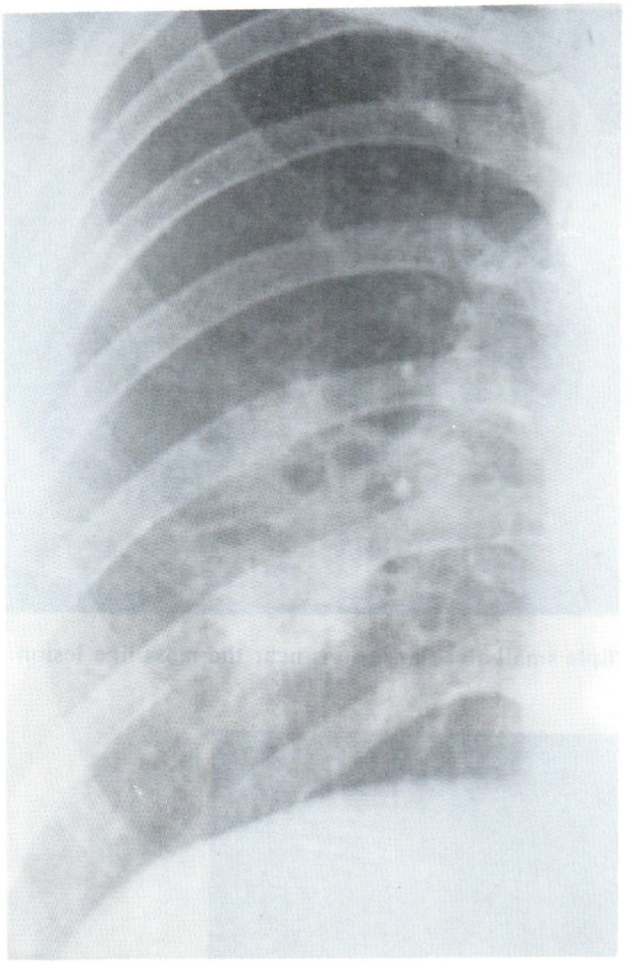

Fig. 4. Plain film of the chest at right lower lobe, 2 months away from Samitivej Hospital, showed widened area of the lesion, probably due to inadequate treatment.

phragm into the liver and create intercostal fistulae along the way (8). CT scanning have been advocated as useful procedures to determine the presence and extent of chest wall involvement (9). Rarely, the disease becomes disseminated, with the development of a miliary pattern roentgenographically.

Our patient had a chronic course and had received some antibiotic treatment for pneumonitis for a year. The presented images were those of mass lesion and cavities, besides surrounding alveolar process. The received prior antibiotic helped to prevent pleural and chest wall complication. Some improvement was shown after 7 days treatment with penicillin, however, the treatment at her hometown might be inadequate and discontinuous, so that the area of the involvement was widened. More prolonged antibiotic treatment was even more important in this diabetic patient. Earlier aspiration of the lesion for diagnosis should be performed whenever the lesion did not response to conventional antibiotic treatment for pneumonia.

REFERENCE

1. Fraser RG, Pare JAP, Fraser RS, Genereux GP. Infectious disease of the lung; in Diagnosis of disease of the chest, 3rd ed. Philadelphia, W.B. Saunders, 1989.
2. Pine L: Actinomyces and microaerophilic actinomucetes, in Braude AI, Davis CE, Fierrer J (eds): Medical microbiology and infectious Diseases, Philadelphia, WB, Saunders, 1981, p 448.
3. Rippon SW:Medical mycology: The pathogenic fungi and the pathogenic actinomycetes. 3rd ed. Philadelphia, WB Saunders, 1988.
4. Harvey JC, Cantrell JR, Fisher AM: Actinomycosis: Its recognition and treatment. Ann Intern Med 46:868,1957.
5. Flynn MW, Felson B: The roentgen manifestations of thoracic actinomycosis Am J Roentgenol 110:707,1970.
6. Slade PR, Slesser BV, Southgate J: Thoracic actinomycosis. Thorax 28:73, 1973.
7. Bennhoff DF: Actinomycosis: Diagnostic and therapeutic considerations and a review of 32 cases. Laryngoscope 94: 1198,1984.
8. Schwarz J, Baum GL: Actinomycosis. Semin Roentgenol 5:58,1970.
9. Webb WR, Sagel SS: Actinomycosis involving the chest wall: CT findings. Am J Roentgenol 139:1007,1982.

CT IMAGING OF MADELUNG DISEASE: A CASE REPORT

Patchrin PEKANAN[1], Supawadee PRAKUNHANGSIT[2],
Supranee NIRAPATHPONGPORN[1], Wiwattana THANOMKIAT[1,3].

Madelung Disease was first described by Launois and Bensaude in 1898 (1). Its synonyms are Launois-Bensaude disease, Buschke disease, cervical lipomatosis, Madelung neck and multiple symmetrical lipomatosis (2). It is characterized by progressive growth of fat masses which are located symmetrically at the neck, shoulders, chest, abdomen and groin (3). The disease seems to be more frequent in the Mediterranean regions, and approximately 97% of those affected are men.

We report a case of Madelung disease in a 38 years-old Thai male patient.

CASE REPORT

A 38 years-old Thai male patient from Ubolrajthani, a province in the north-eastern part of Thailand, came to the Ramathibodi Hospital due to the presence of neck mass for 2 years. At first, the soft and bulky mass appeared at the anterior chest wall; then it grew slowly up to the anterior and posterior part of the neck. He was not dyspneic. The systemic symptoms did not exist. He drank alcohol for 15 yrs, 2 times a week and smoked for 10 yrs. Non I.V. contrast CT scan of the neck, performed at Subprasithprasong Hospital in Ubolrajathanee (see figure 1) , showed markedly increased fatty tissue around the central structures of the neck without distorting them. The airway was not narrowed. The fatty tumors were unencepsulated, so that the borders between tumors and surrounding tissue are not defined. The histology confirmed the mass to be lipoma.

DISCUSSION

Studies have linked Madelung disease to a specific defect in the regulation of catecholamine-induced lipid mobilization (4,5); thus it could be considered a "triglyceride storage disease" involving adipose tissue. Clinical manifestations are as followings; 1) the onset is in adulthood 2) massive lipomatosis (normal fat that often begins on the back of the neck and extends anteriorly to the submental region and to the thorax in a symmetrical fasion) may spread to the scrotal region 3) respiratory system symptoms related to tracheal compression and recurrent palsy 4) venous stasis of the chest wall in association with mediastinal involvement 5) neuropathy (sensory, motor, autonomic) 6) muscular weakness, tendon areflexia, muscle atrophy, tremor, cramps, loss of vibratory sensation, hypoesthesia, sciatica-like pain, trophic changes, segmental hyperhidrosis, gustatory sweating, impotence, tachycardia at rest etc. 7) metabolic abnormalities, marked increase in adipose tissue lipoprotein lipase activity, plasma hyperalpha-lipoproteinemia, defect in the adrenergic stimulated lipolysis in lipomatous tissue, hyperuricemia, reduced glucose tolerance, renal tubular acidosis 8) red blood cell macrocytosis, macrocytic anemia 9) abnormal liver function test results related to elevated alcohol intake 10) no signs of abdominal or pelvic involvement 11) sudden death.(7-10).

Familial occurrence has been described (11-13). A hyperplastic mechanism has been postulated, with in vitro studies demonstrating a defect

[1]Department of Radiology, Ramathibodi Hospital, Rama 6 Street, Bangkok 10400, Thailand.
[2]Department of E.N.T., Ramathibodi Hospital.
[3]Department of Radiology, Songklanakarin University Hospital, Hardyai, Songkla.

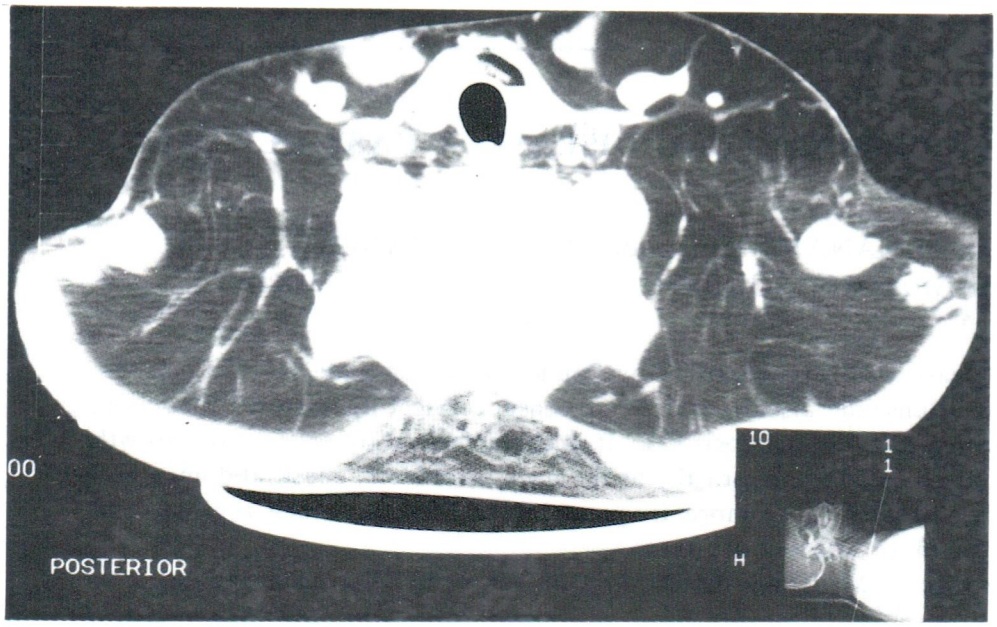

Fig. 1A.
Non I.V. enhanced CT scan of the lower neck showed diffuse fatty tissue infiltration around the central part of the neck.

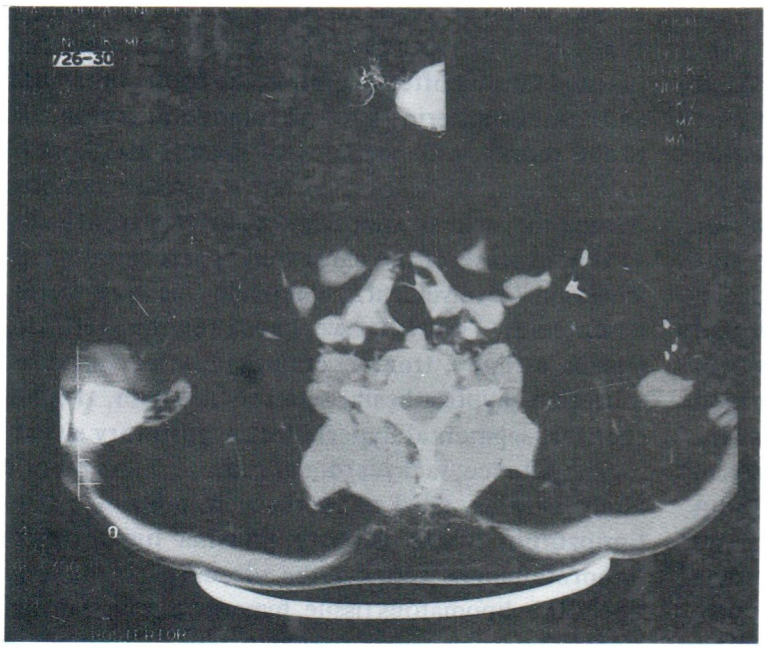

Fig. 1B.
Soft tissue window of the same image as in fig. 1A. showed no distortion of the central structures.

in adrenergic-stimulated lipolysis of lipomatous tissue (4,5). The uninvolved subcutaneous fat is usually very poorly represented of frankly atrophic, and signs of mediastinal compression have often been described (14,15,16). No abnormal deposition of fat in the anterior mediastinal region (17), cardiophrenic angle, or retropleural locations was seen, contrary to observations in patients with long term steroid treatments (18-20), Cushing syndrome (21,22), or obesity (23-25).

Radiologic manifestations in 15 patients with Madelung disease described by Enzi (3) were 1.) Lipomatosis (neck, mediastinum, below the trapezius muscle) 2.) Calcification/ossification within the lipomatous masses 3) tracheal narrowing and deformity 4) venous stasis 5) absence of pericardial, intraabdominal, retroperitoneal and pelvic lipomatosis 6) Large amount of fat at anterior abdominal wall and pubic region.

REFERENCE

1. Launois PE, Bensaude R. De L. adeno-lipomatose symetrique. Bull Mem Soc Med Hop Paris 1898; 1:298-317 (Fre).
2. Taybi H, Lachman RS. Madelung disease: in Radiology of syndromes, metabolic disorders, and skeletal dysplasias, pp 282-283; 3rd Ed.1990 Chicago, Year book medical publishers, inc.
3. Enzi G, Biondetti RP, Fiore D, Mazzoleni F. Computed tomography of deep fat masses in multiple symmetrical lipomatosis. Radiology 1982; 144: 121-124.
4. Enzi G, Inelmen EM, Baritussio A, et al. Multiple symmetric lipomatosis: a defect in adrenergic-stimulated lipolysis. J Clin Invest 1977;60:1221-1229.
5. Enzi G, Favaretto L, Dorigo P, et al. Defects of lipolysis in human lipomatosis. In : Enzi G, Crepaldi G, Pozza G, Renolds AE, eds, Obesity: pathogenesis and treatment. New York: Academic Press, 1981:161-165.
6. Boonichon PH, et al: Maladie de Launois-Bensaude, Traitment par large cervicotomie trasversale. Presse Med. 1986:15:2247.
7. Buschke A, et al: Die traumatische Atiologie und die Begutachtung der symmetrischen Lipmatose. Klin. Wochenschr. 1929;8:880.
8. Enzi G, et al: Sensory, motor, and autonomic neuropathy in patients with multiple symmetric lipomatosis. Medicine (Baltimore) 1986;64:388.
9. Gate A, et al: Le syndrome de Launois-Bensaude: A propos de 12 cas cliniques, Ann. Chir. Plast. 1966;11:193.
10. Madelung O: Ueber den Fetthals (diffuses Liom des Halses). Arcj. Klin. Chir. (berlin) 1888;37:106.
11. Michon P. Adenolipomatose symetrique familiale. Presse Med 1936;44: 663-664 (Fre).
12. Kurzweg FT, Spencer R. Familial multiple lipomatosis. Am J Surg 1951;82:762-765.
13. McKusick VA. Mendelian inheritance in man. Catalogs of autosomal dominant, autosomal recessive, and x-linked phenotypes. 5th ed. Baltimore: Johns Hopkins University Press, 1978:242-243.
14. Mounier-Kuhn P, Haguenauer JP, Localisation laryngree d une maladie de Launois Bensaude. J Franc Otorhinolaryngol 1967;16:603 (Fre).
15. Chahrokhi K, La Lipomatose symetrique diffuse a predominance cervicale. Rev Laryngol (Bordeaux) 1960;81:551-578. 16. Comings DE, Glenchur H. Benign symmetric lipomatosis. JAMA 1968; 203:305.
17. Heitzman ER. The mediastinum. Radiologic correlations with anatomy and pathology. St. Louis, Mo:Mosby 1977.
18. Koerner HJ, Sun DI-C. Mediastinal lipomatosis secondary to steroid therapy. AJR 1966;98: 461-464.
19. Teates CD. Steroid induced mediastinal lipomatosis. Radiology 1970; 96:501-502.
20. Schuman BM. Mediastinal lipomatosis complicating steroid therapy of regional enteritis. Gastroenterology 1971;61:244-246.
21. Bodman SF, Condemi JJ. Mediastinal widening in iatrogenic Cushing's syndrome. Ann Intern Med 1967;67:399-403.
22. Santini LC, Williams JL. Mediastinal widening (presumable lipomatosis) in Cushing's syndrome. N Engl J Med 1971;284:1357-1359.
23. Price JE Jr, Rigler LG. Widening of the mediastinum resulting from fat accumulation. Radiology 1970;96:497-500.
24. Steckel RJ. Mediastinal pseudotumors associated with exogenous obesity. Radiology 1976;119:74.
25. Lee WJ, Fattal G. Mediastinal lipomatosis in simple obesity. Chest 1976;70:308-309.

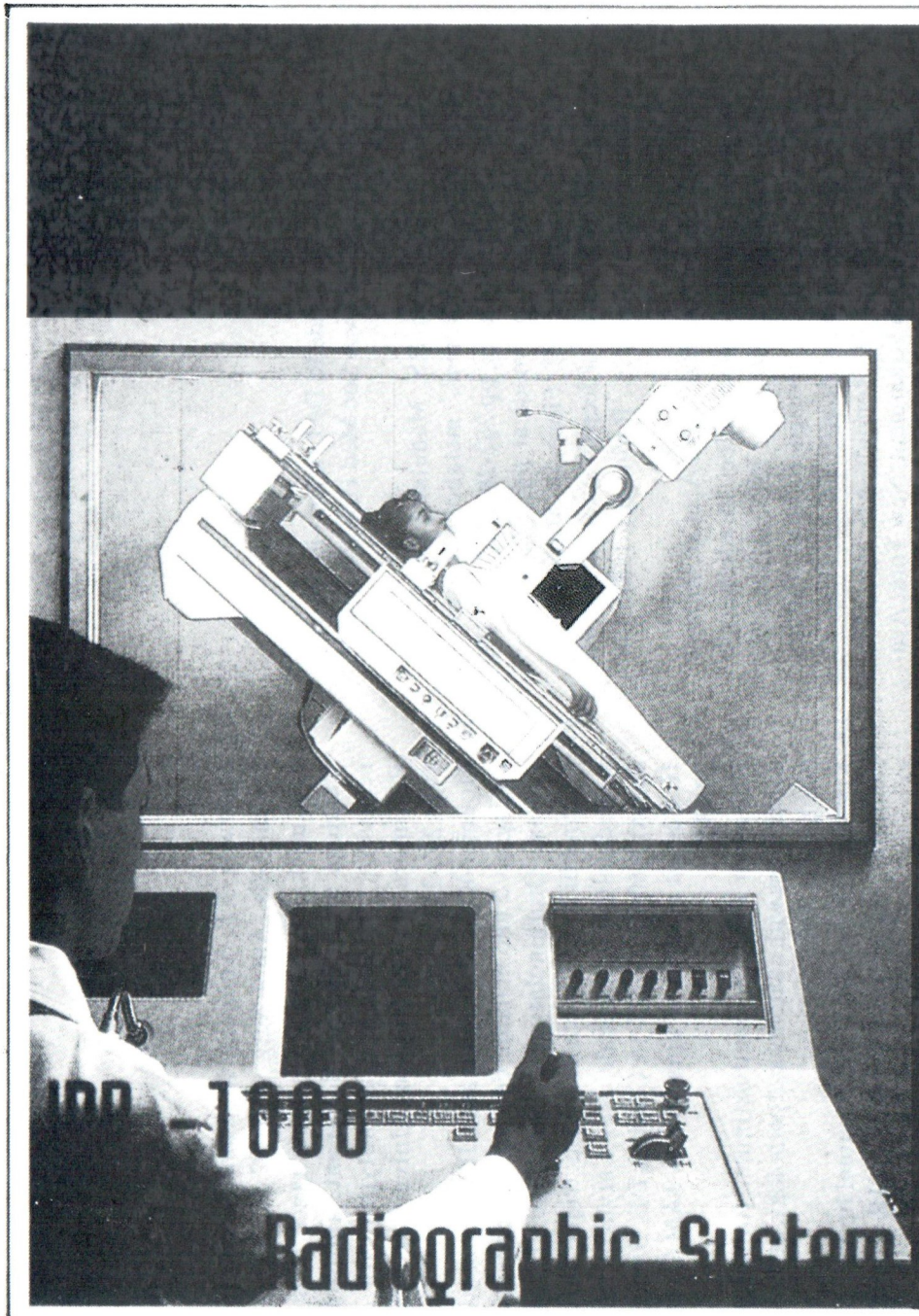

SHIMADZU

INVERTERTYPE Mobile X-ray system

SCT-4800T WHOLE BODY CT SCANNER

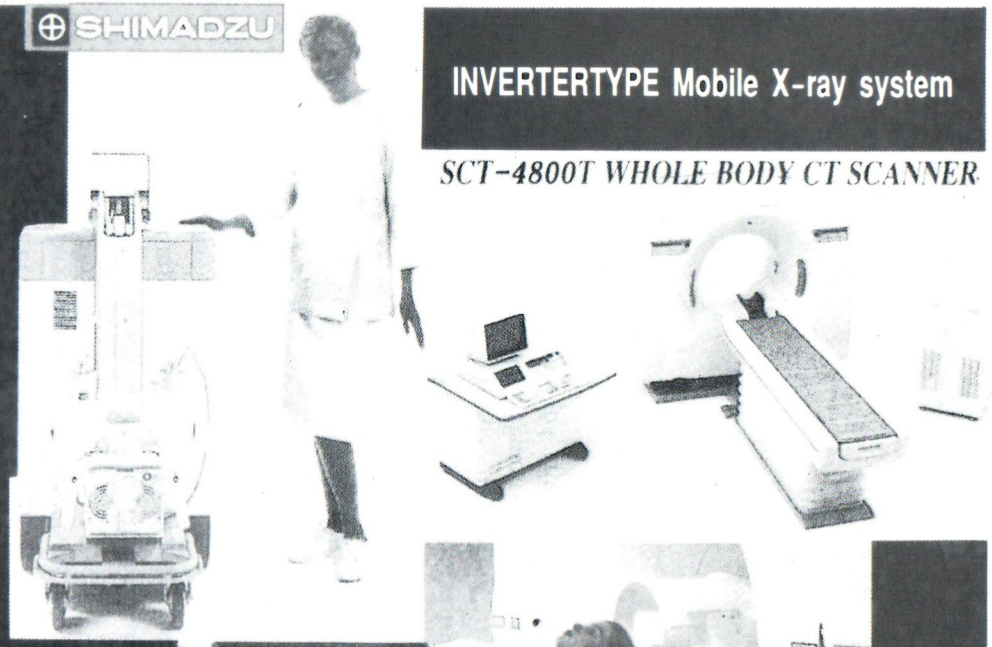

MAGNETIC RESONANCE IMAGING

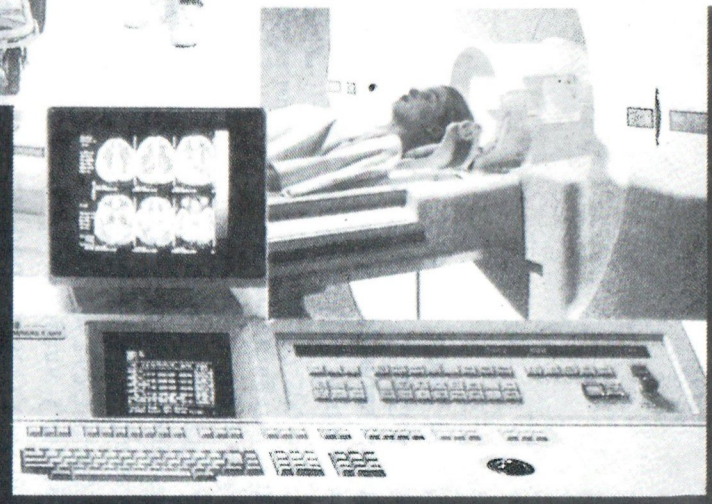

บริษัท รังสิภัณฑ์ จำกัด

RADIOLOGICAL EQUIPMENT CO.,LTD.

170-172/1 (ชั้น 2-3) ถนนบริพัตร ป้อมปราบ กรุงเทพฯ 10100

170-172/1 (Floor 2-3) BORIPHAT ROAD BANGKOK 10100 THAILAND

TEL: 2212386,2237954,2239791,2243402 TELEFAX: (02) 2251657

DIAGNOSTIC IMAGING OF THE LATERAL NECK MASSES IN ADULTS: A STUDY IN RAMATHIBODI HOSPITAL.

Kunchitthape TANPOAPONG[1], Boonchu KULPADITHAROM[1], Patchrin PEKANAN[2].

ABSTRACT

The retrospective study of roentgenographic evaluation for solely lateral neck mass in 146 adult patients at ENT clinic, Ramathibodi Hospital, during 1987-94 prior to panendoscopy with random-guided- directed biopsy of upper aerodigestive tract was proposed. X-ray chest (PA view) showed abnormal in 21.3%. Tuberculosis, non-tuberculosis, pulmonary mass, hilar or mediastinal mass and miliary infiltration were 5.5,6.2,2.7, 6.2 and 0.7% respectively. Panendocopic finding was abnormal only in 1 case. Barium swallowing in 67 cases had sensitivity, specificity, accuracy, positive predictive value and negative predictive value of 50.0,96.6,91.1,66.7 and 93.4%. It was necessary to be done in swallowing disorder patients. CT scan of the head and neck region in 18 patients, 16 had abnormal findings; it was recommended in suspected nasopharyngeal cases or lessions difficult to be palpated. Other investigations such as thyroid scan, neck ultrasonography, sialography or angiography was used when they were indicated. Roentgenographic cost had an importnat role in order to choose the suitable investigation and gave maximal benefit for patients.

Keywords: lateral neck mass, roentgenography, adult

INTRODUCTION

Lateral neck masses are usually caused by lymphadenopathy. The primary source may be within or outside the head and neck region and the only chance for cure or palliation is to find and treat the primary site. There is a significant incidence of multiple separate primary malignancies of the head and neck, so that, a divergent opinion as to the optimum diagnostic management of these patients exists. The improvements in physical examination techniques and the introduction of new endoscopic techniques have led to the ability to diagnose the vast majority of upper aerodigestive tract carcinomas (1,2,3). The fine needle biopsy and improved cytologic techniques, have contributed to the improved management of these patients (4,5). The imaging modalities, both conventional and high technology types, also have the similar importance (6-11).

To define the role of the diagnostic imaging in the evaluation of the patients presented with lateral neck masses, we conducted a retrospective study in 146 patients.

PATIENTS AND METHODS

A retrospective study of 146 patients (between 1987-1994) who presented at the department of Otolaryngology, Ramathibodi Hospital with the lateral neck masses. There were 98 males and 48 females. The age ranged between 21-74 years old. The mass was present for 2 days to 8 years.

[1]Department of Otolaryngology, Ramathibodi Hospital, Rama 6 Street, Bangkok 10400, Thailand.
[2]Department of Radiology, Ramathibodi Hospital.

The time used for the diagnosis was 2 weeks to 7 months. The total admission time was 2 to 4 days. The follow up time was 4 weeks to 5 years. The clinical information and the results of the diagnostic tests were reviewed from the patients' files. The detailed information was shown in table 1-8. The location of the lymph node or mass in the lateral part of the neck was illustrated in figure 1.

DISCUSSION

Evaluation of the patients with lateral neck masses by imaging modalities, we should begin with plain film of the chest which enable us to visualize the mass larger than 1 cm of the bronchus. If the mass is larger than 2 cm in the main bronchus near hilar area or in the mediastinum, it will be detected (6), but the false negative result varied from 0-56% (12-16). The mediastinal widening or hilar mass could be seen from malignant lymphoma.

Barium swallow could detect cancer in the upper aerodigestive tract, up to 90% for the superficial type. For the flat type or the spreading type, larger than 1 cm, only the panendoscope could detect it and the false negative could vary from 0-75% (7,15,17,18).

Sialography should be done only in some selective cases, e.g. increasing in size of the mass related to the food ingestion or salivation.

Ultrasonography helped to differentiate between cystic and solid lesion, enlarged nodes, abscess, salivary gland lesion and mass near the large vessels. The lesion hidden by the bony part of the face could be missed. Evaluation of the thyroid gland by this modality is 90% accuracy (19,20). In addition, the fine needle aspiration biopsy, guided by ultrasonography was very helpful.

Carotid angiography was used in the diagnosis of the pulsatile or expansile mass, the mass with bruit, e.g. hemangioma, arteriovenous malformation and paraganglioma. Intra-arterial embolization, before surgery helped to reduce the amount of blood loss.

CT scan was used in the submucosal lesion of the upper aerodigestive tract (8,21) or lesion deep in the neck which was not render for palpation (22,23). Evaluation of the extension of the disease was quite accurate, CT scan and valsalva maneuver could be used in the case of laryngeal cancer spreading to the preepiglotic space, subglottic area, Morgagni's ventricle or pyriform sinus (24,25). Multiple sites of the thyroid cancer with lateral neck metastases and substernal involvement were well shown by CT study (26).

MRI study gives more information about the vascular invasion, involvement of the muscles, aerodigestive tract (27), the tumor of the tonsil, the anterior floor of the mouth and the base of the tongue (28,29). In addition, there is no hazard of radiation from MRI machine.

Thyroid scan scintigraphy is not very useful due to the lateral location of the neck masses. The technetium pertechnitate radionuclide scan is used in the diagnosis of the salivary gland tumor such as Warthin's tumor or oncocytoma(11).

Several conclusion could be drawn from this study

1. Plain roentgenography of the chest should be performed in every patient before endoscopy was made. The study was cheap and eligible. One patient with abnormal chest film (mass) and abnormal endoscope (bronchial bleeding) was shown to be carcinoma by neck mass biopsy. Every normal chest film also had normal bronchoscopy.
2. Barium swallow was not helpful for the patients who had no symptom of dysphagia.
3. CT scan was useful in the cases of nasopharyngeal mass, mass at head and neck which was difficult for palpation and helpful in the staging of the disease.
4. MRI scan gave more detail of the mass except the associated bone lesion.
5. Our ultrasonographic cases were too few in number to made a conclusion.
6. Sialography should be used in the enlarging mass relating to tasty food ingestion, or salivation.
7. Angiography would be used in the cases of pulsatile or expansile mass.
8. Serum for EBV titer and fine needle aspiration biopsy of the lateral neck mass before imaging study may helped in detecting many lesions e.g. malignant lymphoma, tuberculous adenitis, branchial cleft cyst etc.

Table 1. Incidence of the pathology of the 146 patients

Pathology	No. of cases	(%)
Cancer of the upper aerodigestive tract	76	(52)
Malignancy of the lymph nodes	17	(12)
Tuberculous adenitis	24	(16)
Others*	29	(20)

* reactive hyperplasia of the nodes, neurilemoma, branchial cleft cyst, lymphadenitis, carotid body tumor, pleomorphic adenoma, pleomorphic lipoma, cavernous hemangioma and chronic sialadenitis

Table 2: Incidence of the diagnostic imaging examination

Types of investigation	No.of pts (%)	No.of abn.cases (%)
Conventional imaging		
Plain film of the chest (PA view)	146 (100)	28 (19)
Barium swallow	67 (46)	10 (15)
Sialography - Parotid gland	3 (2)	3 (100)
- Submaxillary gland	2 (1.5)	2 (100)
High-technology imaging		
CT scan of the head & neck	18 (12)	16 (89)
CT scan of the chest	1 (1)	1 (100)
MRI of the head & neck	1 (1)	1 (100)
Thyroid scintigraphy	16 (11)	2 (12.5)
Ultrasonography of the neck	3 (2)	3 (100)
X-ray mammography	2 (1.5)	0 (0)
Carotid angiography	2 (1.5)	0 (0)

Table 3. The incidence of the results of the chest roentgenography in 146 studied patients

Pathology*	No. of cases	(%)
Normal	118	(81)**
Pulmonary fibropatchy infiltration or calcified granuloma (Tbc)	8	(5.5)
Pulmonary infiltration (non-Tbc)	9	(6)
Pulmonary nodule or mass	4	(3)
Miliary pattern	1	(1)
Widening of the mediastinum, hilar mass	9	(6)

* in 3 patients there are 2 different abnormal findings.

**also had normal upper airway endoscopy

Table 4. The abnormalities that were seen at barium swallow study of 10 patients and at panendoscopy, random-guided-directed biopsy (RGDB) in 13 patients

Panendoscopy	RGDB	Barium swallow
1. Rt. tonsillar polyp	SCCA*	Lt pyriform mass
2. Swelling of post cricoid and arytenoid area	Negative	Lt pyriform mass
3. Arytenoid cyst	Chr.inflammation	Lt pyriform mass
4. Esophageal mass,	Sq.metaplasia tracheal compression	Upper esophageal irregularity
5. Esophageal irregularity	Acute ulceration	Upper esophageal narrowing
6. Negative	Negative	Vallecular irregularity
7. Negative	Negative	Prominent upper esophageal mucosa
8. Negative	Negative	Hypopharyngeal incoordination
9. Negative	Negative	Minimal aspiration
10. Negative	Negative	Minimal aspiration
11. Bulging nasopharynx	Anaplastic carcinoma	Negative
12. Negative	Nasopharyngeal SCCA	Negative
13. Negative	Nasopharyngeal SCCA	Negative
14. Bronchial mass	Caseous granuloma	Negative
15. Hypopharyngeal mass	SCCA	Negative
16. Pyriform mass	Negative	Negative
17. Tongue base induration	Negative	Negative

*SCCA-Squamous cell carcinoma

Table 5. Relationship between barium swallow, panendoscopy and random-guided - directed biopsy (RGDB) in 67 patients

		Panendoscopy and RGDB	
		Positive	**Negative**
Barium swallow	**Positive**	**4**	**2**
	Negative	**4**	**57**

The sensitivity of barium swallow was 50%, the specificity was 97%, the accuracy was 91%, the positive predictive value was 67% and the negative predictive value was 93%.

Table 6. Comparison of the abnormalities detected by CT scan of the head and neck in 18 patients with panendoscopy and random-guided-directed biopsy (RGDB).

CT scan	Panendoscopy	RGDB	Diagnosis
1. NP	Irregular base of tongue	mild dysplasia	Ca, Primary ?
2. NP	Contact bleeding of vallecula and NP bulging	CA vallecula, Normal NP	Ca Vallecula
3. NP	Normal	Ca	Ca-NP
4. NP	Normal	Normal	Reactive hyperplasia
5. NP	Normal	Normal	Ca, Primary ?
6. NP	Normal	Normal	Ca, Primary ?
7. NP,LN	Normal	Normal	Ca, Primary ?
8. NP,LN	Normal	Ca	Ca, NP
9. Multiple LN	Normal	Normal	Ca, Primary ?
10. spinal accessory LN	Normal	Normal	Ca, Primary ?
11. Cervical cyst and mass	Normal	Normal	Brancheal cleft cyst
12. Parotid space mass	Normal	Normal	Ca-parotid gl.
13. Parapharyngeal mass	Normal	Normal	Ca parapharyn
14. Hypopharyngeal mass	Normal	Normal	Tuberculosis
15. Pyriform mass	Pyriform mass	Ca	Ca-pyriform
16. Carotid body tumor	Normal	Normal	Schwannoma
17. Normal	Normal	Normal	Ca, Primary ?
18. Normal	Normal	Normal	Ca, Primary ?

NP = nasopharyngeal irregularity, prominent or mass
LN = cervical lymph nodes
Ca = carcinoma
Diagnosis = final diagnosis by fine needle aspiration biopsy or cervical mass excision.

Table 7. Expense for each imaging modality

Type of Examination	Price in Baht	
	Service	Private
1. Plain x-ray Chest	100	120
2. Barium Swallow	400	500
3. Sialography (Parotid or Submaxillary)	600	1,200
4. CT scan of the head neck	4,000	4,500
5. MRI of the head and neck	8,000	10,000
6. Thyroid scintigraphy	500	500
7. Ultrasonography of the neck	300	400
8. X-ray mammography	400	600
9. Carotid angiography	3,500-6,500	3,500-6,500

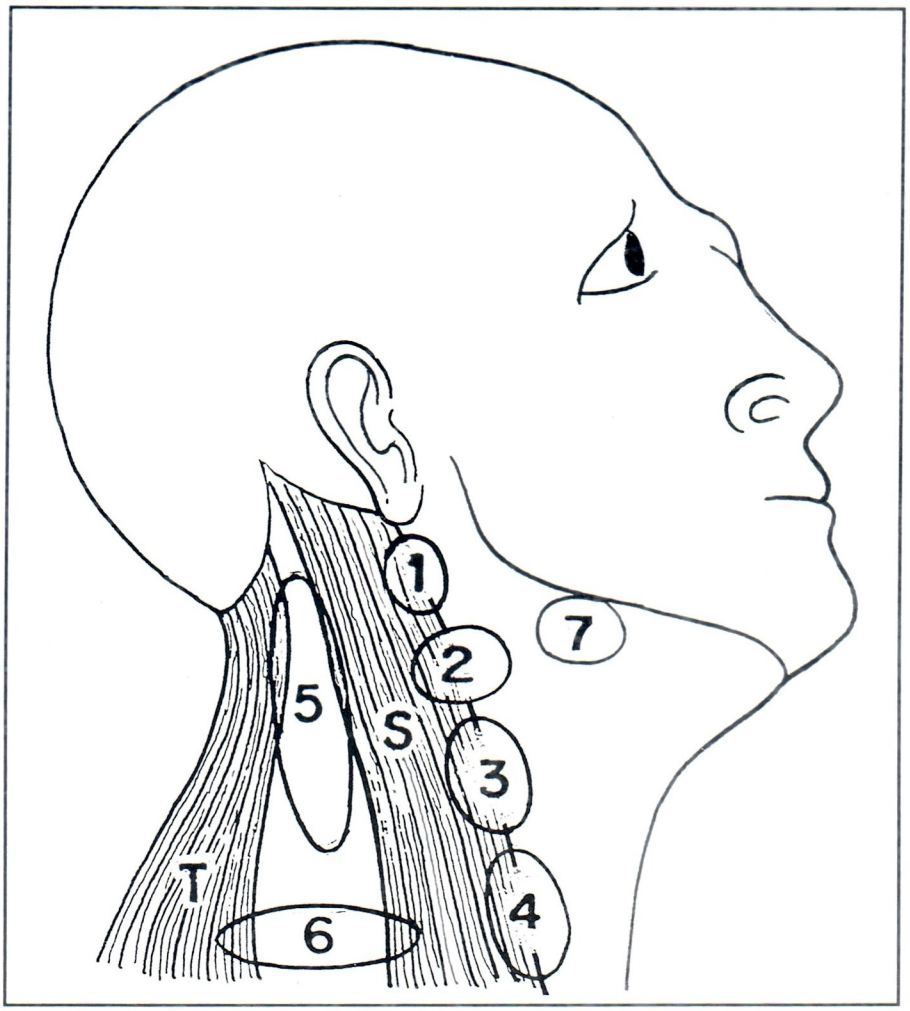

FIG.1. LOCATION OF LYMPH NODE OR MASS IN LATERAL NECK.

1. SUPERIOR 2.&3. MIDDLE 4. INFERIOR (1,2,3,4 = INTERNAL JUGULAR CHAIN)
5. POSTERIOR TRIANGLE
6. SUPRACLAVICULAR 7. SUBMANDIBULAR
S = Sternocleidomastoid muscle
T = Trapezius muscle

REFERENCES

1. Muraki As, Mancusa AA, Harnsberger HR. Metastatic cervical adenopathy from tumors of unknown origin:the role of CT. Radiology 1984;152:749-753.
2. Nahum AM, Decision management of the solitary neck mass. Trans Pac. Coast Oto-Ophthalmol Soc 1972;53:71-81.
3. MacComb WS, Diagnosis and treatment of metastatic cervical cancerous nodes from an unknown primary site. Amer J Surg 1972;124: 441-449.
4. Meyers DS, Templer J, Davis WE, Balch JA. Aspiration cytology for diagnosis of head and neck masses. Otolaryngology 1978;86:650-655.
5. Miller D, Ervin T, Weichselbaum R, Fabian RL, The differential diagnosis of the mass in the neck. A fresh look. Laryngoscope 1981;91:140-145.
6. Filder AE, Shaw C, Matthay RA. Lung cancer:Part I:Etiology,pathology. natural history, manifestation and diagnostic techniques. Invest Radiol 1986:21;80-90.
7. Ott DJ, Gelfand DW, Wu Wc. Sensitivity of single contrast radiology in esophageal disease: a study of 240 patients with endoscopically verified abnormality. Gastrointest Radiol 1983:8;105-10.
8. Premachandra DJ, Makae D, Primley P, Biopsy of neck lumps in adults should be the examination of the upper aerodigestive tract. Post grad med J.1990:66:113-5.
9. Gluckman JL, Robbins KT, Fried MP, Cervical metastasis squamous cell carcinoma of unknown or occult primary source. Head Neck Surgery 1990:12:440-3.
10. Baatenburg de Jong RJ, Rongen RJ, Lameris JS, Metastatic Neck disease: palpation VS ultrasound examination. Arch Otolaryngol 1989;115:689-91.
11. Greyson ND, Noyek AM, Radionuclide Salivary Scanning. J Otolaryngol 1982;11:1-4.
12. Maisel RH, Vermeersch H, Panendoscopy for second primaries in head and neck cancer. Ann Otol Rhinol Laryngol 1981:90:460-4.
13. Leipzig B, Bronchoscopy in the staging and evaluation of head and neck carcinoma. Ann Otol Rhinol Laryngol 1983:92;373-6.
14. Denneny JC, Keane WM, Atkins JP., Fiberoptic bronchoscopy:review of 1000 cases. Ear Nose Throat J 1983:62;540-50.
15. Leipzign B.Zellmer JE, Klug D, The role of endoscopy in evaluating patients with head and neck cancer: a multi-institutional prospective study. Arch Otolaryngol 1985:111;589-94.
16. Vrabec DP., Multiple primary malignancy of the upper aerodigestive system. Ann Otol Rhinol Laryngol 1979:88;846-54.
17. Shapshay SM.Hong WK,Fried WP., Simultaneous carcinoma of the esophagus and upper aerodigestive tract. Otolaryngol Head Neck Surg 1980:88;373-7.
18. Grossman TW,Kita MS.Toohill RJ., The diagnosis accuracy of pharyngoesophagram compared to esophagoscopy in patients with head and neck cancer. Laryngoscope 1987: 97;1030-2.
19. Noyek AM, Finkelstein DM, Kirsh JC., Diagnostic imaging of the thyroid gland. In:Falk SA, ed. Thyroid disease. Endocrinology surgery, nuclear medicine, radiotherapy. New York:Raven Press, 1990.
20. Simeone JF, Mueller PR, Ferucci JT., High resolution real time sonography of the thyroid. Radiology 1981:165:745-50.
21. Mancuso AA, Hanafee WN, Elusive head and neck carcinomas beneath intact mucosa. Laryngoscope 1983;93:133-6.
22. Mancuso AA, Hanafee WN., Computed tomography and magnetic resonance imaging of the head and neck. 2nd ed. Baltimore: William & Wilkins 1985.
23. Muraki AJ, Mancuso AA, Harnsberger HR. Metastatic cervical adenopathy from tumours of unknown origin:the role of CT. Radiology 1984; 152:749-52.
24. Gamsu G, Webb WR, Shallit JB., Computed tomography in carcinoma of the larynx and pyriform sinus. Value of phonation scans. Am J Roentgenol 1981;136:577-80.
25. Shulman HS, Noyek AM, Steinhart MI., CT of the larynx. J Otolaryngol 1982;11:395-9.
26. McShane DP, Freeman JL, Noyek AM, A review of conventional and CT imaging in the evaluation of thyroid malignancies. J Otolaryngol 1987;16:1-6.
27. Shapiro MD, Som PM, MRI of the paranasal sinuses and nasal cavity. Radiol Clin North Am 1989;27:447-9.
28. Som PM., Lymph nodes of the neck. Radiology 1987; 165:593-7.
29. Dooms GC, Hircak H, Croks LE., Magnetic resonance imaging of the lymph nodes:comparison with CT. Radiology 1984; 153:719-22.

APEX **Helix**

The first Slip-Ring nuclear imaging system

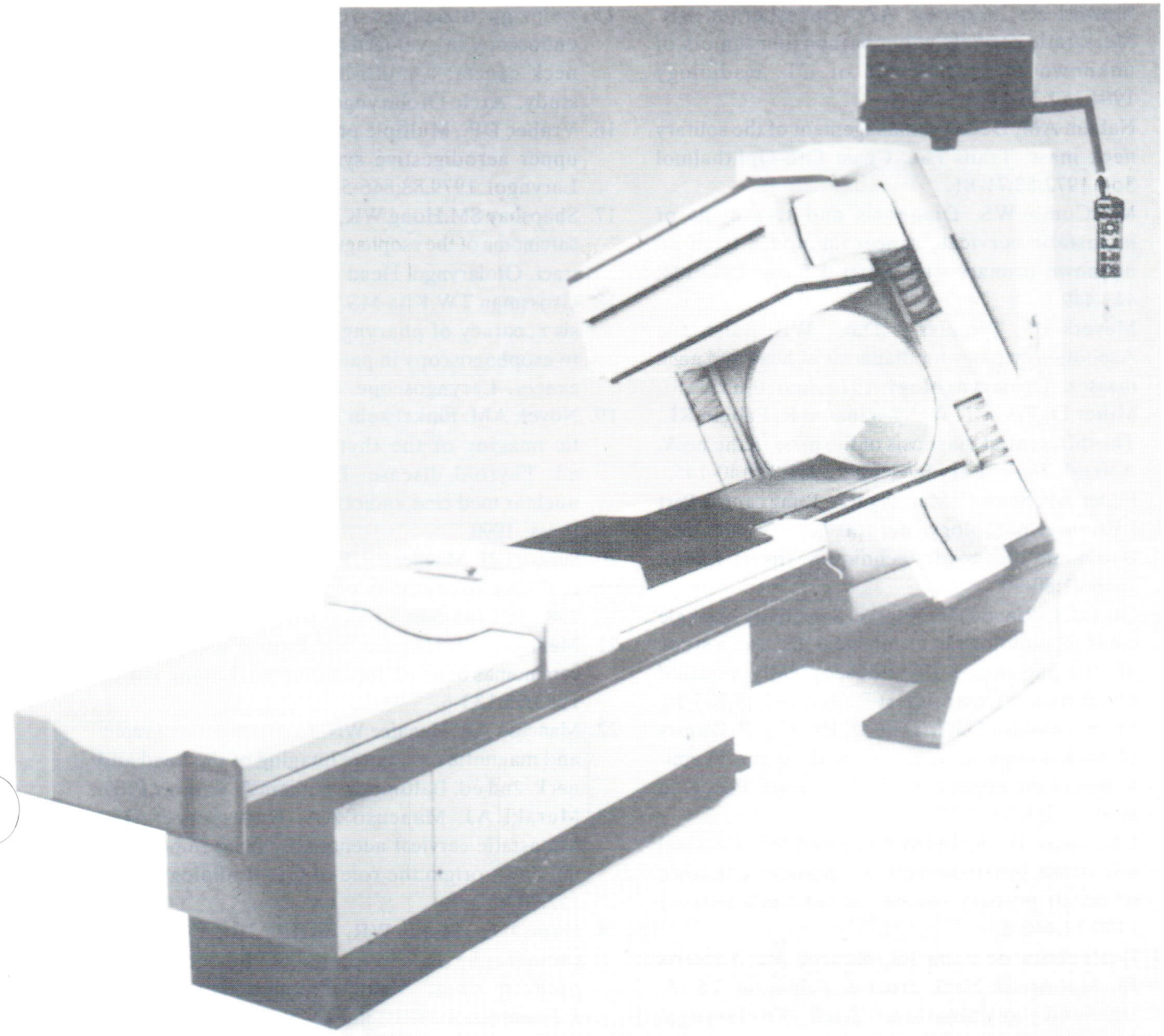

Dual Head, Multi-Purpose Camera

Distributed By

supreme PRODUCTS CO.,LTD.

163/81 82 Prapinklao Road. Bangkok 10700

Fax: No.<662> 4333971

Tel: 4340040,4340050 Service Dept. 4340060

RADIOGRAPHIC APPEARANCE OF THE INTRATHORACIC TUBERCULOSIS IN 20 HIV-POSITIVE PATIENTS

Supranee NIRAPATHPONGPORN[1], Sutarat TANSAGUNWATTANA[1,2], Patchrin PEKANAN[1].

ABSTRACT

Retrospective analysis of the roentgen findings in intrathoracic tuberculosis of 20 HIV positive patients were performed. Prominent features were mediastinal and hilar lymphadenopathy. Pulmonary infiltration had more or less interstitial component. Cavitation was rare. Pleural effusion was quite common. The pulmonary infiltration involved both upper and lower lung zones, diffuse and perihilar distribution; however, the upper lung zones still predominated.

The pandemic of AIDS has had a major impact on the worldwide tuberculosis problem. Tuberculosis usually occurs early in the course of AIDS and may even be the sentinel infection. The diagnosis is difficult because the characteristic pulmonary symptoms, signs, and radiographic appearance are often absent (1). Disease tends to be extrapulmonary, disseminated and lymphatic. Pulmonary lesions, when present, often are noncavitary and nonapical.

The studies of intrathoracic tuberculosis in AIDS patients had been reported by several Thai authors (2,3,4). We conducted the study to compare the results with other reports from Thailand and from other countries.

MATERIAL AND METHODS

The chest radiographs and medical records of 20 patients who visited the infectious clinic of Ramathibodi Hospital between January 1991 to February 1994 were reviewed. All patients were seropositive to HIV infection and sputum was positive for tuberculosis. The routine PA chest film was obtained on the day of 1st visit and follow up film chest was done after treatment. In all cases, the abnormal x-ray findings were analyzed by the radiologist, documenting the presence or absence of the following findings; 1) the pattern of parenchymal infiltration and its location 2) cavitation 3) adenopathy (hilar and mediastinum) and 4) pleural effusion.

RESULTS

The patient consisted of 17 males and 3 females, age group ranged from 19 to 65 years old, as shown in table 1. The radiographic findings showed high percentage of hilar and mediastinal lymphadenopathy. Most of the cases had pulmonary infiltration of interstitial type or mixed interstitial and alveolar types. Associated cavities were rare. There was only one case of miliary tuberculosis. Pleural effusion was not uncommon, occurring alone in 3 cases. Upper zone infiltration occurred slightly more than the lower zone infiltration. The detailed information of the roentgen abnormality and the comparison with findings reported by other authors was presented in the table 2. The radiographs of the parenchymal infiltration, adenopathy and pleural effusion were illustrated in figure 1,2,3 and 4.

[1]Department of Radiology, Ramathibodi Hospital, Rama 6 Street, Bangkok 10400, Thailand.
[2]Radiologic section, Central chest hospital, Ministry of Public health.

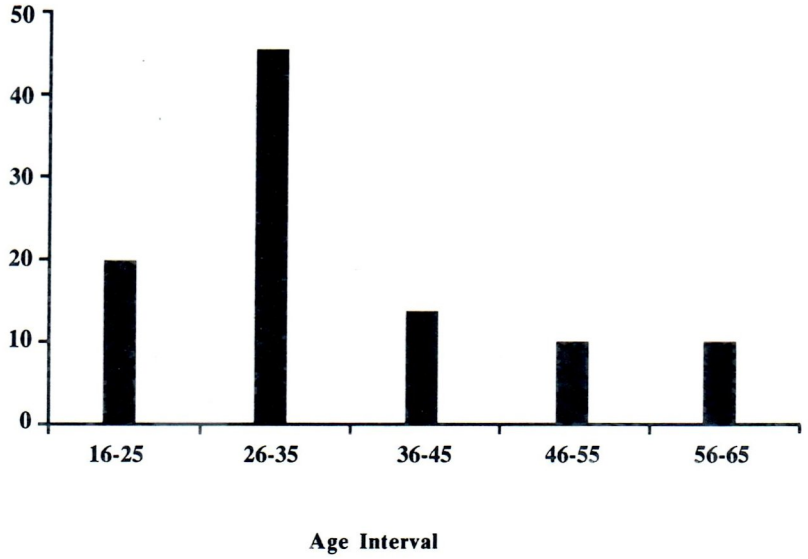

Table 1. Frequency of the patient's age group.

Table 2. Detail information of the roentgen findings in 20 AIDS- patients with intrathoracic tuberculosis

Case No.	Adenopathy	Infiltration & Location	Miliary	Effusion
1	M	RU,LL (I)	–	–
2	M	–	–	LT
3	–	LU, LL (I)	–	RT
4	–	–	–	RT
5	–	–	P	–
6	H	–	–	Bilateral
7	–	–	–	LT
8	M & H	Perihilar (I)	–	–
9	M & H	RL (A)	–	–
10	M & H	LU (I)	–	–
11	–	RU, RL (I & A)	–	–
12	M	RU (I & A)	–	–
13	–	RU (C) (I)	–	–
14	M & H	Diffuse (I)	–	–
15	–	LU, LL (I)	–	–
16	–	RL (C) (I & A)	–	–
17	–	Perihilar (I & A)	–	–
18	M	RU, RL (A)	–	–
19	–	–	–	RT
20	M & H	Diffuse (I)	–	–

M = Mediastinal
H = Hilar
I = Interstitial
A = Alveolar
C = Cavity
P = Presence

RU = right upper lung zone
RL = right lower lung zone
LU = left upper lung zone
LL = left lower lung zone

Table 3. Percentage of abnormalities, compared with other authors

Roentgen Abn	USA	Can	SPA	AFI	THA	RAMA
Normal chest	12	13	6	–	–	–
Adenopathy	59	39	32	50	–	50*
Pulmonary infilt.	47	74	38	11	90	75**
Cavitation	0	44	10	38	60	10
Miliary	18	–	12	8	10	10
Pleural effusion	12	–	10	38	–	30
Total cases	23	57	49	61	40	20

USA = United States of America, 1985 Pitchenik & Rubinson (5)
CAN = Canada, 1991 Long & Maycher (6)
SPA = Spain, 1991 Gutierrez & Miralles (7)
AFI = South Africa, 1992 Saks & Posner (8)
THA = Thailand, 1992 Punnotok & Subhannachart (4)

* Mediastinal nodes alone 40%, Hilar nodes alone 10%, Mediastinal and hilar nodes 50%
** Interstitial infiltration 53%, interstitial & Alveolar 26%, alveolar 14%
** Infiltration of upper zone & lower zone 36%, upper zone 22%, lower zone 14%, perihilar 14% and diffuse 14%

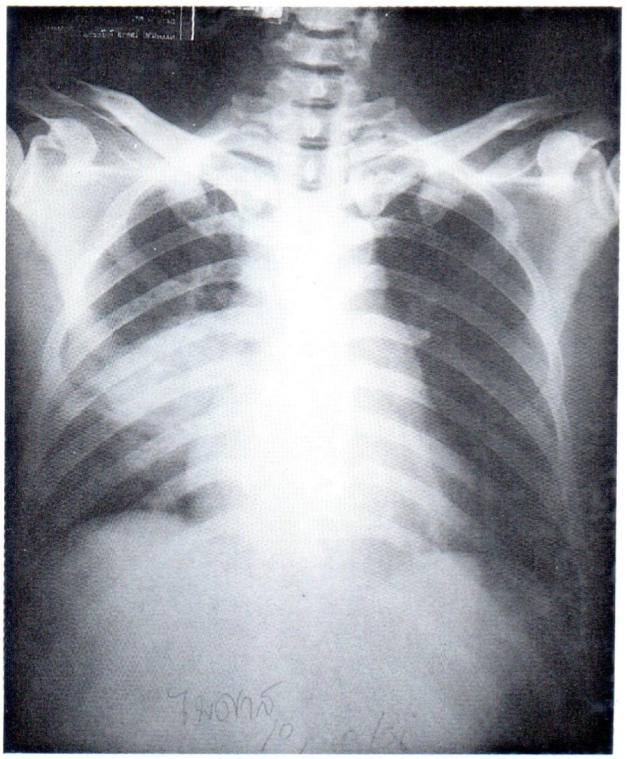

Fig.1A. PA chest film of the patient No.9

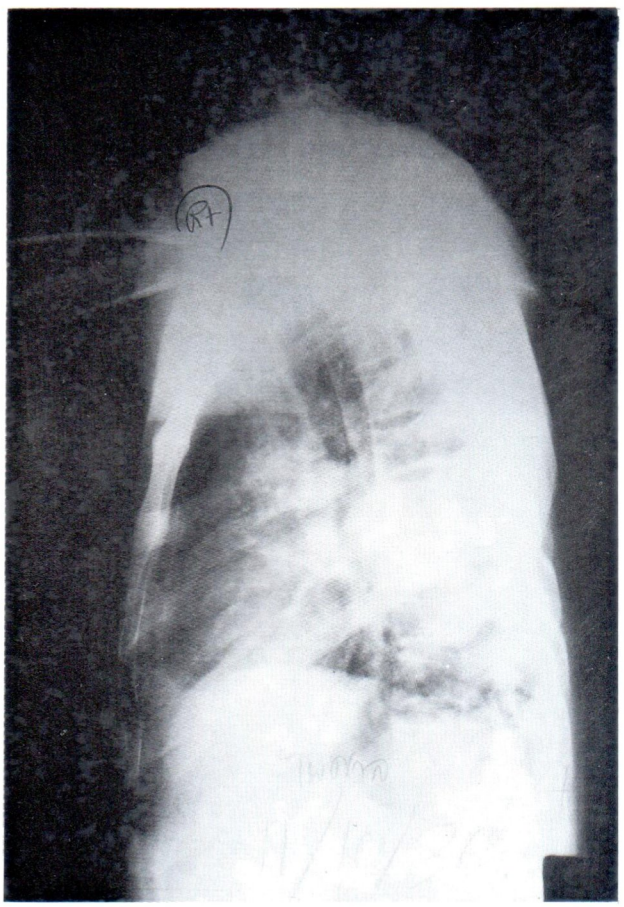

Fig.1B. Lateral chest film of the patient No.9

Fig.1A,1B. PA and lateral chest film showed consolidation of superior segment of right lower lobe with mediastinal and hilar adenopathy.

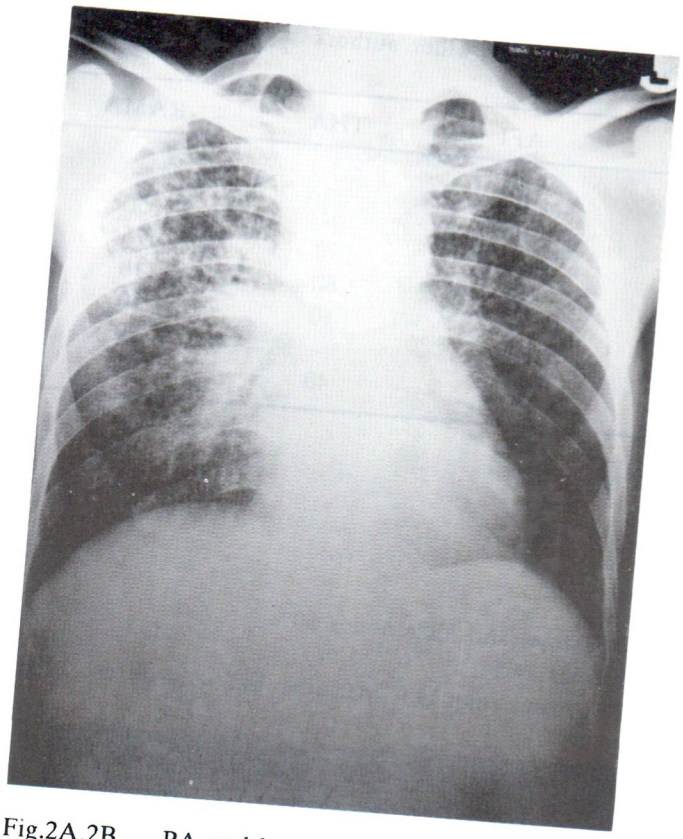

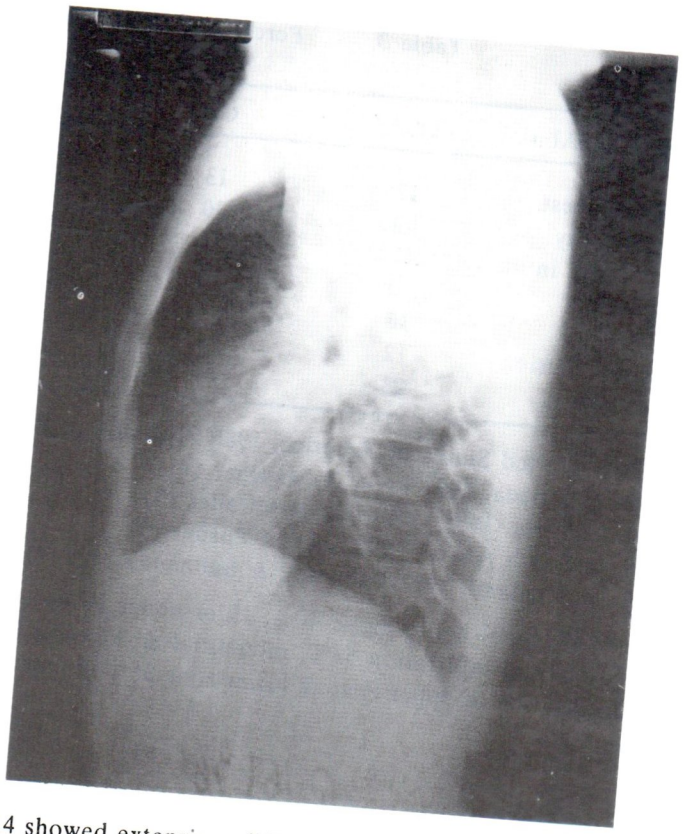

Fig.2A,2B. PA and lateral chest films of the patient No.14 showed extensive diffuse reticulonodular lesion in both lungs, most intensely present at perihilar area. Mediastinal and hilar nodes were shown.

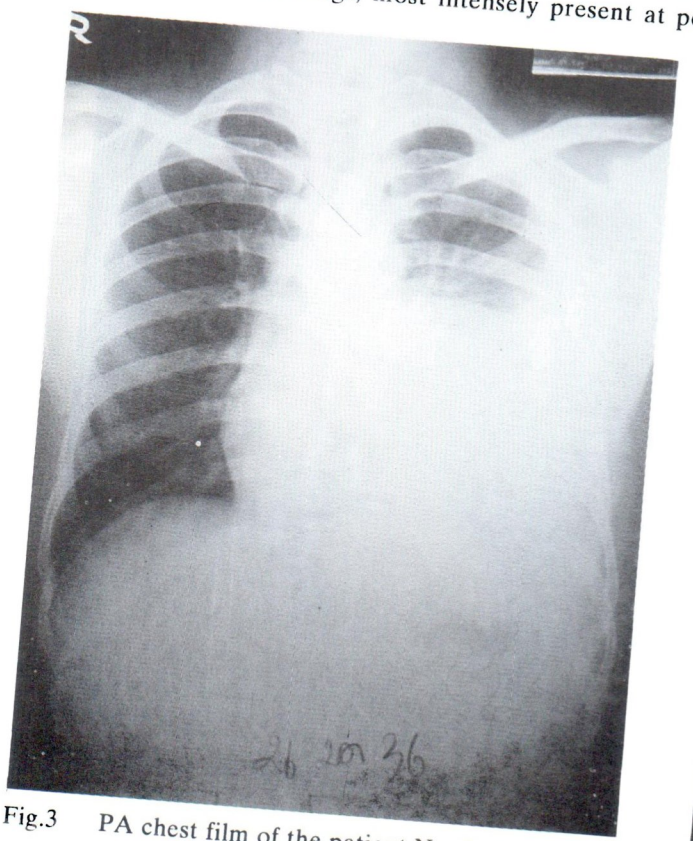

Fig.3 PA chest film of the patient No. 7 showed isolated massive pleural effusion, left side.

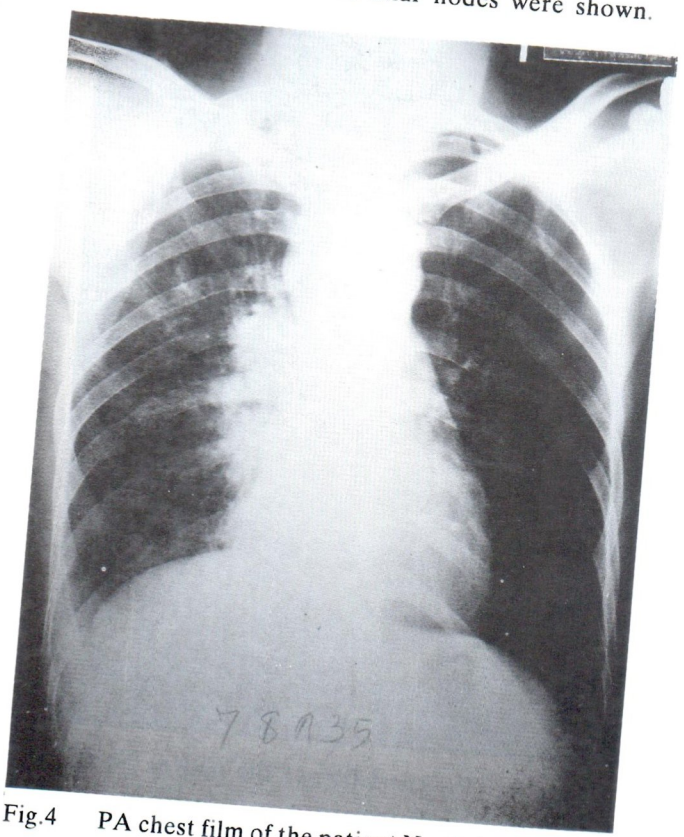

Fig.4 PA chest film of the patient No. 8 showed right perihila interstitial process with right hilar and mediastinal adenopathy.

DISCUSSION

Pulmonary tuberculosis had been divided into primary tuberculosis, postprimary tuberculosis or reactivated pulmonary tuberculosis and miliary tuberculosis(8). Primary tuberculosis develops via inhalation of infected airborne droplets. It occurs in childhood and becomes commoner in adults. It is characterized by consolidation in any areas of the lungs, however favoring lower lung fields. Hilar and mediastinal lymphadenopathy and plerual effusion is common. The reactivation tuberculosis is due to reactivation of focus acquired in childhood or initial infection in individual vaccinated with BCG or continuation of initial infection. It occurs predominantly in adulthood. The infiltration is in apical plus posterior segments of upper lobes and the rest is in the superior segment of lower lobe and in mixed location. The infiltration is divided into local exudative tuberculosis and local fibroproductive tuberculosis. Cavitation is common in extensive disease. The miliary pulmonary tubeculosis is the massive hematogenous dissemination of organsisms anytime after primary infection. The causes are severe immuno-depression during postprimary state of infection or impaired defenses during primary infection.

Presence of adenopathy and multiple areas of involvement in the lungs is similar to the primary tuberculosis. Predominated interstitial process is similar to the fibroproductive tuberculosis of reactivated type. If we compared intrathoracic tubercosis in HIV-negative patients, studied by Long (6), we can see that in our HIV-positive patients, there are more incidence of lymphadenopathy and pleural effusion and there are less incidence of parenchymal infiltration and cavitation.

REFERENCE

1. Wolinsky E. Tuberculosis, Diseases due to mycobacteria; pp 1741-1742 in Cecil Textbook of Medicine. Wyngaarden, Smith and Bennett; editors 19th ed. Philadelphia, W.B. Saunders Company.
2. Chuchotetavorn J, Buranajaru B, Stanondsakul S, Panyatangskul P. Incidence of HIV infection in adult Thai patients with tuberculosis. Thai J Tuberc Chest Dis 3:149-156,1989.
3. Pratyanond B, Nujprayoon C. AIDS and Tuberculosis. Thai J Tuberc Chest Dis 9:85-88,1988.
4. Punnotok J, Subhannacheart P, Chaisuksuwan R. Pulmonary tuberculosis among intravenous drug users with human immunodeficiency virus infection. Thai J Tuberc Chest Dis 1991;12: 15-24.
5. Pitchenik AE, Rubinson HA. The radiographic appearance of tuberculosis with acquired immune deficiency syndrome (AIDS) and pre-AIDS. Am Rev Respir Dis 1985:131;393-396.
6. Long R, Maycher B, Scalcini M, Manfreda J. The chest roentgenogram in pulmonary tuberculosis. Chest 1991;99: 123-127.
7. Gutierrez R, Miralles JC et al. Radiographic findings in pulmonary tuberculosis; the influence of human immunodeficiency virus infection. European Journal of Radiology 1991;12:234-237.
8. Saks AM, Posner R. Tuberculosis in HIV positive patients in South Africa: A compariative radiological study with HIV negative patients. Clinical Radiology 1992;46: 386-390.
9. Daehanert W.Radiology review Manual, 2nd ed.pp 332-333 Baltimore, Williams & Wilkins.

Leader Medical Equipment

Sole Distributor

supreme
PRODUCTS CO.,LTD.

บริษัท สุพรีม โพรดักส์ จำกัด

163/81-82 Phar Pinklao Rd.,Bangyeekan Bangpat,Bangkok Thailand 10700 Tel. 434-0040,435-0050, Service 435-0060

CT FINDINGS IN HYPERTENSIVE INTRACRANIAL PARENCHYMA HEMORRHAGE

Wiwatana THANOMKIAT[1], Patchrin PEKANAN[1],
Siriporn HIRUNPAT[1], Achara SANGSAI[1].

ABSTRACT

A retrospective study of the CT scans of the patients with hypertensive intracranial parenchymal bleeding, was performed in 141 patients. Bleeding at the putamen/ external capsule, thalamus, subcortical white matter, cerebellum, brain stem and internal capsule was seen in 42, 26, 12, 10, 9 and 1 percents of cases respectively. The incidence of rupture of the hematoma into the ventricles from the sites mentioned above was 44, 75, 41,43,30 and 0 percents of the total hematomas at each site respectively.

Focal brain hemorrhage occurs spontaneously in three common settings: hypertension, ruptured AVM's and amyloid angiopathy (1). Additional contributing causes are excessive anticoagulation, systemic bleeding diatheses, and trauma. Hypertensive bleeding is believed to result from rupture of microaneurysms in small, intracerebral arteries and necrotic vascular degeneration.

A retrospective study of the CT scan was performed in the patients who bled into the brain parenchyma due to high blood pressure, to determine the sites of bleeding and the pattern of spreading of the hematoma.

PATIENTS AND METHODS

We reviewed 141 cranial CT scans in the cases of hypertensive intracranial parenchymal hemorrhage. The films were collected from January 1989 to December 1993. The study was concerned about the location of the hematoma, the ventricular rupture and the pattern of spreading.

RESULTS

One hundred and forty one patients were consisted of 97 males and 64 females and the ratio of male to female was 1.5:1. Only one site of the hematoma was found in each patient. Most of the patients had essential hypertension and only four patients had known underlying causes; 2 cases had chronic renal failure and another two cases had renal arterial stenosis. The mean age of the patients who had essential hypertension was 62.6 years old. Fifty one percents of the patients were below 60 years old and 20.4% were below 50 years old. The locations of the hematomas were shown in Table 1. The most common location was putamen/external capsule and the second most common location was thalamus. The incidence of ruptured hematoma to the ventricular system was shown in Table. 2. The thalamic hematoma was associated with the highest incidence of ventricular rupture. All of the thalamic hematomas dissected along the paraventricular white matter superiorly and broke into the nearby ventricle, shown in Fig. 1. The patterns of spreading of the hematomas

[1]Department of Radiology, Ramathobidi Hospital, Rama 6 Street, Bangkok 10400, Thailand.

in the other locations were variable and will not mention here. The CT images of the hematomas at putamen/external capsule, subcortical area, cerebellar hemisphere, brain stem and internal capsule were illustrated in Fig. 2,3,4,5,6, respectively.

DISCUSSION

Hypertensive intracerebral hemorrhage (HICH) has a predilection for areas supplied by penetrating branches of the middle cerebral and basilar arteries. It therefore preferentially involves the external capsule and putamen, thalamus, and pons. (2). Large hematomas often extend beyond the putamen to include the globus pallidus and internal capsule (3). Clot dissection into the ventricular system occurs in about half the cases of hypertensive ICH and is associated with poor prognosis (4), particularly when intraventricular hematoma involves the fourth ventricle (5). Lobar white matter hemorrhage is seen in 15% to 20% of ICH cases (6).

The cerebellum is a relatively common site of hypertensive hemorrhage; the midbrain, medulla and spinal cord are rarely involved (2). Cerebellar hemorrhages typically originate near the dentate nucleus along perforating branches of the superiorcerebellar or posterior inferior cerebellar arteries (7,8).

The mean age of the patients who had essential hypertensive bleeding was similar to a report published in Thailand (9) and worldwide (10,11,12). The two most common locations were similar to other reports. The most common site was the putamen/external capsule. They were very characteristically lens-shaped hematoma, situated between lenticular nucleus and the insula, displacing the surrounding tissue without destroying them or destroyed only a small part (13). Some authors preferred using the term "putaminal hematoma" and there were many debates whether the putamen or the external capsule was the primary site of bleeding (14,15). We have found no cases of hematoma at the caudate or globus pallidus.

The subcortical white matter hematoma (lobar hematoma) was found in higher frequency than the autopsy report (16), and in similar frequency to the study by CT scan (6). The hematoma at brain stem and cerebellum occurred in about equal frequency.

Table 1. The location of the hematomas detected by CT scan of the brain and the number of the patients

Location	No. of Patients	(% of total patients)
Putamen/External capsule	59	(42)
Thalamus	36	(26)
Subcortical white matter (lobar	17	(12)
Cerebellum	14	(10)
Brain stem *	13	(9)
Internal capsule	2	(1)
Total	141	(100)

*13 Brain stem hematomas included 7 pontine and 6 midbrain hematomas

Table 2. The incidence of ventricular rupture at each site

Location	No. of ruptured hematomas	(% of all hematomas of that region)
Putamen/External capsule	26/59	(44)
Thalamus	27/36	(75)
Subcortical white matter (lobar)	7/17	(41)
Cerebellum	6/14	(43)
Brain stem	4/13	(30)
Internal capsule	0/2	(0)

The incidence of rupture of the hematoma into the ventricles was highest at thalamus and was about equally occurred at putamen/external capsule, cerebellum and subcortical white matter. Less incidence was shown in the brain stem hematoma and none at internal capsule.

Epidemiologic data strongly suggest that control of hypertension reduces the risk of hypertensive intraparenchymal hemorrhage (1).

REFERENCES

1. Pulsinelli WA, Levy DE: Cerebrovascular diseases. In Wyngaarden JB, Smith LH, Bennett JC, editor: Cecil Textbook of medicine, 19th ed, pp 2167-2168, Philadelphia, W.B. Saunders, 1992.
2. Okasaki H: Cerebrovascular disease. In Fundamentals of Neuropathology, pp 27-93, New York: Szaku-Shoin, 1989.
3. Bae HG, Lee KS, Yun IG et al: Rapid expansion of hypertensive intracerebral hemorrhage, Neurosurg 31:35-40, 1992.
4. Franke CL, van Swieten JC, Algra A, van Gijn J: Prognostic factors in patients with intracerebral hematoma, J Neurol Neurosurg Psychiat 55:653-657, 1992.
5. Gras P, Giroud M, Dumas R: Intracerebral hemorrhage, Neurol 42:1852 (letter), 1992.
6. Loes DJ, Smoker WRK, Biller J, Cornell SH: Nontraumatic lobar intracerebral hemorrhage: CT/angiographic correlation, AJNR 8:1027-1030,1987.
7. Gokaslan ZL, Narayan RK: Intracranial hemorrhage in the hypertensive patient, Neuroimaging Clin N Amer 2:171-186, 1992.
8. Osborn AG: Intracranial hemorrhage. In Osborn AG, editor: Diagnostic Neuroradiology, pp 197, St. Louis, Mosby-Year Book,1994.
9. Issaragrisil R, Bhoopat W, Khanjanasthiti P: Computed tomography in intracranial hemorrhage, J Med Ass Thailand 69:641-648, 1986.
10. Laissy JP, Normand G, Monroe M, et al: Spontaneous intracerebral hematoma from vascular causes. Neuroradiol 33:291-295, 1991.
11. Liu HC, Chu By, Chiang BN and Wang SP: Stroke, a clinico-pathological study. Chinese Med J (Taipei) 20:170-177, 1973.

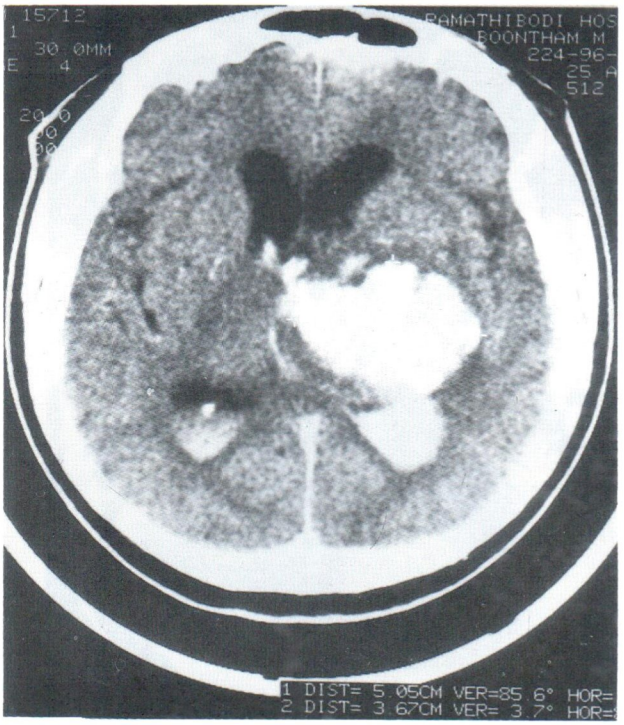

Fig. 1A. CT shows large hematoma in left thalamus and blood in the occipital horns and third ventricle

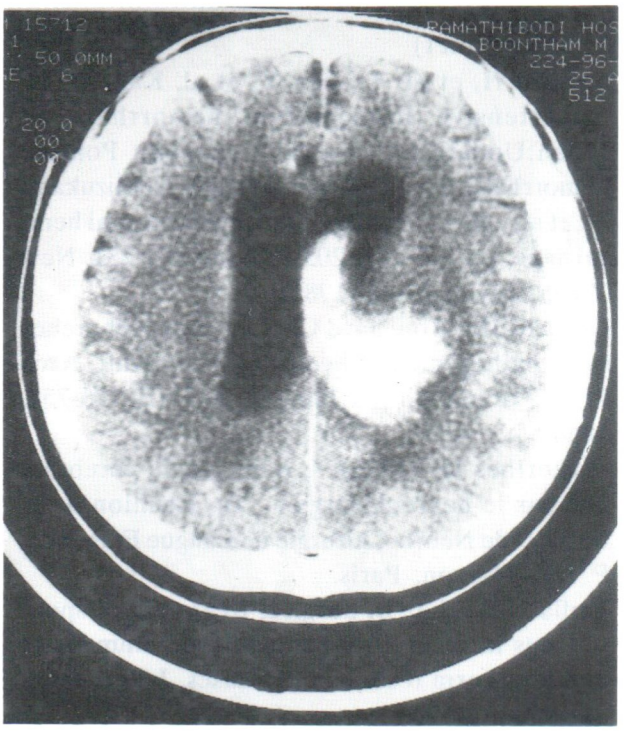

Fig. 1B. Thalamic hematoma dissected superiorly along the paraventicular white matter and ruptured into the lateral ventricle

Fig. 2 CT shows hematoma in the location of left putamen-external capsule

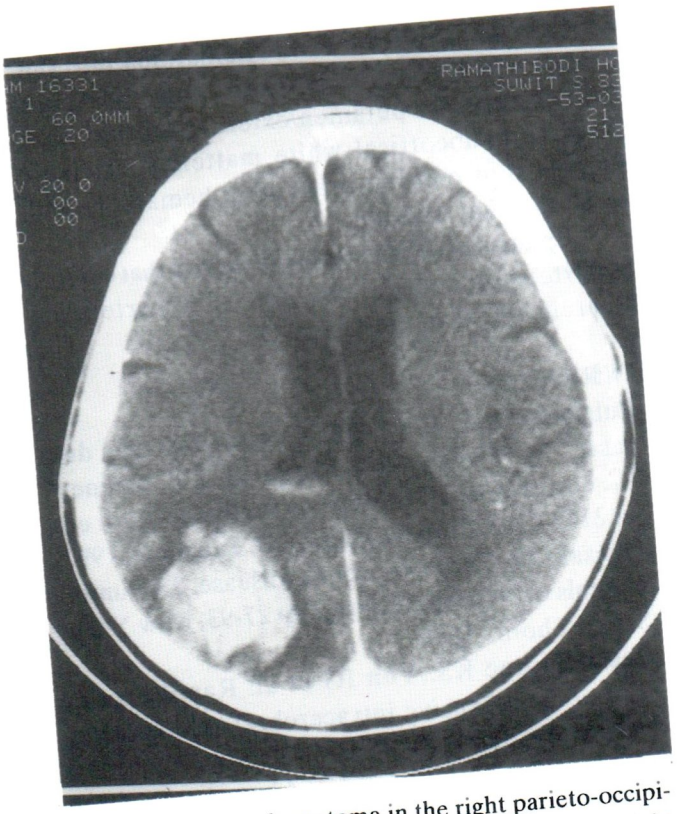

Fig. 3 CT shows hematoma in the right parieto-occipital subcortical area and thin layer of blood in right lateral ventricle

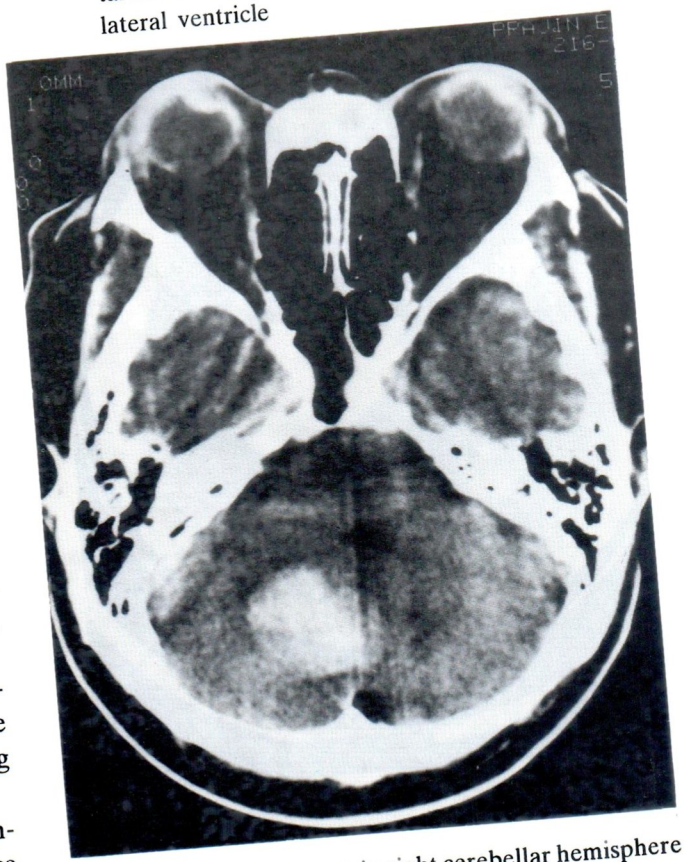

Fig. 4 CT shows hematoma in right cerebellar hemisphere

References: (con't)

12. Kanaya H, et al, Tanaka Y, et al, Kagawa M: Hypertensive intracerebral hemorrhage in Japan:Update on surgical treatment: Pontine hemorrhage: Thalamic hemorrhage. In Mizukami M, et al, editor: Hypertensive intracerebral hemorrhage, pp 147-163, 205-214 and 225-231, New York, Raven Press, 1983.
13. Charcot JM, Bouchard C: Nouvelles recherches sur la pathogenic de 1 hemorragie cerebrale. Arch Phys Norm Pathol 1:110-127, 643-675,725-734. 1868.
14. Lazorthes G. (1956): L hemorragie cerebrale vuc par le neurochirurgien. In: Reunion de la Societe' de Neuro-Chirurgie de Langue Francaise, P 122, Masson, Paris.
15. Paillas JE, Aliez B. Surgical treatment of spontaneous intracerebral hemorrhage. Immediate and long-term results in 250 cases. J Neurosurg 39:145-151,1974.
16. Broderick J, Brott T, Tomsik T et al. Lobar hemorrhage in the elderly: the undiminishing importance of hypertension. Stroke 14:49-51,1993.

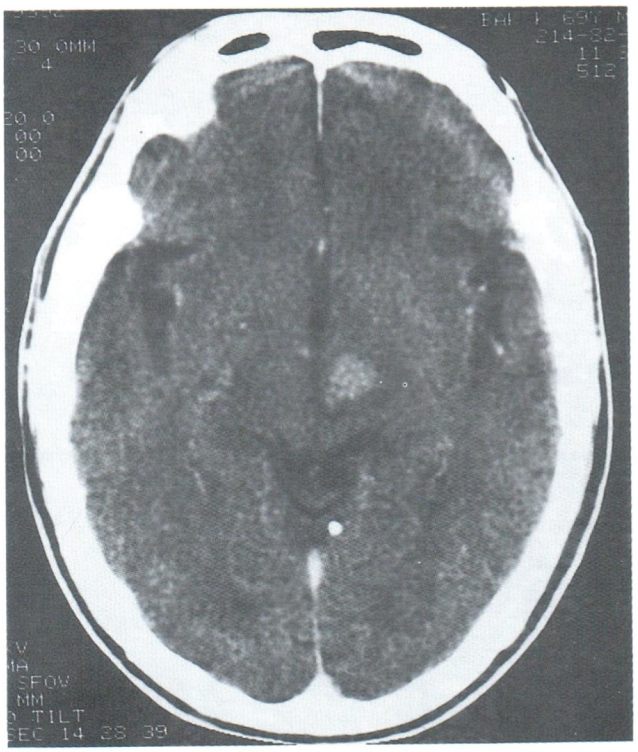

Fig.5A CT shows hematoma in the left mid brain

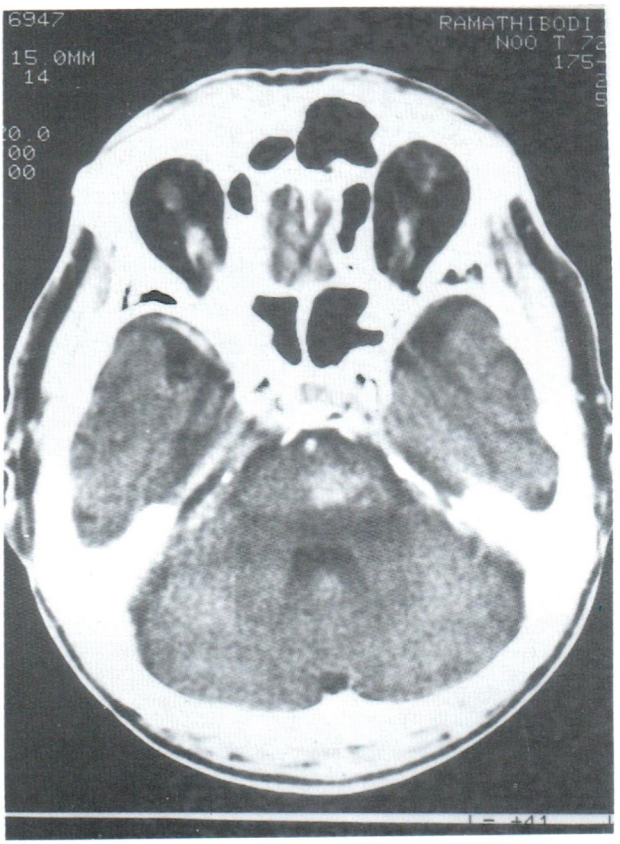

Fig.5B. CT shows left pontine hematoma

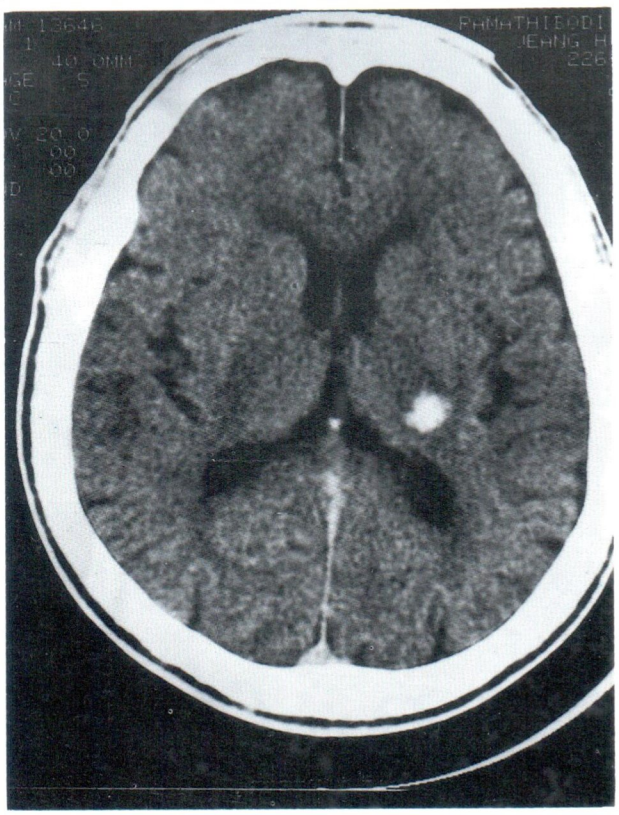

Fig. 6 CT shows small hematoma at left internal capsule

ACOUSTIC IMAGING
A Dornier Company

Presents...

HIGH PERFORMANCE, COST EFFECTIVE ULTRASOUND FOR:

- ABDOMINAL
- OBSTETRICS
- GYNECOLOGY
- VASCULAR
- PROSTATE
- MUSCULOSKELETAL
- SMALL PARTS
- MAMMOGRAPHY
- PEDIATRICS

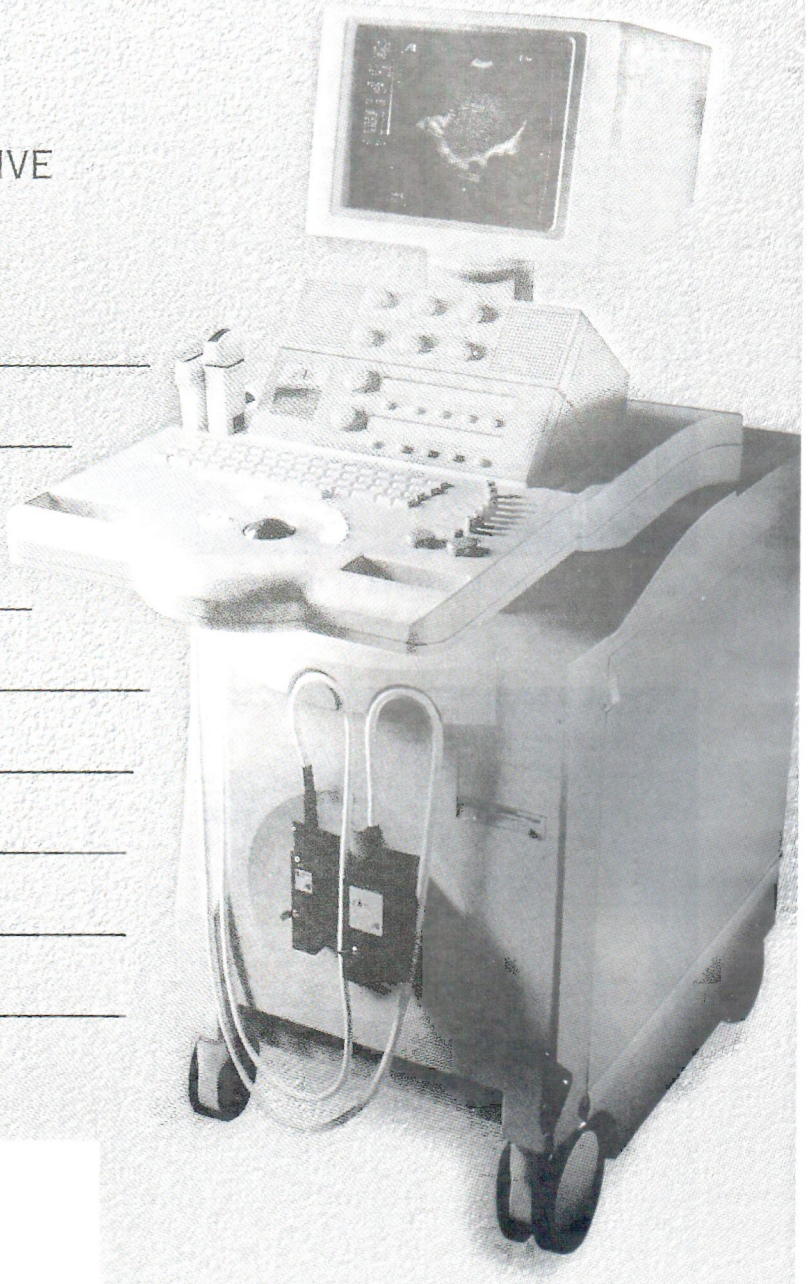

MEDICAL MEDIA PRODUCT CO., LTD.

บริษัท เมดิคอล มีเดีย โปรดักส์ จำกัด

633/14 ถนนสาธุประดิษฐ์ เขตยานนาวา กรุงเทพฯ 10120

โทร. (662) 2943364-8 โทรสาร : (662) 2943373

Performa™

High resolution ultrasound imaging scanner

EVALUATION FOR CT CRITERIA OF GRANULOMATOUS INFECTION AND TUMOUR OF SPINE

Napaporn CHOTIKA, Pimjai SIRIWONGPAIRAJ, Suphaneewan JAOVISIDHA, Suvipaporn SIRIPORNPITAK, Manee AIMACHARIYACHAI.

ABSTRACT

To develop criteria to distinguish between granulomatous infection and neoplastic process in the spine by mean of the computed tomography scan (CT scan), the authors retrospectively analyzed 31 cases of granulomatous infection and 13 cases of neoplastic disease. The result was that the reliable criteria for granulomatous infection were diffuse bony destruction, contiguous levels of spinal involvement, absence of posterior element involvement, presence of "complete" pattern of prevertebral soft tissue, and presence of disc involvemant. Neoplastic diseases were characterized by focal bony destruction, seperated levels of spinal involvement, presence of posterior element involvement, "partial" pattern of prevertebral soft tissue, and absence of disc involvement. Blinded testing of these criteria is potential for improving diagnostic accuracy in clinical practice.

INTRODUCTION

Computed tomographic examination of the spine is an available method in Thailand for diagnosis and characterization of vertebral lesions. The importance of CT is underscored by the fact that clinical assessment and conventional radiographic analysis are occasionally inconclusive in distinguishing between granulomatous infection and neoplastic process of the spine. This retrospective study was designed to identify reliable CT criteria for distinction between these two major categories of disease involving the spine.

MATERIALS AND METHOD

Transaxial CT image from a total of 44 cases of granulomatous infection and neoplastic disease affecting the spine were retrospectively evaluated. The pathologic identity of each lesion was determined with surgical specimen (36/44) and assumed on the basis of known widespread metastasis in the remainders (8/44).

There are 31 cases of granulomatous infections and 13 cases of neoplastic diseases examined. The types of tumor included adenocarcinoma from unknown primary site, breast carcinoma, lung carcinoma, hepato-cellular carcinoma, multiple myeloma, and hemangioma. The authors defined the CT findings for which each site of involvement would be evaluated in an attempt to identify distinguishing features between the two pathologic categories.

Each CT study was assessed for [1]

a. Presence or absence of prevertebral (anterior to lamina) soft tissue involvement, and when present, whether this was partial or complete (lamina to lamina) (Fig. 1,3).
b. Presence or absence of bony destruction and whether this was focal, multifocal or diffuse (Fig 2,4,5).
c. Presence or absence of posterior element involvement (Fig.1,3)

Department of Radiology, Faculty of Medicine at Ramathibodi Hospital, Mahidol University, Rama 6 street, Bangkok 10400, THAILAND.

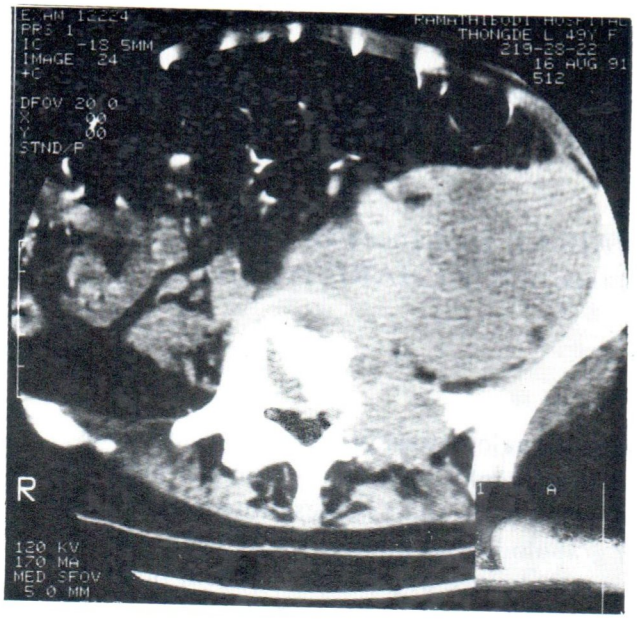

Fig 1. Breast carcinoma metastasized to L_5. Characteristic features are posterior element involvement and partial prevertebral soft tissue involvement.

Fig 2. The same case as fig 1. The image viewed in bone window also showed focal bony destruction

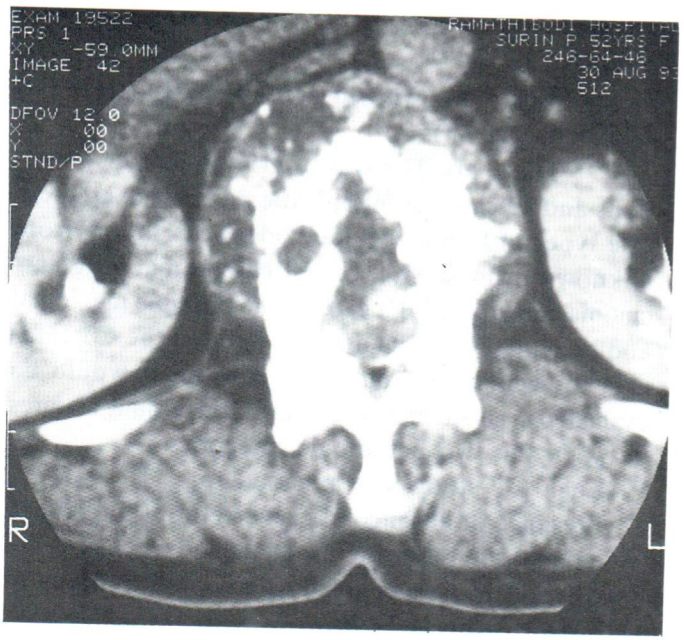

Fig 3. Pathologic tissue proved to be caseous granulomatous infection at L_1. Complete pre-vertebral soft tissue involvement and extension into the spinal canal are noted.

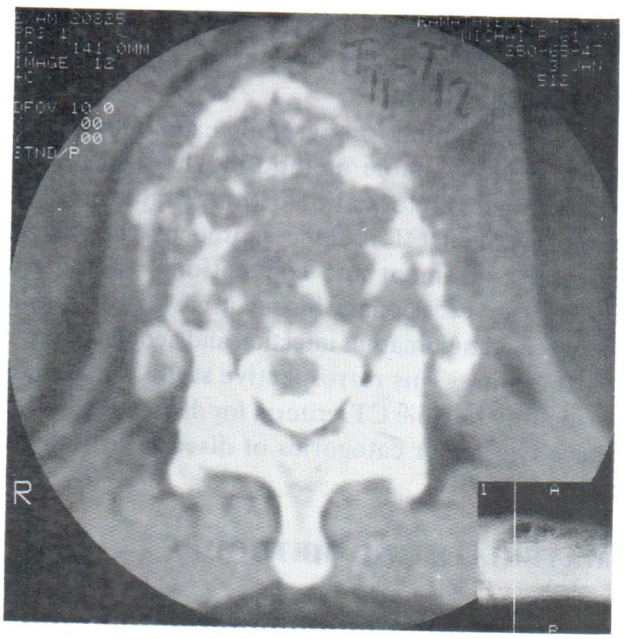

Fig 4. Pathologic tissue proved to be granulomatous infection at T_{11}. The image revealed diffuse bony destruction

d. Presence or absence of multilevel disease and whether this was contiguous (across an intervertebral disc space) or seperated.
e. Presence or absence of disc involvement.

A statistical analysis of the results were performed to determine which CT findings were most valuable in distinguising between granulomatous infection and tumoral process.

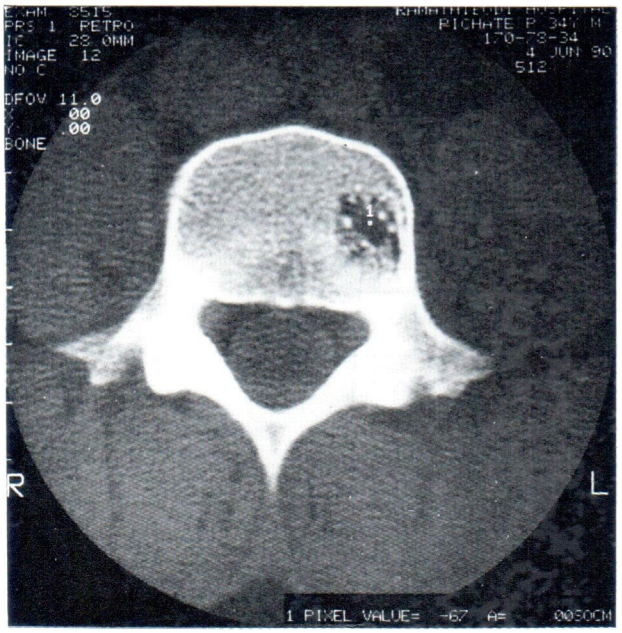

Fig 5. Pathologic tissue proved to be haemangioma of L_4. The image showed focal bony destruction

DISCUSSION

Granulomatous infection are grouped with similarities in clinical presentation and histologic feature of granulomatous identification on frozen section. They may caused by fungi, certain bacteria and spirochetes. The most common granulomatous spinal infection in the world by far is tuberculosis. As in our study, all granulomatous infection (31 cases) are tuberculosis. These infections spread hematogenously and subligamentously [2,3,4,5]. The latter route of spreading causes more prevertebral soft tissue (sensitivity 1.0, specificity 0.53, p = 0.00004) and contiguous levels of spinal involvement (sensitivity 1.0, specificity 0.25, p = 0.042) than those in neoplastic processes. Criteria of diffuse bony destruction in granulomatous diseases in this study (sensitivity 0.86, specificity 0.67, p = 0.004) differs from the previous study of Van Lom et.al [1]. They reported criteria of focal bony destruction in this disease (sensitivity 1.0, specificity 1.0). This was likely due to late presentation of many cases of granulomatous infection in Thailand. Absence of posterior element involvement is also a reliable criteria for granulomatous infection (sensitivity 0.61, specificity 0.84, p = 0.014) due to in this disease there are three major primary foci of spinal involvement : peridiscal, central body and anterior body locations. In one series of 914 cases, the disease was at peridiscal location 33% , central body 11.6% , and anterior body in 2.1%. In 52.8% of cases, the disease was widespread at presentation [5].

Neoplastic process of the spine arises from focal lesions or from distant malignancy. Local involvement of the spine may result from primary lesion arising in the spinal cord, its coverings, or contiguous spread of tumour from the paraspinous

Results

Table 1

		Granulomatous infection	Tumor	
Prevertebral soft tissue	Presence	31	6	37
	Absence	0	7	7
		31	13	44

Analysis of Single Table Odd ratio : Undefined

Chi-Squares		P-values
Yates corrected	16.03	0.0000624
Fisher exact 1-tailed P-value		0.0000448
2-tailed P-value		0.0000448
Sensitivity	1.0	
Specificity	0.53	

Table 2

		Granulomatous infection	Tumor	
Prevertebral soft tissue	complete	24	0	24
	partial	7	6	13
		31	6	37

Analysis of Single Table Odd ratio : Undefined

Chi-Squares		P-values
Yates corrected	10.04	0.0015301
Fisher exact 1-tailed P-value		0.0007381
2-tailed P-value		0.007331
Sensitivity	0.77	
Specificity	1.0	

Table 3

		Granulomatous infection	Tumor	
Pattern of bony destruction	diffuse	26	3	29
	focal	4	6	10
		30	9	39

Analysis of Single Table Odd ratio = 13.00

Chi-Squares		P-values
Yates corrected	7.72	0.0054599
Fisher exact 1-tailed P-value		0.0038571
2-tailed P-value		0.0038571
Sensitivity	0.86	
Specificity	0.67	

soft tissue and lymphatics. Regional and distant spread of metastatic disease to spine may occur with almost any of the solid tumour of the body, with osseous malignancy of appendicular skeleton, and with systemic lymphoreticular malignancy such as multiple myeloma and lymphoma. Metastases are the most common skeletal tumour , and the spine is the most common site of skeletal involvement. They are most common secondary to carcinoma of the breast, lung and prostate gland. [5,6]

Absence and partial prevertebral soft tissue involvement in neoplastic processes of the spine is

Table 4

		Granulomatous infection	Tumor	
Posterior element involvement	absence	19	2	21
	presence	12	11	23
		31	13	44

Analysis of Single Table Odd ratio : 8.71

Chi-Squares		P-values
Yates corrected	6.01	0.0142584
Sensitivity	0.61	
Specificity	0.84	

Table 5

		Granulomatous infection	Tumor	
Multiple levels of spinal involvement	contiguous	29	6	35
	seperated	0	2	2
		29	8	37

Analysis of Single Table Odd ratio = Undefined

Chi-Squares		P-values
Yates corrected	3.55	0.0593750
Fisher exact 1-tailed P-value		0.042042
2-tailed P-value		0.042042
Sensitivity	1.0	
Specificity	0.25	

a reliable criteria (sensitivity 0.53, specificity 1.0, p = 0.00004 and sensitivity 1.0, specificity 0.77,p = 0.0007 respectively) because most neoplasm spread by hematogenous and lymphatic routes, but less likely by subligamentous route. These also caused more presence of multiple seperated levels of spinal involvement (sensitivity 0.25, specificity 1.0, p = 0.042) than in granulomatous infections. Criteria of focal pattern of bony destruction (sensitivity 0.67, specificity 0.86, p = 0.004) is reliable due to marrow replacement in any degree by the tumour cells but granulomatous infection usually causes diffuse fragmentation of the vertebral bodies [8]. The intervertebral discs are spared in tumoural process (sensitivity 1.0, specificity 1.0) owing to their resistance to tumour invasion and is a reliable criteria for tumoural process, while presence of disc involvement (sensitivity 1.0, specificity 1.0) is observed in granulomatous infection.

Table 6

		Granulomatous infection	Tumor	
Disc involvement	presence	31	0	31
	absence	0	13	13
		31	13	44

Analysis of Single Table Odd ratio : Undefined

Chi-Squares		P-values
Yates corrected	39.33	0.0000
Sensitivity	1.0	
Specificity	1.0	

Table 7

		Tumor	Granulomatous infection	
Prevertebral soft tissue	absence	7	0	7
	soft tissue	6	31	37
		13	31	44

Analysis of Single Table Odd ratio = Undefined

Chi-Squares		P-values
Yates corrected	16.03	0.0000624
Fisher exact 1-tailed P-value		0.0000442
2-tailed P-value		0.000448
Sensitivity	0.53	
Specificity	1.0	

The limitation of this study is its purely retrospective nature , and all granulomatous infections in this study were tuberculosis so this study may mainly represents the spinal tuberculosis rather than other granulomatous infections.

In conclusion, under these criteria for CT interpretation of spinal pathology, it can be practical benefit in the patients with clinical undiagnostic between granulomatous infection (particularly tuberculosis) and neoplastic process [7].

ACKNOWLEDGEMENT :

We would like to thank Ms.Amarin Taksinsathian for the statistical analysis

Table 8

		Tumor	Granulomatous infection	
Prevertebral soft tissue	partial	6	7	13
	complete	0	24	24
		6	31	37

Analysis of Single Table Odd ratio : Undefined

Chi-Squares		P-values
Yates corrected	10.04	0.0014301
Fisher exact 1-tailed P-value		0.0007381
2-tailed P-value		0.0007381
Sensitivity	1.0	
Specificity	0.77	

Table 9

		Tumor	Granulomatous infection	
Bony destruction	focal	6	4	10
	diffuse	3	26	29
		9	30	39

Analysis of Single Table Odd ratio = Undefined

Chi-Squares		P-values
Yates corrected	7.72	0.0054599
Fisher exact 1-tailed P-value		0.0038571
2-tailed P-value		0.0038571
Sensitivity	0.67	
Specificity	0.86	

REFERENCE

1. Van Lom KJ, Kellerhouse LE, Pathria MN, et al. Infection versus Tumor in the Spine : Criteria for Distinction with CT. *Radiology* 1988 ; 166 : 851-855
2. Smith AS, Blaser SI. Infection and Inflammatory Process of the spine. *Radiol Clin North Am* July 1991 ; 29 (4) : 809-827
3. Latchaw RE. *MR and CT Imaging of The Head, Neck and Spine* , 2nd Ed. St.Louis ; Mosby 1991 : 1183-1221
4. La Berge JM, Brant-Zawadzki M. Evaluation of Pott's disease with computerized tomography. *Neuroradiology* 1984 ; 26 : 429-434

Table 10

		Tumor	Granulomatous infection	
Posterior element involvement	presence	11	12	23
	absence	2	19	21
		13	31	44

Analysis of Single Table Odd ratio = 8.71

Chi-Squares		P-values
Yates corrected	6.01	0.0142584
Sensitivity	0.84	
Specificity	0.61	

Table 11

		Tumor	Granulomatous infection	
Multiple levels of spinal involvement	seperated	2	0	2
	contiguous	6	29	35
		8	29	37

Analysis of Single Table Odd ratio = Undefined

Chi-Squares		P-values
Yates corrected	3.55	0.0593750
Fisher exact 1-tailed P-value		0.0420420
2-tailed P-value		0.0420420
Sensitivity	0.25	
Specificity	1.0	

5. Rothman RH, Simeone FA. *The Spine* , 3rdEd. Philadelphia ; W B Saunder 1992 : 1279-1303, 1352-1364
6. Masaryk TJ. Neoplastic disease of the Spine. *Radiol Clin North Am* July 1991 ; 29 (4) : 829-845
7. Redmond J, Spring DB, Munderloh SH, et al. Spinal Computed Tomography Scanning in the Evaluation of Metastatic Disease. *Cancer* 1984 ; 54 : 253-258
8. Chongchitnant P. Computed Tomography of Spinal Tuberculosis. *J Med Asso Thai* Oct 1992 ; 75(10) : 560-564

Table 12

		Tumor	Granulomatous infection	
Disc involvement	absence	13	0	13
	presence	0	31	31
		13	31	44

Analysis of Single Table Odd ratio = Undefined

Chi-Squares	P-values
Yates corrected 39.33	0.00000
Sensitivity 1.0	
Specificity 1.0	

Table 13

Retrospective analysis of CT examinations reveals the reliable criteria as followed :

	Sensitivity	Specificity	P-values
Reliable criteria for granulomatous infection of spines			
- presence of prevertebral soft tissue	1.0	0.53	0.00004
- complete pattern of prevertebral soft fissue	0.77	1.0	0.0007
- diffuse bony destruction	0.86	0.67	0.004
- absence of posterior element involvement	0.61	0.84	0.014
- contiguous levels of spinal involvement	1.0	0.25	0.042
- presence of disc involvement	1.0	1.0	–
Reliable criteria for neoplastic process of spines			
- absence of prevertebral soft tissue	0.53	1	0.00004
- partial pattern of prevertebral soft tissue	1.0	0.77	0.0007
- focal bony destruction	0.67	0.86	0.004
- presence of posterior element involvement	0.84	0.61	0.014
- seperated levels of spinal involvement	0.25	1.0	0.042
- absence of disc involvement	1.0	1.0	–

Our new laser imager reviews films before you do

The new 3M Model 969 HQ Laser Imager doesn't perform diagnoses. But it does review images before you see them. If the quality doesn't meet your preset requirements, it makes the necessary adjustments — automatically.

This revolutionary Automatic Image Quality Control System from 3M ensures that each film meets your expectations the first time, every time. It frees your staff from the time-consuming task of monitoring and adjusting the printing process. And it provides radiologists with the image quality and consistency they need to perform fast, accurate diagnoses.

The 3M Model 969 HQ Laser Imager is the first to offer Automatic Image Quality Control. But that shouldn't surprise anyone. After 20 years of industry leadership, the medical imaging world expects "firsts" from 3M.

For a more detailed review of the new 3M Model 969 HQ Laser Imager, call the 3M THAILAND LIMITED

3M THAILAND LIMITED

159 Sermmit Tower 12th Floor, Sukhumvit 21, Bangkok 10110
Tel: 2608577 (50 lines), 5790023 ext. 301
Fax: 2617535, 5614052

3M *Innovation*

INTRAVENTRICULAR MENINGEAL HEMANGIOPERICYTOMA CT DIAGNOSIS.

Patchrin PEKANAN[1], Panpen UTTAMAKUL[1,2],
Wiwattana THANOMKIAT[1,2], Supranee NIRAPATHPONGPORN[1].

ABSTRACT

A report case of hemangiopericytoma detected by CT scan in a 59-year old patient was performed. The tumor was partly in left posterior horn of the lateral ventricle and partly in the deep left parietal lobe. The tumor was lobulated and solid. The density was isodensity with central low density. The enhancement was dense at the isodensity area. The left choroidal vessel at the medial part of the mass, facing the posterior horn was dilated. There was a moderate degree of peritumoral white matter edema. Meningeal hemangiopericytoma should be kept in mind if the appearance of the CT scan was similar to this case and the pathological report was that of meningioma. More aggressive treatment and follow up should be offered to the patient.

Key words Meningeal, hemangiopericytoma, CT scan.

Meningeal hemangiopericytoma was first described by Stout and Murray in 1942(1). This tumor was actually classified in 1938 by Cushing and Eisenhardt as angioblastic meningioma(2). Despite the difference in opinion regarding the terminology, meningeal hemangiopericytoma has a propensity for both local recurrence and extraneural metastasis(3). Hemangiopericytomas arise from the pericytes of blood vessels. They adhere to the meninges with a smooth but unencapsulated surface and contain areas of hypocellularity, necrosis and cyst formation (4). Meningeal hemangiopericytomas account for 2.4% of all meningiomas and less than 1% of all CNS tumor (3). Reports of this tumor by imaging were not present often. We report a case of the tumor, originating from posterior horn of the lateral ventricle, displayed by CT scan.

CASE REPORT

A 59-year-old male patient was presented to the Ramathibodi Hospital with the complaint of right hemiparesis for 2 weeks. The patient had severe headache for 3 months. He had fever, alteration of consciousness, nausea and vomiting for 3 days. Physical examination showed right sided motor weakness, grade 0, right papilledema, presence of right Babinski's sign and right sided clonus.

Plain CT scan of the brain showed an iso plus low density solid mass, size 5 x 6 x 6 cm at deep part of the left parietal lobe, obliterating left posterior horn. There is surrounding white matter edema, involving left putamen, left thalamus, left internal capsule, left occipital lobe, left parietal and temporal lobe and splenium of corpus callosum.

[1]Department of Radiology, Ramathibodi Hospital, Rama 6 Street, Bangkok 10400, Thailand.
[2]Department of Radiology, Songklanakarin University Hospital, Haadyai, Songkla, Thailand.

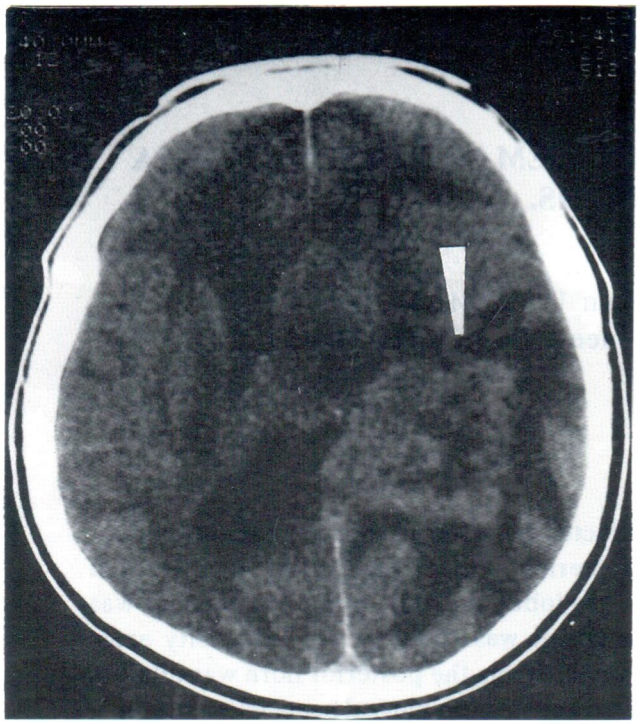

Fig. 1. Non-contrast CT scan of the brain showed a mixed iso and low density mass at deep left parietal lobe with surrounding white matter edema.

Subfalcine herniation was noted with midline shift of the lateral ventricle to the right for 1.7 cm. (Fig.1). The enhancement CT scan showed dense inhomogenous enhancement with tendency to enhance more at the peripheral aspect of the mass. The left choroidal vessel to the peripheral-medial aspect of the mass was enlarged(Fig. 2).

Operation was performed and the mass was nearly totally removed. The Histology was shown to be hemangiopericytoma with massive necrosis.

CT scan 11 months later showed recurrence of the tumor to nearly the same size as that before the operation. His complaint this time was severe headache, unable to walk, poor memory, bilateral papilledema, and right hemiparesis (motor power, grade III).

DISCUSSION

In 1989, Guthrie(5) reported 44 cases of meningeal hemangiopericytoma. It was found that the tumor is extremely vascular and appears to arise from the meninges, to which it tenaciously adheres. The patients were predominately male(55%) and the average age at the diagnosis (38-42 years) is younger than that of patients with meningiomas (early

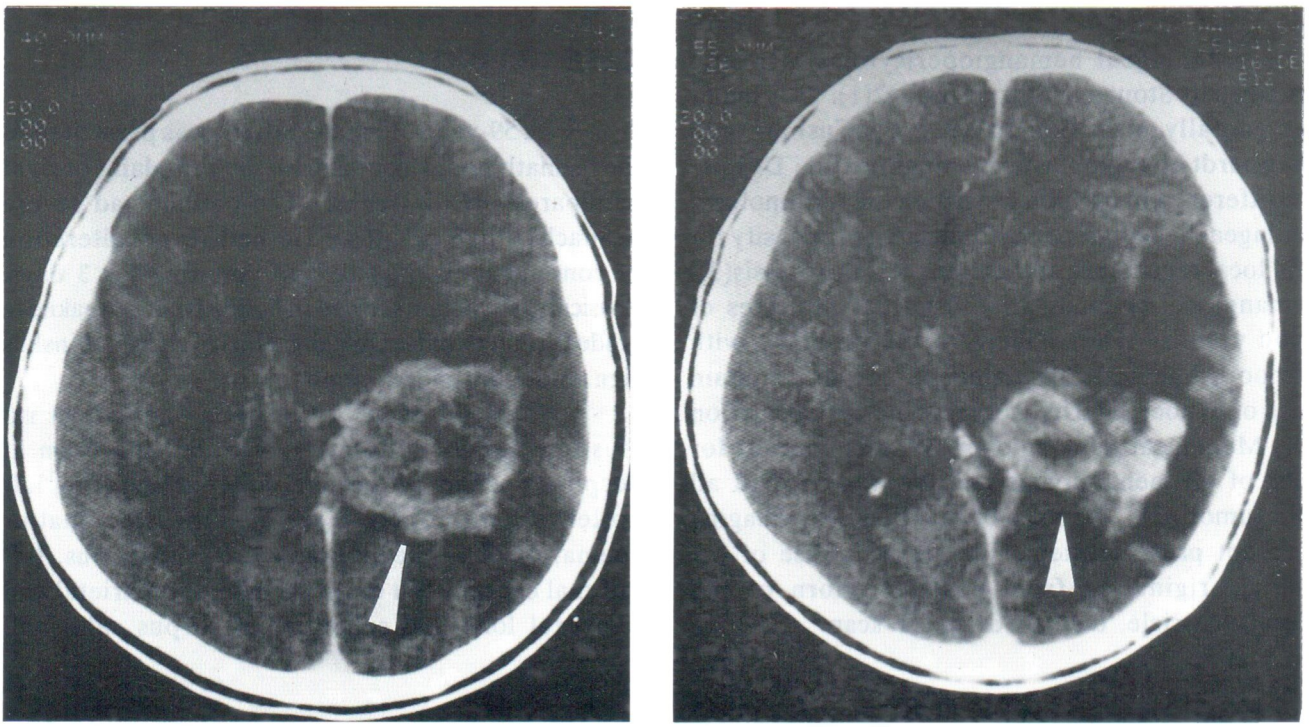

Fig. 2. I.V. enhanced CT scan of the lesion showed nodular and ring enhanced area in the mass. The choroidal vessel to the medial aspect of the mass was enlarged. The left posterior horn blended with the mass.

fifties). The average survival period is 84 months, shorter than that for ordinary meningioma (more than 100 months)(6,7). The tumor behaves as if it had a moderate to rapid growth rate, and patients are plagued by its marked tendency to recur and its high rate of eventual extraneural metastasis. Recurrence is likely in patients who survive for more than 5 years. Metastasis is likely in patients who survive for more than 15 years. Guthrie(5) found that the optimum time to benefit the patient is at the first operation, subsequent operations are less successful.

The histological features of the tumor and the patient's age and sex are not prognostically significant. Tentorial tumors or those in the posterior fossa were more lethal than supratentorial tumors. Incomplete tumor removal was followed by an average survival period of 65 months, as opposed to 93.5 months following complete removal. Metastasis occurred at an extremely long interval and was a poor prognostic sign, hastening patient's death. Radiation therapy was found to significantly prolong the recurrence-free interval and to extend survival.

Guthrie(5) recommended aggressive treatment for patients who have meningeal hemangiopericytomas. Resonable effort should be made to completely excise the tumor at the first operation Radiation therapy is strongly recommended, even if no gross tumor remnants are seen, particularly if the tumor is at a difficult operative site. Doses in excess of 5100 cGy should be used, treating with a localized field that includes the primary tumor (or operative bed) plus a minimum margin of 2 cm, similar to recommendations for radiation of intracranial meningiomas (8). Follow up of the patient should be vigilant, with frequent assessment for local recurrence. Chest x-ray at 6 to 12 month intervals should be obtained for as long as the patient survives, and any complaint of bone pain should be prompt to workup for metastasis.

Radiologically, the appearance of meningeal hemangiopericytomas varies. They are included among the angioblastic meningiomas in the discussion (9). Unlike fibroblastic and transitional meningiomas, angioblastic and syncytial meningiomas display heterogeneous attenuation with low density cystic areas, poorly defined tumor margins, marked peritumoral edema, absence of calcium aggregates, and heterogeneous enhancement with nonenhancing cystic areas (10). Angioblastic meningiomas, including meningeal hemangiopericytomas, are generally larger and more heterogeneous, with more cystic areas than the syncytial type. Our case showed similar CT appearance to that mentioned by Vasilouthis (10).

Radiotherapy was not given in this case, because the pathologist's first report of the tumor was meningioma and hemangiopericytoma was only a retrospective review after the 2nd operation for the recurrence.

REFERENCES

1. Stout AP, Murray MR: Hemangiopericytoma: Study of 25 new cases. Cancer 1942;2:1027-1035.
2. Cushing H, Eisenhardt L: Meningiomas: Their Classification. Regional Behavior Life History and Surgical End Results. Spring-field, LL, Charles C Thomas, 1938.
3. Enzinger FM, Smith BH: Hemangiopericytoma. An analysis of 106 cases. Hum Pathol 1976;7:61-82.
4. Burger PC, Vogel FS. The intracranial meninges: Surgical pathology of the nervous system and its coverings. 2nd ed. New York:Wiley Medical, 1982:92.
5. Guthrie BL, Ebersold MJ, Scheithauer BW and Shaw EG. Meningeal hemangiopericytoma: Histopatholigcal features, treatment, and long-term follow-up of 44 cases. Neurosurg 1989;25:514-521.
6. Chan RC, Thompson GB: Morbidity, mortality, and quality of life following surgery for intracranial meningiomas. J Neurosurg 1984;60:52-60.
7. Mirimannoff RO, Dosoretz DE, Linggood RM, Ojemann RG, Martuza RL: Meningioma: Analysis of recurrence and progression following neurosurgical resection. J Neurosurg 1985;62:18-24.
8. Carella RJ, Ransohoff J, Newall J: Role of radiation therapy in the management of meningioma. Neurosurgery 1982;10:332-339.
9. Daryl RP, Eschelman DJ, Gibbens DT, Rabinov JD, O'Connor JF. Neuroradiology case of the day. AJR 1991:156:1307-1313.
10. Vasilouthis J, Ambrose J. Computerized tomography scanning appearance of intracranial meningiomas. J Neurosurg 1979;50:320-327.

multi DIAGNOST 3

The multi-functional system with unrivalled accessibility

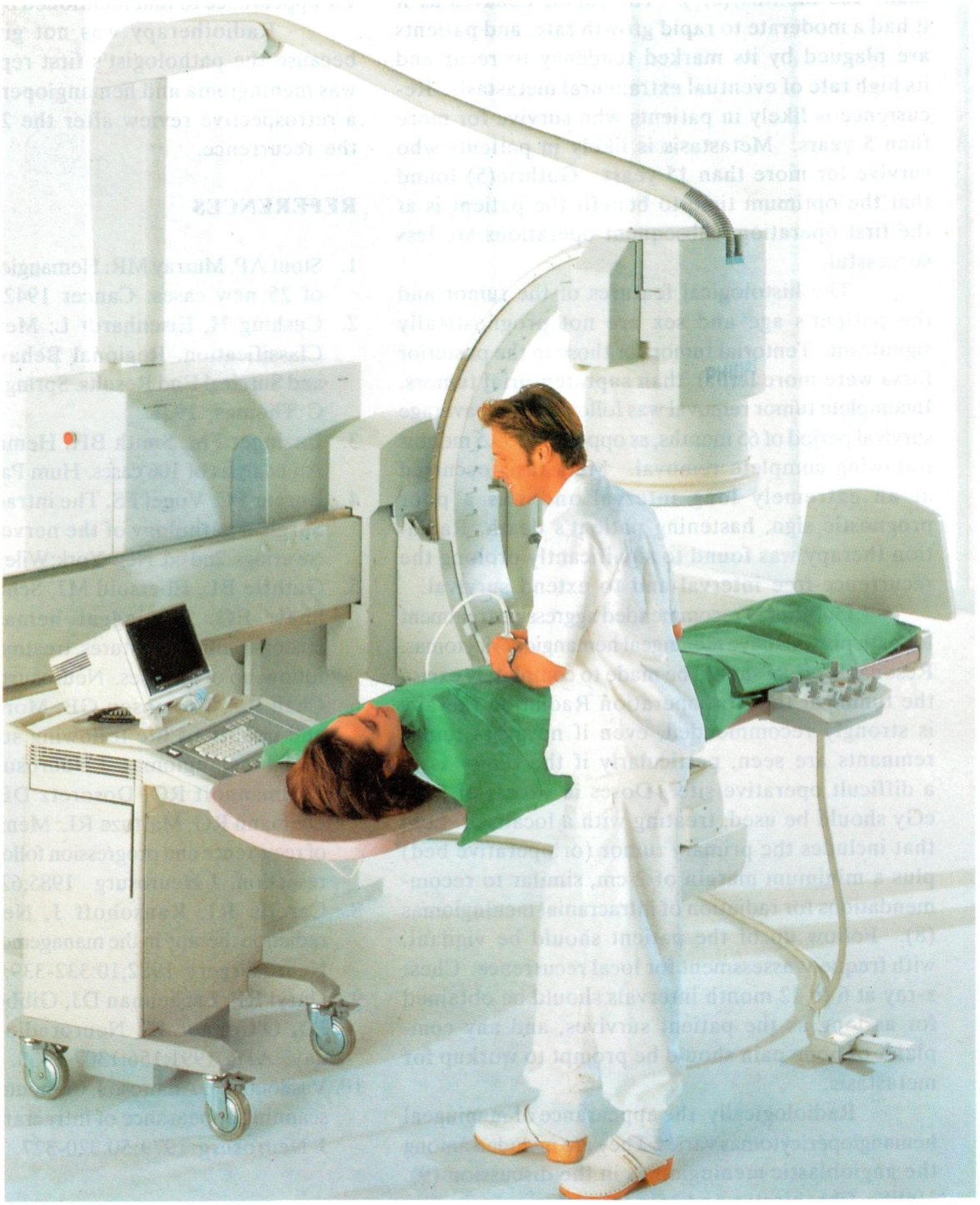

Philips Medical Systems

For more Information please contact
Philips Electronics (Thailand) Ltd.
tel. 745-4090

PHILIPS...MOVING AHEAD IN ELECTRONICS.

PHILIPS

"GAS IN THE AORTIC WALL" : A CT FINDING IN SALMONELLA ABDOMINAL AORTIC ANEURYSM.

Komgrit TANISARO, MD.,

ABSTRACT

Two cases of Salmonella Abdominal Aortic Aneurysm (AAA) in diabetic elderly are presented. CT scan in both cases reveal "gas in the aortic wall" which were seldom reported in Salmonella infection. This sign and other CT findings of Salmonella AAA are reviewed and discussed.

INTRODUCTION

Infected of Mycotic Abdominal Aortic Aneurysm (AAA) is a rare fatal condition. Salmonella species account for 1/3-1/2 of these cases. (1-4) The increasing incidence of Salmonella infection was thought to be associated with antibiotic therapy which prolongs the fecal excretion and increases the frequency of resistant stool isolate. (5) Despite advanced medical and surgical treatment, overall mortality is still more than fifty percents.

CT scan is proved to be the most useful radiologic modality for this condition and several CT signs have been reported. (1,6,7) This report describes two pateints with "gas in the aortic wall"

CASE 1

A 63 year-old diabetic male presented with two-day history of backpain, dysuria and low grade fever. Group D1 Salmonella enteritides was isolated from urine and blood when the patient manifested symptom and sign of sepsis.

An abdominal CT scan performed on day 14 of admission showed periaortic soft tissue density and gas collection with area of extraluminal enhancement at mid and lower abdominal aorta. (Fig.-1) Aortograms revealed irregular and narrowed aorta with saccular leakage of contrast material on delayed phase. (Fig.-2)

Abdominal pain and distension were observed on the later day and he was dead because of hypovolumic shock. Autopsy revealed severe artherosclerosis of aorta with acute aortitis. A leakage is noted with large retroperitoneal hematoma and 1,000 ml, of blood clot in the abdominal cavity.

CASE 2

An 81 year-old diabetic and cirrhotic female had a fever and diarrhea for three weeks prior to admission. Group B Salmonella enteritides was isolated from blood. Abdominal pain with radiated back pain occured during the course of treatment. CT scan showed lower AAA with thrombus and gas collection in the aortic wall. (Fig.-3)

Aneurysmectomy with axillofemoral and femorofemoral bypass surgery was done. However, the patient died on postoperative day 18. Pathological specimen revealed artherosclerosis with thrombus and periaortic inflamation.

DISCUSSION

Different machnisms of mycotic aneurysm have been postulated. Three types of vascular lesions may result from Salmonella infection. First, a diffused suppurative arteritis may cause arterial rupture resulting in a saccular or false aneurysm. Second, Salmonella may initiate focal arteritis that leads to

Department of Radiology,Prince of Songkla University Hospital Hatyai, Songkla, Thailand 90112

weakening of arterial wall and formation of a true infected aneurysm. Third, Salmonella may infect a pre-existing aneurysm. (5)

Salmonella are gram- negative flagellated bacteria of family Enterobacteriaceae. Three predominanting serotypes are S. typhimurium, S. enteritides, and S. typhi, The most commonly isolated from infected or mycotic aortic aneurysm are S. choleraesuis, S. typhimurium, and S. enteritides. (8) In addition to arterial infection, meningitis, pleuropulmonary disease, endocarditis, and osteomyelitis have been reported. (9-11)

Fever, backpain, and palpable pulsatile abdominal mass are triads which found in only forty percents of Salmonella AAA. Blood culture is positive in seventy - three percents. (1) This disease frequently affects the immunocompromised elderly. (6) Both reported cases are also the old diabetics.

Many radiologic investigations including ultrasonography, nuclear scanning, angiography, and CT scanning have been successfully used in diagnosis of infected or mycotic AAA. (1,6,12-15) CT scan is the most useful diagnostic test and several CT findings were reported. (1,6,13,16-20) Few studies have described CT apearance of Salmonella AAA which, in fact, resemble to findings of AAA from other infectious etiology, They are

1. par-aortic soft tissue density mass or collection.
2. contiguous vertebral destruction or osteomyelitis. (7,10)
3. change in size of aorta and saccular aneurysm in otherwise normal- looking aorta. (19,21)
4. gas in the aortic wall, (22)

Some of the above CT signs were found in our report and "gas in the aortic wall" was a shared finding. This CT sign is thought to be pathognomonic of infected aorta (21) but is not specific for Salmonella infection. (6) It was seldom found in literature and firstly reported by Kario K, et al. in 1991. (22) The second and third are our reported cases. Other organisms responsible for this same finding include Staphyllococus and E. coli. (18,23)

In conclusion, we believe that "gas in the aortic wall" is pathognomonic of infected or mycotic AAA, but is not specific for Salmonella infection. Clinical manifestation and positive blood culture remain essential in identification of the causative organism.

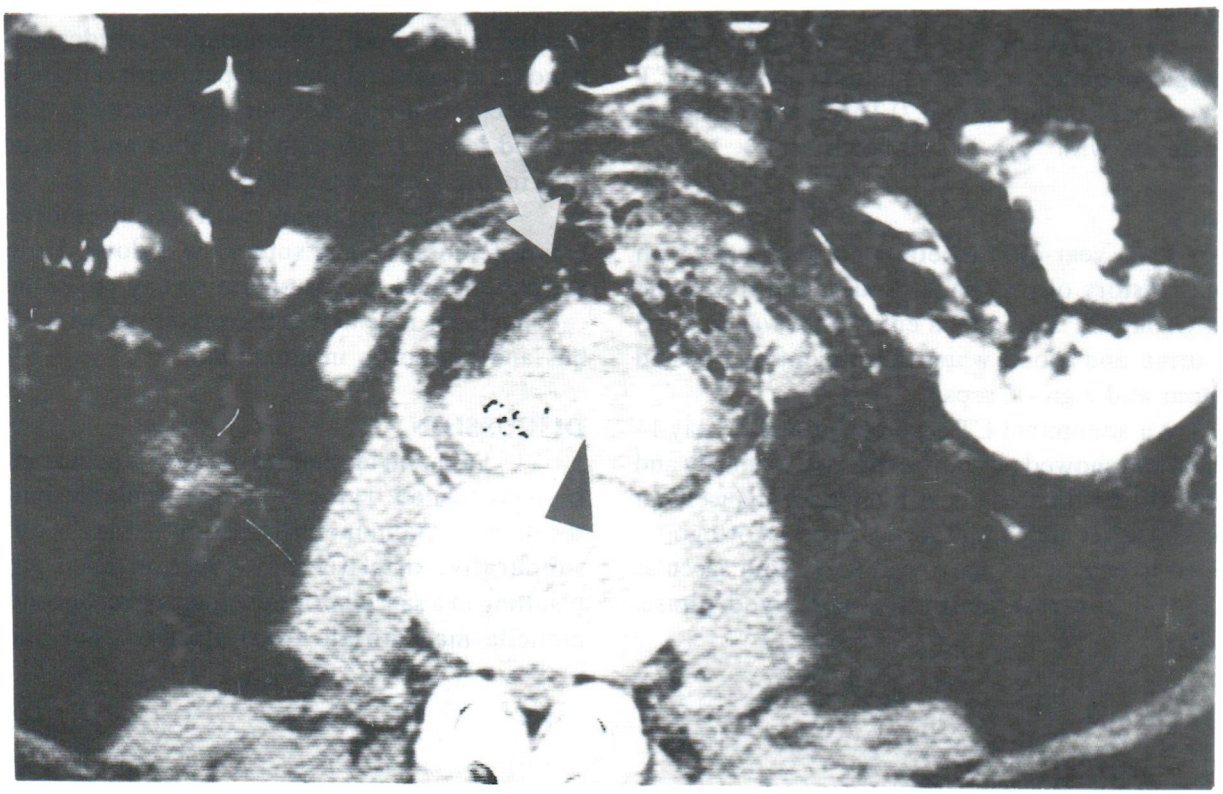

Figure-1 : CT image of lower abdominal aorta reveals periaortic soft tissue density and gas collection (arrow). There are also extraluminal leakage of contrast materials (black arrowhead)

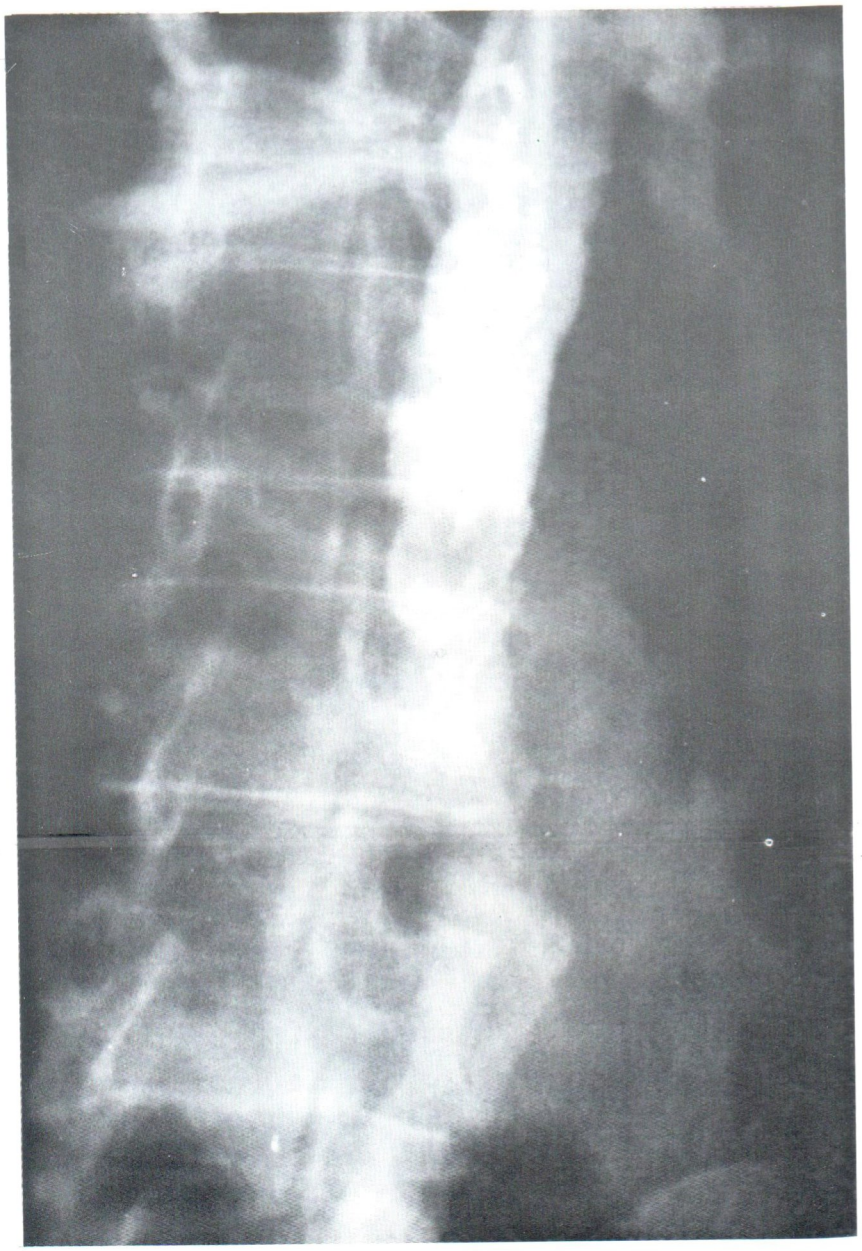

Fig. 2 a: Abdominal aortogram reveals irregular and narrowed aorta. Saccular leakage of contrast materials (black arrowhead) on delayed phase (b)

REFERENCES

1. Katz SG, Andros G, Kohl RD. Salmonella infection of the abdominal aorta. Surgery 1992;175: 102-106.
2. Mendelwitz DS, Ramstedt R, Yao JST, Bergan JJ. Abdominal aortic salmonellosis. Surgery 1979;85:514-519.
3. Anderson CB, Butcher HR, Ballinger WF. Mycotic aneurysms. Arch Surg 1974;109:712-716.
4. Davies OG, Thronborn JD, Powell P. Cryptic mycotic abdominal aortic aneurysms. Am J Surg 1978;136: 96-101.
5. Wiison SE, Veith FJ, Hobson RW, Williams RA. Vascular surgery. Newyork: McGraw-Hill 1987; 519-520.
6. Flamand F, Haris KA, Derose G, Karam B, Jameison WG. Arteritis due to Salmonella with aneurysm formation: two cases. CJS 1992;35: 248-252.
7. Atlas SW, Vogelsang RL, Bressler EL, Gore RM, Bergan JJ. CT diagnosis of mycotic aneurysm of the thoracoabdominal aorta. J Comput Assist Tomogr 1984;8:1211-1212.
8. Kanwar JS, Malhotra V, Anderson BR, Pilz CG, Salmonellosis associated with abdominal aortic aneurysm. Arch Intern Med 1974;134:1095.
9. Sower ND, Whelan TJ. Supperative arteritis due to Salmonella. Surgery 1967;52:851 (abstract)
10. Reichele FA, Tyson RR, Soloof LA, Lautsch EV, Rosemond GP. Salmonellosis and aneyrysm of the distal abdominal aorta:case report with a review. Ann Surg 1970;171:219 (abstract)
11. Simon DR, Wishnow RM. An unusual presentation of Salmonella aortitis. South Med J 1991;84:657-659.
12. Gonda RL, Guitierrez OH, Azodo MVU. Mycotic aneurysms of the aorta: Radiologic features. Radiology 1988;168:343-346.
13. McHenry MC, Rehm SJ, Krajewski LP, Duchesneau PM, Levin HS, Steinmuller DR. Vertebral osteomyelitis and aortic lesions; case roport and review. RID 1991;13:1184-1194.
14. Reddy DJ, Shepard AD, Evans JR, Wright DJ, Smith RF, Ernst CB. Management of infected aortoiliac aneurysms. Arch Surg 1991;126:873-879.
15. Edwards PR, Moody P, Harris PL. Salmonella infection of aorta. J R Coll Edinb 1991; 36: 181-183.

References: (con't)
16. Reed DH. Case report: pseudo aneurysm of descending thoracic aorta associated with vertebral osteomyelitis. Clini Radiol 1990;41:427-429.
17. Vogelzang RL, Soheay R. Infected aortic aneurysm: CT apearance. J Comput Assist Tomogr 1989;13: 101-104.
18. Pripstein S, Cavoto FV, Gerristen RW. Spontaneous mycotic aneurysm of the abdominal aorta. J Comput Assist Tomogr 1979;3:681-683.
19. Blair RH, Resnik MD, Polga JP. CT appearance of mycotic abdominal aortic aneurysms. J Comput Assist Tomogr 989;13:101-104.
20. Vogelsang RL, Soheay R. Infected aortic aneurysms: CT appearance. J Comput Assist Tomogr 1988;12: 109-112.
21. Oz MC, Brenner BJ, Buda JA et al. A ten-year experience with bacterial aortitis. J Vasc Surg 1989;10: 439-449.
22. Kario K, Mizuno Y, Kanatsu K, Tankawa H, Ikeda M. Infected abdominal aortic aneurysm due to Salmonella: CT evaluation. Cli imag 1991;15:261-264.
23. Reed DH. Case report: Mycotic pseudoaneurysm of the descending thoracic aorta associated with vertebral osteomyelitits. Clin Radiol 1990;41: 427-429.

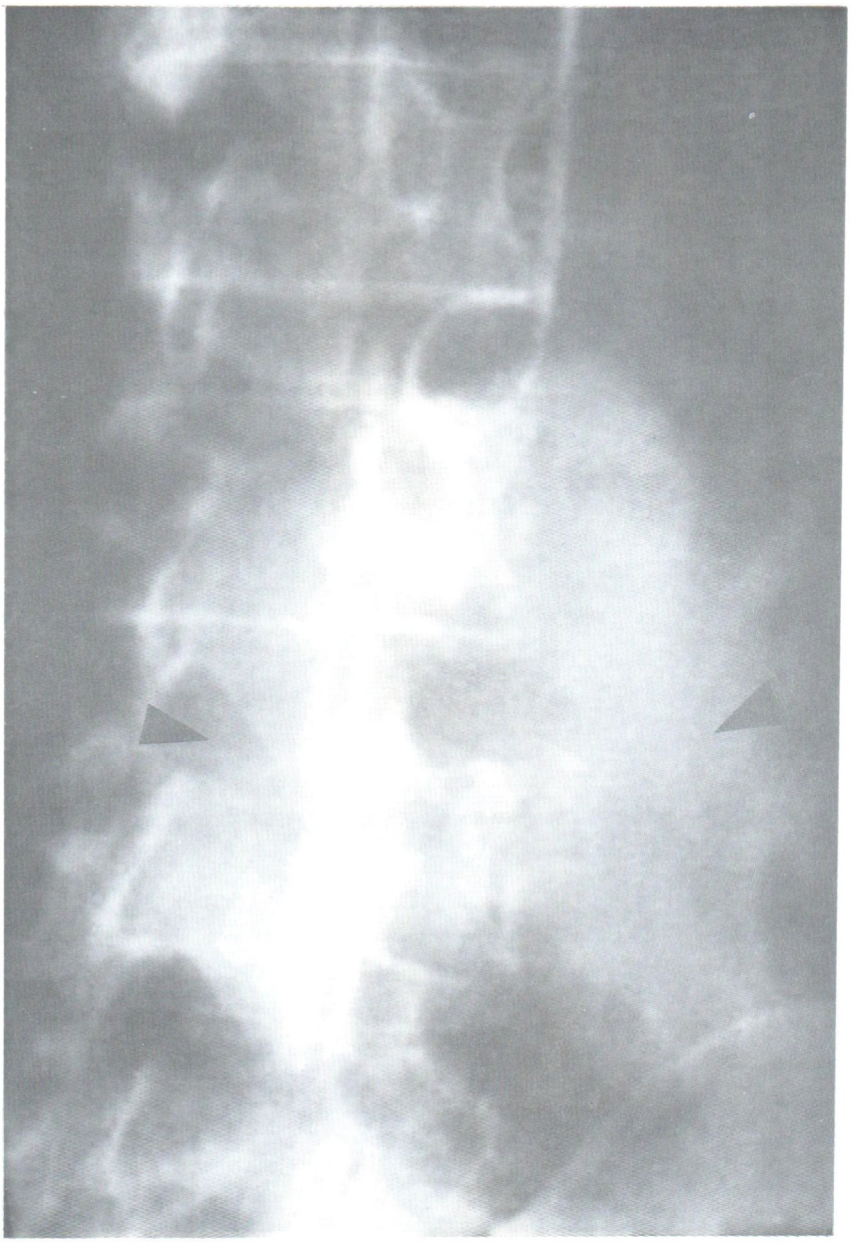

Fig. 2 b : Saccular leakage of contrast materials (black arrowhead) on delayed phase.

Fiqure-3 : CT image of lower abdominal aorta reveals aneurysm with intraluminal thrombus and gas collection in the aortic wall (arrow). Calcified intema is shown (arrowhead).

บริษัท คงศักดิ์เอ็กซเรย์การแพทย์อุตสาหกรรม จำกัด
KONGSAK X-RAY MEDICAL INDUSTRY COMPANY LIMITED
212/1 PHAHONYOTHIN SOI 55 BANGKHEN BANGKOK 10220
TEL. 5213214, 5511794 CABLE: KELEX FAX: 5523744

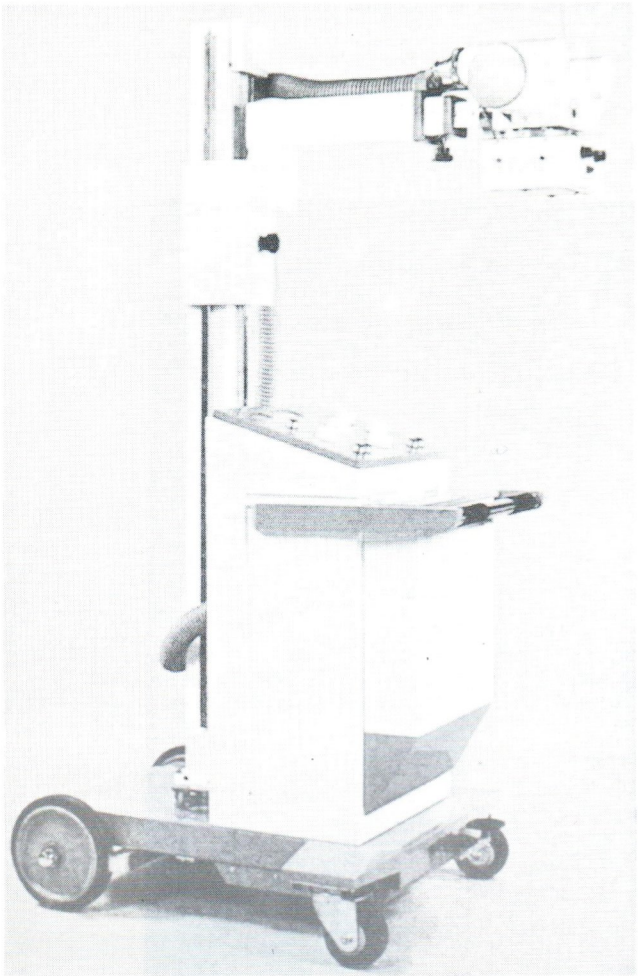

KELEX
50 mA 100 KV MOBILE TYPE DIAGNOSTIC X-RAY UNIT MODEL MD 50-99

- # เหมาะสำหรับคลินิคเอกชนและโรงพยาบาลทั่วไป
- # มีช่างผู้ชำนาญให้การบริการ ตลอดอายุการใช้งาน
- # พร้อมทั้งจำหน่ายอุปกรณ์เอ็กซเรย์

KELEX
MD 100-99 X-RAY SYSTEM
FULL WAVE 100 MA 100 KV

RETROPHARYNGEAL SPACE, PREVERTEBRAL SPACE INFECTION AND EPIDURAL ABSCESS:MULTI-IMAGING-MODALITIES-DEMONSTRATION IN A DIABETIC PATIENT.

Wiwattana TANOMKIAT[1,2], Patchrin PEKANAN[1], Teeratorn PULKES[3]. Suphaneewan JAOVISIAHA[1].

ABSTRACT

A case of pyogenic infection in retropharyngeal and prevertebral space with epidural abscess in a diabetic adult patient was reported. The infectious process began as an acute osteomyelitis of the great toe's phalanges. Plain film, CT scan and MRI studies showed the spread extension nicely in different aspects.

Key words Infection retropharyngeal space, prevertebral space, epidural space, osteomyelitis.

INTRODUCTION

The retropharyngeal space (RPS) and prevertebral space (PVS) are distinct midline spaces of the extracranial head and neck that extend from the skull base to the upper mediastinum and form an integral part of the suprahyoid neck. They are bounded by the middle and deep layers of the deep cervical fascia. Lymph nodes and fat are found in the RPS while muscles, vertebral artery, clivus and cervical vertebrae are found in the suprahyoid PVS (1)(Fig.8). Diseases processes in this space are relatively uncommon. CT and MRI are the primary imaging modalities for the evaluation of the pathology in this space and related structures (2-5). Inflammatory lesions represent a significant portion of PVS pathology and may present as abscess. Etiologies include tuberculous spondylitis and pyogenic vertebral osteomyelitis.

We present a diabetic case with pyogenic retropharyngeal and prevertebral space infection, extending to anterior epidural space, demonstrated by plain film, CT scan and MRI scan.

CASE REPORT

A 54-years old male patient was admitted to Ramathibodi Hospital due to headache for 5 weeks. He was known as a poorly controlled diabetes mellitus case for 10 years. He had low grade fever and headache several days after he stepped on a lighting cigarette which caused him an ulcer with pus at his left foot. His body temperature at the time of admission was 37.8 degree celsius, pulse rate was 120/min. The stiff neck and kernig's sign was positive. White blood cell count was 15,000 cell/mm^3 with predominant PMN. Lumbar puncture showed high pressure of 30 mm H_2O, WBC count 13,000, PMN 90%, low sugar and high protein. CSF culture showed no growth.

Plain film of his left foot showed osteolytic area at distal phalanx of the great toe, cortical destruction along the medial part of proximal phalanx of the great toe and focal osteolytic area at metaphysis of proximal phalanx, compatible with acute osteomyelitis (Fig. 1). Plain film of the cervical spine in lateral view showed prevertebral soft tissue lesion extending from C1 to C3 with forward displacement of the

[1]Department of Radiology, Ramathibodi Hospital, Rama 6 Street, Bangkok 10400, Thailand.
[1]Department of Radiology Songklanakarin Hospital, Hardyai, Songkla, Thailand.
[3]Department of Medicine, Ramathibodi Hospital.

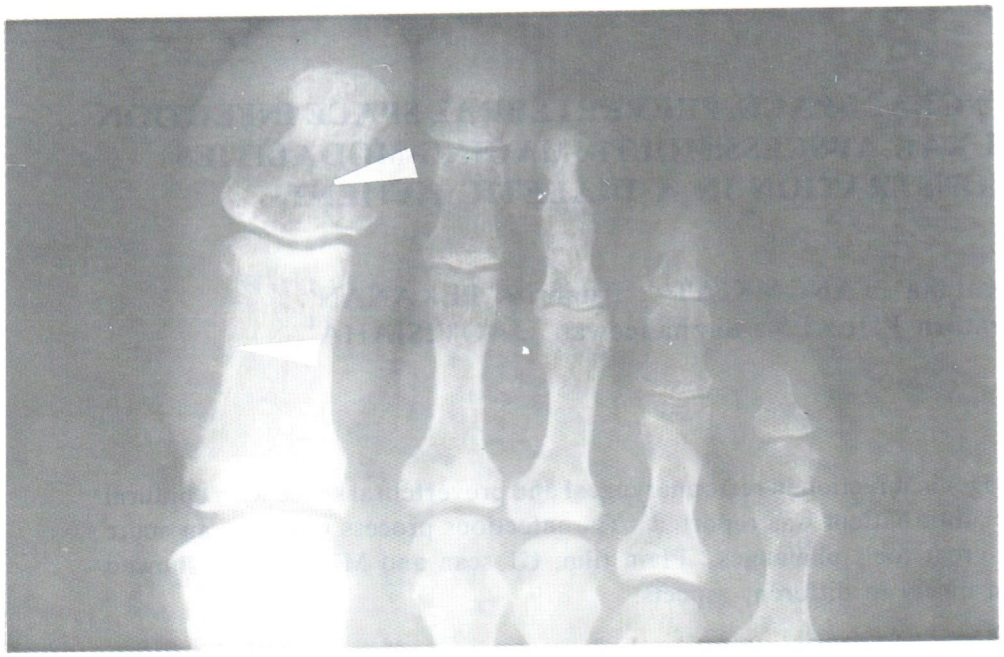

Fig. 1
Plain film, AP view of left foot showed osteomyelitis of distal phalanx and proximal phalanx of the great toe.

compressed nasopharyngeal air way (Fig.2). CT scan of C1-2 level showed osteolytic destruction of the anterior arch of C1(Fig.3) and left inferior clivus (The image is not shown here). T1WI sagittal view of the brain and upper cervical spine showed soft tissue lesion in the anterior central canal of C1-3 and at lower pontine and medullary level. Soft tissue lesion is also shown at retropharyngeal space and prevertebral area. There was a destruction of right part of C1-2 bodies and anterior arch of C1. The cord was compressed and displaced posteriorly(Fig.4). T1WI-sagittal view of the brain and upper cervical spine with Gd-DTPA enhancement showed strongly enhanced lesion at retropharynx, prevertebral area lesion, the region of destruction of C1-2 and partly enhanced lesion in the anterior central canal. Demonstration of the upper cervical cord compression was nicely shown in the post contrast enhancement scan(Fig.5). T2WI-sagittal view of the brain and upper cervical spine showed bright signal in the lesion at retropharyngeal, prevertebral area and in small pre-pontine lesion. Most of the anterior central canal lesion had dark signal similar to the adjacent bone(Fig.6). Demonstrated lesion in T2WI-axial view of C1-2 level was noted in figure 7. Findings were compatible with retropharyngeal and prevertebral space infection with an anterior epidural abscess.

Surgical drainage was performed and pus was found. The smear of the organisms revealed mixed organism (gram positive bacilli and cocci), the aerobic culture was negative.

Fig. 2 Plain film of the neck in lateral view showed a prevertebral and retropharyngeal mass lesion.

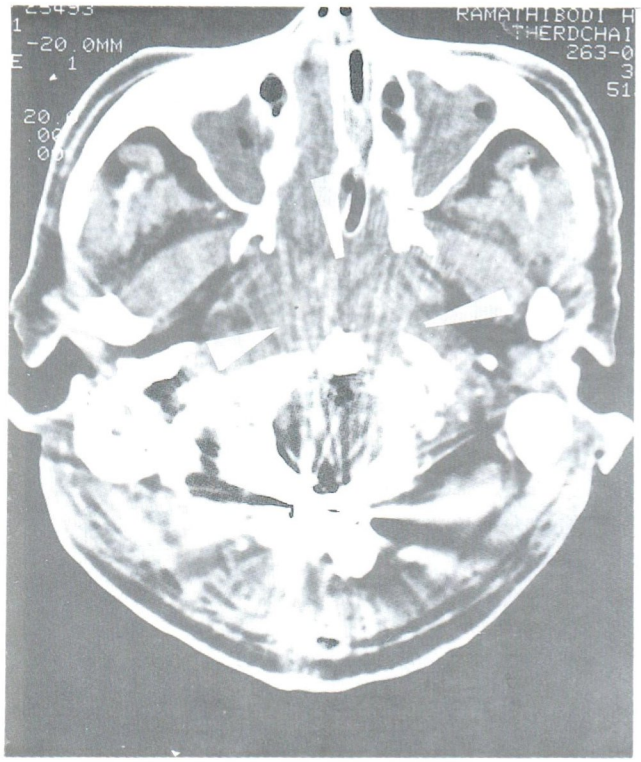

Fig. 3 CT scan at skull base showed osteolytic lesion at left anterior arch of the foramen magnum and prevertebral soft tissue mass. Bilateral maxillary sinusitis was also observed.

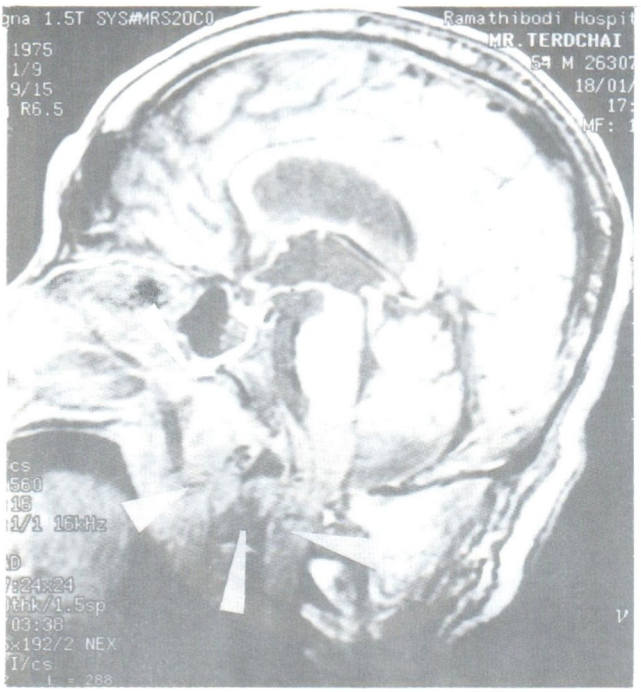

Fig. 4. T1WI sagittal view of the brain and C1-2 region showed isosignal soft tissue lesion at retropharyngeal area, anterior central canal at around the F.Magnum with destruction of odontoid process.

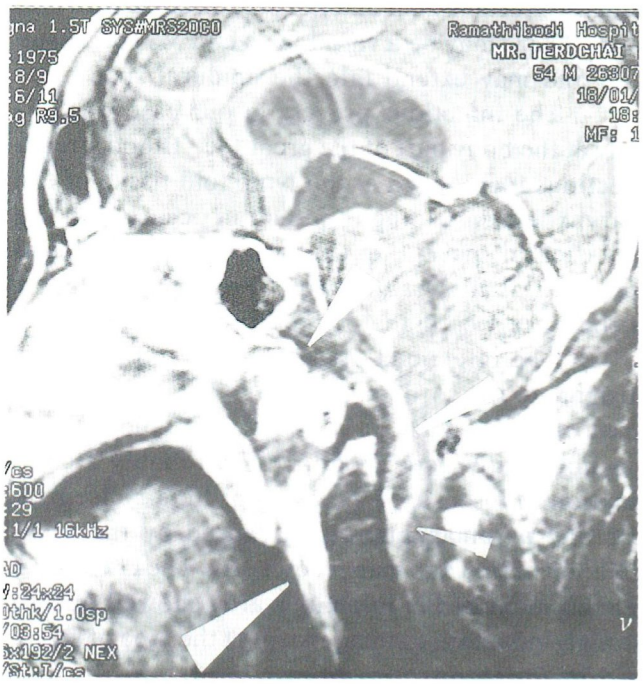

Fig. 5. T1WI sagittal view of the same area as in figure 4, post Gd-DTPA contrast enhancement showed diffuse strongly enhanced lesion except a small part of the anterior spinal canal lesion.

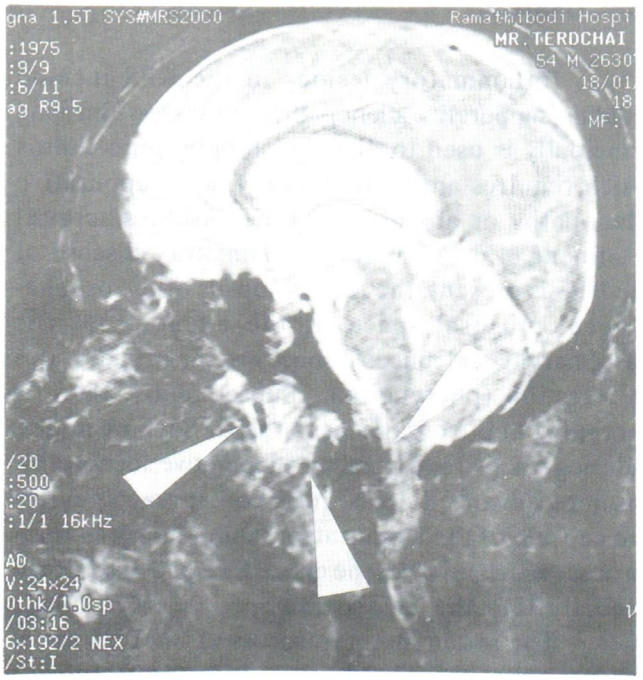

Fig. 6. T2WI sagittal view showed brightness of the infectious lesion except the area of signal drop in the lesion of the anterior central canal

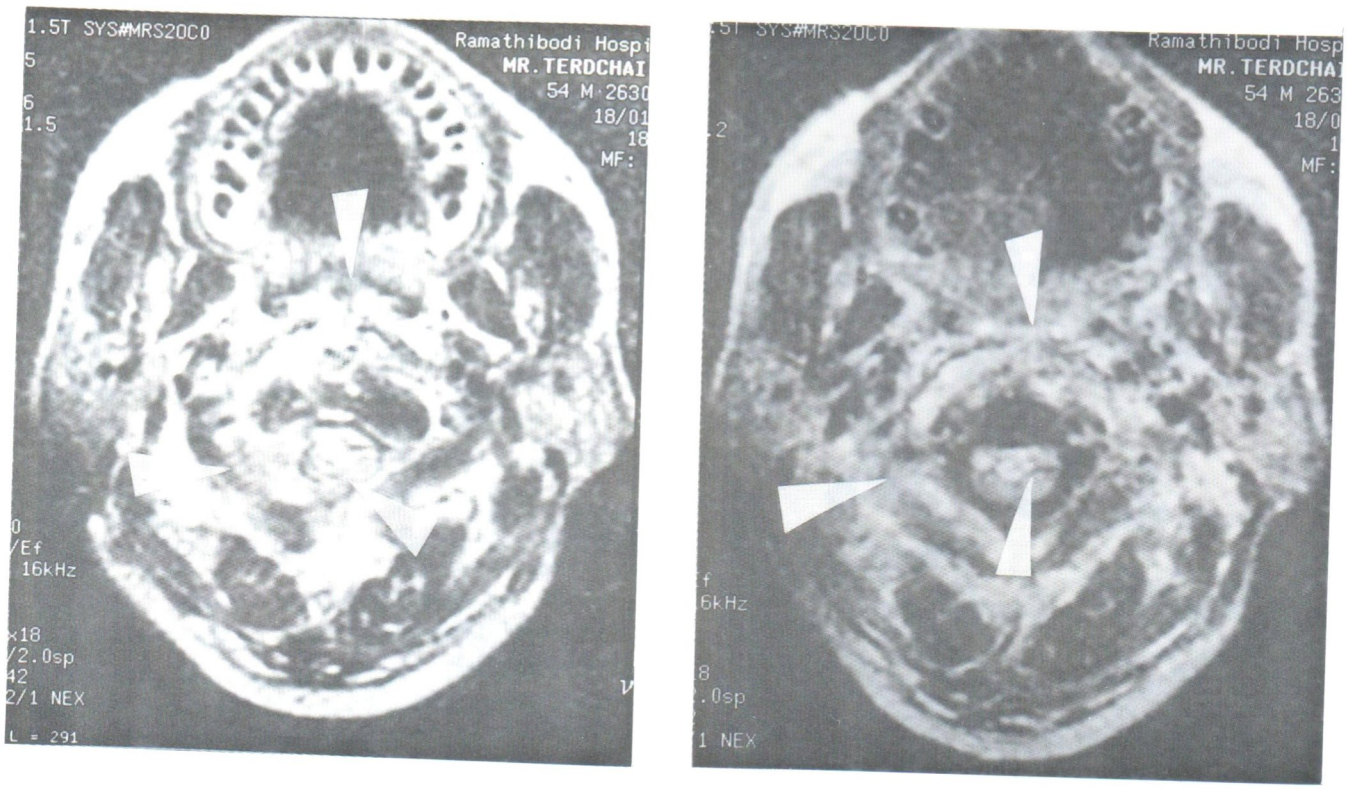

Fig. 7A,B. T2W axial view of the C1-2 level showed a focal destruction of right anterior arch of C2. Other changes were similarly seen as in figure 6.

DISCUSSION

Inflammatory lesions in the RPS include cellulitis, suppurative adenopathy, and abscess. Imaging principally is used to distinguish between cellulitis which requires antibiotic therapy, and suppurative adenopathy or abscess which necessitates surgical treatment (1,6-9). When inflammatory disease of the RPS is present, the faucial tonsils of the oropharyngeal mucosal space or the adenoids of the nasopharynegeal mucosal space are the primary sites of infection (pharyngitis). Subsequently, there is spreading of the organisms to the RPS lymph nodes, inducing reactive and, possibly, suppurative adenopathy. In more advanced cases, infection spreads beyond the capsule of the suppurative lymph nodes to form an abscess that involves the entire RPS and may spread caudally into the mediastinum.

The inflammatory process of the PVS space is centered at the disc space and is associated with partial destruction of the anterior portion of the vertebral body. There may be a variable-sized PVS soft tissue mass and may extend into the epidural space.

The infectious process in our case was initially at the bony part of the great toe. Blood stream infectious foci lodged at the lymphoid tissue of the pharynx and spreading of infection occurred in the prevertebral space, then cervical osteomyelitis and prevertebral abscess followed. Predisposing factor in this case was diabetes mellitus.

The infectious tissue at RVS and PVS was isosignal to the cord on T1WI, and bright on T2WI. Area of drop signal on T2WI in the epidural pus was not totally understood. It is probably a combination of viscosity, increasing protein concentration and paramagnetic effect caused by the accumulation of iron and manganese.(10). The Gd-DTPA enhancement of the infectious area showed diffuse strongly enhanced lesions, except at the area of signal void epidural abscess.

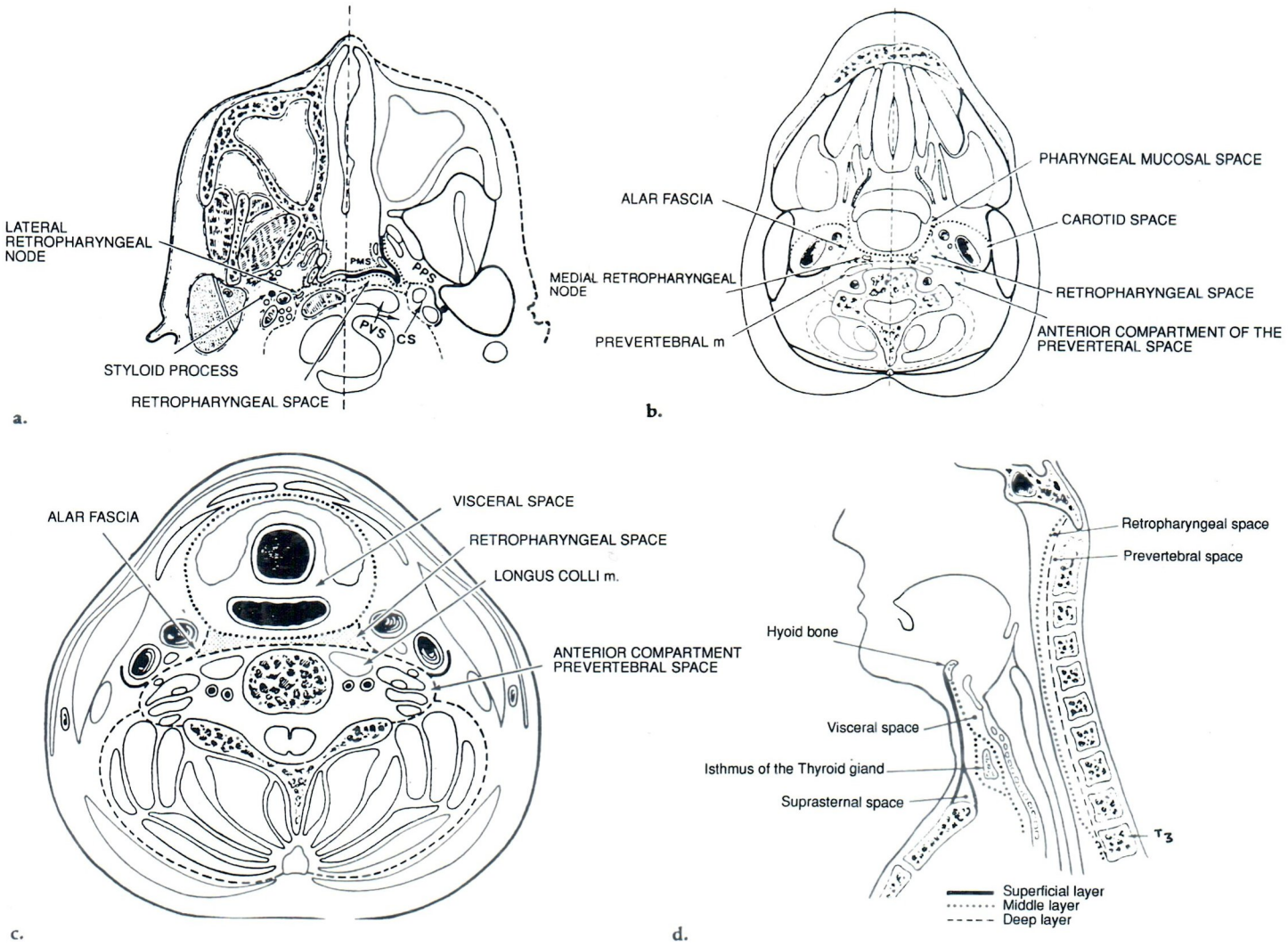

Fig. 8. Drawing of retropharyngeal and prevertebral space.

REFERENCES

1. Davis WL, Smoker WRK, Harnsberger HR. The normal and diseased retropharyngeal and prevertebral spaces. Seminars in ultrasound, CT, and MRI 1990;11:520-533.
2. Dillon WP, Mills CM, Kjos B, et al: Magnetic resonance imaging of the nasopharynx. Radiology 1984;152: 731-738.
3. Silver AJ, Mawad ME, Hilal SK, et al. Computed tomography of the nasopharynx and related spaces. II. Pathology. Radiology 1983;147:733-738.
4. Kumar R, Guinto FC, Madewell JE, et al. Expansile bone lesions of the vertebrae. Radiographics 1988;8: 749-769.
5. Van Lom KJ, Kellerhouse LE, Pethria MN, et al. Infection vs tumor in the spine: Criteria for distinction with CT. Radiology 1988;166:851-855.
6. Nyberg DA, Jeffrey RB, Brant-Zawadzki M, et al. Computed tomography of cervical infection. J Comput Assist Tomogr 1985;9:288-296.
7. Wong YK, Novotny GM. Retropharyngeal space: A review of anatomy, pathology, and clinical presentation. J Otolaryngol 1978;7:528-536.
8. Barratt GE, Koopmann CF, Coulthard SW. Retropharyngeal abscess: A ten-year experience. Laryngoscope d1984;94:455-463.
9. Everts EC, Echevarria J. The pharynx and deep neck infection, in Paparella MM, Shumrick DA (eds): Otolaryngology. Head and Neck, vol 3. Philadelphia, PA, Saunders, 1973, pp 310-340.
10. Som PM, Dillon WP, Fullerton GD, et al. Chronically obstructed sinonasal secretions, observations on T1 and T2 shortening. Radiology 1989;172:515.

HITACHI

Digital Electronic Ultrasound Scanner

EUB-405

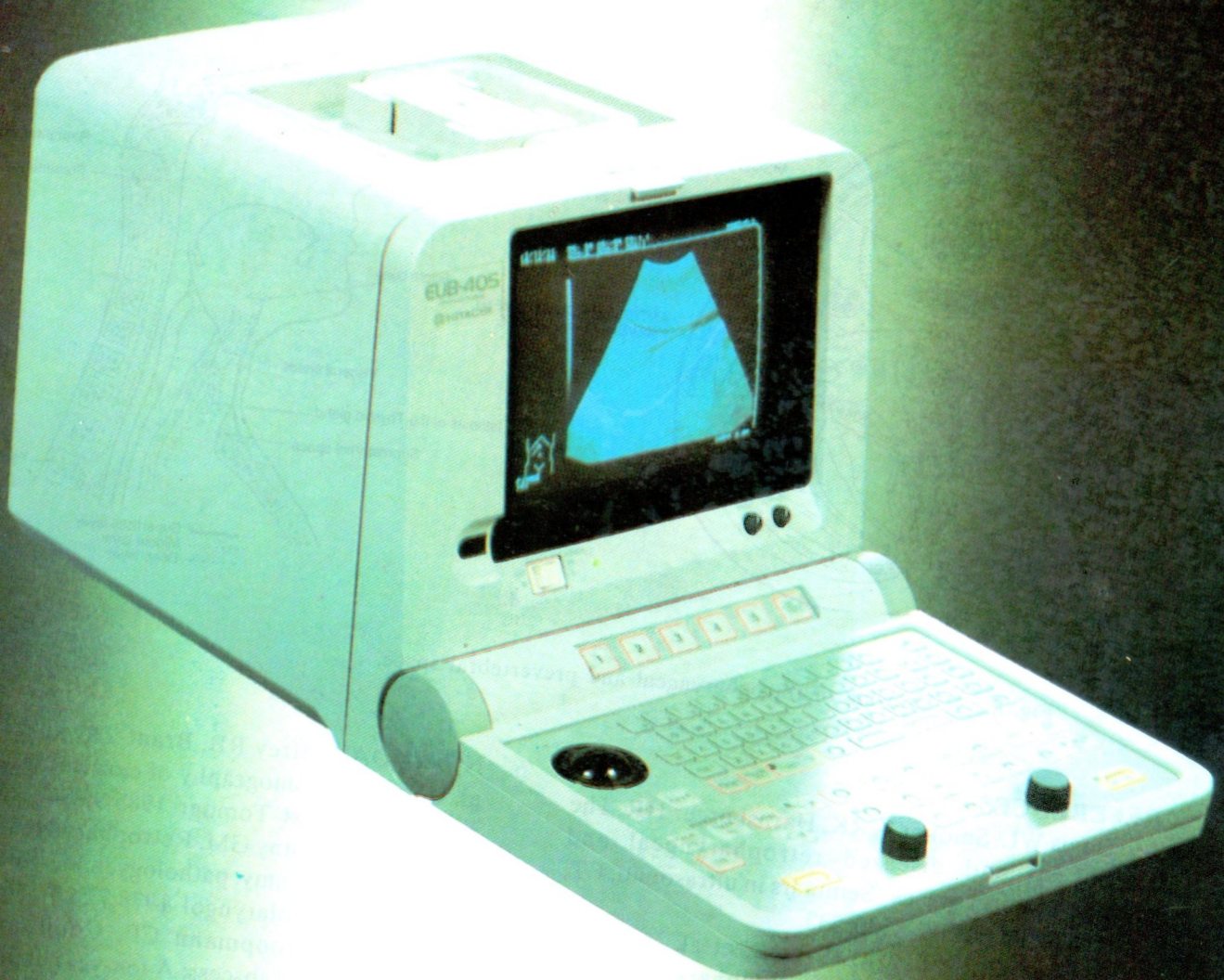

THORACOLUMBAR VERTEBRAL HEIGHT RATIO : NORMAL VALUE IN THAI POPULATION AND SIGNIFICANCE

Pimjai SIRIWONGPAIRAT[1], Chuda SRISUKON[2], Suphaneewan JAOVISIDHA[1], Sarawut KITTIPEERACHOL[1], Chatchai THANUDUMRONG[1].

ABSTRACT

The vertebral height (anterior height, central height and posterior height) of thoracolumbar spine, Th12 to L4, were measured in 398 normal subjects by standard lateral radiographs, and the vertebral height ratios were calculated in both females and males to evaluate normal value in Thai population. A fracture was considered to be present if the anterior or central height was decreased by 20% comparing to the posterior height.

INTRODUCTION

Osteoporosis is nowadays observed to be an increasing problem in the Far East. It is characterized by decrease in amount of bone, leading to increased risk of fracture after minimal trauma (1). In primary osteoporosis, it relates to aging and also estrogen deprivation in postmenopausal women in the absence of other recognizable causes of bone loss such as renal disease, metabolic bone disease or some medications known to affect bone.

It has been hypothesized that loss of vertebral height in the elderly patient with osteoporosis is the result of compression fractures (2-4), nonskeletal factors such as muscle tone (5) or both (6). Of skeletal cause, some authors graded fracture ratios in osteoporotic women as quantitated with spinal DPA,* however, mild anterior wedging at lower thoracic levels are considered within normal limits.

Vertebral bodies of the spine is the early site of osteoporosis. It is composed of predominantly trabecular bone which is susceptible to metabolic stimuli and presenting early bone loss. Lateral spinal radiograph is the first method to be used for semiquantitative assessment of the osteoporotic spine and its associated fracture.

In the present study we calculate anterior wedging ratio and central compression ratio at thoracolumbar junction (Th12) and lumber levels (L1-L4) in healthy Thai subjects of different age and gender.

MATERIAL AND METHODS

The studied population consisted of 398 healthy volunteers (245 women, 153 men), 20-80 years old. We confirmed that no of volunteer had a history of metabolic bone disease, trauma or arthritis. Standard lateral radiographs of thoracolumbar spine were obtained, with the patient in left lateral decubitus position. The focal film distance was 40 inches. We used a measurement technique [11] to determine anterior height, central height, and posterior height (Fig. 1) of the thoracolumbar spine ; from Th12 to L4. We also calculate anterior wedging ratio and central compression ratio in each vertebra. All of the radiographic measurements were entered into the personal computer for tabulation and statistical analysis, using Anova technique.

[1]Department of Radiology, Faculty of Medicine at Ramathibodi Hospital, Rama 6 street, Bangkok , Thailand.
[2]Section of Radiology, Noparat Rajathani Hospital, Ram-intra Street, Bangkok, Thailand
*DPA = Dual-photon-absorptiometry

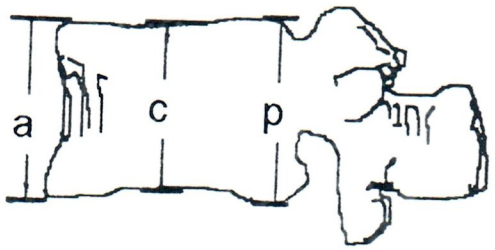

FIG. 1 : Diagram illustrates method for quantitation of vertebral height [8] Anterior wedging ratio (a/p) = anterior height (a) / posterior height (p) Central compression ratio (c/p) = central height (c) / posterior height (p)

RESULT

The results of female anterior wedging ratio (a/p) and central compression ratio (c/p) are shown in Table 1 and 2, and the results of male in Table 3 and 4 respectively, as well as their corresponding line graphs. The average values of the ratios for each vertebral body level are shown in Table 5 and 6.

DISCUSSION

Conventional radiography continues to be the mainstay of any diagnostic investigation of thoracolumbar spine. It should precede any complex imaging procedure. Usually antero-posterior and lateral radiographs are required and the latter is helpful in assessing vertebral height. Because of its availability, the mentioned measurements are usually obtained.

The studied population should represent norm, since osteoporosis was excluded clinically, through laboratory investigation and DXA* measurements of the vertebra and femoral neck. This study shows that the lower limit (average value) of the anterior wedging ratio (a/p) is 0.89 in females and 0.86 in males, and that of the central compression ratio (c/p) is 0.88 in females and 0.89 in males (Table 5 and 6). This lower limit was observed at levels of Th12 and L1, suggesting that Th12 and L1 usually have the normal more anterior wedging than the lower vertebral levels. Our findings of Th12 anterior wedging ratio (0.89 in females and 0.86 in males) are also in accordance with the data obtained by Fletcher et al.(7), who found that wedging ratios of 0.87 in females and 0.8 in males at the Th8 to Th12 levels are within normal limits.

The mechanical testing has shown that vertebral resistance to collapse is highest on the lumbar spine [12]. The lumbar vertebral cortex which is thicker than that of thoracic levels and the normal lumbar lordosis may relatively protects the lumbar vertebrae from anterior wedging forces. As a result, in osteoporotic patient, the loss of trabecular bone results instead in central compression (8).

At the level of L4 in all age groups, especially in female subjects (Table 1), we have observed that the anterior wedging ratios are near or above 1.0. This probably be due to the normal lordotic curve of lumbar spine causing the posterior aspect of the vertebrae to be more compressed than the anterior aspect, and partly due to the more lordosis in pregnant period causing the more posterior compression.

The metabolic turnover rate of trabecular bone is 6 to 8 times higher than that of cortical bone (9). Osteoporosis is characterized by a process removing entire trabeculae,lacing ones that remian more widely separated but only slightly reduced in thickness, as by Parfitt et.al (10). As a result, incomplete fracture of vertebrae are late manifestation of illness and the fracture ratios are relatively insensitive measurement.

In conclusion, we established anterior wedging ratio (a/p) and central compression ratio (c/p) in healthy Thai population. If the value is less than this measurement, particularly decreasing by 20% comparing to the posterior height, compression fracture is suggested although it is the late manifestation of osteoporosis.

ACKNOWLEDGEMENT

We would like to thank Prof.Rajata Rajatanavin for his kind co-operation, and Ms.La-or Chailuekij for the statistical analysis.

* DXA = Dual-X-ray-absorptiometry

TABLE 1 : FEMALE ANTERIOR WEDGING RATIO
(ANTERIOR/POSTERIOR VERTEBRAL HEIGHT)

AGE (YEARS)	NUMBER OF CASES	T12	L1	L2	L3	L4
20-29	30	0.8906	0.9043	0.9272	1.0260	1.0130
30-39	31	0.9001	0.9003	0.9389	0.9763	1.0200
40-49	57	0.8923	0.9014	0.9367	0.9784	1.0160
50-59	49	0.8901	0.8867	0.9411	0.9735	1.0130
60-69	52	0.8829	0.8937	0.9403	0.9831	1.0320
70-80	26	0.8988	0.8731	0.9091	0.9356	1.0041

FIG 2 : LINE GRAPH OF FEMALE ANTERIOR WEDGING RATIO
(Corresponding to Table 1)

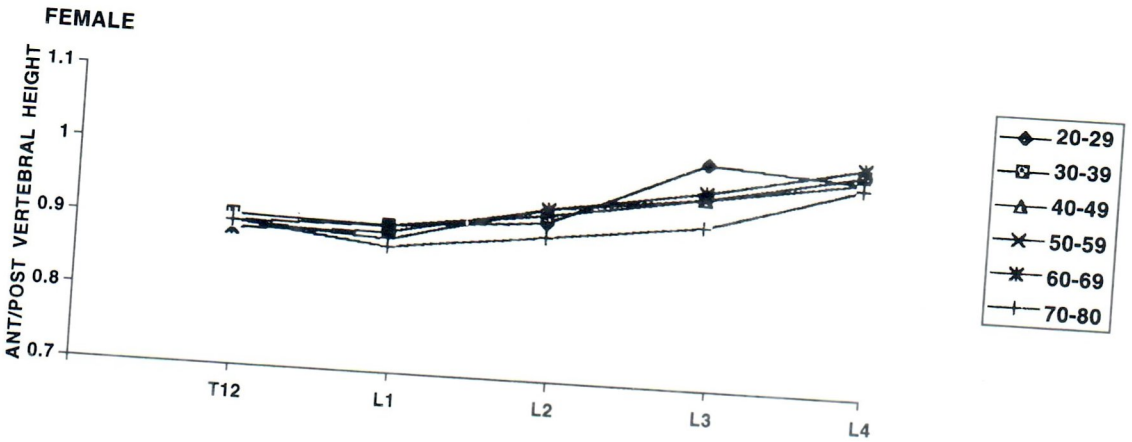

TABLE 2 : FEMALE CENTRAL COMPRESSION RATIO

(CENTRAL/POSTERIOR VERTEBRAL HEIGHT)

AGE (YEARS)	NUMBER OF CASES	T12	L1	L2	L3	L4
20-29	30	0.8584	0.8545	0.8501	0.9331	0.9032
30-39	30	0.8429	0.8693	0.8741	0.8786	0.9137
40-49	57	0.8656	0.8952	0.9096	0.9309	0.9558
50-59	48	0.9185	0.9217	0.9524	0.9590	1.0065
60-69	52	0.8976	0.6069	0.9126	0.9351	0.9762
70-80	26	0.9348	0.9239	0.9343	0.9481	0.9790

FIG 3 : LINE GRAPH OF FEMALE CENTRAL COMPRESSION RATIO

(Corresponding to Table 2)

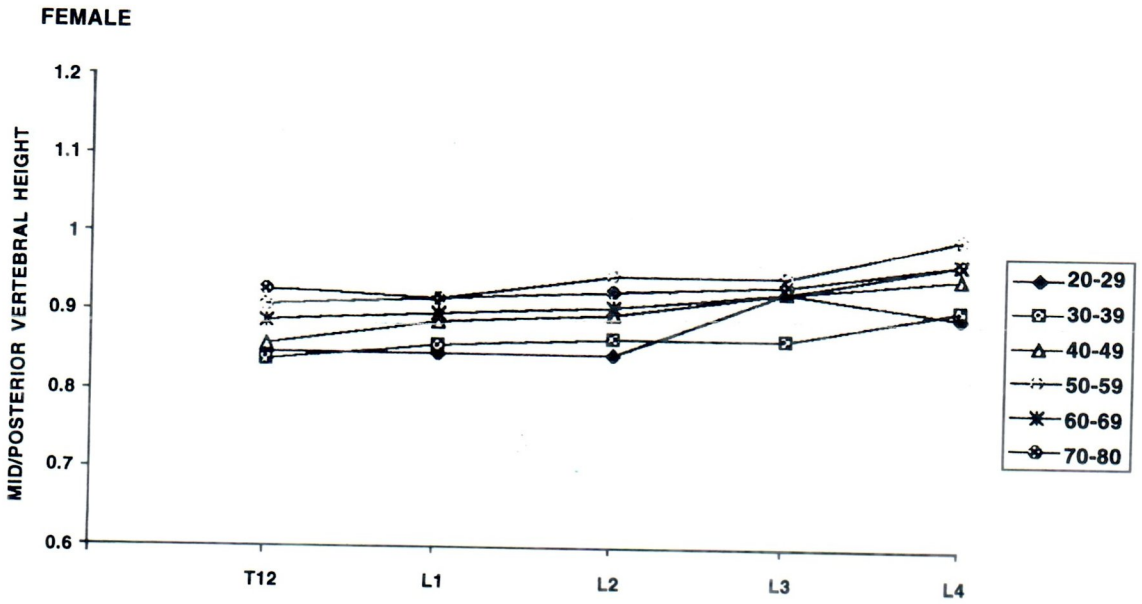

TABLE 3 : MALE ANTERIOR WEDGING RATIO
(ANTERIOR/POSTERIOR VERTEBRAL HEIGHT)

AGE (YEARS)	NUMBER OF CASES	T12	L1	L2	L3	L4
20-29	24	0.8739	0.8520	0.8910	0.9406	0.9916
30-39	25	0.8558	0.8742	0.8876	0.9399	0.9920
40-49	24	0.8636	0.8509	0.8858	0.9393	0.9698
50-59	25	0.8713	0.8582	0.9238	0.9436	0.9830
60-69	24	0.8445	0.8659	0.9190	0.9492	0.9886
70-80	26	0.8681	0.8429	0.8799	0.9379	0.9735

FIG 4 : LINE GRAPH OF MALE ANTERIOR WEDGING RATIO
(Corresponding to Table 3)

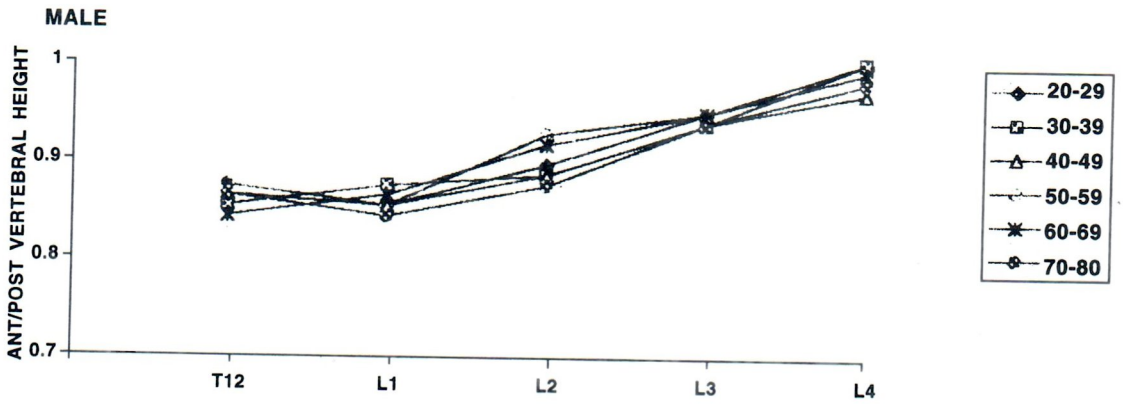

TABLE 4 : MALE CENTRAL COMPRESSION RATIO

(CENTRAL/POSTERIOR VERTEBRAL HEIGHT)

AGE (YEARS)	NUMBER OF CASES	T12	L1	L2	L3	L4
20-29	24	0.9163	0.9086	0.9306	0.9673	0.9828
30-39	25	0.8854	0.9141	0.9079	0.9072	0.9469
40-49	24	0.8954	0.9067	0.9194	0.9444	0.9612
50-59	25	0.9058	0.9046	0.9338	0.9561	0.9951
60-69	24	0.8957	0.9030	0.9217	0.9407	0.9752
70-80	25	0.8968	0.8920	0.9142	0.9453	0.9794

FIG 5 : LINE GRAPH OF MALE CENTRAL COMPRESSION RATIO

(Corresponding to Table 4)

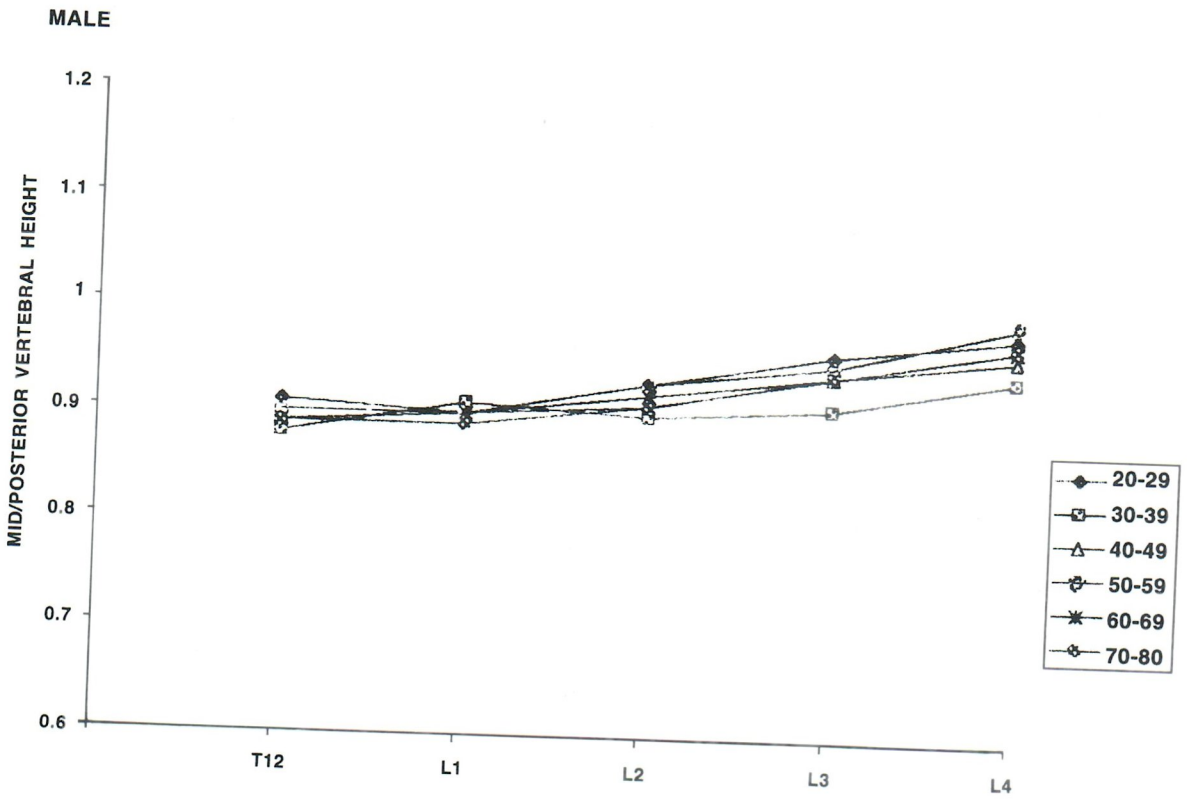

TABLE 5 : AVERAGE VALUES OF THE RATIOS FOR EACH VERTEBRAL LEVEL IN FEMALE

	Th12	L1	L2	L3	L4
a/p	0.8913	0.8940	0.9345	0.9876	1.0176
c/p	0.8866	0.8978	0.9096	0.9330	0.9609

TABLE 6 : AVERAGE VALUES OF THE RATIOS FOR EACH VERTEBRAL LEVEL IN MALE

	Th12	L1	L2	L3	L4
a/p	0.8629	0.8625	0.8977	0.9417	0.9862
c/p	0.8992	0.9048	0.9212	0.9461	0.9734

REFERENCES

1. Consensus Conferences, National Institutes of Health. Osteoporosis. JAMA 1984 ; 252 : 799-802
2. Rose GA. A critique of modern methods of diagnosis and treatment of osteoporosis. Clin Orthop 1967 ; 55 : 17-41
3. Urist MR, Gurvey MS, Fareed DO. Long term observations in aged women with pathologic osteoporosis : including a comment on the significance of the Dowager's hump. In : Barze US, ed. Osteoporosis. New York : Grune & Stratton, 1970 : 3-35
4. Johnston CC, Epstein S. Clinical, biochemical, radiographic, epidemiologic features of osteoporosis. Orthop Clin North Am 1981 ; 12 : 559-569
5. Kalliomaki JL, Siltavuori L, Virtama P. Stature and aging. J Am Geriatr Soc 1973 ; 21 : 504-506
6. Gruber HE, Baylink DJ. The diagnosis of osteoporosis. J Am Geriatr Soc 1981 ; 19 : 490-497
7. Fletcher GH. Anterior vertebral wedging : frequency and significance. AJR 1947 ; 57 : 232-238
8. De Smet AA, Robinson RG, Johnson BE, Lukert BP. Spinal compression fractures in osteoporotic women : Patterns and Relationship to hyperkyphosis. Radiology 1988 ; 166 : 497-500
9. Frost HM. Diagnosis of bone remodelling. In : Frost HM, ed. Bone Biodynamics. London : Little Brown, 1964
10. Parfitt AM, Matthews CHE, Villanuera AR, Kleerekoper M, Frame B, Rao DS. Relationships between surface, volume and thickness of iliac trabecular bone in aging and in osteoporosis : implications for the microanatomic and cellular mechanisms of bone loss. J Clin Invest 1983 ; 72 : 1396-1409
11. Hurxthal LM. Measurement of anterior vertebral compressions and biconcave vertebrae. AJR 1968 ; 103 : 635-644
12. Wehner HW, Dunn WK, Riggs BL. Assessment of bone mineral. J Nucl Med 1984 : 1134-41
13. Grampp S., et al. Radiologic Diagnosis of Osteoporosis. Current methods and Perspectives. Radiol Clin North Am 1993 ; 31(5) : 1133-45

SHIMADZU

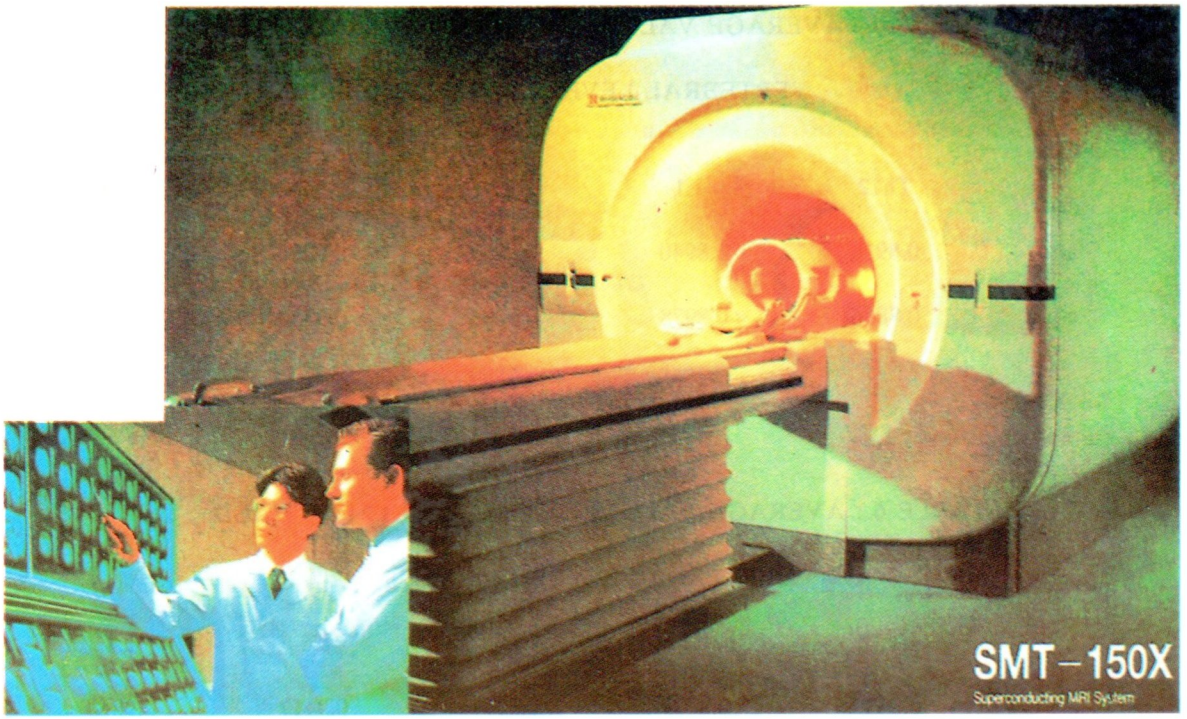

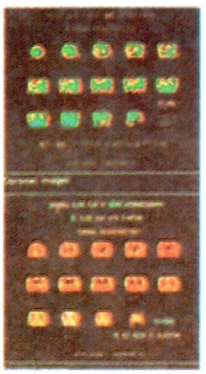

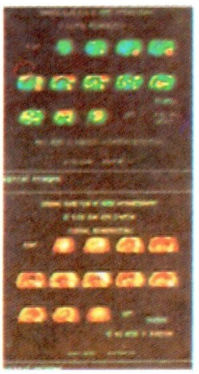

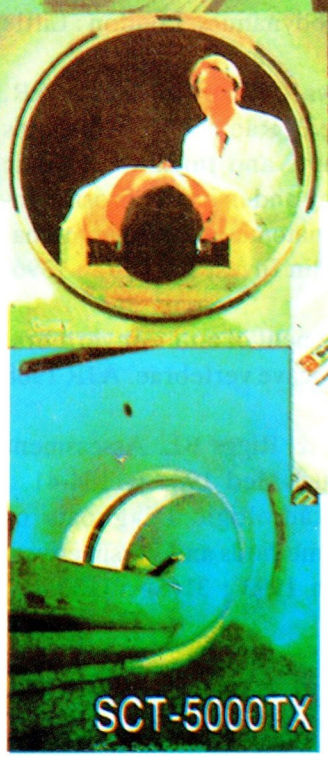

SOLE DISTRIBUTOR :

INTERNATIONAL COSMETICS CO., LTD.

757/10 Soi Pradoo 1, Sathupradit Road, Yannawa, Bangkok 10120

Tel 2949541, 2940292 (Ext 264, 273) Telefax 2949541

THYROID NODULES : EVALUATION WITH COLOR DOPPLER ULTRASONOGRAPHY.

Chutiwan VIWATTANASITTIPHONG, Bussanee WIBULPOLPRASERT, Achara SANGSAI, Chatchai THANUDUMRONG

ABSTRACT

The aim of this study was to assess prospectively the value of thyroid Color Doppler sonographic examination of the patients with a solitary thyroid nodule and correlation with the fine needle aspiration cytology.

Sixty patients with a solitary thyroid nodule underwent Color Doppler sonography with 7.5 MHz transducer which proved histologically to be 10 (15%) malignant and 50 (85%) benign nodules. Perinodular color flow signal were depicted in 6 out of 10 (60%) malignant nodules and 29 out of 50 (58%) benign lesions. Intranodular color flow signal were exhibited in 3 out of 10 (33%) and 2 out of 50 (4%) of malignant and benign lesions respectively. This left 20 out of 60 (33%) to have absence of color flow signal. The malignant nodule showed greater tendency to exhibit intranodular color flow signal than benign lesion but perinodular color flow signal was found in both benign and malignant nodule equally. The quantitative evaluation of the peak flow velocity obtained from the Doppler wave form shows no significant difference of the peak flow velocity between benign and malignant lesion (mean peak flow velocity 15.85 cm/sec of malignant nodule and 13.37 cm/sec of benign lesion.

Management of the solitary thyroid nodule poses a problem for the clinician in the selection of patients who require surgery. 10-20% of solitary thyroid nodules are malignant (1). Clinical history and examination are frequently unable to distinguish between benign and malignant thyroid nodules. (2,3)

Although sonography is widely used as a single and noninvasive diagnostic tool in a wide spectrum of thyoid disease, the lack of histopathological specificity accentuates its limitation. (4) Color doppler sonography provides not only the standard gray scale image but also a color display of blood flow and hence permits the evaluation of vascularity in thyroid tumors and tumorlike lesions. (5,6)

However it is not yet clear that an analysis of flow pattern types could differentiate carcinoma from benign lesions. (7)

The study therefore attemped to assess the characteristic of blood flow within the thyroid nodules with the emphasis on the correlation between flow patterns and pathology with correlation between color doppler patterns and the gray scale appearance of the lesions was also evaluated.

MATERIALS AND METHODS

From february to october 1994, 60 patients with solitary thyroid nodules underwent examination with color doppler sonography at the department of Radiology in Ramathibodi Hospital by the author (*) and confirmed by experienced consultant radiologist (**) prior to the fine needle aspiration cytology (FNAC). Results were recorded prospectively.

The age of patients varied from 20 to 84 years, average 46 years.

Department of Radiology, Ramathibodi Hospital, Rama VI road, Bangkok, Thailand.

Color doppler sonography was performed using a commercially available color doppler system (ALOKA SSD 680) with a 7.5 Mhz, transducer, wall filter of 100 Hz pulse repetition frequency of 100 Hz to 2 Khz, sampling volume 1 mm.

1) The patients first underwent the gray scale scanning to evaluate echo texture.

2) Subsequently color flow imaging and doppler examination were performed.

Color gain was adjusted to a level associated with minimal artifacts. The color flow image was used as a guide to select the points for recording the doppler time-velocity wave form with a sampling volume of 1 mm. (Fig 4.) when no color signals could be depicted, the quantitative doppler examination was not performed.

Flow toward the transducer was displayed as red and blue indicated flow in the reverse direction.

Nodules were classified on the basis of flow distribution as follows :-

TYPE O : Absence of color, singals (Fig.1)

TYPE I : Color flow at the periphery of the nodule (Fig.2)

TYPE II : Mixed peripheral and internal flow signal (Fig.3)

The doppler wave form record at the point with the highest frequency shift was used for statistcal analysis.

RESULTS

The mean patient age was 46.8 years and the female to male ratio was 7.5 to 1 (female 53, male 7).

The histological diagnoses are shown in Table 1.

There were ten (16%) malignant nodules :- seven papillary, three follicular carcinoma, This left 50 patients (84%) with benign lesions.

All 60 patients had thyroid ultrasonography and doppler exam performed. The correlation between pathologic and color doppler findings is summarized in Table 2 and 3, correlation between B-mode images and flow patterns is shown in Table 4.

Color signal could be depicted in 9 out of 10 (90%) malignant tumors and 37 out of 50 (74%) benign lesions. However no specific flow pattern for malignancy could be found.

As regards to flow distribution, type II was seen in 3 out of 10 (33%) malignant lesions and in 2 out of 50 (4%) benign lesions. Malignant nodules showed greater tendency to exhibit type II flow than benign lesion. However no specific flow pattern for malignancy could be found.

No color flow pattern that correlated specifically with the conventional B-Mode characteristics of the nodules and no correlation existed between the presence of color flow signals and peak flow velocity and pathology.

DISCUSSION

The quantitative evaluation of color doppler and flow of this report showed that no correlation existed between pathology and flow pattern and peak flow velocity obtained from the doppler wave form (Chi's Square Test)

Similarly, no correlation was found between conventional B-Mode images and the doppler data.

However, as shown angiographically (8,9) most malignant tumors are rich in irregular, tortuous vessels. This discrepancy might occur because color doppler songraphy is relativelly less "sensitive" in the depiction of fine tumor vessels than angiography.

"sensitivity" in color doppler sonography related to several factors (10) (gain setting, pulse repetition frequency, doppler filter) and technical difficulties also exist in selecting the precise setting at which optimal image would be obtained (10). Depiction of fine vasculature with slow flow is still difficult.

Taylor and coworkers (11) reported that high doppler velocity were detected in primary malignant tumors of the liver, kidney, adrenal gland and pancreas and that such high velocity doppler signals were due to arteriovenous shunting.

In conclusion, the presence of color flow signal and flow distribution within the nodule and peak flow velocity did not establish the differrential diagnosis between benign and malignant thyroid nodule. Doppler pattern could not significantly improve the limitation of the conventional B-Mode scan and the doppler examination would play a limited role in evaluating the nature of disease vasculature within the nodules.

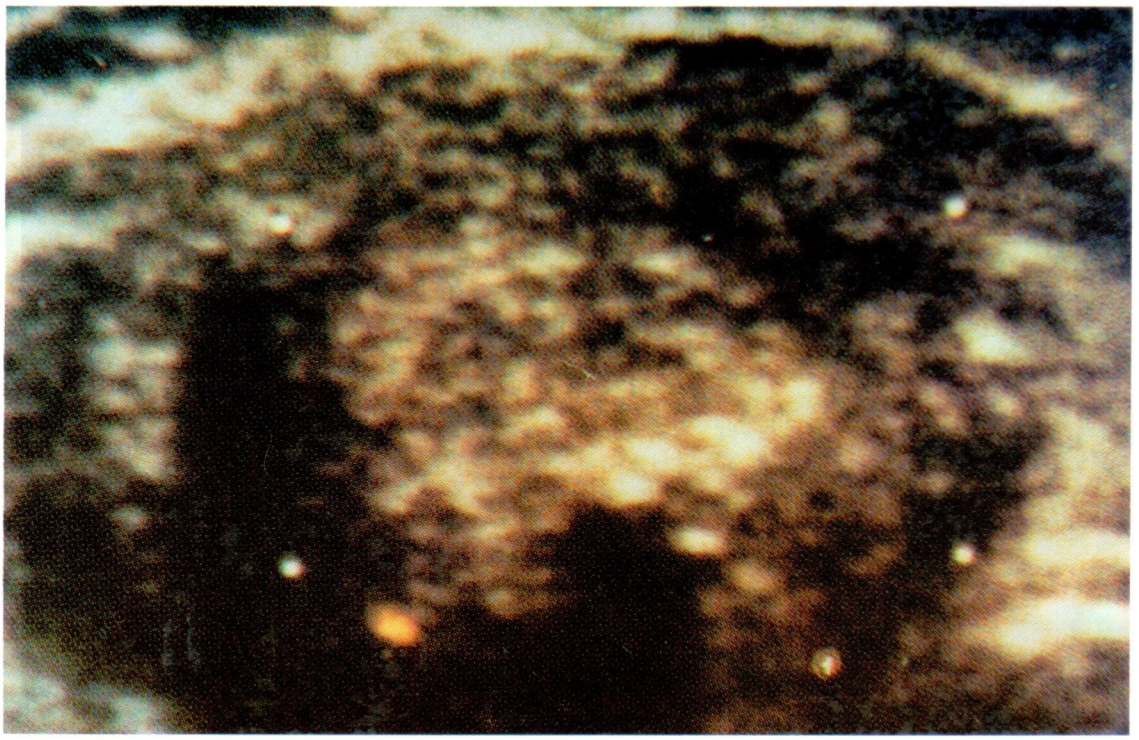

Fig. 1 FLOW DISTRIBUTION TYPE 0
NO COLOR FLOW SIGNAL IS DETECTED IN THE NODULE

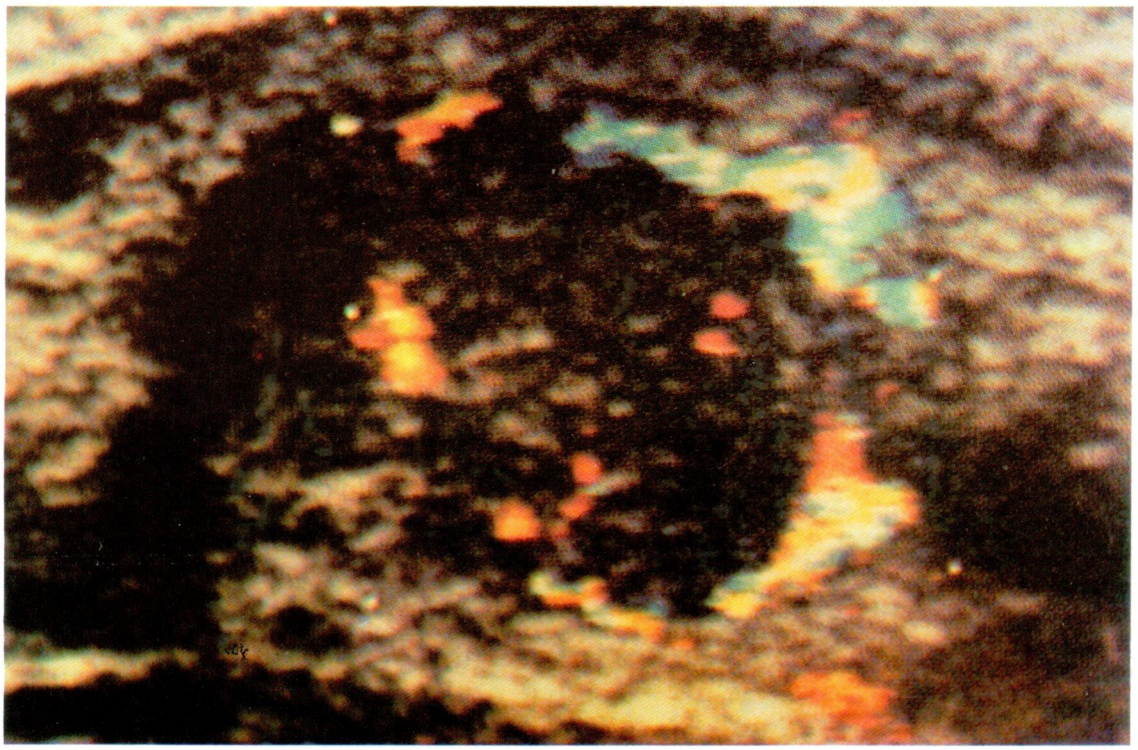

Fig. 2 FLOW DISTRIBUTION TYPE 1
COLOR FLOW SIGNAL IS DEPICTED AT PERIPHERY OF THE NODULE

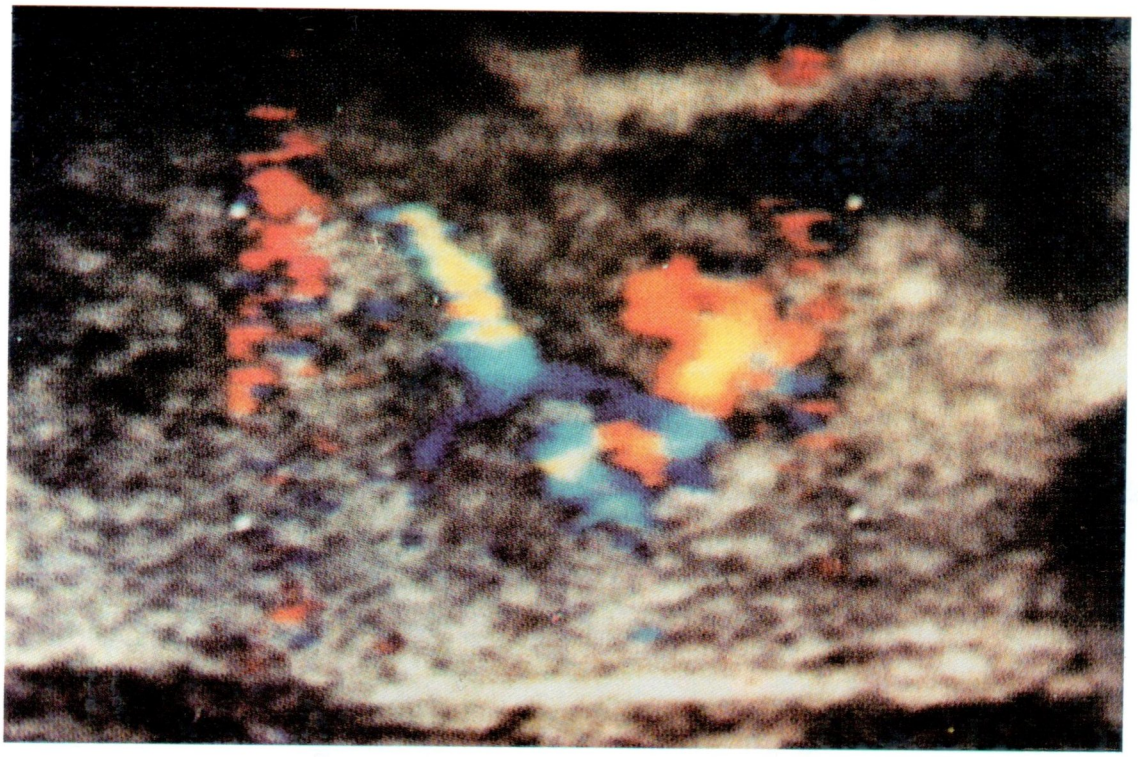

Fig. 3 FLOW DISTRIBUTION TYPE 2
MIXED PERIPHERAL AND INTRANODULAR COLOR FLOW SIGNAL

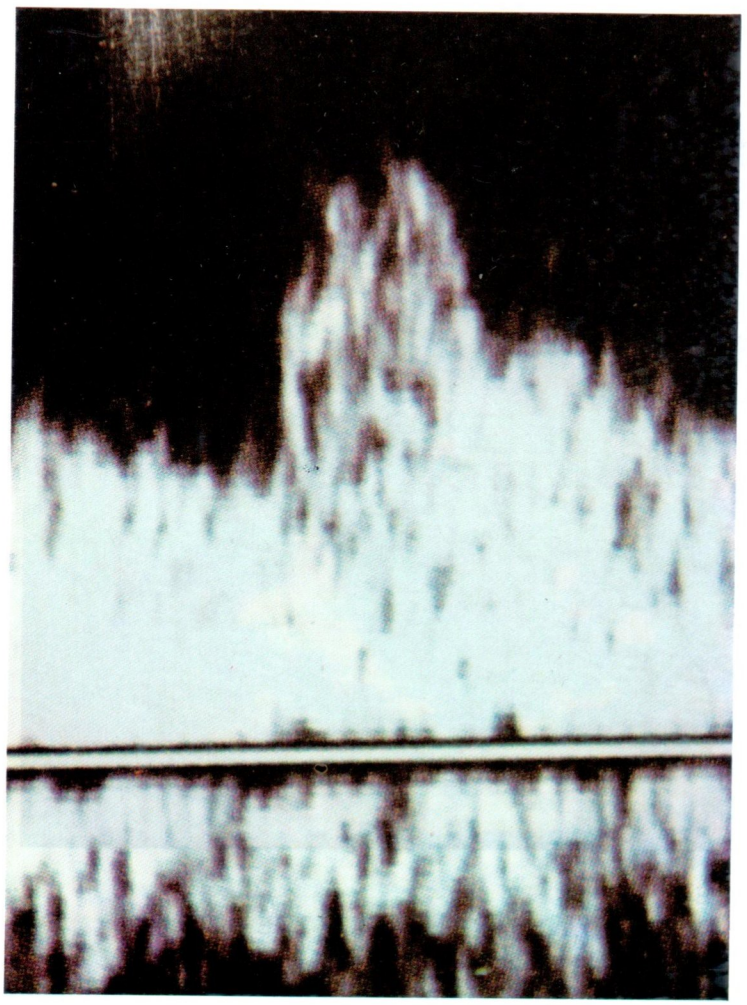

Fig. 4
THE DOPPLER TIME-VELOCITY WAVE FORM SHOWS PEAK FLOW VELOCITY 20.1 Cm/sec

Table. 1 Histological diagnosis of solitary thyroid nodules

Histological diagnosis	No.
Malignant	
papillary carcinoma	7 (11.2%)
Follicular carcinoma	3 (4.8%)
Benign	
Hurthle cell adenoma	2 (3.2%)
Colloid nodule goiter	12 (19.2%)
Cystic nodular	12 (19.2%)
Adenomatous nodule	11 (17.6%)
Hemorrhagic cystic nodular goiter	7 (11.2%)
Cystic colloid goiter	4 (6.4%)
Hemorrhagic colloid nodule	2 (3.2%)
	---
	60 (100%)

Table. 2 Correlation between pathology and Color Doppler findings

Pathology	No. of case	Flow pattern*		
Maligant		O	I	II
Papillary carcinoma	7	1	4	2
Follicular carcinoma	3	-	2	1
Benign				
Adenomatous nodule	12	4	8	-
Colloid nodule	12	3	8	1
Cystic nodular goiter	11	5	6	-
Hemorrhagic cystic nodular goiter	7	4	3	-
Cystic colloid goiter	4	3	1	-
Hemorrhagic colloid nodule	2	-	2	-
Hurthle cell adenoma	2	-	1	1

* For the flow pattern
TYPE O : Absence of color signals
TYPE I : Color flow at the periphery of nodule
TYPE II : Mixed peripheral and internal flow signal

Table. 3 Correlation between pathology and Color Doppler findings

Pathology	No. of case	Peak Flow velocity (cm/sec)	
Maligant		Range	Mean
Papillary carcinoma	7	12.45-22.05	15.65
Follicular carcinoma	3	11.50-18.35	16.06
Benign			
Adenomatous nodule	12	10.95-17.45	14.20
Colloid nodule	12	11.65-19.00	14.10
Cystic nodular goiter	11	9.63-16.85	12.24
Hemorrhagic cystic nodular goiter	7	10.55-14.45	12.05
Cystic colloid goiter	4	9.25-15.00	10.68
Hemorrhagic colloid nodule	2	10.20-17.35	13.77
Hurthle cell adenoma	2	14.60-18.55	16.55

Table. 4 Correlation between B-Mode image and flow patterns

Echogenicity of nodule	No. of case	Flow pattern		
		O	I	II
Anechoic or cystic	22	11	11	-
Hypoechoic	25	5	17	3
Isoechoic or hyperechoic	9	3	5	1
Mixed	4	1	2	1

REFERENCE

1. Brooks JR. The solitary thyroid nodule. Am J Surg 1973 ; 125 : 477-81
2. Haff RC, Schecter BC, Armstrong RC, Evans WE. Factors increasing the probability of malignancy in thyroid nodules. Am J Surg 1976 ; 131 : 707-9
3. Ro jeski MT, Ghirib H. Nodular thyroid disease : Evaluation and management. N ENG J Med 1985 ; 313 : 428-36
4. Cox MR., Marshall SG, Spence RAJ. Solitary thyroid nodule : a prospective evaluation of nuclear scanning and Ultrasonography. Br J Surg 1991 ; 78 : 90-93
5. Ralls PW, Mayekawa DS, Lee KP, et al : Color-flow Doppler Sonography in Graves'disease. AJR 1988 ; 150 : 781
6. Luigi SB, Vincenzo CF, Enrico BR. Thyroid Pathologic Radiology Clinics of North America 1992 ; 30 : 945-950
7. Kazuhiro SM, Tokiko Endo, Takeo Ishigaki, et al : Thyroid Nodules : Evaluation with Color Doppler Ultrasonography. J Ultrasound Med 1993 ; 12 : 673-678
8. Takahashi M, Ishibashi T, Kawanami H : Angiographic diagnosis of benign and malignant tumors of the thyroid. Radiology 1969 ; 92 : 520.
9. Wickbom I, Zachrisson BF : Thyroid angiography. In Abrams HL (Ed) : Angiography, 2 nd edition ; vol 1. Bastom, little, Brown, 1971, P. 677
10. Cape EG, Sung H-W, Yoganathan AP : Basics of Color Doppler imaging. In Lanzer P, Yoganthan AP (Eds) : Vascular Imaging By Color Doppler and Magnetic Resonance. Berlin, Springer-Verlag, 1991, p. 73
11. Taylor KJW, Ramos I, Carter D, et al : Correlation of Doppler US tumor signals with neovascular morphologic feature, Radiology 1988 ; 166 : 57.

MRI OF MARROW CHANGES IN THE VERTEBRAL BODIES ADJACENT TO ENDPLATES IN DEGENERATIVE LUMBAR DISC DISEASE.

Krisna CHITAREE, Pimjai SIRIWONGPAIRAT, Suphaneewan JAOVISIDHA, Achara SANGSAI.

ABSTRACT

MR studies of the lumbar spine in 57 patients [285 disc spaces] were analyzed, to assess the appearance and frequency of the bone marrow signal changes in the vertebral bodies adjacent to the normal and degenerative discs. Degenerative changes were found in 144 of 285 discs. Signal abnormalities of bone marrow adjacent to the endplates were identified in 52 of 144 discs (36.1%). In 44 of 52 discs [84.6%], there is an area of relatively increased signal intensity in T1WI & T2WI in the vertebral bodies adjacent to the endplates. In 6 of 52 [11.5%] decreased signal intensity on both T1WI & T2WI was noted in focal and bandlike appearance. In the other 2 discs [3.9%] decreased signal was noted on T1WI and increased signal evidence in T2WI. These marrow changes were not present adjacent to the normal discs. The signal alteration suggests three patterns of bone marrow change; fat phase, sclerotic phase and edematous phase respectively. The ages of the patients with marrow changes in edematous phase (41 and 43 years old) are less than the mean ages of the other two groups (65.52 and 59.4 years respectively).

We conclude that bandlike and focal areas of signal changes in the bone marrow adjacent to degenerative intervertebral discs can occur on MR images of the lumbar spine and should not be confused with signal changes from tumor or infectious process involving the disc space and adjacent vertebral endplates.

INTRODUCTION

MR imaging is a valuable method for detecting bone marrow abnormalities [1]. Normal vertebral marrow consists of hematopoietic marrow that demonstrates intermediate signal intensity of both T1W and T2W images, and fat marrow which shows increased signal intensity on T1WI and decreased signal on T2WI [2]. Bone marrow changes adjacent to the vertebral endplates have been noted on MR imaging in a variety of pathologic conditions [3]. We have observed focal alterations in bone marrow signal intensity adjacent to endplates in patients with degenerative disc disease. The purpose of this study is to assess the appearance and frequency of this finding in MRI of the spine and to determine the pathophysiologic basis of these marrow changes.

MATERIALS AND METHODS

MR studies were performed with a General Electric 1.5 Tesla superconductive system machine for lumbar spine imaging. All patients were studied at least with T1W (TR = 400-600 msec, TE = 10-20 msec) and T2W (TR = 2000-3000 msec, TE = 90-110 msec) in the sagittal plane and T1W in the axial plane.

Department of Radiology, Ramathibodi Hospital, Rama VI Rd., Bangkok 10400, Thailand.

Fig. 1A.
Areas of marrow signal alteration in focal and bandlike appearance of increased signal intensity on both T1W and T2W images suggesting local increases in marrow fat.
Sagittal midline T1WI (TR/TE = 440/11 msec) of the lower lumbar spine. There is focal increased signal of the marrow at infero-posterior aspect of the vertebral body adjacent to the L5-S1 disc.

MR studies of the lumbar spine were reviewed in 57 patients examined in an 8-month period (January to August 1994); 33 women and 24 men; 21-79 years old: mean age 50.74 years old. These include 49 patients with degenerative disc disease and 8 patients with normal disc appearance on MRI. Totally 285 discs were analyzed and 144 degenerative discs were noted. Disc degeneration was considered to be presented when there was decreased signal intensity of the intervertebral disc on T2WI or narrowing of disc space [3,4].

Fig. 1B. Focal increased signal is also seen on sagittal T2WI (TR/TE = 2300/90 msec. Note decreased signal intensity of the intervertebral disc at this level.

RESULTS

Altered signal intensity in the bone marrow adjacent to the endplates was observed in 52 (36.1%) of 144 degenerative discs. This was not seen at any normal disc level. The marrow signal alteration was bandlike, focal or mixed bandlike and focal on one or both sides of the disc. In 44 of the 52 abnormal disc levels (84.6%), there was increased signal intensity on both T1W and T2W images (Fig.1). In 5 patients (6 discs or 11.5%), decreased signal intensity was demonstrated on both T1W and T2W images (Fig.2). In 2 patients (2 discs or 3.8%), decreased marrow signal intensity on T1WI and relatively increased signal intensity on T2WI was observed (Fig.3).

The patients who have degenerative disc disease with altered marrow signal intensity appeared to be somewhat older than the patients who have degenerative disc disease with normal marrow signal (mean age, 59.55 and 45.2 years, respectively).

The two patients with decreased marrow signal on T1WI and relatively increased signal on T2WI were quite younger (41 and 43 years old) than the other two groups. The mean age of the group with increased marrow signal on both T1W and T2W images and that of the group with decreased signal on both T1W and T2W images were 65.53 and 59.4 years respectively.

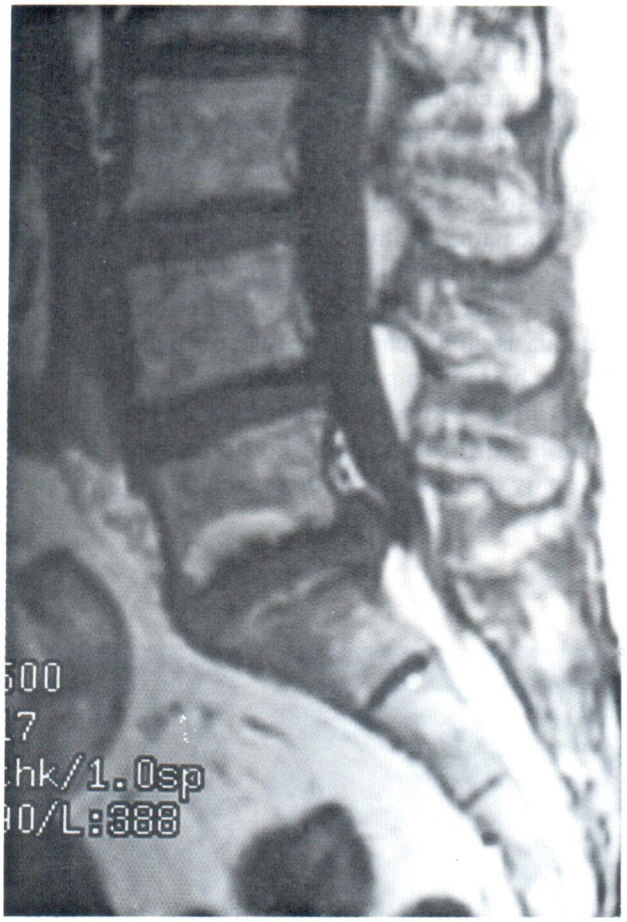

Fig. 1C. Sagittal T1WI (TR/TE=500/17 msec) of the other study. Again there is bandlike increased signal adjacent to the endplate of L5-S1 disc.

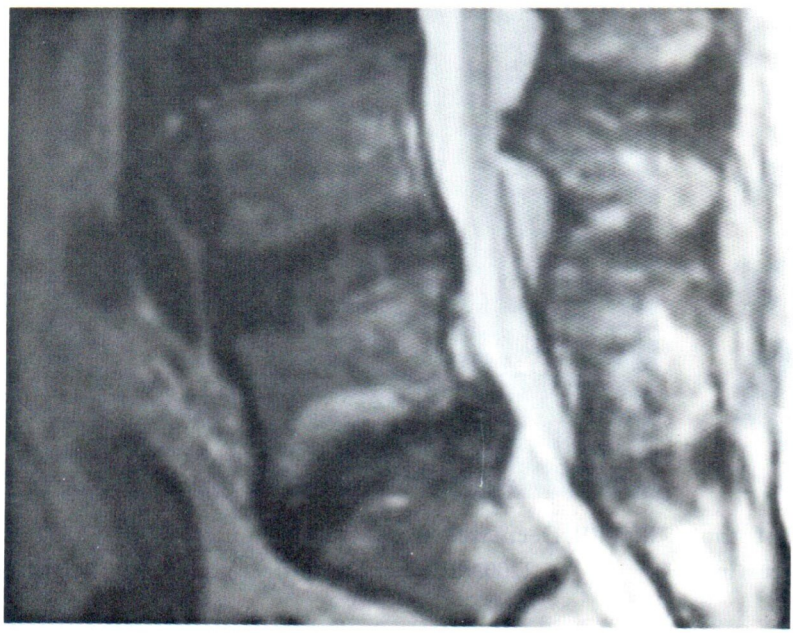

Fig.1D. Sagittal T2WI (TR/TE=3000/108 msec) shows degenerative disc at L4-5 and area of bandlike increased signal intensity.

DISCUSSION

The normal lumbar vertebral body has intermediate to high signal intensity on both T1W and T2W images due to the signal contribution of fat and hematopoietic marrow [2]. The normal intervertebral disc has relatively homogenous low signal intensity on T1WI. On T2WI, the normal nucleus pulposus has a high signal intensity and a central cleft [3,4].

Alterations in marrow signal intensity adjacent to the intervertebral discs was found in 36.1% of cases with degenerative discs. Three basic patterns of marrow change were observed: (1) hypointense T1 and hyperintense T2 = edematous phase, (2) hyperintense T1 and hyperintense T2 = fat phase, and (3) hypointense T1 and hypointense T2 = sclerotic phase [5].

The study about endplate marrow signal alteration in patients with degenerative discs was previously reported by de Roose et al. [6] and revealed similar results. The following study by Modic et al. for assessment of vertebral body marrow change related to degenerative disc disease suggested that there is a spectrum of vertebral marrow signal intensity change that occurs with increasing frequency with age [7]. And from this study, two types of vertebral signal intensity change were identified; type 1 showed decreased signal intensity on T1WI and increased signal intensity on T2WI, type 2 showed increased signal intensity on T1WI and isointense or slightly increased signal intensity on T2WI.

Whether the endplate should be considered as part of the vertebral body or intervertebral disc is a matter of great debate and speculation [8].In infants and young children, blood supply to the cartilagenous endplate and intervertebral disc is from a vascular network which soon atrophies and may disappear by the age of 8-12 years. The metabolism of the intervertebral disc becomes dependent on diffusion of fluid either from the marrow of the vertebral bodies across the subchondral bone or cartilagenous endplate or through the annulus fibrosus from the surrounding blood vessels. During aging, morphologic changes in the vertebral bone and endplate occur. These can interfere with normal disc nutrition and result in one or more

degenerative processes [8]. Focal histologic changes in the cartilagenous endplates appear to precede histologic changes in the nucleus pulposus and annulus fibrosus. With advancing age, a vascular network along the endplates atrophies and local marrow ischemia can cause a conversion of normal hematopoietic marrow to fatty marrow [6,8]. Furthermore, bony trabeculae adjacent to the endplate became thickened, resulting in sclerosis as part of degenerative process [6].

The two patients who have altered marrow signal in edematous phase both presented with acute symptom of back pain and the studies showed disc herniation. Herniated discs always show associated disc degeneration while degeneration may be seen without herniation. All herniated discs eventually degenerate and there is immediate dehydration followed by a temporary gain in water content during a short period. This mechanism also affects the endplate and results in edematous changes in acute phase [3,5]. The younger age of the patients in this group as compared to that of the other two groups is also noted and suggestive of acuteness.

The pattern of hypointense T1 and hyperintense T2 of the marrow adjacent to endplates may conceivably reflect local infection, inflammation and/or ischemia as similar changes in marrow signal intensity which can be seen in patients with ischemic necrosis of the hip [9]. However, this pattern of degeneration can be differentiated from the findings seen in infection by the absence of increased signal intensity of the disc on T2W1 [5,10]

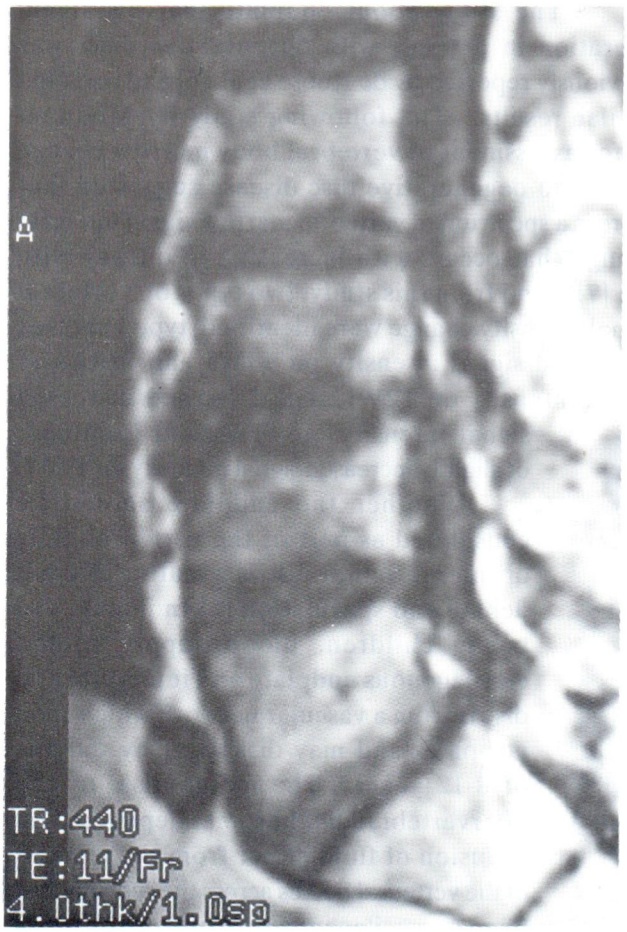

Fig. 2A. Bandlike decreased signal intensity of the marrow in both T1WI and T2WI suggesting sclerotic change.
Sagittal T1WI (TR/TE=440/11 msec) shows decreased signal intensity of the adjacent marrow on both sides of the L3-4 disc.

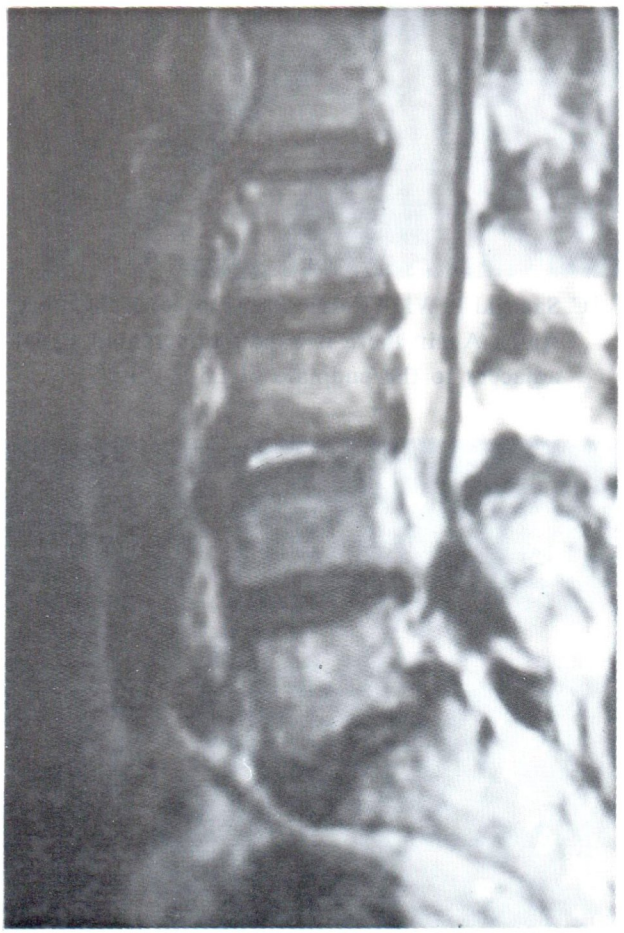

Fig. 2B. Decreased signal is also seen on T2WI (TR/TE = 2200/90 msec). Note decreased disc height.

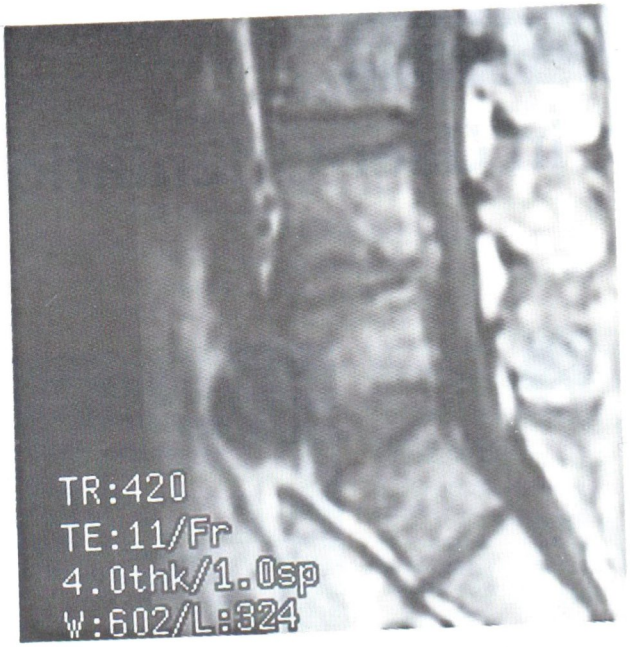

Fig. 3A. Decreased signal intensity in T1WI and increased signal intensity in the marrow adjacent to the endplate suggesting increase in water fraction in the marrow.
Sagital T1WI (TR/TE = 420/11 msec) shows decrease - signal marrow adjacent to L4-L5 disc.

Fig. 3B. The low signal of the marrow on T1WI turns to be high on T1WI (TR/TE = 2300/90 msec). Note disc herniation.

REFERENCES

1. Daffner RH, Lupetin AR, Dash N, Deeb ZL, Sefczek RJ, Schapiro RL. MRI in the detection of malignant infiltration of bone marrow. AJR 1986;146:353-358.
2. Wismer GL, Rosen BR, Buxton R, Stark DD, Brady TJ. Chemical shift imaging of bone marrow: preliminary experience. AJR 1985;145:1031-1037.
3. Modic MT, Pavlicek W, Weinstein MA, et al. Magnetic resonance imaging of intervertebral disk disease: clinical and pulse sequence considerations. Radiology 1984; 152:103- 111.
4. Aguila LA, Piraino DW, Modic MT, Dudley AW, Duchesneau PM, Weinstein MA. The intranuclear cleft of the intervertebral disk:magnetic resonance imaging. Radiology 1985;155:155-158.
5. Pomeranz SJ. Gamuts & pearls in MRI 2nd edition. Ohio: MRI-EFI, 1993:215,218.
6. De Roose A, Kressel H, Sprotzer C, Dalinka M. MR imaging of marrow changes adjacent to endplates in degenerative lumbar disk disease. AJR 1987;149:531-534.
7. Modic MT, Steinberg PM, Ross JS, et al. Degenerative disk disease : assessment of changes in vertebral body marrow with MR imaging. Radiology 1988;166:193-199.
8. Resnick D. Degenerative disease of the vertebral column. Radiology 1985;156:3-14.
9. Mitchell DG, Rao VM, Dalinka M, et al. MRI of the normal and ischemic hips at 1.5 Tesla: observations utilizing T2 contrast. Presented at the annual meeting of the American Roentgen Ray Society,Washington DC, April 1986.
10. Resnick D, Niwayama G. Degenerative disease of the spine. In:Resnick D, Niwayama G eds. Diagnosis of bone and joint disorders. Philadelphia: W.B. Saunders, 1981:1368-1415.

MEDISON

SONOACE SERIES

Gyn-Center: New Approach in User-Orientation

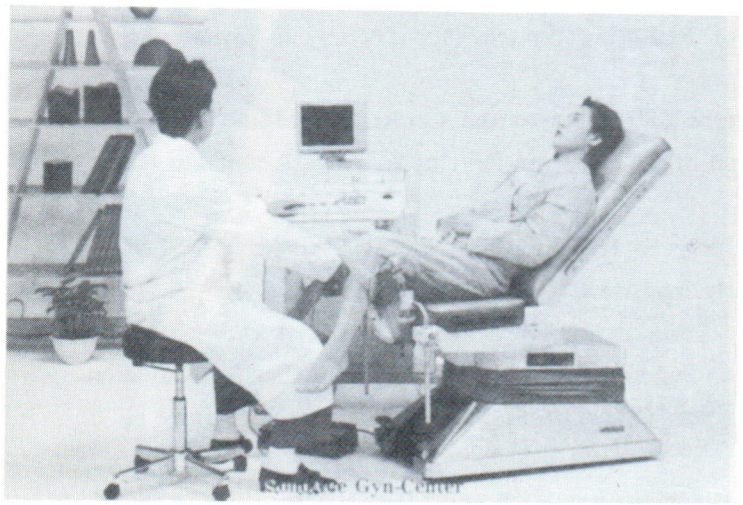

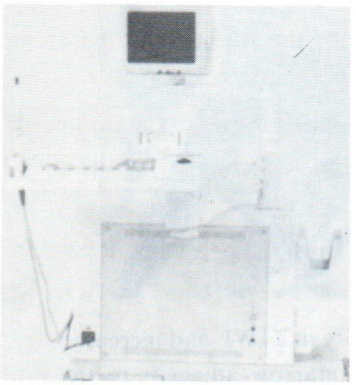

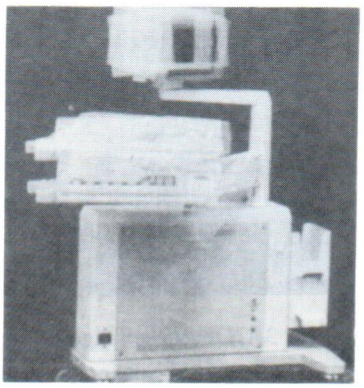

SA-88P

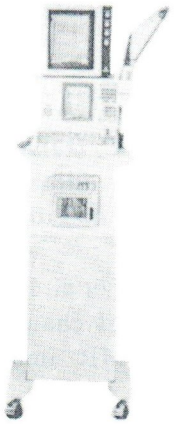

64 Grey scale
Image memory
3 points dynamic focusing
Distance & area measurement
Battery operated(option)
Built-in G.A.Table
M-mode

SA-1500

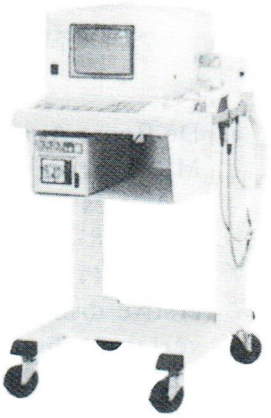

256 Grey scale
2 probes available simultaneously
Track-ball unit as standard
9" built-in monitor
Histogram & Window mode
Diverse applications
Abdomen, endovaginal, small parts, intraoperative biopsy etc.

SA-4800

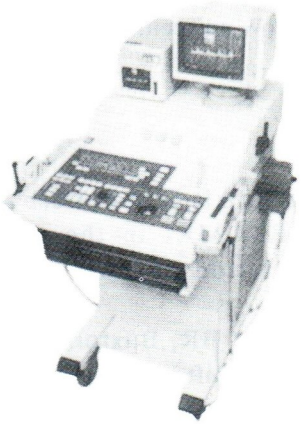

Highly sensitive CW/PW Doppler function(option)
Powerful software package for B/M/D mode
Duplex probes(L/S/C)
ECG, PCG, A-mode(option)

S.J. MEDICAL TRADING CO., LTD.
บริษัท เอส.เจ. เมดิคอล เทรดดิ้ง จำกัด
139/6 หมู่ที่ 6 ซอยชินเขต ถนนงามวงศ์วาน แขวงทุ่งสองห้อง คลองเมือง กทม. 10210
โทร. 589-0520-1, 591-4631-2 FAX: (662) 589-8185

NEUROCUTANEOUS MELANOSIS: MRI FINDINGS IN THE BRAIN WITH REVIEW OF ARTICLES

Patchrin PEKANAN[1], Pimjai SIRIWONGPAIRAT[1], Wiwatana THANOMKIAT[1,2], Panpen UTTAMAKUL[1,2].

ABSTRACT

MRI findings in a 5 years-old boy with neurocutaneous melanosis was described. Melanocytic nodules were shown in the brain parenchyma, meninges and perivascular space. They were seen as hypersignal lesions on T1W1, iso to hyposignal lesions on T2W1. There was no significant enhancement of the nodules. Literatures were reviewed concerning this condition.

Key words Melanosis, brain, MRI

Neurocutaneous melanosis (NCM) is a rare neuroectodermal dysplasia that is characterized by multiple congenital pigmented or giant hairy cutaneous nevi in conjunction with leptomeningeal proliferation of melanin-producing cells (1). Forty percents of the patients develop primary malignant melanoma of the CNS (2). Its synonyms are Rokitansky van Bogaert syndrome and neurocutaneous syndrome (3). NCM was first described by Rokitansky (4) in 1861 and almost a century later in 1948 by Van Bogaert (5).

We report an outpatient case of this syndrome, investigated by MRI study.

CASE REPORT

A 5-months-old Thai boy, was sent from other hospital to the Ramathibodi hospital for an MRI study of the brain. He had generalized congenital giant hairy nevi at the skin. He developed convulsion without neurological deficit.

MRI study showed scattered nodules, size 2 mm to 2 cm, found at left cerebellar hemisphere, pons, both medial temporal lobes, roof of the third ventricle, grey matter of high parietal lobes on both sides and at midline frontal base. In addition, there were small plaque like lesions at the meninges of both supratentorial and infratentorial levels. These nodules and plaque like lesions were hyperintense on T1W1 sequence (TR 640, TE 11/Fr, G.E. Signa 1.5T)(Fig. 1). The signal of the lesions dropped to iso to hyposignal on T2W1 sequence (TR 2800, TE 85/Ef)(Fig.2). Gd-DTPA contrast enhancement on T1W1 (TR 640,TE 11/Fr) showed no significant enhancement of the lesions.(Fig.3) There were no other abnormality in the brain.

DISCUSSION

The mature melanocyte is one of a number of cell line that are derived from a common neural crest stem-cell pool (6). Melanocytes are normally found within the basal layer of the epidermis and also in the pia mater investing the brain and spinal cord.

[1]Department of Radiology, Ramathibodi Hospital, Rama 6 Street, Bangkok 10400, Thailand.
[2]Department of Radiology, Faculty of Medicine, Songklanakarin University, Hardyai, Songkla, Thailand.

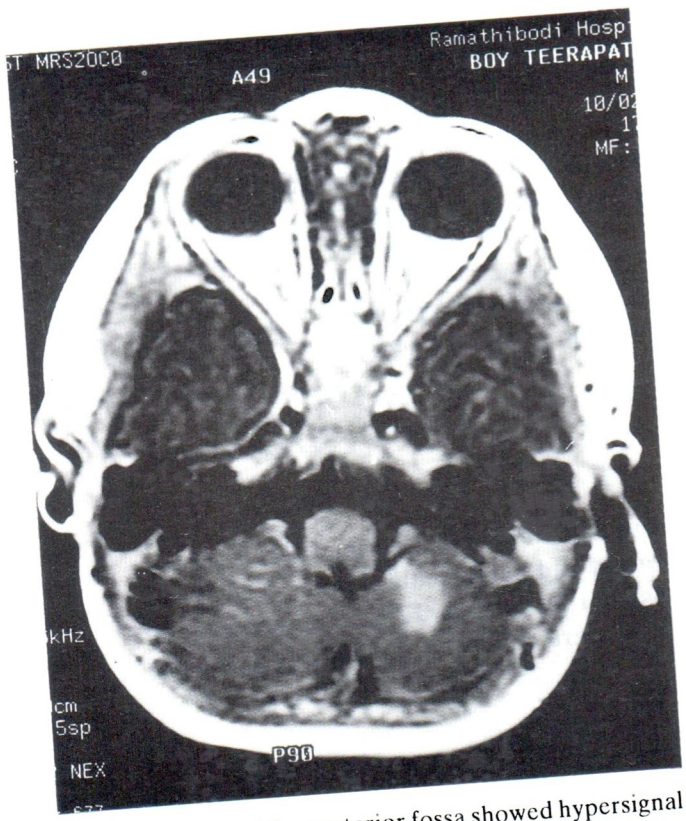

Fig. 1A. T_1WI of the posterior fossa showed hypersignal nodule at left cerebellum.

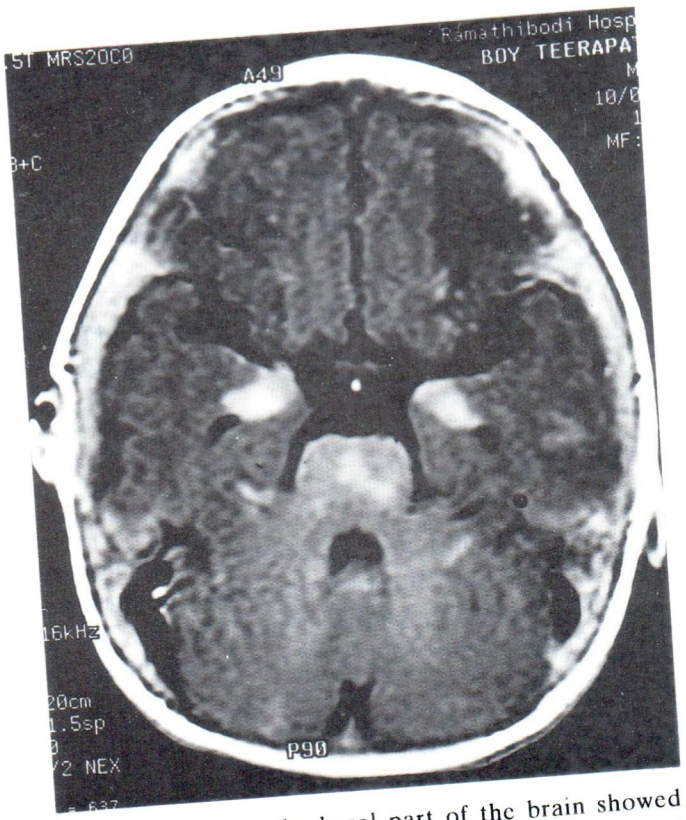

Fig. 1B. T_1WI of the basal part of the brain showed hypersignal lesions at both medial temporal lobes, pons, left cerebellum, vermian and peripheral aspect of left temporal lobe.

Neurocutaneous melanosis is thought to represent an embryonal neuroectodermal dysplasia in which excessive accumulation of melanin-producing cells occurs in a focal or diffuse distribution, within the skin and the leptomeninges (7). The pia and arachnoid membrane exhibit varying degrees of infiltration by melanotic cells. Melanotic cell infiltration may extend along the Virchow-Robin space, (8). These cells have been found also within the ventricular ependyma (9) and within the choroid plexus (10). It is frequently accompanied by a second cell type, called "melanophore". These represent melanin-laden macrophages, and it is these cells that are responsible for the parenchymal pigmentation which has been described in the basal ganglia (11), dentate nucleus (12), cerebellar hemisphere (13), pons (14), thalamus (15) and amygdaloid body (16).

The frequency of the CNS melanoma development remains unclear but was reported to be infrequent (17). Other clinical features that have been described in NCM include stillbirth (15), epilepsy (18), psychiatric disturbance (19), meningeal hemorrhage (19), cranial nerves palsies (20), subdural hemorrhage (19), and intracranial hemorrhage (22) and hydrocephalus due to obstruction of CSF circulation either at the fourth ventricle outlets or within the basal subarachnoid cisterns (7).

Involvement of the spinal cord and its coverings is variable. The cord and leptomeninges may be normal (17) or there may be varying degrees of leptomeningeal infiltration and thickening to the extent that the subarachnoid space is obliterated and the spinal cord distorted (23). Melanotic cells may infiltrate the Virchow-Robin space of the cord (11). A single malignant melanoma has been reported arising from the cord meninges (24). Associated syringomyelia was reported by Leaney (7).

Scattered abnormal areas of calcification and irregular contrast enhancement in the suprasellar cistern, in the right Sylvian fissure and the left occipital lobe were described by Leaney (7).

The lesions in our case were present both

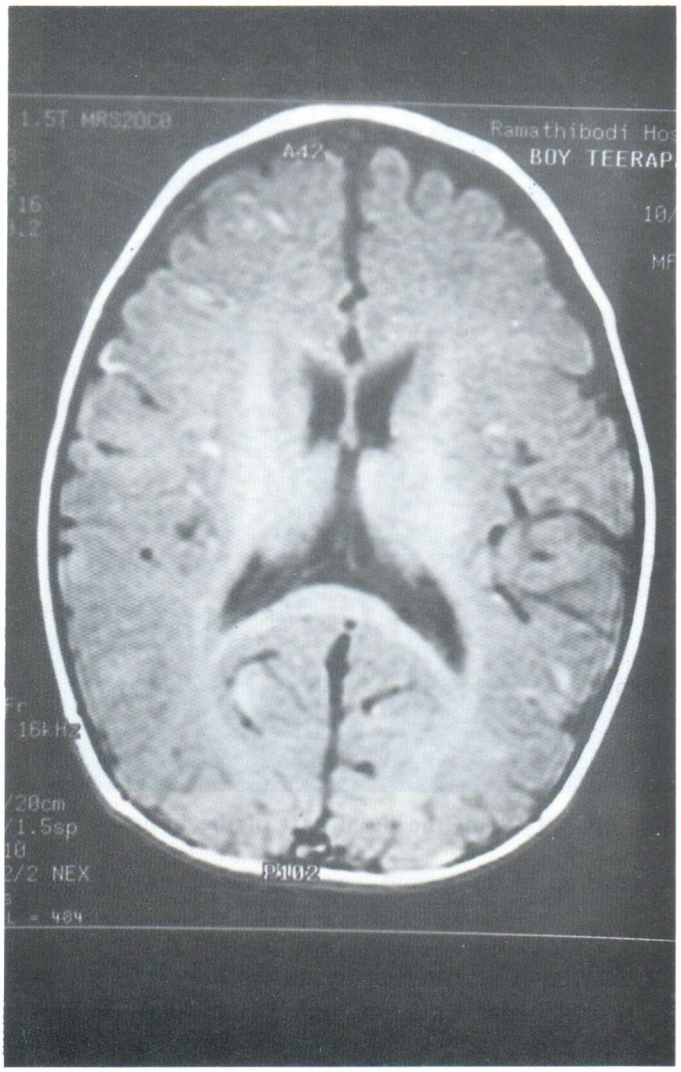

Fig. 1C. T_1WI of the brain at mid ventricular level showed hyper signal lesions scattering at convexity meninges and perivascular space.

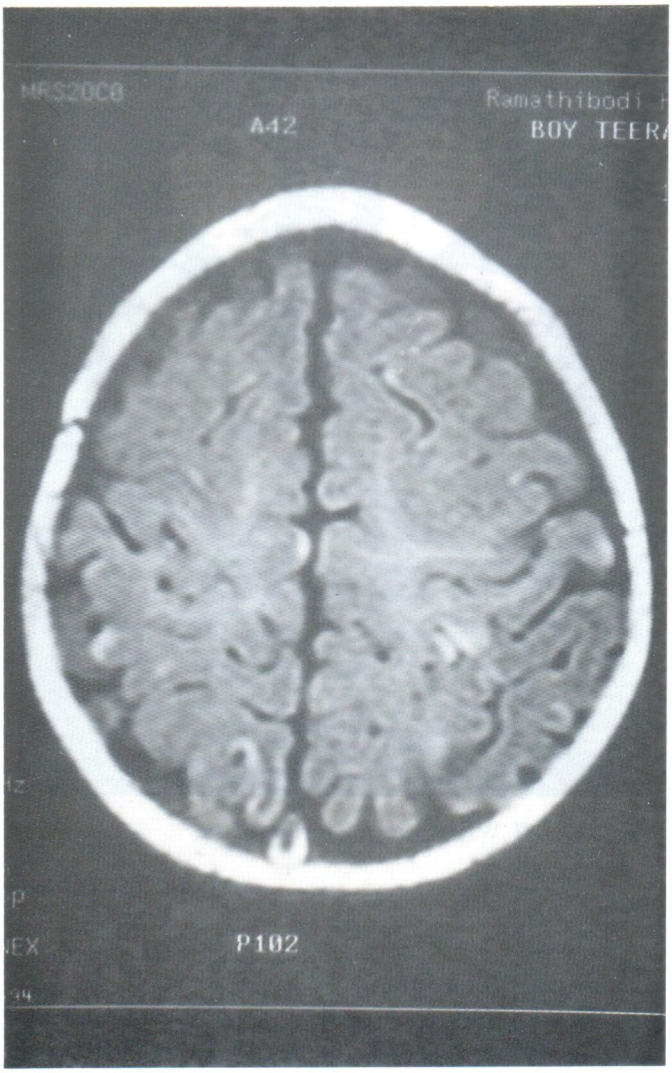

Fig. 1D. T_1WI of the brain near vertex showed bright signal lesions depositing at meninges.

in the brain parenchyma and leptomeninges, including perivascular space. The brain lesions in our case have both T1 and T2 shortening; it appears to be due to enhanced proton relaxation caused by a dipole interaction, secondary chelated metal ions within the melanin itself. Contrast enhancement showed no significant enhancement, either in the nodules or in the leptomeninges. A case report from Rhodes (1) showed strong leptomeningeal enhancement, howevere, no parenchymal nodule was present.

REFERENCES:

1. Rhodes RE, Friedman HS, Halter HP Jr et al: Contrast enhanced MR imaging of neurocutaneous melanosis. AJNR 1991;12:380-382.
2. Pont MS, Elster AD. Lesions of skin and brain. Modern imaging of the neurocutaneous syndromes. AJR 1992; 158:1193-1203.
3. Taybi H, Lachman RS: Neurocutaneous melanosis sequence;pp 329-310 in Radiology of Syndromes, Metabolic Disorders, and Skeletal Dysplasia; 3rd Ed, 1990, Chicago, Year book medical publishers, Inc
4. Rokitansky J: Ein ausgezeichneter Fall von Pigment-Mal mit ausgebreiteter Pigmentierung der inneren Hirnhaute und Ruecken-markshaeute. Allg Wien Med Ztg 1861;6:113-116.
5. Van Bogaert LC: La melanose neurocutanee diffuse heredofamiliale. Bull Acad Roy Med Belg 13:1948;13: 397-427.

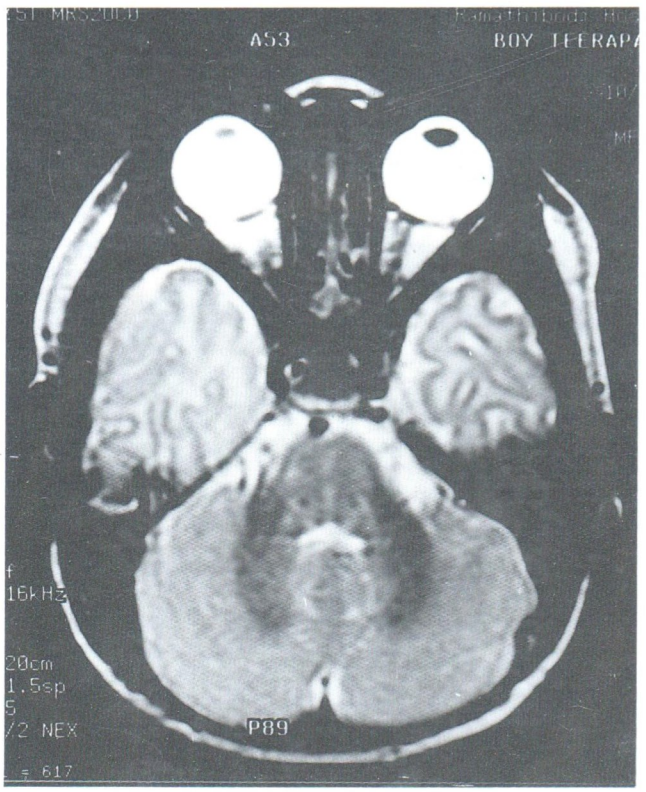

Fig. 2A. T_2WI of the posterior fossa.

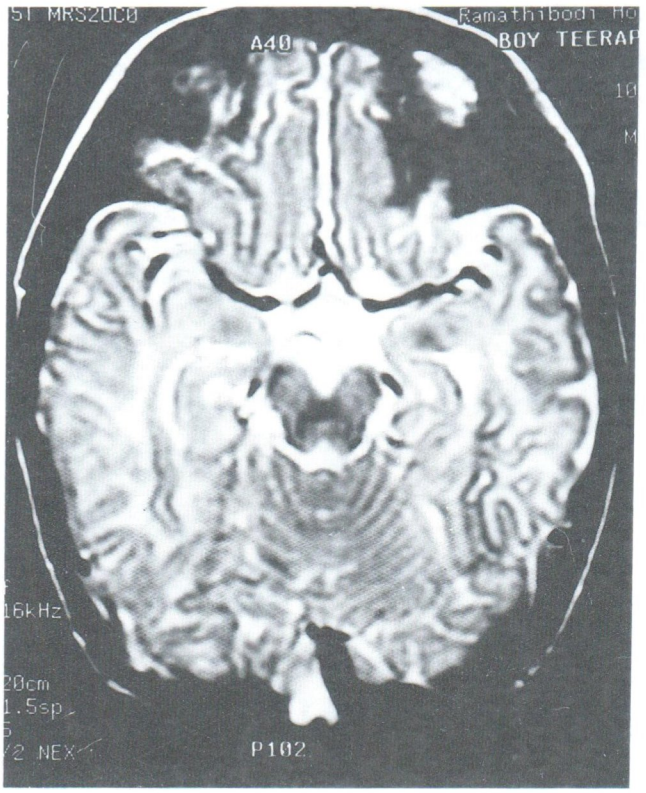

Fig. 2B. T_2WI of the basal part of the brain

Both figures showed signal drop of the lesions.

References (continued)

6. Weston JA: The regulation of normal and abnormal neural crest cell development, in Riccardi VM, Mulvihill JJ (eds): Neurofibromatosis (Von Recklinghausen Disease). Genetics, Cell Biology, and Biochemistry. Advances in Neurology, Vol 29. New York: Raven Press, 1981, pp 77-96.
7. Leaney BJ et: Neurocutaneous melanosis with hydro- cephalus and syringomyelia. J Neurosurg 1985;62: 148-152.
8. Bouton J: Primary melanoma of the loptomeninges. J Clin PATHO 1958;11:122-127.
9. Harper CG, Thomas DGT: Neurocutaneous melanosis. J Neurol Neurosurg Psychiatry 1974;37:760-763.
10. Fox H: Neurocutaneous melanosis, in Vinken PJ, Bruyn GW (eds): The Phakomatoses. Handbook of Clinical Neurology, Vol 14. Amsterdam: North-Holland, 1972, pp 414-428.
11. Slaughter JC, Hardman JM, Kempe LG, et al: Neurocutaneous melanosis and leptomeningeal melanomatosis in children. Arch Pathol 1969;88: 298-304.
12. Berlinger W: Ein Beitrag zur epithelialen Genese des Melanins. Virchows Arch (Pathol Anat) 1915;29: 328-365.
13. Fox H, Emery JL, Goodbody RA, et al: Neurocutaneous melanosis. Arch Dis Child 1964;39:508-516.
14. Farnell FJ, Globus JH: Primary melanoblastosis of the leptomeninges and brain. Arch Neurol Psychiatry 1931; 25:803-823.
15. Grahl F: Angeborener ausgedehnter Naevus pigmentosus in Verbindung mit Pigmentflecken im Gehirn. Beitr Pathol Anat 1906;39:66-81.
16. Ishikawa T, Nishi T, Shimada H, et al: Two cases of melanose neurocutanee with development of malignant melanoma: a microspectrophotometric and electron microscopic study. Gann 1975;66:277-289.
17. Bjoerneboe M: Primares Melanosarkom des Gehirns, massenhafte Naevi pigmentosi der Haut, ausgedehnte Neurofibromatose der Hautnerven. Frankfurt Z Pathol 1934;47:363-373.
18. Brandt RA, Schwartzman JS, Naspita C: (Neurocutaneous melanosis. Report of a case). Arq Neuropsoquiatr 1978 (Por); 36: 147-154.

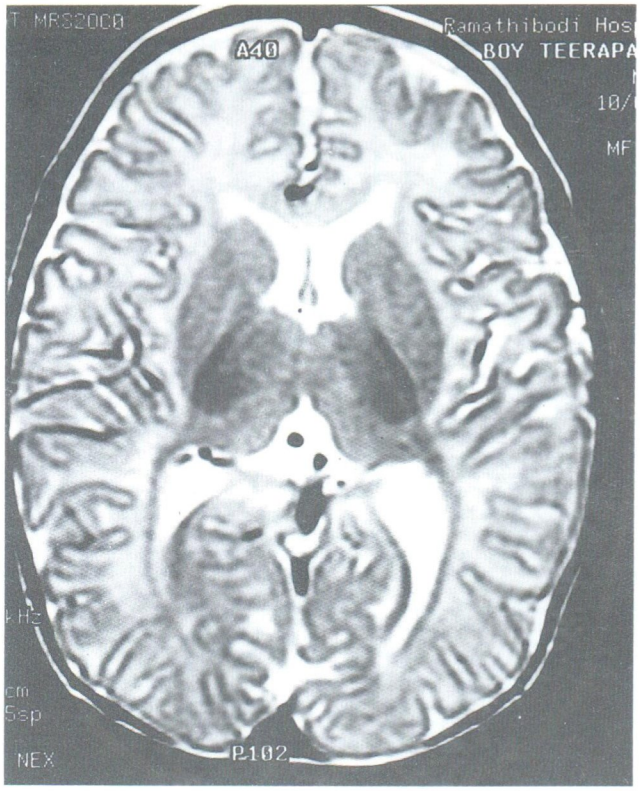

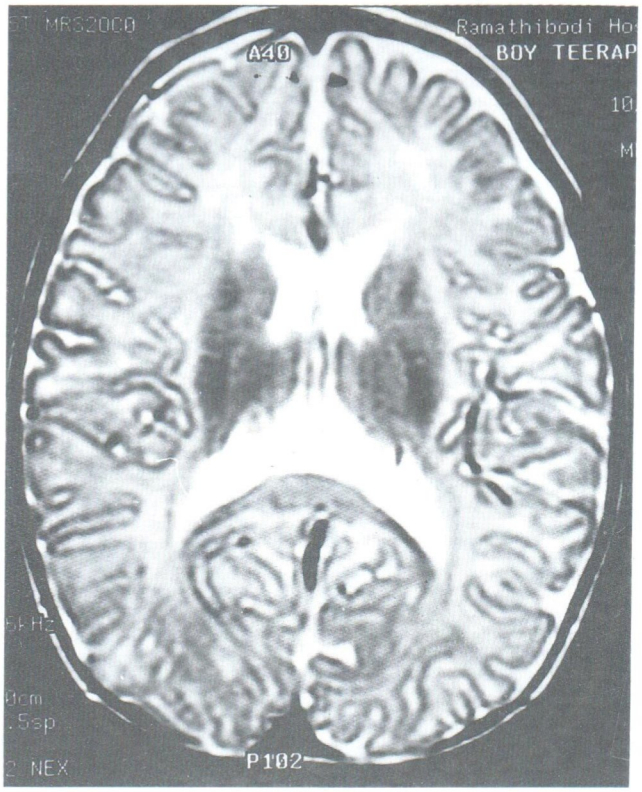

Fig. 2C. and Fig. 2D. showed T_2WI of the brain, the bright mass of the CSF obscured the bright signal deposits at the meninges.

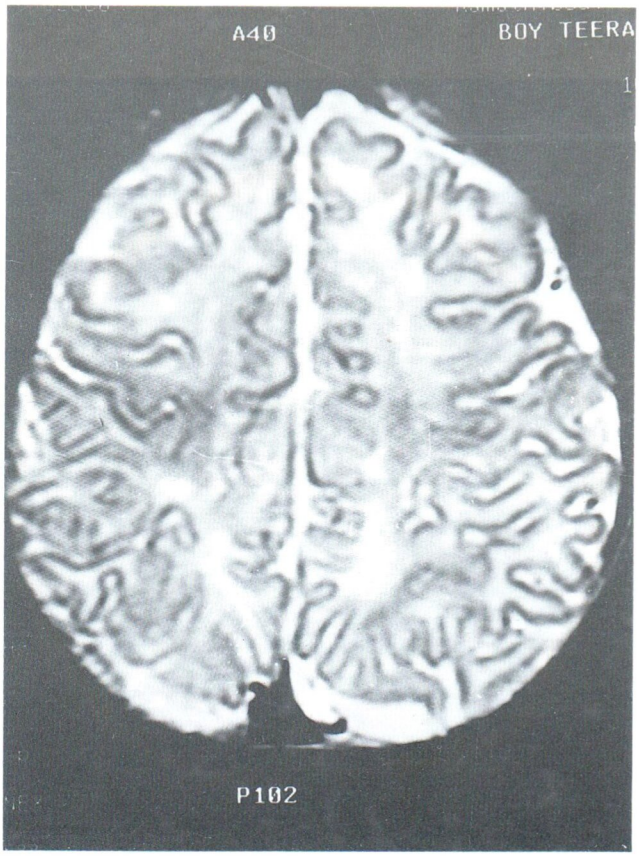

Fig. 2E. T_2WI of the brain at vertex showed obscuration of the meningeal deposits by the bright CSF signal.

References (continued)

19. Daily R, Forthomme J, Samson M, et al: Melanose neuro-cutanee a evolution tumorale. Une observation anatomo-clinique. Presse Med 1965;73:2867-2872.
20. Reed WB, Becker SW, Becker SW Jr, et al: Giant pigmented nevi, melanoma, and leptomeningeal melanocytosis. A clinical and histopathological study. Arch Dermatol 1965;91:100-119.
21. Komatus S,Takaku A, Suzuki J: (Neurocutaneous malanosis with chronic subdural hematoma on the left side and later on the right side-a case study). Clin Neurol 1974 (Jpn);14:855-860.
22. Medoc J, Folle JA: Malignant diffuse melanosis of the meninges of the neuro axis causing a hemorrhagic cerebrovascular type accident. Acta Neurol Lat Am 1969;15:106-114.
23. Hoffman HJ, Freeman A: Primary malignant leptomeningeal melanoma in association with giant hairy nevi. Report of two cases. J. Neurosurg 1967; 26:62-71.
24. Fasske E:Zur Genese der primaren Melanosarkome der Leptomeninx bei Saeuglingen. Zentrabl Allg Pathol 1958;98:113-121.

Fig.3A. T1WI of the brain showed a large hyper-signal nodule at 3rd ventricular roof and smaller meningeal deposits at convexity and at both thalami.

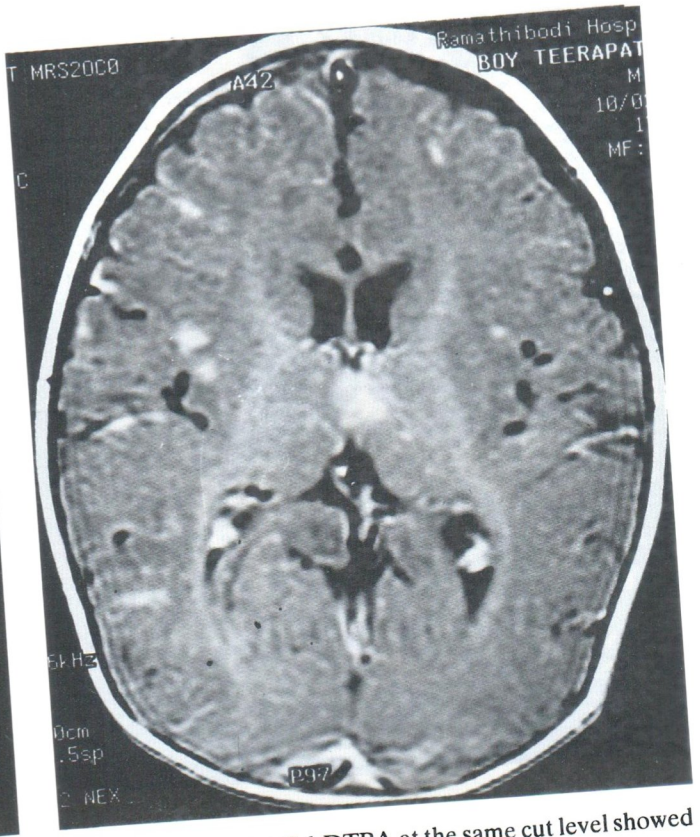

Fig. 3B. T1WI post Gd-DTPA at the same cut level showed no significant enhancement of the lesions.

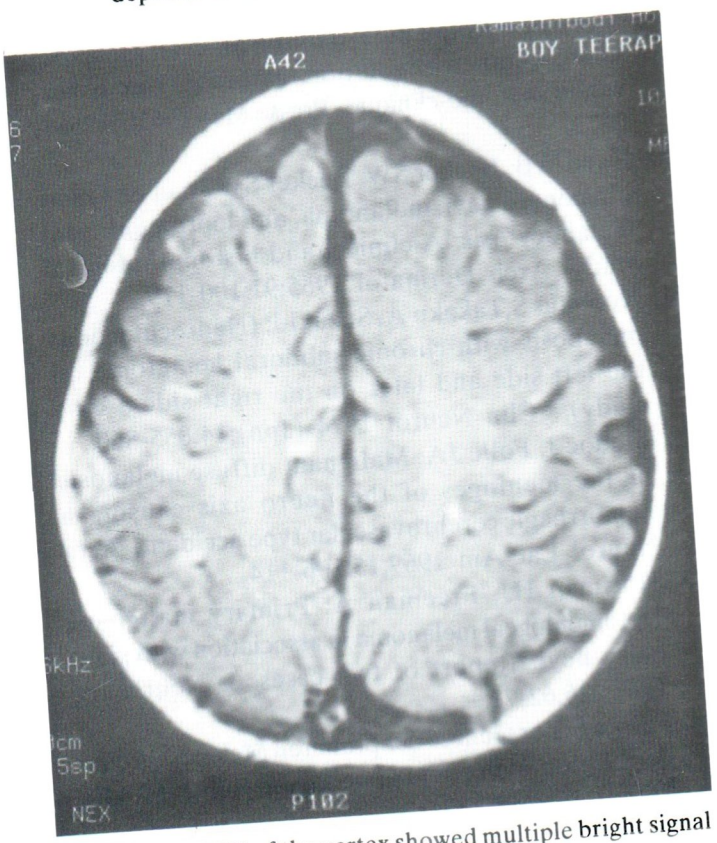

Fig. 3C. T1WI of the vertex showed multiple bright signal meningeal deposits

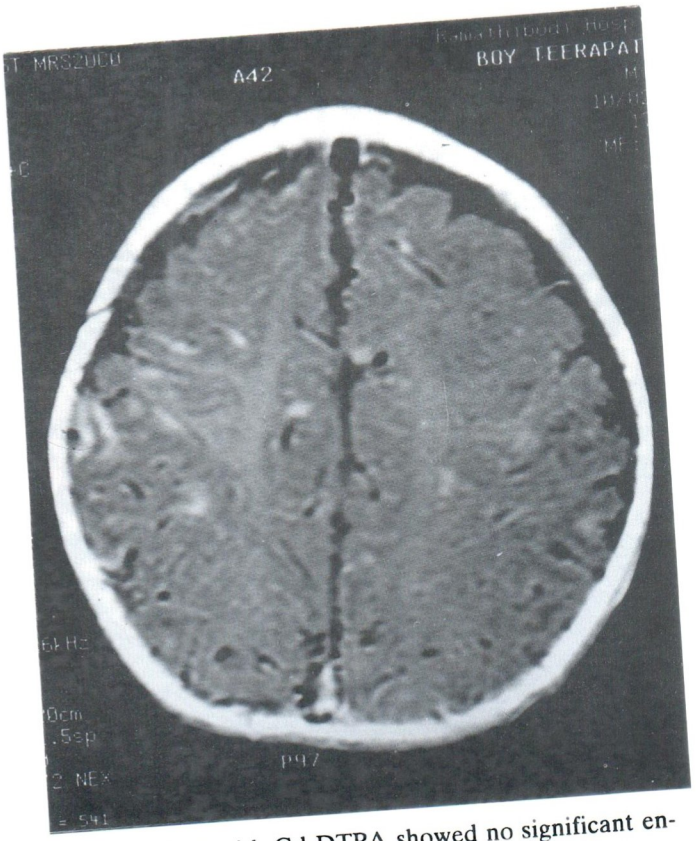

Fig. 3D. T1WI with Gd-DTPA showed no significant enhancement of the lesion .

DUCTAL LUCENCY IN X-RAY MAMMOGRAPHY

Suphaneewan JAOVISIDHA[1], Kamolpong, OSATHAVANICHVONGS[2], Patchrin PEKANAN[1], Pimjai SIRIWONGPAIRAT[1]

ABSTRACT

x-ray mammography is a widely performed procedure in the diagnosis of the diseases of the breast,and is able to reveal ductal abnormalities such as ductal dilatation & calcification. We, hereby, report a case of ductal lucency demonstrated by X-ray mammography, which is an uncommon finding. It may represent normal physiology or pathological processes.

INTRODUCTION

Ductal lucency is an uncommon mammographic finding, described when the decreased-density ductal arborization is observed through the density of surrounding breast tissue. Due to the larger size of the lactiferous ducts as they converging to areolar area, demonstration of ductal lucency is more easily in central part of the breast. In this report, we present a non-lactating patient coming to the surgical clinic with a suspected mass in her Rt. breast, and further mammographic study disclosed lucency of the ducts in another breast.

CASE REPORT

In May 1993, a 26-year-old Thai female came to the surgical clinic due to suspicion of mass in her Rt. breast. She was single, and had no history of pregnancy, nipple discharge, or previous surgery. The breast examination reveals nodularity of right breast at the upper-inner and upper-outer quadrants. The left breast and both axillary areas were unremarkable. Physical chest examination revealed normal heart and lungs. Abdominal examination showed no abnormality. X-ray and ultrasonographic mammography were performed. The right breast was normal, as well as the ultrasonographic mammography of the left breast. The interesting finding was the lucency of the ductal arborization in her left breast seen in X-ray mammography. (Fig. 1-4)

Since the patient had no symptom concerning the left breast, specific treatment was not given at that time. The patient was followed up at the surgical clinic at 2, 6, & 12 months after the X-ray mammography for the right breast nodularity. There was still no problem in her left breast.

DISCUSSION

In the adult mammary gland, there are 15 to 20 irregular lobes of breast tissue converging to the nipple, seperated by thin fibrous septa that are irregular and poorly defined. Each lobe is drained by its own lactiferous duct. On cross section of the nipple, each major duct can be seen, 2 to 4.5 mm in diameter, lined by stratified squamous epithelium. The ducts end in a local dilatation beneath the areola, the sinus lac-

[1] Department of Radiology, Faculty of Medicine at Ramathibodi Hospital : Rama 6 street, Bangkok 10400, Thailand
[2] Institute of scientific, development & technology, Mahidol University : Pinklao-Nakornchaisri Street, Bangkok Thailand

tiferous. Each duct is constricted as it passes to the summit of the nipple and ends as an independent opening, 0.4 to 0.7 mm in diameter; or several ducts may join below the summit of the nipple and drain through a common orifice. Thus, the excretory ducts may be as few as six to eight. Distention of the subareolar ducts with inspissated secretions and epithelial debris is considered a normal anatomic variation [1].

The breasts also have cyclic variation with the endometrium [2,3,5,6,7]. During the **"proliferative phase"** of the menstrual cycle (days 3-7) there is an increase in the number of mitoses of the acinar cells of the lobules without secretions. In **"follicular phase"** (days 8-14), the acini appear to have more collagen, while mitotic activities diminished. **"Luteal phase"** occurs between days 15-20, revealing vacuolization in the cells of the lobule and secretions are visible in the ducts. Loosening of the stroma within the lobules are noted followed by true apocrine secretion into the distended duct lumen during **"secretory phase"**(days 21-27). The tissue within the lobules become edematous and there is venous congestion, which probably accounts for some of the discomfort many women experienced premenstrually. Active secretion appears to end during the **"menstrual phase"** of day 28 to day 2, and then the cycle repeat itself [2,3].

The lobular as well as the ductal systems are capable of secretion and absorption. Evidence of *milk secretion* may even be found in the normal breast during non-lactating periods in the form of *secretory lobules*. But even apparently resting lobules and ducts produce small amount of secretory products e.g. various mucosubstances and fluid which are partly re-absorbed and partly transported to the surface via the ductal system [5]. The concentration of fat in these secretions, if high, will account for the ductal lucency observed in X-ray mammography performed in non-lactating patient, and the nipple discharge may not be found

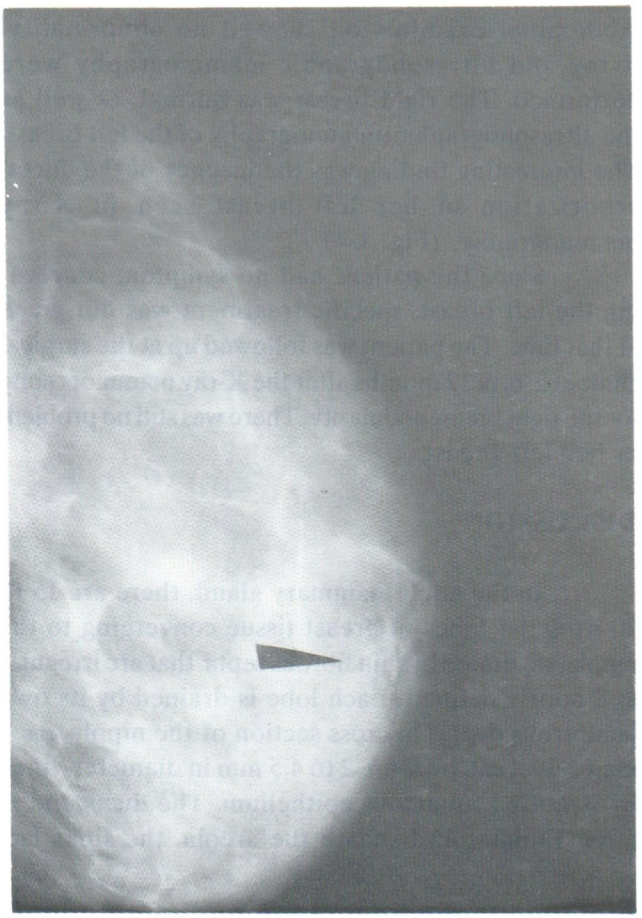

Fig. 1

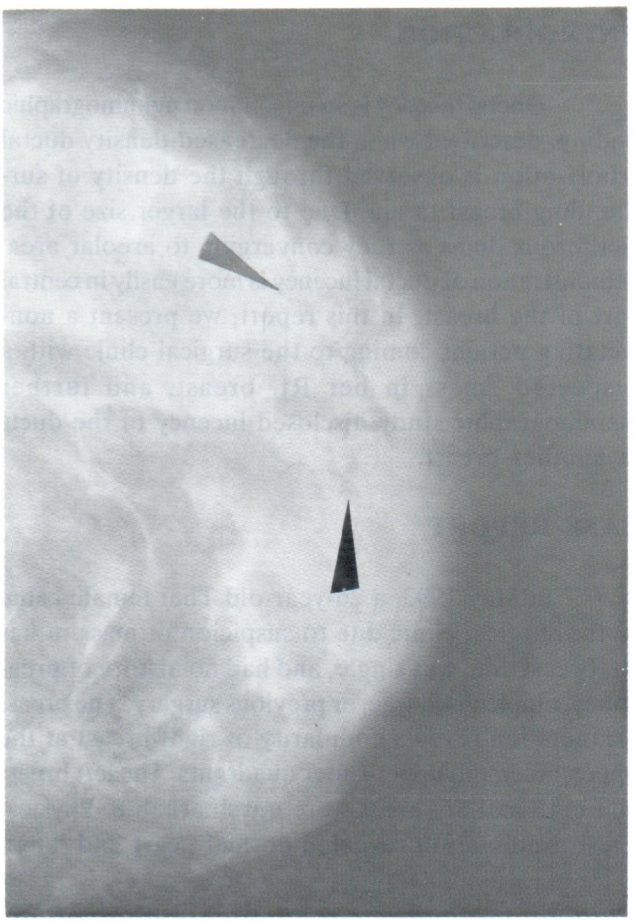

Fig. 2

X-ray mammography in medio-lateral oblique projection (Fig.1) and cranio-caudal projection (Fig.2) of the patient's left breast showed ductal lucency at juxta-areolar and subareolar area

due to resorption of the secreted materials by the lobular and ductal systems.

Occasionally, breast lobules may contain dilated ductules with epithelial changes identical to those seen in pregnancy or lactation. This pregnancy-like change occurs in women who are neither pregnant nor lactating. Some women are nulliparous. The frequency of this change is remarkably constant in both autopsy and surgical series, which is about 3% in each series [6].

The ductal lucency also can be seen if we perform the mammogram during lactation, owing to when lactation takes place, milk from apocrine cells and membrane-encapsulated fat globules from the epithelial cells are secreted to fill the lactiferous ducts results in widening of their caliber [2,4]. Following the end of lactation, the milk secretion ceases, generally some ductal ectasia remains and involution of the lactiferous ducts may be prolonged [4]. It takes at least 3 months after cessation of lactation for the breast to return to its nonlactational histologic appearance [6].

The **Chiari-Frommel Syndrome** is a condition in which there is prolonged lactation which may persist for months or years after pregnancy. It appears to be related to abnormal secretory and neural ovarian function. Other components of the syndrome include uterine atrophy, secondary amenorrhea, headache, back pain and depression. The Chiari-Frommel syndrome is rare and should not be confused with the much more frequent occurrence of persistent serous breast secretion following cessation of lactation. The latter belongs to the spectrum of **"secretory disease"** and is caused by incomplete or prolonged involution of lactiferous ducts. This condition may be verified with ductography. A natural contrast ductogram results whenever there is a high concentration of fat in the ductal contents, resulting from pathological lactation [4].

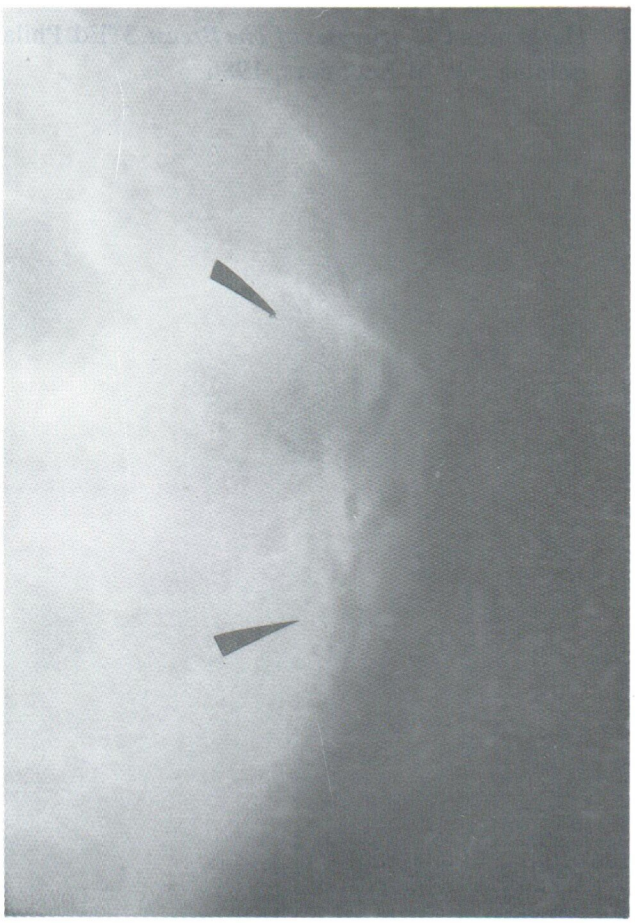

Fig. 3

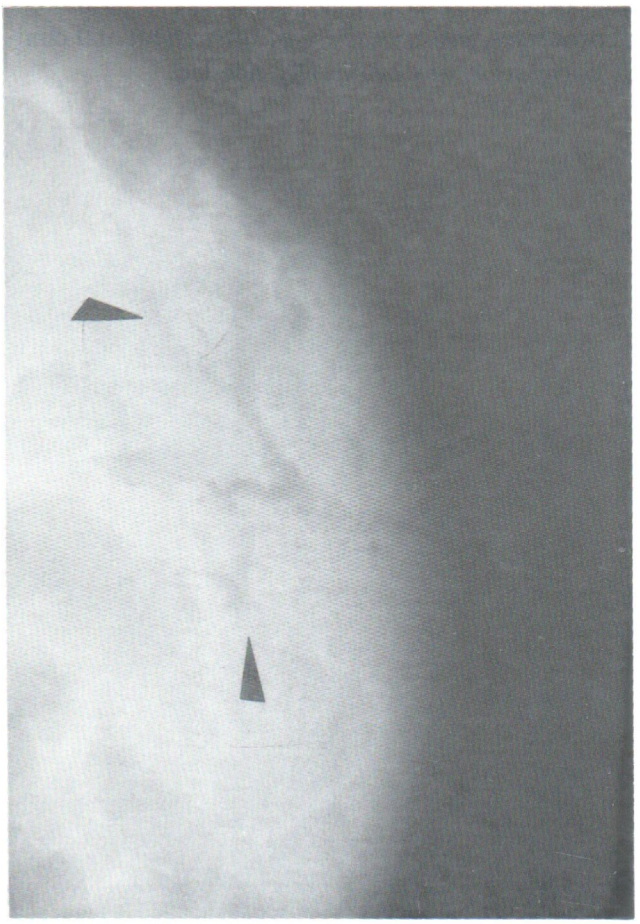

Fig. 4

Fig.3-4 : Magnification view of the lucent ducts from Fig.1 and Fig.2 respectively

A variant of Chiari-Frommel syndrome is the **Forbes-Albright syndrome** which consists of amenorrhea and galactorrhea associated with acromegaly, without any preceding pregnancy [4].

Spontaneous lactation has been documented followingchest wall trauma . Surgery on the chest wall that may or may not involve the breast may produce spontaneous lactation. The patient, after one week of resection of pulmonary hamartoma, was reported to begin lactating normal milk which change to serous discharge with menstruation but returned to normal milk following menstruation [1].

In conclusion, we have reported a case of mammographically demonstrated ductal lucency. This is an uncommon finding, and particularly uncommon when observed in the patient without preceding pregnancy, chest wall trauma, history of nipple discharge, or any complaint about that breast. According to one-year follow up without any sign or symptom, we considered that the ductal lucency in this patient is due to the normal physiologic variation of the breast. However, the ductal lucency in X-ray mammography can represent either normal physiology or pathological processes, history review of the patient and clinical correlation are eventually needed.

ACKNOWLEDGEMENT :

We would like to thank Urupong Medical Center for providing materials in this study, and Mrs.R. Jaovisidha for preparing the manuscript.

REFERENCES

1. Egan RL. *Breast Imaging : Diagnosis & Morphology of Breast Diseases.* Philadelphia : W B Suanders, 1988
2. Kopans DB. *Breast Imaging.* Philadelphia : J B Lippincott, 1989
3. Vogel PM, Georgiade NG, Fetter BF, et al. The correlation of histologic changes in the human breast with the menstrual cycle. *Am J Pathol* 1981;104(1):23
4. Hoeffken W, Lanyi M. *Mammography.* Stuttgart : Georg THieme Publishers 1977
5. Linell F, Ljungberg O. *Atlas of Breast Pathology.* Copenhagen : Munksgaard, 1984
6. Fechner RE, Mills SE. *Breast Pathology : Benign Proliferation, Atypias, and In Situ Carcinomas.* Chicago: ASCPPress, 1990
7. Haagensen CD. *Diseases of The Breast*, 3rdEd. Philadelphia : W B Saunders, 1986

BENIGN BREAST MASSES SIMULATING CARCINOMA: MAMMOGRAPHIC FINDINGS

Malai MUTTARAK, M.D.,* Hongsin TRAKOONTIVAKORN, M.D.,**
Benjaporn CHAIWUM, M.D.,***

ABSTRACT

Mammography is now a more widely used procedure in the diagnosis of breast disease. The only breast diagnosis of importance is carcinoma because it can cause a woman's death. The pitfalls of mammographic diagnosis are increasingly recognised. The roentgen appearance of some benign disease process may simulate carcinoma. Accurate diagnosis depends on a wide knowledge of various disease processes. We present 23 cases of different benign lesions that may be easily confused with carcinoma.

INTRODUCTION

The goal of accurate mammographic interpretation is to identify malignancy of the breast and distinguish between normal and abnornal breast tissue. An irregular marginated mass on mammography is a primary sign of breast carcinoma. However, a variety of benign lesions may also present as an irregularly marginated mass radiographically. (1) We present various benign lesions that may simulate carcinoma on mammography and suggest criteria for a differential diagnosis.

MATERIALS AND METHODS

We have collected a total of 23 cases of ill-defined or irregularly marginated mass on mammography which proved to be benign lesions. Mammograms were obtained with dedicated screen-film mammographic units (Lorad MII or MIII). Standard craniocaudal and mediolateral oblique views of each breast were obtained and magnification or other supplemental views were taken when indicated. Sonograms were obtained in all patients using 5-7.5 MHz linear array transducers (Aloka SSD-630,650). Excisional biopsy was done in 7 cases, incision and drainage in 1 case, and aspiration in 4 cases. Culture was obtained in 5 cases. Seven cases were treated conservatively.

RESULTS

Table 1. lists the diagnosis and number of patients.

There were 9 cases of abscess in the non-lactating breast. Mammography showed an ill-defined mass (Fig 1A) and sonography showed an ill-defined echoic mass with central low echo (Fig 1B). Histologic section revealed abscess in one case. Cultures were reported as having no growth in 2, staphylococcus in 2 and proteus in one case. Three cases were treated conservatively with antibiotics.

The histopathological diagnosis of fibroadenoma was confirmed in two cases. One was 54 years old and the other one was 47 years old. Mammograms showed an irregular mass (Fig 3) with solid appearance from ultrasound in both cases.

Biopsy findings confirmed fat necrosis in two irregular masses (Fig 4).

*Department of Radiology,**Department of Surgery, ***Department of Pathology,
Faculty of Medicine, Chiang Mai University, Chiang Mai 50200 THAILAND.

Localized fibrocystic change was pathologically proved in two cases (Fig 5&6), one presenting as an irregular mass and the other as an ill-defined mass.

Three cases of hematoma were diagnosed, two resulting from surgery and one from blunt trauma. Mammographic findings were irregular mass, (Fig 7) ill-defined mass and well-defined mass with partlially irregular margin (Fig 8) in one case each. Sonography showed mixed echoic mass in all cases. Symptomatic treatment showed resolution of the lesions in all cases.

Post surgical scar was diagnosed in two cases that had irregular mass lesions (Fig 9). Follow up study showed stability of the lesion in one case and resolution of the lesion in the other one.

Three cases showed triangular density at the medial aspect of the breast on the craniocaudal view (Fig 10) with no palpable mass. No definite lesion was found on sonography. Sternal insertion of the pectoral muscle was diagnosed in these cases.

DISCUSSION

Abscess of the breast in the lactating period is a well known disease, and the diagnosis can be easily

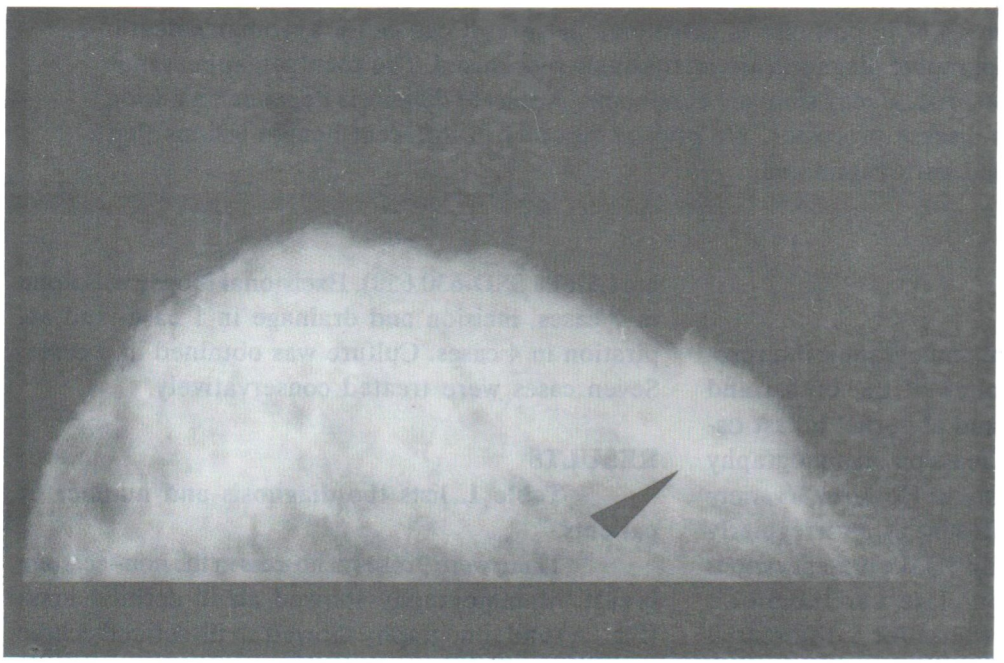

Fig 1A.
43-year-old woman with mass and pain in the right breast. Exagerated craniocaudal view of the right breast showing an ill-defined mass (arrow head) in the tail of the breast.

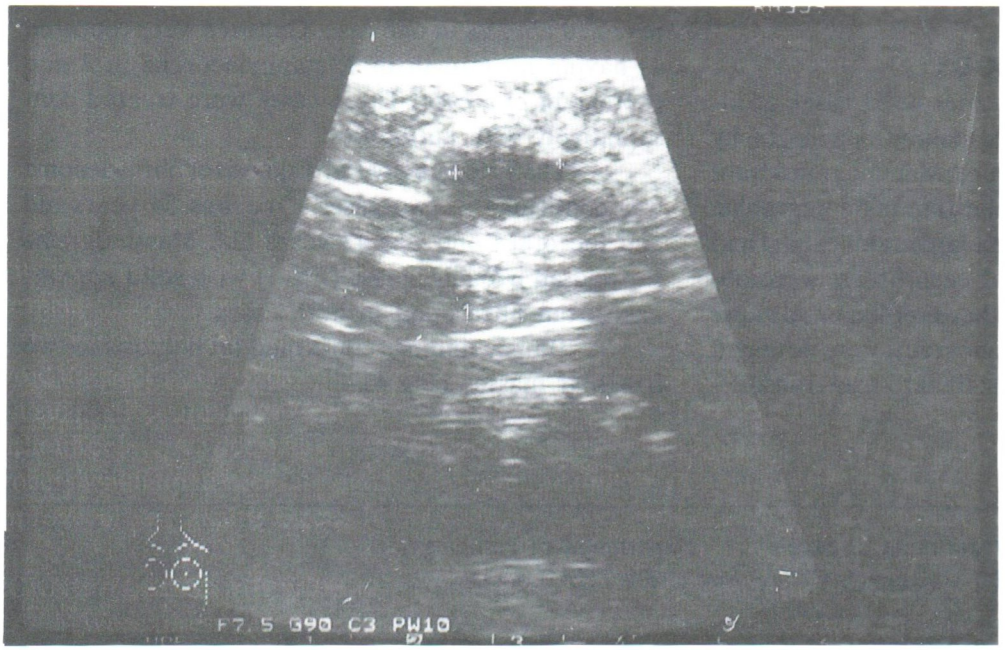

Fig 1B.
Ultrasound: an ill-defined echoic mass with central low echo.

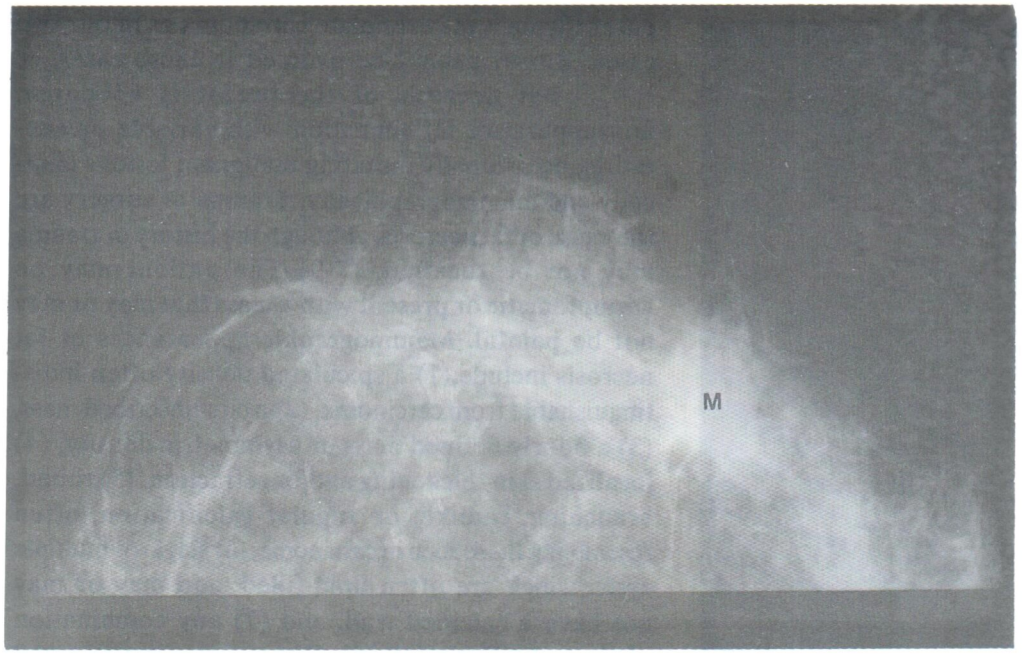

Fig 2.
42-year-old woman with pain in the right breast. Craniocaudal view of the right breast showing an irregular mass (M). Aspiration obtained pus.

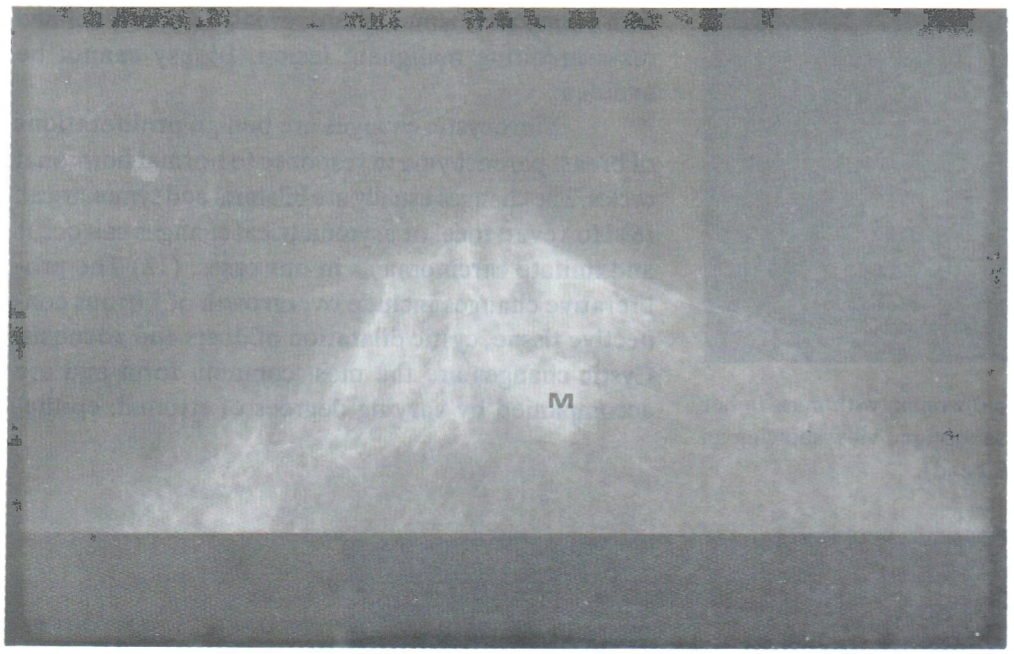

Fig 3.
Fibroadenoma. 54-year-old woman, had a history of right mastectomy for breast carcinoma 2 year ago. She was referred for her first routine follow-up mammograms. Left craniocaudal view showing a well circumscribe mass but indistinct anterior border (M). Biopsy was recommended and revealed fibroadenoma.

made from clinical presentation. Abscess in the non-lactating breast, however is less common and more difficult to diagnose. (2) The patients may present with a breast mass without typical signs of inflammation, and mammography will therefore play a role to exclude malignancy. The most common mammographic findings were a focal area of increased density with spiculation or architectural distortion which can simulate carcinoma. (3-4) Sonographic findings of ill-defined echoic mass with central low echo are helpful for diagnosis of abscess. (5) Diagnostic aspiration and antibiotics might be definitive and prevent unnecessary surgery.

Fibroadenoma is an estrogen-induced tumor of the breast, which usually appears before the age of 30 years. Mammographic findings of a fibroadenoma are a very well defined, round, ovoid or lobulated lesion. This tumor usually regresses after menopause because of mucoid degeneration hyalinization and involution of epithelial components. (6) When fibroadenoma occurs in a patient over 30 years, uncalcified and partially obscured by overlying breast

Fig 4. Fat necrosis. 42-year old woman with mass in her left breast. Mediolateral oblique view showing an irregular mass (arrow head).

parenchyma it may simulate carcinoma as in our two cases. Biopsy cannot be avoided in these cases.

Fat necrosis of the breast is a benign, nonsuppurative inflammation with variable presentation, occasionally imitating malignant lesions clinically and mammographically. Trauma or surgery are the cause of fat necrosis, although the history of trauma may not be recalled. (7-9) The patient may be asymptomatic or present with a mass that may or may not be painful. Mammographic appearances of fat necrosis include;(1) a spiculated density often indistinguishable from carcinoma, (2) a circumscribed mass, (3) a poorly defined mass or asymmetric density, (4) localized skin thickening and/or retraction, (5) round, branching, rodlike, or angular calcification, often resembling those seen in carcinoma, (6) single or multiple cysts, which are often lipid-filled, and may or may not have a calcified wall, and (7) any combination of these findings. (10-11) Our two cases presented with a lump and mammograms revealed a poorly defined mass imitating malignant lesion. Biopsy cannot be avoided.

Fibrocystic changes are benign proliferations of breast parenchyma in response to normal hormonal cycles. The changes usually are bilateral and symmetrical. (6) However, focal or asymmetrical changes can occur and imitate carcinoma as in our cases. (12) The proliferative changes include overgrowth of fibrous connective tissue, cystic dilatation of ducts and adenosis. Cystic changes are the most common form and are accompanied by varying degrees of stromal, epithe-

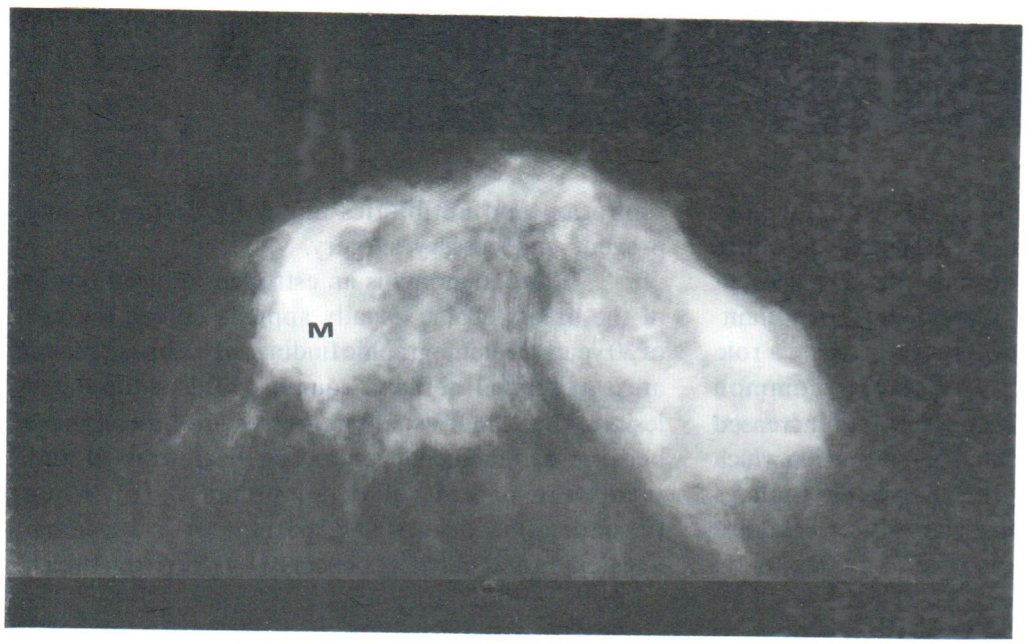

Fig 5.
Focal fibrocystic change. 40-year-old woman with mass in her right breast. Craniocaudaul view showing an irregular mass (M).

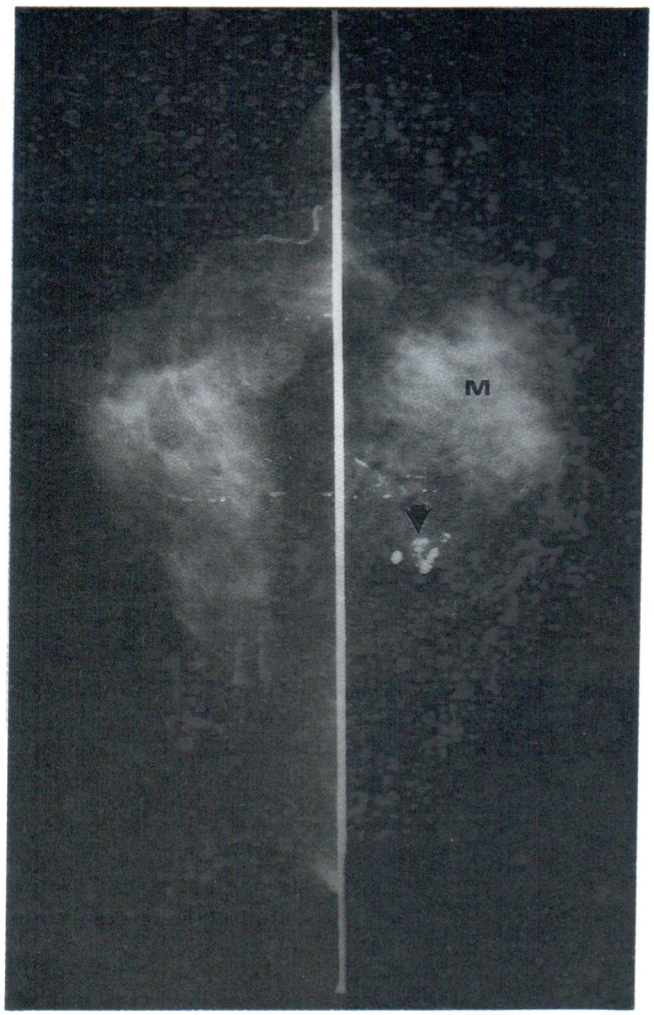

Fig 6. Focal fibrocystic change. 64-year-old woman with mass in her left breast. Bilateral craniocaudal views showing an ill-defined mass in the left breast (M). Calcified degenerating fibroadenoma is also seen (arrow head.)

lial hyperplasia and apocrine metaplasia. Fibrous connective tissue proliferation is probably the least common form and is responsible for many so-calles clinical "thickenings" of the breast. We can not avoid biopsy in these two cases.

Hematoma may result from blunt or surgical trauma. It may be loculated and appear as a well-defined mass or be interstitial and dissect through the tissues, creating a diffuse density on mammography. Sonographic appearance of an acute hematoma is a mixture of echogenic areas and hypoechoic fluid pockets. Mature hematoma has the typical sonographic appearance of a well-circumscribed, anechoic mass with posterior enhancement. (6,13-15) Overlying skin ecchymosis or surgical scar may suggest the diagnosis. Hematoma usually resolves within 2-4 weeks, although some persist 8 weeks or longer. The combination of history, mammographic and sonographic appearance can suggest the diagnosis and avoid unnecessary biopsy.

Intraparenchymal scars after biopsy appear as poorly defined masses, often with spiculated margins. The rate of scar formation depends on the size of parenchymal resection, volume of post surgical fluid collection and whether it was drained postsurgically. Benign biopsy changes often resolve more quickly and completely. Radiolucencies within the central area of soft-tissue density suggest scarring. The spicules of carcinoma are symmetrically placed around the periphery of the tumor mass and are extremely straight, but the spicules of scarring are asymmetric and somewhat curvilinear. (14-18) However, Sickles et al did

Fig 7.
Hematoma. 25-year-old woman with mass in her right breast. She had history of nipple operation 1 month earlier. Right craniocaudal view showing an irregular mass (M).

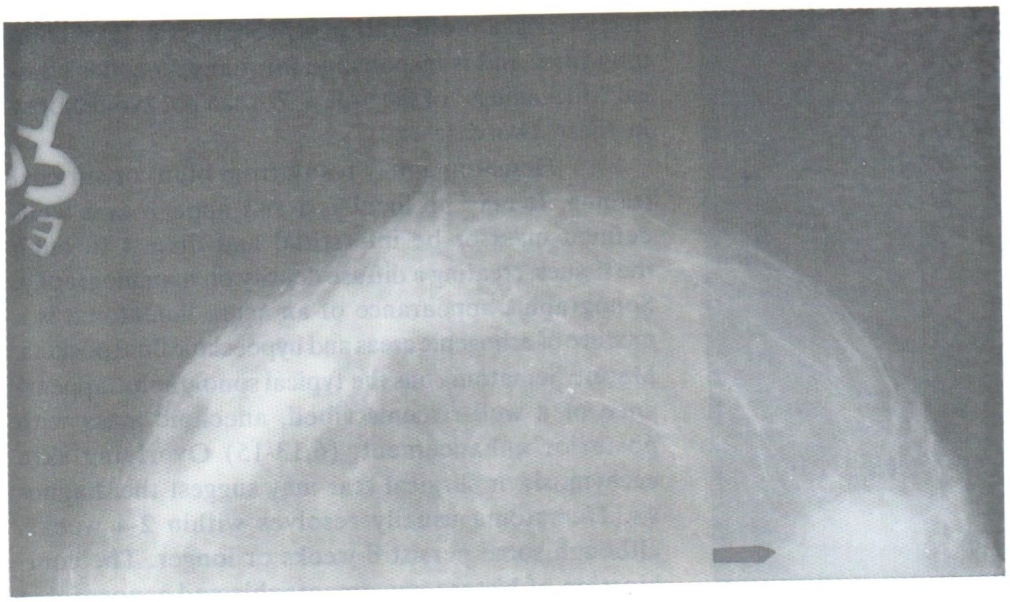

Fig 8A.
Hematoma. 40-year-old woman with history of blunt trauma and a lump in her left breast. A. craniocaudal view of the left breast showing a well-defined mass with partially irregular border (arrow).

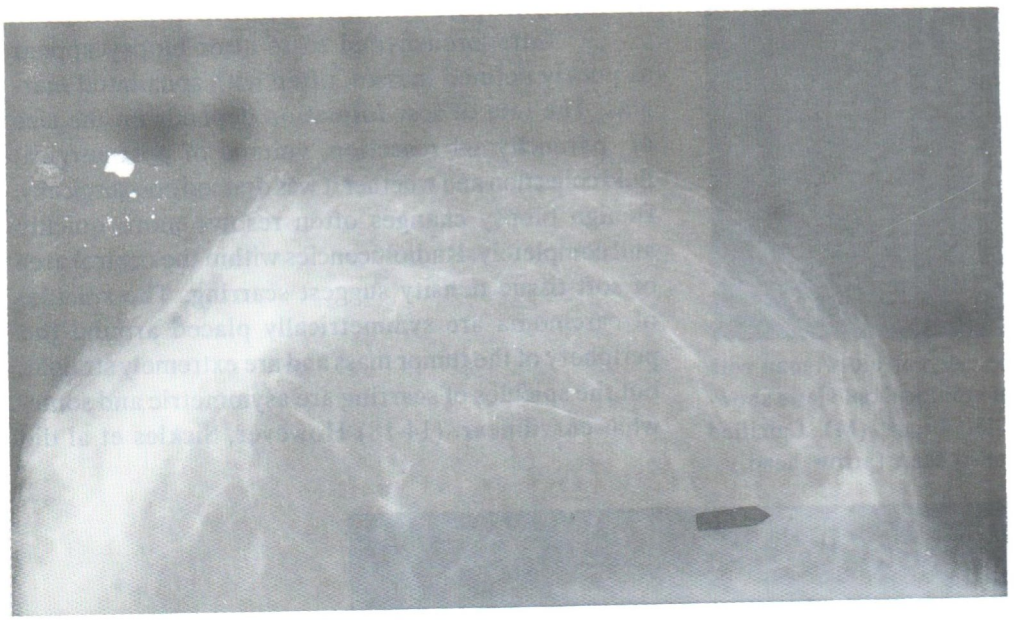

Fig 8B.
follow up study 2 weeks later showing resolution of hematoma.

not rely on these criteria. The clinical history, physical examination and comparison with previous studies are necessary for management. (16,17) On physical examination scarring uncomplicated by fat necrosis is perceived as induration rather than a mass. On sequential studies, scar should decrease in size. Progression of abnormalities should prompt immediate biopsy.

Britton et at reported the presence of a rounded or triangular density at the medial aspect of the breast on craniocaudal view with no palpable mass. This density represents the medial portion of the pectoral muscle, which is included because of vigorous retraction of the breast and slight external rotation during positioning for the craniocaudal view. (19) It may be seen unilaterally, bilaterally or may not be imaged in other women due to a variety of normal appearances of the pectoral muscle. Familiarity with its typical appearance can prevent biopsy of this normal structure.

In summary, the key mammographic feature distinguishing carcinoma from benign breast masses

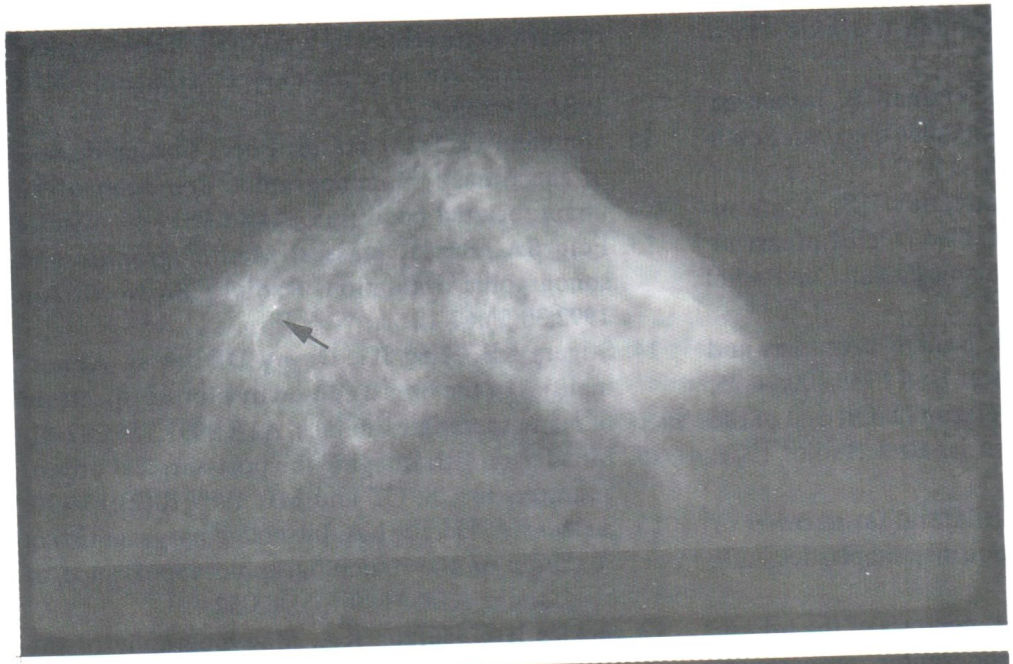

Fig 9.
Post surgical scar. 40-year-old woman, post excision benign breast mass on the right side 1 year earlier (same case as Fig.5). Craniocaudal view of the right breast showing a stellate mass (arrow) with no palpable mass.

Fig 10.
Sternal insertion of pectoral muscle. Screening mammography of a 40 year-old-woman showing a triangular soft tissue density (arrow head) at the medial aspect of the right breast on craniocaudal view.

is its irregular or ill-defined margin. However, there are many breast lesions having these features. Awareness of the varied mammographic features is essential to avoid unneccessary biopsy, but lesions in which there is a suggestion of malignancy should undergo biopsy without delay. A wide knowledge of various disease process will help in accurate diagnosis and ultimately improve breast health care.

ACKNOWLEDGEMENT

We express our appreciation to Dr.Ezekiel Freed (Northridge Medical Center, LA, USA) for reviewing this manuscript.

REFERENCES

1. Gold RH, Montgomery CK, Rambo ON. Significance of margination of benign and malignant infiltrative mammary lesions: Roentgenographic pathological correlation. AJR 1973;118:881-93.
2. Ekland DA, Zeigler MG. Abscess in the non-lactating breast. Arch Surg 1973;107:398-401.
3. Van Overhagen H, Zonderlan HM. Lameris JS.

Radiodiagnostic aspects of non-puerperal mastitis. ROFO-Fortschr-Geb-Rontgenstr-Nuklearmed. 1988;149:294-7.
4. Reddin A, McCrea ES, Keramati B. Inflammatory breast disease: Mammographic spectrum. South-Med-J, 1988;81:981-4,988.
5. Hayes R, Michell M, Nunnerley HB. Acute inflammation of the breast: The role of breast ultrasound in diagnosis and management. Clin Radiol 1991;44:253-6.
6. Paulus DD, Holbert MJ. Benign processes and tumors of the breast. Cancer Bull 1988;400:14-25.
7. Andersson I, Fex G, Pattersson H. Oil cyst of the breast following fat necrosis. Br J Radiol 1977; 50:143-6.
8. Baber CE, Libshitz HI. Bilateral fat necrosis of the breast following reduction mammoplasties. AJR 1977;128:508-9.
9. Orson LW, Cigtay OS. Fat necrosis of the breast: Characteristic xeromammographic appearance. Radiology 1983;146:35-8.
10. Bassett LW, Gold RH, Cove HC. Mammographic spectrum of traumatic fat necrosis: The fallability of "pathognomonic" signs of carcinoma. AJR 1978;130:119-22.
11. Bassett LW, Gold RH, Marra JM. Nonneoplastic breast calcifications in lipid cysts: Development after excision and primary irradiation. AJR 1982;138:335-8.
12. Heimann G, Schwartz IS. Focal fibrous disease of the breast: Mammographic detection of an unappreciated condition. AJR 1983;140: 1245-6.
13. Feig SA. Breast masses: Mammographic and sonographic evaluation. Radiol Clin North Am 1992;30(1):67-12.
14. Stigers KB, King JG, Davey DD, et al. Abnormalities of the breast caused by biopsy: Spectrum of mammographic findings. AJR 1991;156:287-91.
15. Mendelson EB. Imaging the post-surgical breast. Seminars in US, CT and MR 1989;10(2):154-70.
16. Sickles EA, Herzog KA. Intramammary scar tissue: A mimic of the mammographic appearance of carcinoma. AJR 1980;135:345-52.
17. Sickles EA, Herzog KA. Mammography of the postsurgical breast. AJR 1981;136:585-8.
18. Mendelson EB. Evaluation of the postoperative breast. Radiol Clin North Am. 1992;30(1):107-138.
19. Britton CA, Baratz AB, Harris KM. Carcinoma mimicked by the sternal insertion of the pectoral muscle. AJR 1989;153:955-6.

Table 1. Diagnosis and number of cases

Diagnosis	Number of cases
Non-lactating abscess	9
Fibroadenoma	2
Fat necrosis	2
Focal fibrocystic change	2
Hematoma	3
Scar	2
Sternal insertion of pectoral muscle	3

CARCINOMA OF THE BREASTS: THE IMPORTANCE OF BREAST-PALPATION AND THE DETECTION OF THE CANCER LESIONS BY X-RAY AND ULTRASONOGRAPHIC MAMMOGRAPHY.

Supranee NIRAPATHPONGPORN[1,2], Patchrin PEKANAN[1,2], Chirote SUCHATO[2], Manee AIMACHARIYACHAI[1,2].

ABSTRACT

A retrospective study of 26 breast cancer-cases in Samitivej hospital was performed to determine the importance of breast palpation and the detection of the cancer lesions by x-ray and ultrasonographic mammography. The patient's age was 30-76 years old. The main presenting symptom was palpable mass. Twenty-nine percents of the lesions could be detected by every modality, 14% could be detected only by palpation and more lesions could be detected by ultrasonography compared with x-ray mammography. Microcalcification was the only finding that x-ray mammography was more superior than the palpation and ultrasonography by this study. Biopsy was suggested in every palpated lesion though the lesion could not be visualized by x-ray and ultrasonographic mammography. Needle guided biopsy was useful for the lesions containing microcalcification.

Key words: Breast carcinoma, x-ray mammography

INTRODUCTION

Until mammography becomes an integral part of the medical evaluation of every woman, history and physical examination remain the key elements in providing care for breast problems (1). Physical examination of the breast includes inspection and palpation conducted with the patient in both the erect and the recumbent positions. Despite its usefulness, mammography is not infallible, and the radiologist is at times chagrined to learn that a carcinoma proved by biopsy was not apparent on the film.

A retrospective study of 26 patients with breast cancer was performed to evaluate the importance of the breast palpation and mammography in the non palpated cases.

PATIENTS AND METHODS

A retrospective study was performed in 26 breast-cancer patients during January 1988 and May 1990, in Samitivej Hospital. Data concerning clinical information, x-ray and ultrasonographic, mammographic findings and the results of the pathology were recorded. X-ray mammography of each patient was routinely performed in mediolateral view (M-L view) and craniocaudal view (C-C view) and magnification view of the suspected lesion. Ultrasonography was performed in also suspected cases. The films were reviewed to evaluate the area of malignancy. Mammographic unit was Hospitech 600, T-C GR. The sonographic unit was Aloka 650, real time machine, using 7.5 Mhz transducer.

[1]Department of Radiology, Ramathibodi Hospital, Rama 6 street, Bangkok 10400, Thailand.
[2]Department of Radiology, Samitivej Hospital, Sukhumvit 49, Bangkok, Thailand.

RESULTS

The 26 patients consisted of all female patients, the age range was 30-76 years old. The mean age was 40 years old. The presenting symptoms were mainly palpable mass, as shown in Table 1. There were only 2 check-up cases. The detailed information, mammographic findings and the results of the pathology were presented in table 2.

From the data in table 3, twenty-nine percents of the palpated lesions were also positive by x-ray and ultrasonographic studies. Considerable number of lesions (14%) that were palpated and not shown by imaging techniques of mammography. In cases of palpable lesions, ultrasonography could detect more lesions (18%) than x-ray mammography (3.5%). X-ray mammography helped to detect lesion in the non-palpated cases only via the demonstration of microcalcification. There were no cases of positive ultrasonographic study only. Illustration of cases No.1. 26, 20, and 25 were shown in figure 1,2,3 and 4 respectively.

DISCUSSION

Breast cancer is a major cause of morbidity and mortality,and many methods have been advocated for early detection of breast cancer(2). Mammography is probably the best imaging technique for the early detection and diagnosis of breast cancer. The technique is not without shortcomings that limit its sensitivity and specificity(3). The sources of diagnostic error using x-ray mammography were stated by Egan(1) as followings 1) improper radiographic technique 2) the density of the breast as related to that of the lesion 3) interpretative error. Some benign processes such as infected cysts, abscess, fibrosis, fat necrosis, extra-abdominal desmoids, chronic inflammatory process, sclerosing adenosis, indurative process or mastopathies could be interpreted as carcinoma. False negative diagnosis could occur in 1) a lesion that is too small to produce a recognizable density or that is the same density as the surrounding tissues 2) a carcinoma that is discounted as part of a benign process 3) a carcinoma that is partially or completely obscured by a benign process 4) a carcinoma usually in the extreme periphery of the breast, medially or just below the clavicle, that is not projected onto the mammogram.(7). The degree of reliability of the procedure depends on the relative amount of fat and fibroglandular tissue in the breast.

The lesions were detected only in mediolateral projection in our case No. 4,7, and 24. This observation was different from that of Helvie which stated that craniocaudal view was more superior due to thickness difference of the compressed breast. This leads to the conclusion that the lesion seen in any projection only should not be ignored.

For palpable masses, reported accuracies of the breast cancer ranged from 72 to 92% by ultrasonography (5-8) and 72% (13/18 cases) in our serie. Kobayashi (7) reported 85% breast cancer detection rate with ultrasonography for lesions of all sizes and 83% detection rate with x-ray mammography; this was shown to be 68% (15/22 cases) for ultrasonography and 57% for x-ray mammography in our cases.

There were four breast cancer cases that the mass could not be palpated and x-ray mammography was most helpful in detecting microcalcification and led to needle-localized biopsy.

Panjapiyakul (9) reviewed 838 mammograms in Samitivej Hospital, microcalcification was seen in 6.5% (55/838) and 28.5% of these were malignant lesion.

Table 1. Presenting symptoms in 26 patients with Ca breast

Presenting symptoms	No. of patients
Palpable mass	23
Ulceration of the nipple	1
Discharge per nipple	1*
Check up	2**

* the patient also had palpable mass

**one patient had tumorectomy in the breast 5 years ago

From our results, most of the malignant breast lesions were palpated (82% 23/28 cases); all of the nonpalpated lesions contained microcalcification detected by x-ray mammography. Slightly more lesions could be shown by ultrasonography (68%) as compared to the x-ray mammography (57%). These lead to an observation that there must be a number of cases that escape detection if they are non-palpated and contain no microcalcification.

Table 2. Information about the 26 patients with CA breast

No.	Age(yrs)	Clinical finding	X-ray mammography	Ultrasonography	Pathological findings
1	33	Palpable mass	Negative	Multiple iso and low echoic Nodes	Infiltrative ductal Ca
2	62	Palpable mass	Mass	Not done	Infiltrative intraductal Ca
3	42	Palpable mass	Normal	Not done	Infiltrative intraductal Ca
4	49	Palpable mass	Ill defined border increased density only in M-L view	Echogenic mass	Infiltrative intraductal Ca
5	61	Palpable mass	Lobulated mass	Low echoic mass	Papillary Ca
6	48	Check up post tumorectomy 5 yrs.	Localized micro calcification at tumor bed	Negative	Intraductal Ca
7	43	Palpable mass + nipple discharge	Mass only in M-L view	Low echoic mass	Invasive lobular Ca
8	34	Palpable mass	Negative	Cystic lesion	Infiltrative intraductal Ca
9	34	Palpable mass	Negative	Negative	Intraductal Ca
10	38	Palpable mass	Negative	Echoic mass	Intraductal Ca
11	60	Palpable mass	Irregular border mass	Not done	Medullary Ca
12	45	Palpable mass	Microcalcification	Low echoic mass	Infiltrative medullary Ca
13	60	Palpable mass Rt. breast	Negative Rt breast Microcalc, Lt. breast	Not done	Medullary CA Rt. breast Infiltrative intraductal Ca Lt. breast
14	45	Palpable mass	Dense subareolar lesion	Low echoic mass	Adenocystic Ca
15	45	Palpable mass	Negative	Negative	Intraductal Ca at subareolar area
16	64	Palpable mass	Microcalcification	Negative	Invasive ductal Ca
17	66	Ulceration at Lt nipple 7 yrs	Microcalcification	Negative	Infiltrative ductal Ca
18	30	Palpable mass	Negative	Negative	Cystosarcoma Phylloides
19	35	Palpable mass	Negative	Negative	Cystosarcoma Phylloides
20	52	Check up	Mass Rt breast Microcalc. Lt.	cystic mass Rt	Infiltrative colloid Ca Rt. breast Normal Lt breast
21	40	Palpable mass	Positive for mass	Echogenic mass	Infiltrative ductal Ca
22	36	Check up	Bilat. Microcalc.	Fibrocystic ds both breasts	Ca left breast
23	76	Mass	Not clear	Not done	Infiltrative ductal Ca subareolar area
24	40	Palpable mass	Mass is seen only in M-L view	Ill defined low echoic mass	Intraductal Ca
25	30	Palpable mass	Negative	Low echogenic mass	Infiltrative ductal Ca
26	50	Palpable mass	dense breast	Low echoic mass	Infiltrative intraductal Ca

Table 3. Correlation between palpable lesion, x-ray and ultrasonography mammography in cancer lesion of the breast

Type of lesions	No. of lesions (%)
+ palpation, +x-ray, + U/S	8 (29)
+ palpation, - x-ray, - U/S	4 (14)
+ palpation, +x-ray, - U/S	1 (35)
+ palpation, - x-ray, + U/S	5 (18)
- palpation, - x-ray, - U/S	0 (0)
- palpation, +x-ray, + U/S	2 (7)
- palpation, - x-ray, + U/S	0 (0)
- palpation, +x-ray, - U/S	2 (7)
+ palpation, +x-ray, U/S-not performed	2 (7)
+ palpation, - x-ray, U/S-not performed	3 (11)
- palpation, +x-ray, U/S not performed	1 (3.5)
Total	28 (100)

Fig.1A.
Normal mediolateral view x-ray mammography of the patient No. 1, the case of infiltrative intraductal Ca.

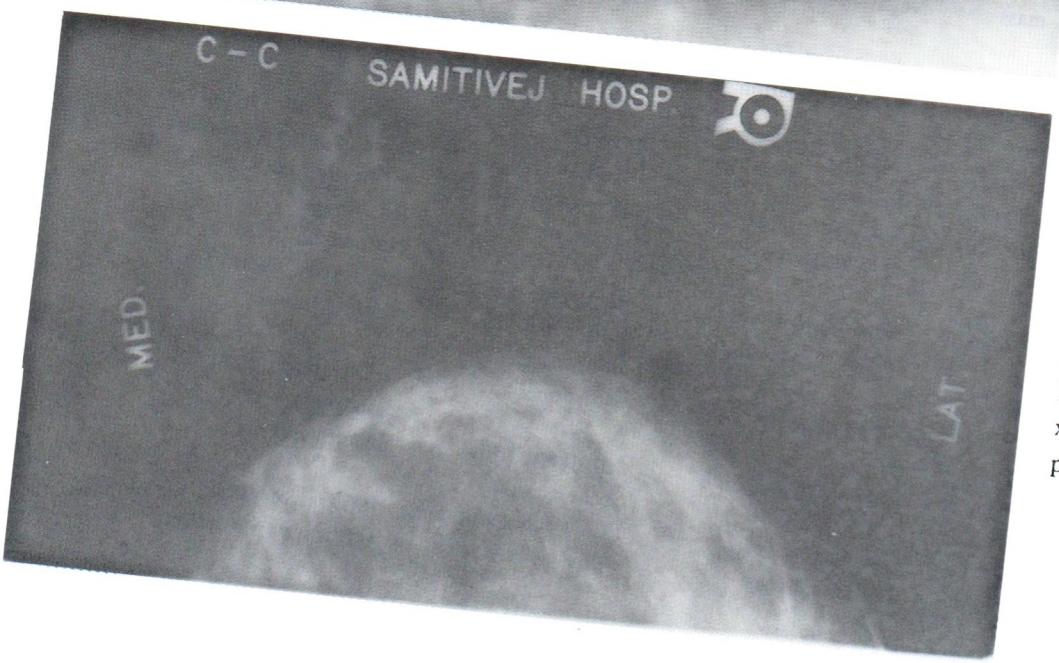

Fig.1B.
Normal craniocaudal view x-ray mammography of the patient No.1.

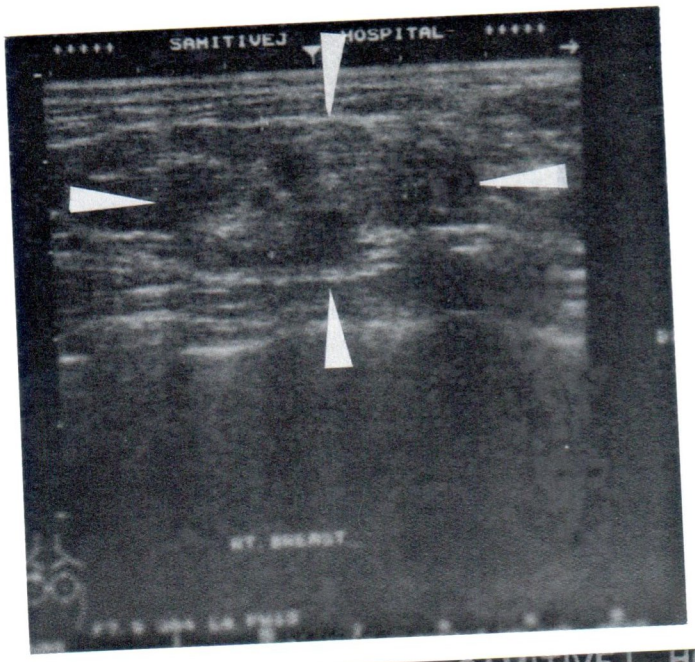

Fig.1C. Ultrasonography of the palpable lesion in the breast of the patient No.1 showed multiple iso and low echoic nodules.

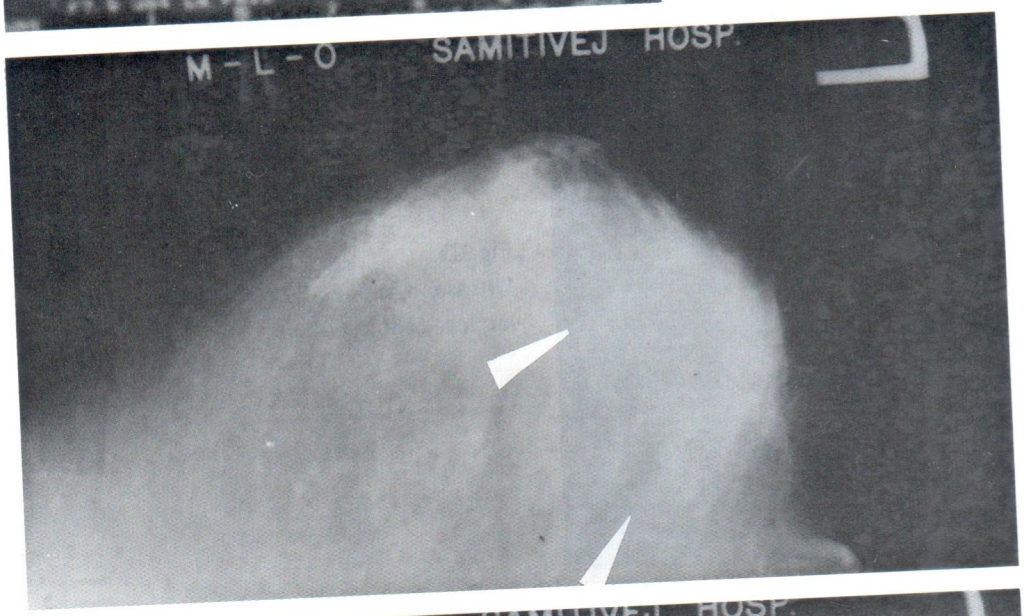

Fig.2A.
Medio-lateral x-ray mammography of the patient No. 26 showed dense breast tissue at inferior part of the breast. The case of infiltrative intraductal Ca.

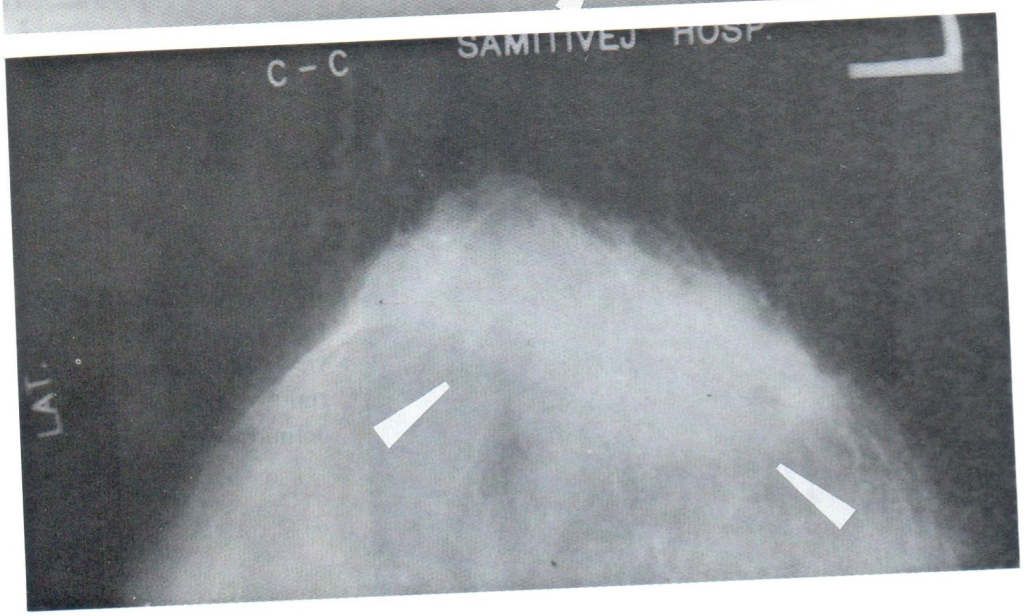

Fig.2B.
Cranio-caudal projection showed dense breast tissue at medial aspect of the breast

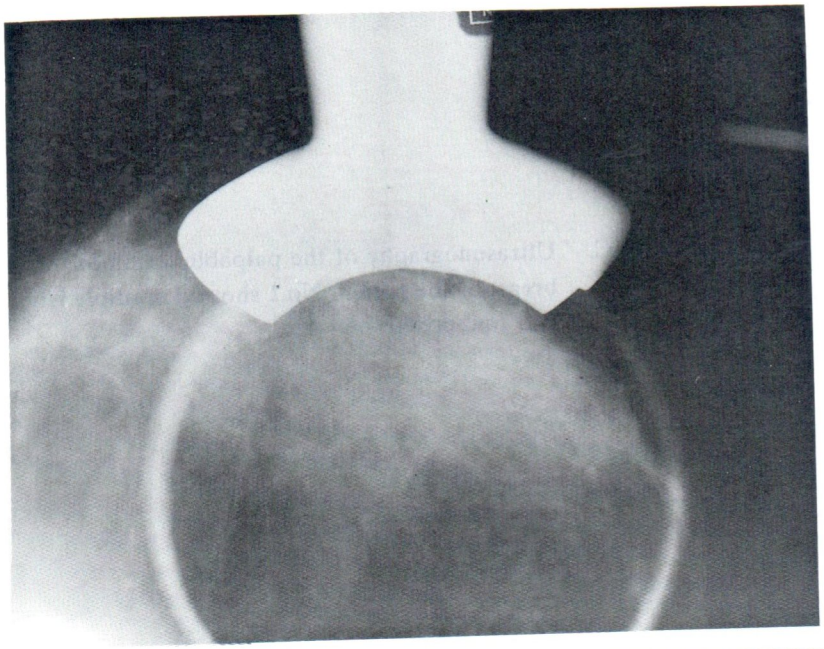

Fig.2C.
Magnified view at the medial part of left breast, showed no definite mass

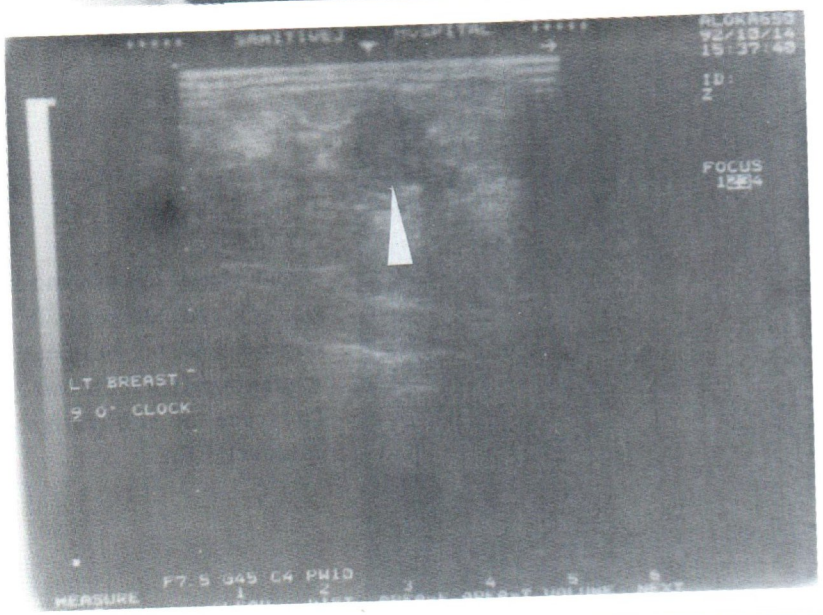

Fig.2D.
Ultrasonography at 9 o'clock showed irregular low echoic nodule

Fig.3A.
Infiltrative colloid Ca, patient No. 20 medio lateral view x-ray mammography of right breast showed no definite mass.

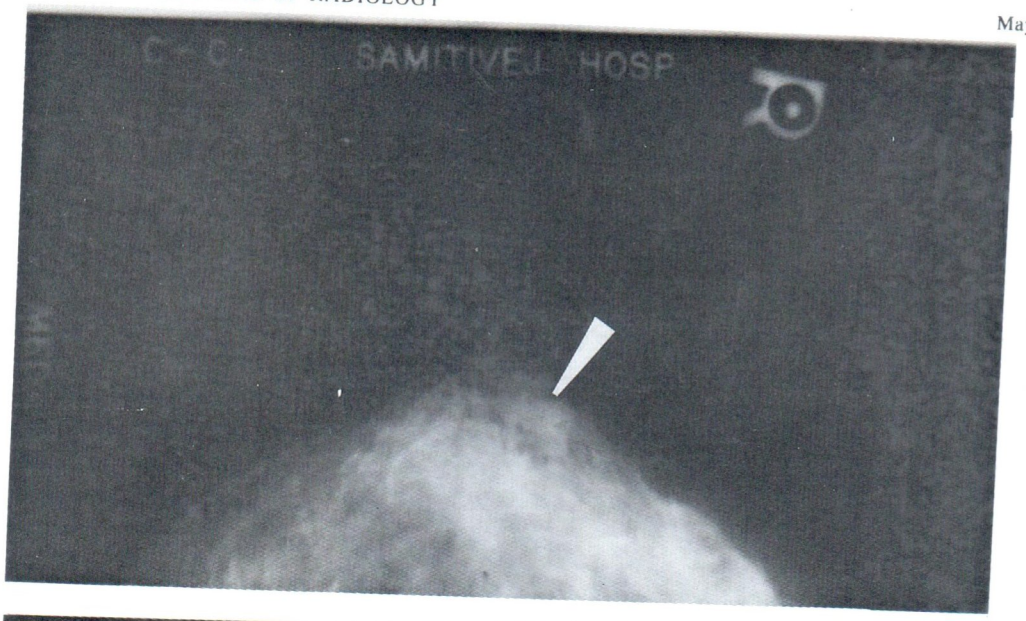

Fig. 3B.
Craniocaudal view x-ray mammography of right breast showed iso dense nodule at lateral aspect of subareolar region.

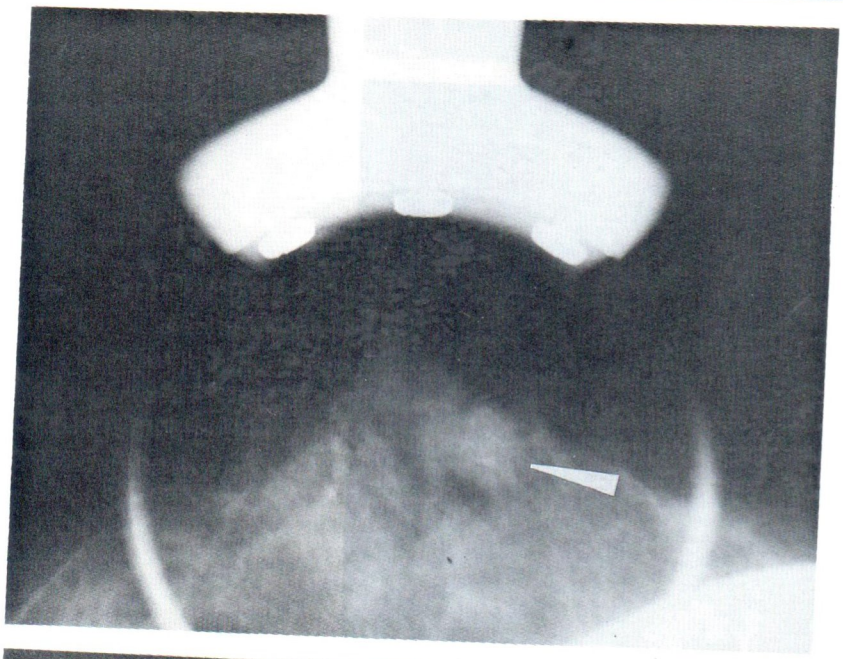

Fig.3C.
Magnified view at the lesion showed calcified area in the iso dense nodule, at the lateral subareolar region.

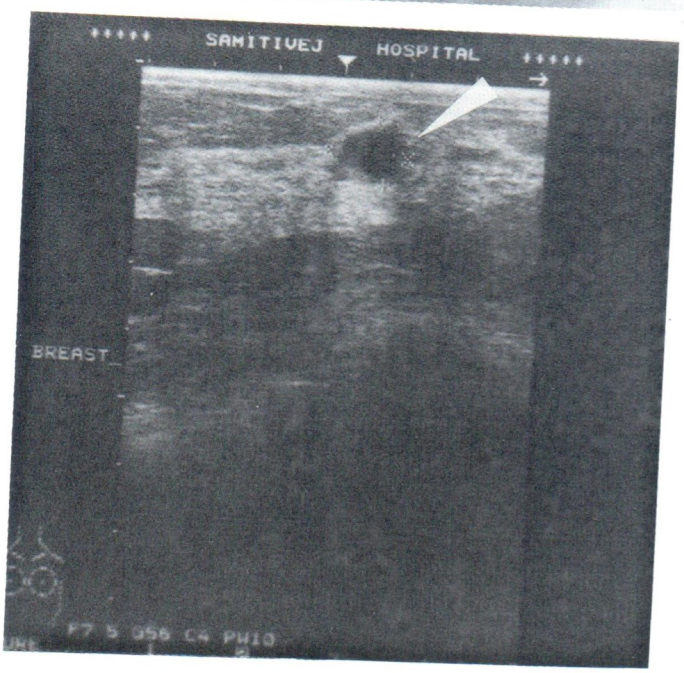

Fig.3D.
Ultrasonography showed low echoic and cystic nodule with posterior enhancement. Aspiration yielded bloody fluid.

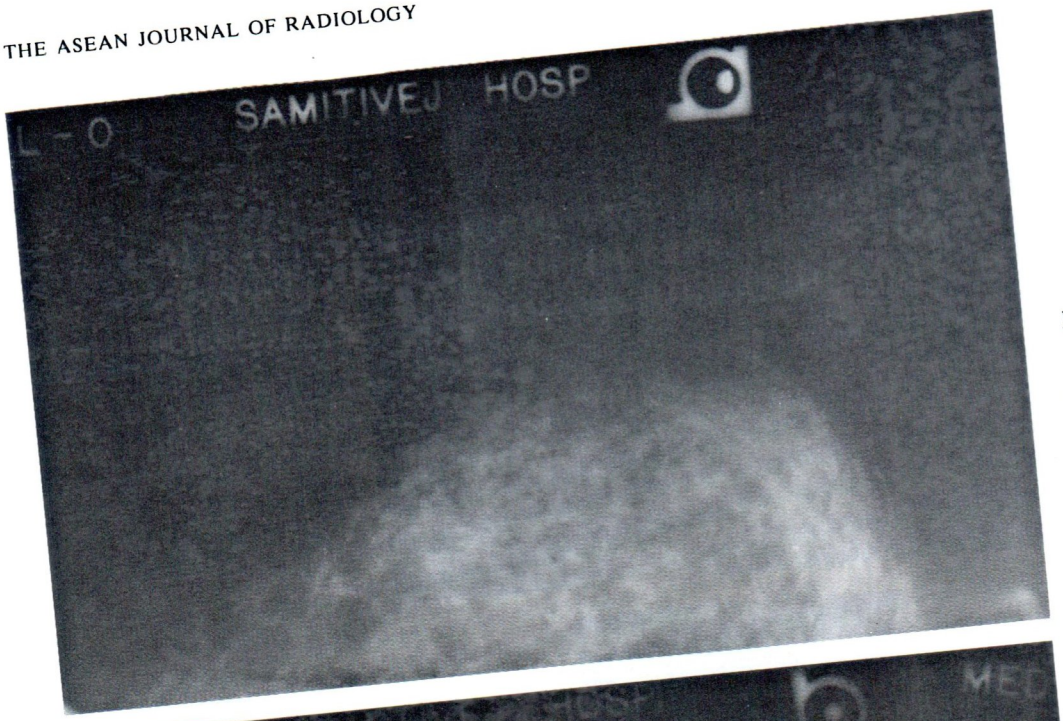

Fig.4A.
Infiltrative intraductal Ca, patient No. 25. Medio lateral view x-ray mammography showed no abnormality.

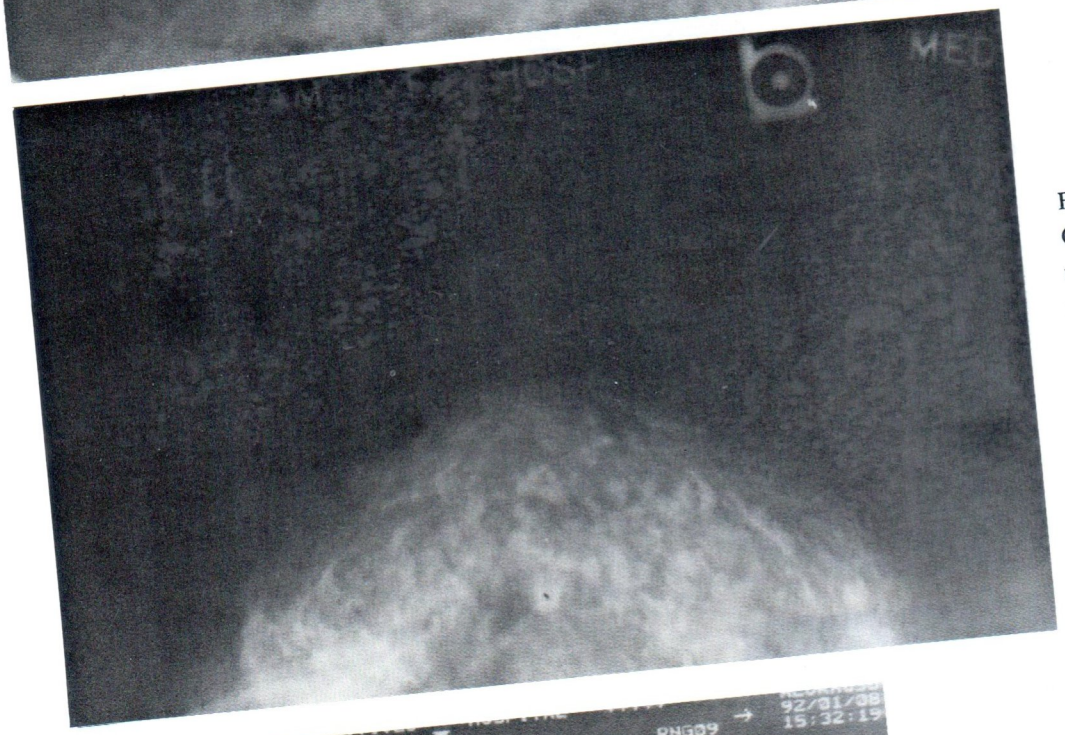

Fig.4B.
Craniocaudal view x-ray mammography showed no mass lesion.

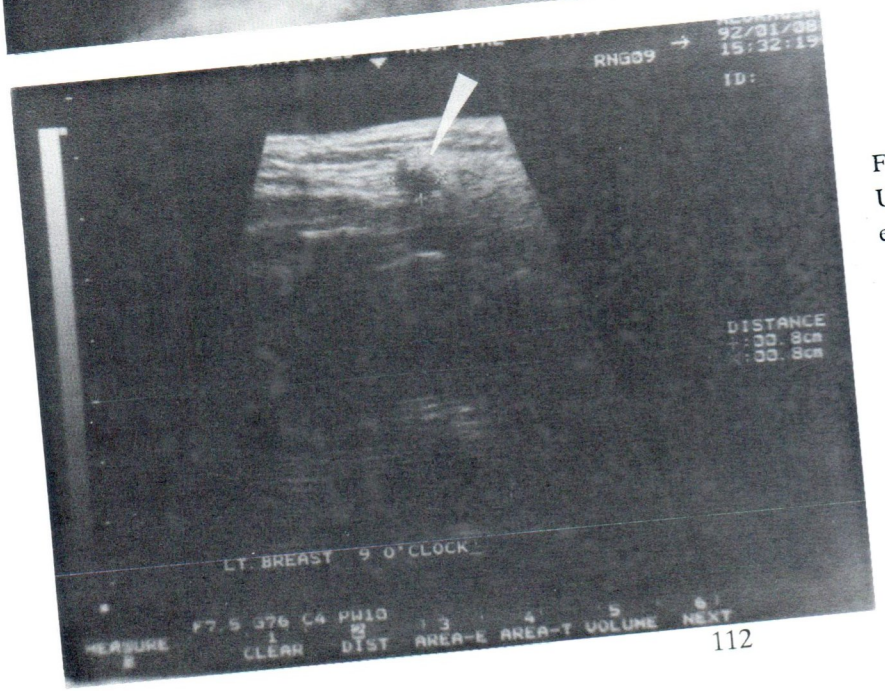

Fig.4C.
Ultrasonography showed an irregular low echoic nodule at 9 o'clock.

REFERENCES

1. Egan RL: Breast imaging: Diagnosis and morphology of breast diseases. Ed. 1988, Philadelphia, W.B. Saunders Company.
2. Pollei SR, Mettler FA, Bartow SA, Moradian G, Moskowitz M. Occult breast cancer: Prevalence and radiographic detectability. Radiology 1987; 163:459-462.
3. Adler DD, Wahl RL, New methods for imaging the breast : Techniques, Findings, and Potential. AJR 1995;164:19-30.
4. Helvie MA, Chan HP, Adler DD, Boyd PG. Breast thickness in routine mammographs: Effect on image and radiation dose. AJR 1994;163:1371-1374.
5. Cole-Beuglet C, Beique RA: Continuous ultrasound B-scanning of palpable breast masses. Radiology 1975;117:123-128.
6. Jellins J, Kossoff G, Reeve TS: Detection and classification of liquid filled masses in the breast by gray scale echography. Radiology 1977;125: 205-212.
7. Kobayashi T: Gray-scale echography for breast cancer. Radiology 1977;122:207-214.
8. Teixidor HS, Kazam E: Combined mammographic sonographic evaluation of breast masses. AJR 1877; 128:409-417.
9. Panjapiyakul C, Suwanraks C, Shaipanich T, Suchato C, Suwanwilai C, Jotisakulratana V, Supromajakr B, Pramyothin P. Impact of mammography in management of breast cancer. The Thai journal of surgery 1991:12:57-62.

CONVENTIONAL RADIOGRAPHY ANALYSIS OF 70 CASES OF PROVED APPENDICULAR-SKELETAL-RELATED OSTEOSARCOMA IN RAMATHIBODI HOSPITAL

Pimjai SIRIWONGPAIRAT, Sarawoot KITTIPERACHOL, Patchrin PEKANAN, Laksana POCHANUGOOL, Supaneewan JAOVISIDHA, Janjira JATCHAVALA.

ABSTRACT

A retrospective analysis of conventional radiographic appearance of the appendicular skeletal related osteosarcoma patients, who came for pre-operative chemoembolization was presented in 70 cases. The most common age range was 16-20 years old. Male to female ratio was 1.3 to 1.

The presenting symptoms were pain and soft tissue mass. Central osteosarcoma occupied 90% of cases and the rest was its variant-telangiectatic type. Around knee involvement was the most common area. Long bones predominated with rare flat bones involvement.

Every region of the bone may be involved, but 85% included metaphyseal region. There was no isolated epiphyseal involvement. Usually the radiographic pattern was mixed lytic and blastic and purely lytic lesion. There was no good correlation between the roentgen appearance and the histologic type. The osteoid matrix represented 74%, chondroid matrix 14% and unclassified 13%. 81% had associated mass, and more than half of them were larger than 5 cms. The sunburst or sunray, the Codman's triangle or combined pattern represented 66%, the rest was spiculated pattern and combined spiculated and Codman's triangle. The finding were not different from those reported by previous authors, except epiphyseal plates were involved mainly in young children whose growth plates were not closed.

INTRODUCTION

Osteosarcoma or osteogenic sarcoma is second in frequency only to plasma cell myeloma as a primary malignant neoplasm of the bone (1). It is characterized histologically by proliferating tumor cells that, in most instances, produce osteoid or immature bone. Infrequently, such cells remain so immature that osteoid or bone is not elaborated, leading to difficulties in tumor classification and to considerable interest in identifying diagnostic methods not dependent on routine microscopy. Extensive modifications in the classification scheme of osteosarcoma have appeared in recent years. Traditional systems using the designations of conventional and parosteal tumors have been replaced owing to the identification of many clinical, radiologic, and histologic varieties of osteosarcoma, although no single method of classification is accepted uniformly. Available systems (2, 3, 4) employ such features as the precise location of the tumor within the bone (intramedullary or central, intracortical, surface, periosteal, or parosteal); the degree of cellular differentiation (high grade or low grade) ; the histologic composition (osteoblastic, chondroblastic, fibroblastic, fibrohistiocytic, telangiectatic, small cell); the number of foci of involvement (single or multicentric); and the status of the underlying bone (normal or the site of disease such as Paget's disease, of injury as occurs with a vascular insult or following irradiation, or of another neoplasm, such as an osteochondroma, chondroma, or osteoblastoma).

This study was a retrospective analysis of the roentgenographic imaging of the proved cases of osteosarcoma in 70 patients who came to receive the chemoembolization of the tumors during the year 1987 and 1993, in Ramathibodi Hospital.

Department of Radiology, Ramathibodi Hospital, Rama 6 Street, Bangkok 10400, Thailand

PATIENTS AND METHODS

Plain films of the involved bones of 70 patients were reviewed. The information concerned were the sites of involvement, the radiographic patterns, the associated soft tissue mass, the types of the periosteal reaction and the types of the matrix. The presenting symptoms were studied from the hospital data. The types of histology were correlated with the radiographic patterns.

RESULTS

There were 39 males and 31 females ostesarcomatous patients. The age ranged from 5 to 48 years old, the most common range was between 16-20 years old. The males to females ratio was 1.3 : 1. Table 1 showed the frequency of the presenting symptoms. Pain was the most common presenting symptom and some patients were thought to have myalgia or tendinitis at first. The duration of the symptoms before the diagnosis was 4 weeks to 1 year, average time was 1-4 months. Conventional osteosarcoma was the most common type (63/70 or 90%). Its correlated histology was shown in table 2. The osteoblastic type was the most common one, followed by chondroblastic, mixed form and fibroblastic types. The unusual variants named telangiectatic type was seen in 10%.

The knee was the most common location to be involved by the tumor, representing 48/70 (69%) ; the distal femur was twice as common as the proximal tibia. The proximal humerus was the third most common site.

Metaphyses of long bones were the most common location, appeared in 93% of cases. The epiphyseal involvement alone was not present. Epiphyseal growth plate extension occurred in 5/70 cases (7%) and involved mainly the young children whose growth plates were not closed. The frequency of the involved bones and their sites were presented in table 3 and 4.

More than half of the patients had mixed osteolytic and osteoblastic radiographic appearance. The purely osteolytic destruction pattern showed permeative and/or moth eaten destruction. Some patients had geographic destruction, causing difficulty in differentiating from other primary bone tumors, such as giant cell tumor, aneurysmal bone cysts, fibrosarcoma or metastatic lesion. The correlation of the radiographic pattern and the histology of osteosarcoma was performed and illustrated in the table 6. It seemed to show no definite correlation.

The osteoid tumor matrix, appearing as cloudlike density was the most common associated matrix. The frequency of types of the matrix was shown in the table 7.

The frequency of the mass and periosteal reactions appeared in the table 8 and 9. The sun-ray , the Codman's and the combination of both types were among the majority. Usually, the tumor penetrated the cortex into the surrounding soft tissue, causing palpable mass and/or pathological fracture. We found 14/70(20%) of the patients had pathologic fracture at the presentation. The central osteosarcoma showed fracture 10/63 cases (16%) and the telangiectatic type 4/7 (57%).

The mixed osteolytic and osteoblastic osteosarcoma with osteoid matrix, sunray periosteal reaction and associated mass was shown in Fig. 1. The osteolytic type with Codman's periosteal reaction was shown in Fig. 2. The osteoblastic type with spiculated periosteal reaction was demonstrated in Fig. 3. The epiphyseal location with chondroblastic matrix and soft tissue mass was in Fig. 4. The expanding lesion simulated Giant cell tumor was in Fig. 5. The osteoblastic type at the right clavicle with spiculated periosteal reaction was in Fig. 6. The spiculated osteoblastic osteosarcoma of the calcaneum was shown in Fig. 7. The involvement of the growth plate was seen in the case of Fig. 8. The pathological fracture in the osteolytic type of the tumor was shown in Fig. 9.

DISCUSSION

The larger series of roentgenologic analysis of the osteosarcoma in Thailand was presented by Kaewjinda(5), in 1988. One hundred and twenty five cases were studied, including bones of the extremities, extremities-related bones, rib, skull, spine, mandible and maxilla. However, there was no histologic correlation as in this study.

Conventional osteosarcoma generally is seen in the second and third decades of life (6-8), although the neoplasm has been identified in patients of all ages, including infants and very young children (9,10) and the elderly (11,12). Clinical manifestations include pain and swelling, restriction of motion, warmth and pyrexia (6,7).

Most of the cases develop in the osseous structures about the knee; it is the distal portion of the femur and the proximal portions of the tibia and

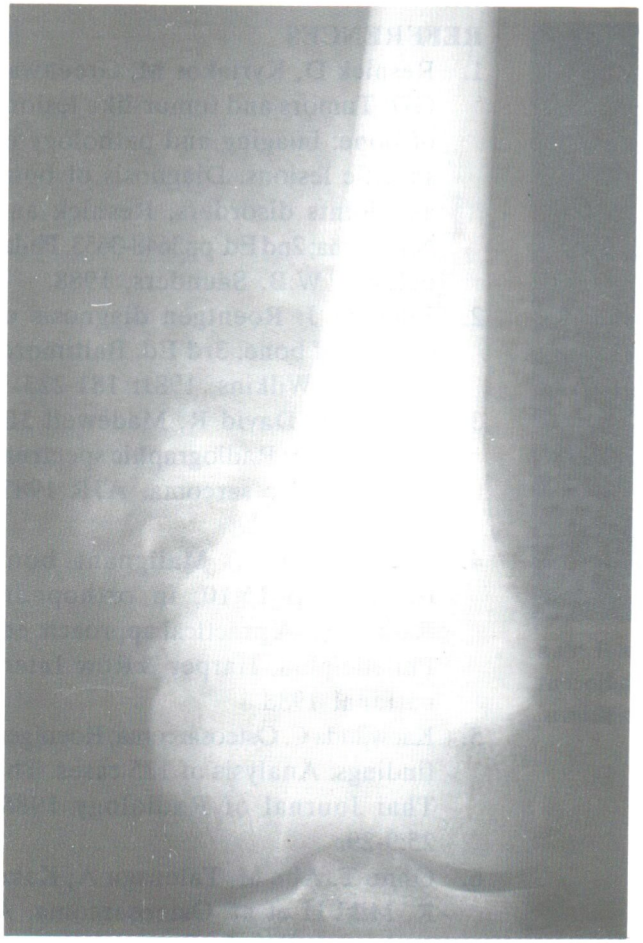

Fig 1. Mixed lytic and blastic osteosarcoma arising in meta-diaphysis of distal femur shows dense cloud like osteoid tumor matrix, classical sunray periosteal reaction and large soft tissue mass.

Fig. 2 . Lytic type osteosarcoma in meta-epiphysis of proximal tibia with large area of bony destruction, soft tissue extension and characteristic codman periosteal reaction were shown.

humerus that represent the areas involved most frequently (6,13-16). With regard to the long tubular bones, metaphyseal location predominates. Initial involvement of the diaphysis occur in 2 to 11 percent of cases (17-21). Although osteosarcoma may extend into the epiphysis (22), especially when the physis is closed (23, 24), a primary epiphyseal origin is quite rare (25,26).

The roentgenographic findings usually are obvious at the time of the initial examination of the patient. A mixed pattern consisting of both osteolysis and osteosclerosis is most typical, with purely osteolytic or osteosclerotic lesions being encountered less frequency (27). Osteolysis is especially characteristic of the telangiectatic variety. With regard to the tubular bones of the appendicular skeleton, conventional osteosarcoma usually is evident as an ill-defined, intramedullary, metaphyseal lesion that has extended through the cortex and produced a sizable soft tissue mass (28). Periosteal reaction in the form of Codman' s triangle or with a " sunray " appearance (29, 30) and uncommonly, a pathologic fracture (6) are additional radiographic features.

Five to 10 percent of osteosarcoma involve the flat bones and may be more frequent in older patients (12). Our results were similar to those reports by other authors, except that the epiphyseal plates involvement occurred in the children whose growth plates were not closed.

Resnick (1) emphasized that the "gold standard "in the specific diagnosis of this tumor remains the conventional radiograph and that those other techniques (bone scintigraphy, arteriography, computed tomography and magnetic resonance) are more useful in defining the extent of the neoplasm and its relationship to surrounding neurovascular structures and in evaluating the response of the tumor to therapy.

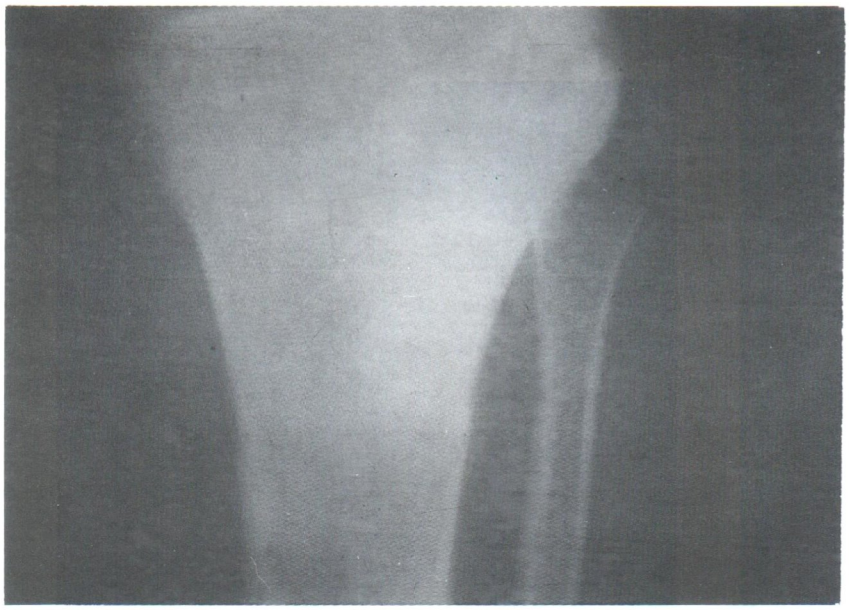

Fig. 3 Purely blastic type osteosarcoma in metaphysis of proximal tibia with cloud like tumor matrix at the lesion extending into the adjacent soft tissue was noted. Spiculated periosteal reaction was shown.

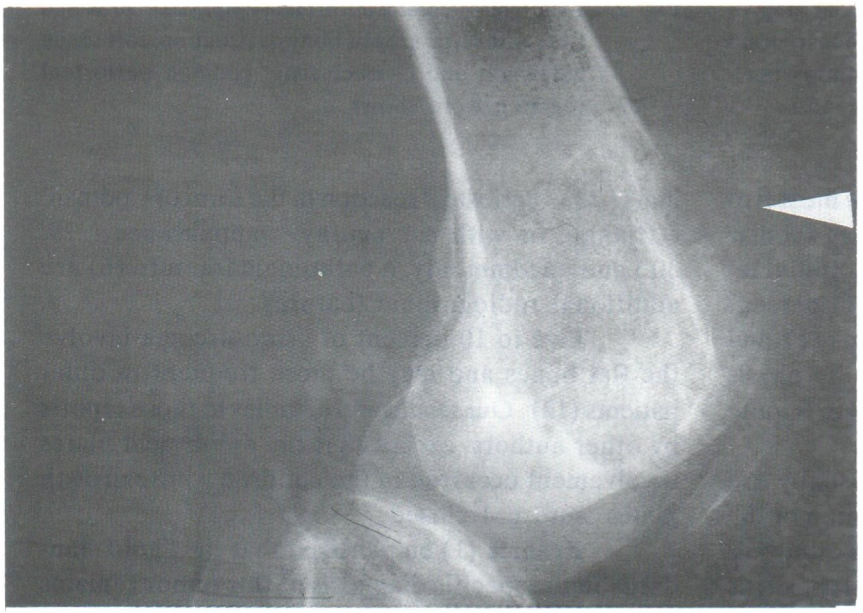

Fig. 4 Epiphyseal location of mixed largely lytic and few blastic osteosarcoma arising in distal femur was demonstrated. There is cortical destruction at anterior aspect of the lesion with extension of tumor containing chondroblastic type tumor matrix into the adjacent soft tissue.

REFERENCES

1. Resnick D, Kyriakos M, Greenway GD: Tumors and tumor-like lesions of bone: imaging and pathology of specific lesions. Diagnosis of bone and joints disorders. Resnick and Niwayama; 2nd Ed. pp3648-3653, Philadelphia, W.B. Saunders, 1988.
2. Edeiken J: Roentgen diagnosis of disease of bone. 3rd Ed. Baltimore: William&Wilkins, 1981: 181-223.
3. Kumar R, David R, Madewell JE, Lindell MM: Radiographic spectrum of osteogenic sarcoma. AJR 1987; 148:767-772.
4. Greeenspan A. Malignant bone tumors, pp 16.10, in orthopedic Radiology, A practical approach. ed. Philadelphia, Harper &Row International 1988
5. Kaewjinda C. Osteosarcoma; Roentgen findings: Analysis of 125 cases. The Thai Journal of Radiology 1988; 25:9-29.
6. Ohno T, Abe M, Tateusgu A, Kako K, Miki H et al. Osteosarcoma. A study of one hundred and thirty cases. J Bone Joint Surg (AM) 57: 397,1975.
7. Wu kk, Guise ER, Frist HM, Mitchell CL: Osteogenic sarcoma.Report of one hundred and fifty-seven cases. Henry Ford Hosp Med J 24: 213,1976.
8. Enneking WF. Springfield DS: Osteosarcoma. Orthop Clin North Am 8:785,1977.
9. Levy ML, Jaffe N: Osteosarcoma in early childhood. Pediatrics 70: 302,1982.
10. Siegel GP, Dahlin DC, Sim FH: Osteoblastic osteogenic sarcoma in a 35 - month - old girl: Report of a case. Am J Pathol 63: 886,1975.
11. De Santos La, Rosengren JE, Wooten WB, Murray JA: Osteogenic sarcoma after the age of 50: A radiographic evaluation. Am J Roentgenol 131: 481, 1978.
12. Huvos AG: Osteogenic sarcoma of bones and soft tissues in older patients. A clinicopathologic analysis of 117 patients older than 60 years. Cancer 57: 1442, 1986.

Fig. 5 Lytic expanding type osteosarcoma involving metaphysis and epiphysis of distal femur, simulated Giant cell tumor. Note the focal increased density of cloud like tumor matrix at proximal part of the lesion, suggested bone forming tumor of osteosarcoma.

Fig . 6 Blastic osteosarcoma in right clavicle with soft tissue mass, and dense spiculated periosteal reaction were demonstrated.

References (continued)

13. Dahlin DC: Bone tumors, General Aspects and Data on 6,221 Cases. 3rd Ed. Springfield, III, Charles C Thomas, 1979.
14. Huvos AG: Bone tumors. Diagnosis, Treatment and Prognosis. Philadelphia, WB Saunder Co. 1979.
15. Schajowicz F: Tumors and Tumorlike lesions of bone and joints. New York, Springer-Verlag, 1981
16. Sujut HJ, Dorfman HD, Fechner RE, Ackerman LV: Tumor of Bone and Cartilage. Atlas of Tumor Pathology. Second Series., Fascicle 5. Washington, DC, Armed Forces Institute of Pathology, 1971.
17. Ellman H, Gold RH, Mirra JM: Roentgenographically "benign" but rapidly lethal diaphyseal osteosarcoma. A case report.J Bone Joint Surg (AM) 56: 1267, 1974.
18. Gold RH, Ellman H, Mirra JM: Case report 23. Skel Radiol 1:235, 1977.
19. Koziowski K: Osteosarcoma with unusual clinical and/or radiographic appearance. Pediastr Radiol 9: 167, 1980.
20. Haworth JM, Park WM, Watt I: Sclerotic medullary spread in diaphyseal osteosarcoma. Skel Radiol 4: 212, 1979.
21. Haworth JM, Watt I, Park WM, Roylance J: Diaphyseal osteosarcoma. Br J Radiol 54: 932, 1981.
22. Simon MA, BosGD: Epiphyseal extension of medullary osteosarcoma in skeletally immature individuals. J Bone Joint Surg (AM) 62: 195, 1980.
23. Campanacci M, Cervellati G: Osteosarcoma. A Review of 345 cases. Ital J Orthop Taumatol 1: 5, 1975.
24. Cohen P: Osteosarcoma of the long bones. Clinical observations and experiences in the Netherlands. Eur J Cancer 14:995, 1978.
25. Unni KK: Case report 214, Skel Radiol 9:129, 1982.
26. Mink JH, Gold RH, Mirra JM, Grant TT, Eiber FR. Case report 65. Skel Radiol 3:69, 1978.
27. de Santos LA, Edeiken B: Purely lytic osteosarcoma. Skel Radiol 9:1, 1982.

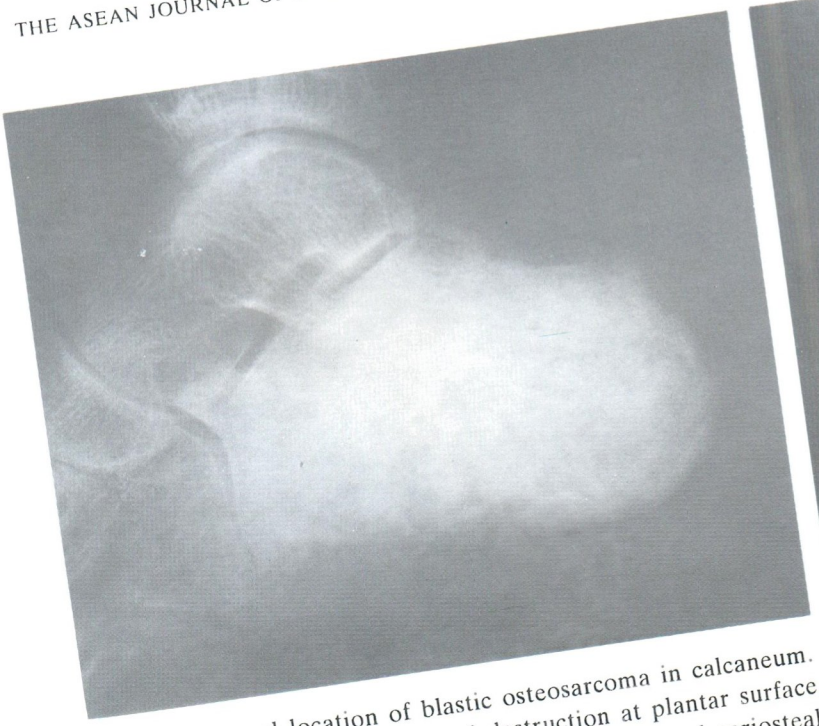

Fig. 7 Unusual location of blastic osteosarcoma in calcaneum. The lesion shows cortical destruction at plantar surface with soft tissue extension and faint spiculated periosteal reaction.

Fig. 8 Epiphyseal extension of the severe blastic osteosarcoma in proximal metaphysis of tibia. The growth plate is involved definitely. Dense cloud like tumor matrix, associated soft tissue mass and combination of sunray and spiculated periosteal reaction were shown.

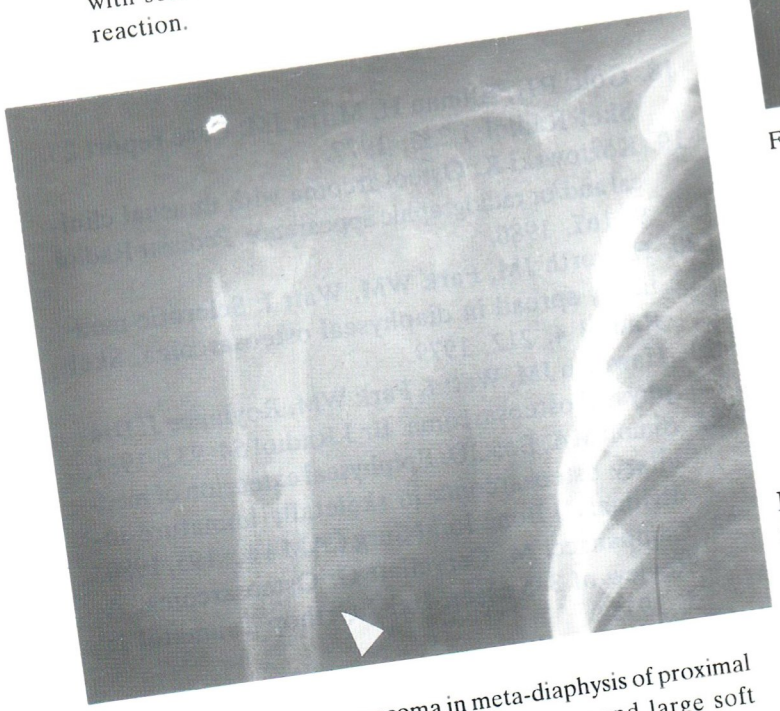

Fig. 9 Lytic type osteosarcoma in meta-diaphysis of proximal humerus shows pathologic fracture and large soft tissue mass. Codman's triangle periosteal reaction is noted at proximal diaphyseal area.

References (continued)
28. Dahlin DC, Unni KK: Osteosarcoma of bone and its important recognizable varieties. Am J Surg Pathol 1:61, 1977.
29. Azouz EM, Esseltine DW, Chevalier L, Gledhill RB: Radiologic evaluation of osteosarcoma, J Can Assoc Radiol 33:167, 1982.
30. Faure C, Boccon - Gibod K, Barcovy M : Case report 257. Skel Radiol 11:73 , 1984.

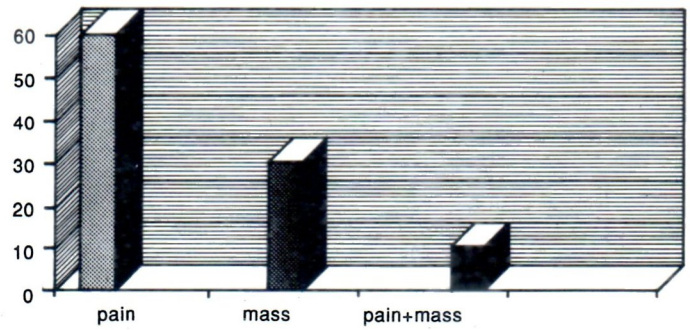

PAIN	42 CASES (60%)
MASS	21 CASES (30%)
PAIN & MASS	7 CASES (10%)

Table 1 : Frequency of the presenting symptoms

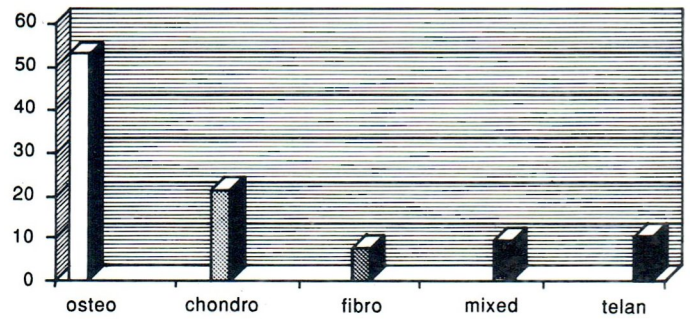

OSTEOBLASTIC	37 CASES (53%)
CHONDROBLASTIC	15 CASES (21%)
FIBROBLASTIC	5 CASES (7%)
MIXED	6 CASES (9%)
TELANGIECTATIC	7 CASES (10%)

Table 2 : Frequency of the histologic type of tumor

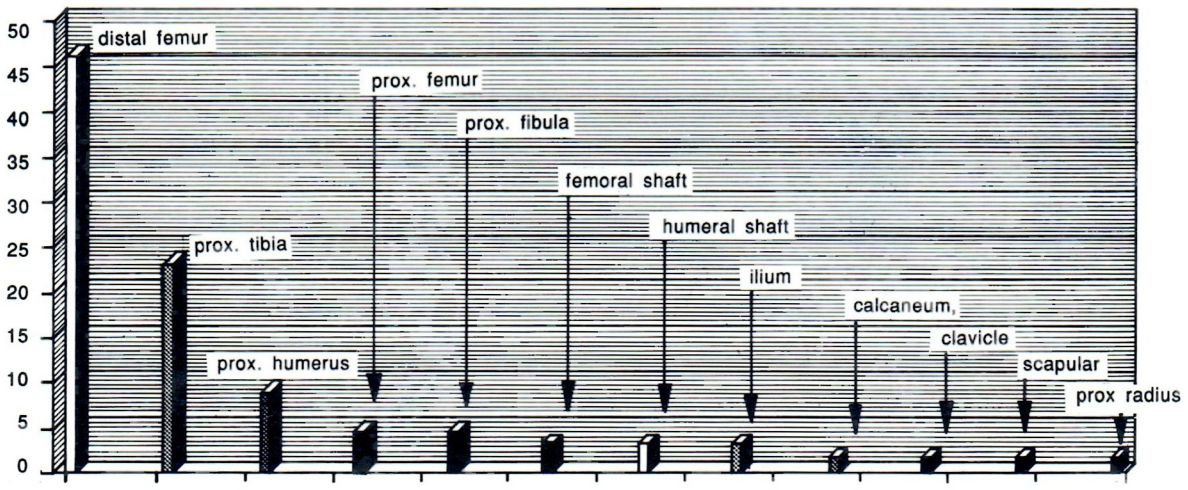

Table 3: Frequency of the sites of involvement

DISTAL FEMUR	32	(46%)
PROXIMAL TIBIA	16	(23%)
PROXIMAL HUMERUS	6	(9%)
PROXIMAL FEMUR	3	(4.5%)
PROXIMAL FIBULA	3	(4.5%)
FEMORAL SHAFT	2	(3%)
HUMERAL SHAFT	2	(3%)
ILIUM	2	(3%)
CALCANEUM	1	(1.5%)
CLAVICLE	1	(1.5%)
SCAPULA	1	(1.5%)
PROXIMAL RADIUS	1	(1.5%)

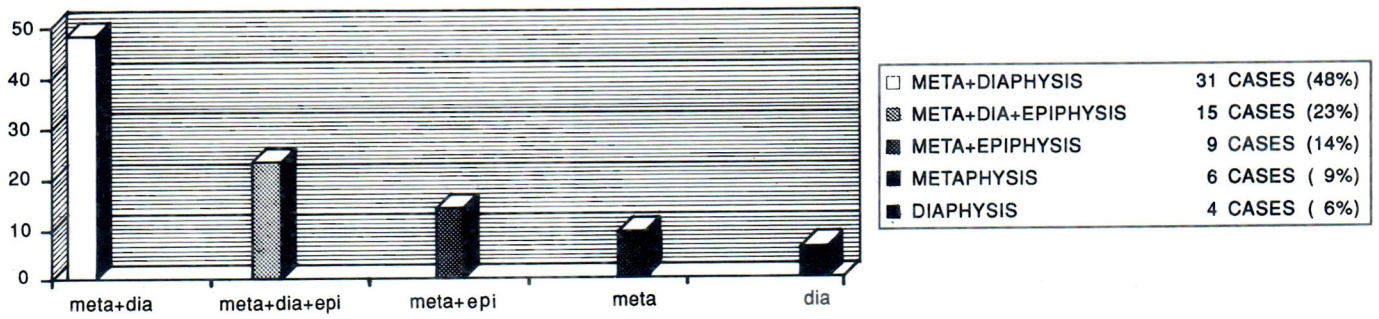

Table 4 : Frequency of involved location in the bones

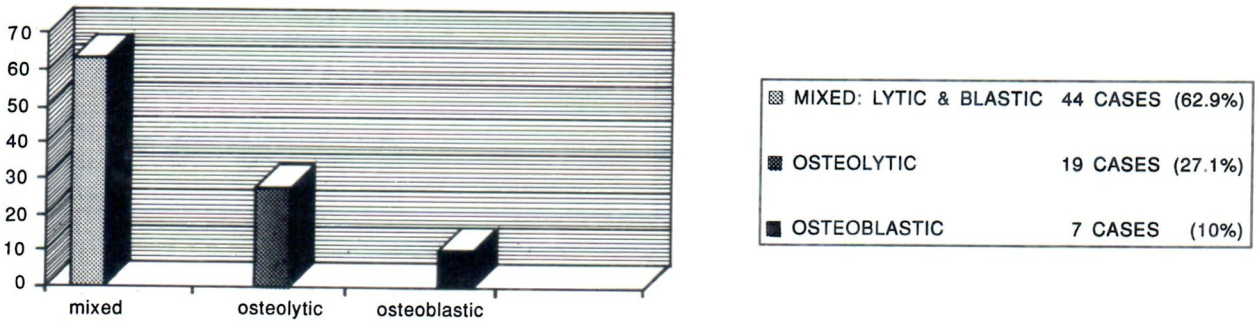

Table 5: Frequency of the radiographic patterns

PATHOLOGY

FINDING	OSTEOBLASTIC	CHONDROBLASTIC	TELANGIECTATIC	FIBROBLASTIC	MIXED
MIXED	22	12	2	3	4
LYTIC	11	2	5	2	-
BLASTIC	3	2	-	-	2

Table 6: Correlation of the radiographic finding and pathology

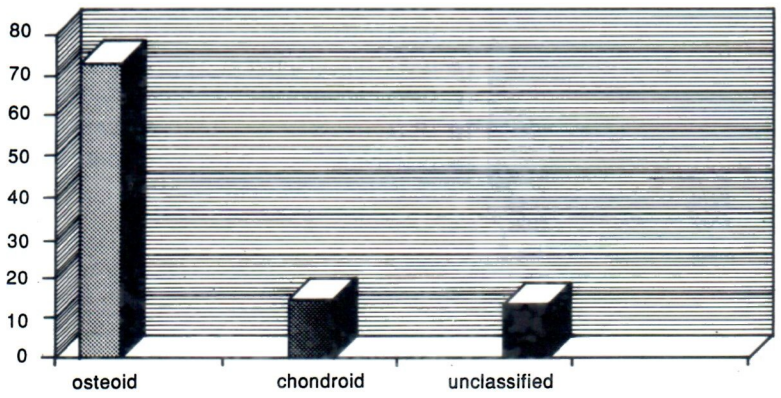

OSTEOID	51	(73%)
CHONDROID	10	(14%)
UNCLASSIFIED	9	(13%)

Table 7: Frequency of types of matrix

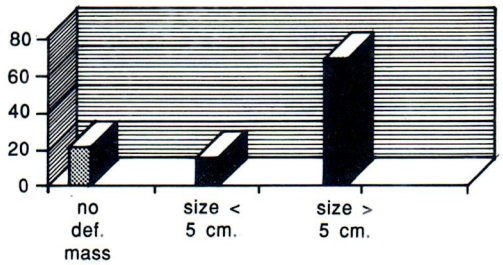

NO DEFINITE MASS	13	(19%)
SIZE < 5 CM.	10	(14%)
SIZE > 5 CM.	47	(67%)

Table 8: Frequency of the associated mass

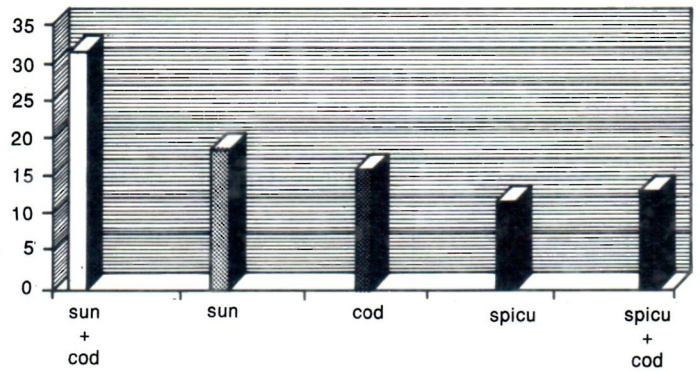

SUNRAYS & CODMAN	22	(31%)
SUNRAYS	13	(19%)
CODMAN	11	(16%)
SPICULATED	8	(11%)
SPICULATED & CODMAN	9	(13%)

Table 9: Frequency of the periosteal reaction

LOW DOSE RATE BRACHYTHERAPY CAESIUM-137 AFTERLOADING IN THE TREATMENT OF CARCINOMA OF UTERINE CERVIX IN SRINAGARIND HOSPITAL : ANALYSIS OF ACTURIAL SURVIVAL RATE

Montien PESEE M.D*, Vorachai TANGVORAPHONKCHAI M.D*
Tweesak REAMSIRI M.Sc* (Med. Phys),
Wichit KIRDPON M.Sc. (Med. Phys), Ph.D (Pharm.Sci)
Kawee TUNGSUBUTRA M.D, D.M.R.T. (England), F.R.C.R.T. (Thailand)**
Kuakoon KHWAKONG*, Naowarat NGAMNASEOW*

ABSTRACT

From October 1982 to December 1985, 412 patients with invasive uterine cervical carcinoma were treated with radiotherapy alone at the Division of Radiotherapy, Department of Radiology, Faculty of lledicine, Khon Kaen University, Khon Kaen, Thailand. The patients were in stages IB, IIA, IIB, IIIA, IIIB, IVA and IVB with 13, 5, 176, 5, 164, 14 and 15 cases respectively. Treatment methods were external irradiation 5000 cGy in 5 weeks in addition to intracavitary low dose rate brachytherapy 5400 mghr once or 3600 mghr twice after external radiotherapy. 66.4% of patients received brachytherapy after teletherapy more than 2 week interval. The average point A dose was 89.63 Gy and point B dose was 61.59 Gy. The acturial 3 year survival rates for stage IB, IIA, IIB, IIIA, IIIB, IVA and IVB were 89%, 100%, 70%, 60%, 56%, 28%, and 29% respectively. The 5 year acturial survival rates for stage IIB and IIIB which represent the highest number of the populations in this study were 63% and 39% respectively. The 5 year acturial survival rates for small size tumor less than 2 cm in diameter and tumor size larger than 2 cm in diameter were 74% and 56% respectively. Our study had been reported previously about residual tumors and complications.[1,2]

INTRODUCTION

Carcinoma of the uterine cervix is still the major problem of malignant disease in Thai women. Even now it is still the highest incidence of malignancy in the Northeastern Thai women. In Srinagarind Hospital, Faculty of Medicine, Khon Kaen University there were more than four hundred new cases of patients with uterine cervical carcinoma every year as table 1.[3-8]

Most of the patients were in advanced stages burdened with larged tumor volume and radiotherapy remains the most generally applicable method for controlling inoperable tumors of uterine cervical carcinoma. Our results and been reported previously about residual tumors and complications.[1,2] This study will be the analysis of acturial survival rate.

MATERIAL AND METHODS

During October 1982 to December 1985, there were 412 patients with histologically proven invasive carcinoma of the uterine cervix treated with radiotherapy alone in Radiotherapy Division, Depertment of Radiology, Srinagarind Hospital. All patients were

* Division of Radiotherapy, Department of Radiology, Srinagarind Hospital,
**Professor and Expert in Radiotherapy, Founder Dean and Faculty consultant.
Faculty of Medicine, Khon Kaen University, Khon Kaen, Thailand. 40002

Table 1 Statistical incidence

Year	% of total cancer cases in female	No of CA.Cervix cases
1988	26.26%	483
1989	29.11%	605
1990	26.10%	541
1991	25.50%	552
1992	22.50%	522
1993	26.20%	596

jointly evaluated by gynecologists and radiotherapists for clinical staging according to the International Federation of Gynecology and Obstetrics (1973)[3]. Patients were followed periodically by the radiotherapist for an average time about 2 years or until lost to follow up or death occured. Informations were available either from the Division of Radiotherapy records, Cancer Unit records or letter of follow up through direct communication with the patients or relatives. Acturial survival rate analysis was performed according to life-table method[10].

TREATMENT
EXTERNAL RADIATION THERAPY

All patients were treated with Cobalt-60 teletherapy units. Most of the patients received 5000 cGy in 5 weeks to the whole pelvis through AP and PA 15x15 cm^2 or 16x16 cm^2 port. The ports were extended to 18x15 cm^2 for the patients with stage IIIA. In small size tumors, the patients received 2000-3000 cGy to the whole pelvis. Tumor dose of 180-200 cGy were treated daily in five fractions per week. The lead block size 9x4x5 cm^3 for midline shielding was used in some patients whose tumor shrinked or disappeared during external radiotherapy or after intracavitary insertion.

BRACHYTHERAPY

Low dose rate intracavitary caesium-137 was performed by using Fletcher afterloading technique. All doses were prescribed in mg-hr Radium equivalent. Standard source loaded by 15-10-10 mg in tandem and 20 mg sources in each of standard vaginal ovoids were practiced.

More than two weeks after completion of teletherapy, the brachytherapy doses of 5400 mghr once or 3600 mghr for two intracavitary insertions were practiced in most patients due to limitation of our facilities and only 4 patients can be treated per week. (two brachytherapy service beds)

PARAMETRIAL BOOST

In addition to the external irradiation, parametrial boosts of 200 cGy for 3 days after the completion of brachytherapy were treated to the patients in stage IIIB with massive tumors at the parametrium.

RESULTS

Four hundred and twelve patients with uterine cervical carcinoma were treated with radiotherapy alone during October 1982 to December1985. The patient characteristics are given in Table 1. The residual tumors and radiation complications had been reported previously.[1,2]

DISCUSSION

The aim of radiotherapy in malignancy is to obtain the highest possible tumor control, the best survival, the lowest possible incidence of major radiation complications and good quality of life of the patients.

Many prognostic factors influencing on radiotherapy in uterine cervical carcinoma are size of tumor, gross appearance of lesions, histologic type or degree of differentiation, staging as well as host prognostic factors including hemoglobin level.[11,12]

Table II Dose rate at point A and point B from caesium-137 (Standard Manchester Technique)

Year	Point A Gy/hr	Point B Gy/hr
1982	0.55	0.173
1983	0.54	0.169
1984	0.52	0.166
1985	0.51	0.162

Our results revealed that patients with small tumor size less than 2 cm in diameter had 5 year acturial survival rate 73% but the patients with large tumor size more than 2 cm in diameter had 5 year acturial survival rate 56%. (Table 4)

In patients with stage IIB and IIIB which were the highest number of populations in this study had 5 year acturial survival rate 63% and 39% respectively. (Table 5)

This data may support the hypothesis that large tumor volume or advanced carcinoma of the cervix contain cores of hypoxic cells which resist to conventional radiation therapy. Attia AB, et al. (1985)[13] reported that tumor size of uterine cervical carcinoma less than 2 cm, 2-4 cm, more than 4 cm in diameter revealed pelvic node involvement 7.5%, 27.5% and 45%, respectively, Conclusion can be drawn that pelvic node involvement rate increases when tumor size increases and this may be another reason for the decreased survival rate in large size tumor.

For exophytic lesions and ulcerative lesions we found that 5 year acturial survival rates were 50.3% and 58.2%, respectively. (Table 6)

From a report on 1013 uterine cervical cancer patients treated with radiotherapy alone, the 5 year survival rates for stage I, II, III and IV were 73.2%, 48.6%, 25.2% and 6.8%, respectively. The pathological report was squamous cell carcinoma 89.5% and adenocarcinoma 8.7% (Tepmongkol P, 1985).[14]

In addition, the 5 year survival rates of another report studied in 845 cases treated by radiotherapy in stage I and II of uterine cervical carcinoma were 69.1% and 48%, respectively. (Benerjee SK, et al 1985)[15]

Jampolis S, et al (1975)[16] also reported that 5 year survival rates on 916 squamous cell carcinoma patients who received radiotherapy alone in stage IIA, IIB, IIIA and IIIB were 91%, 82%, 65%, 54% and 40%, respectively.

Perez CA, et al.(1986)[17] reported that 5 year survival rates on 970 patients treated with radiotherapy alone, stage I, IIA, IIB and III were 89%, 70%, 68% and 45%, respectively. This study revealed that over 90% of the patients had squamous cell carcinoma.

Our results on 5 year acturial survival rates for stage IIB and IIIB were 63% and 39% respectively. (Table 5)

According to the pathology,we found 51% 5 year acturial survival rate for squamous cell carcinoma and 58% for adeno-carcinoma (Table 7). However in our study there were about 87.1% of cases had squamous cell carcinoma and only 10.4% had adenocarcinoma.

All the above mentioned reports showed the result of survival by using the low dose rate brachytherapy. From other reports[18,19], 5 year survival rate by using low dose rate brachytherapy for stage I, II, III and IV were 85-90%, 68-85%, 39-62% and 17-30%, respectively.

CONCLUSION

It can be concluded from our data that radiotherapy remains the useful modality in the treatment of uterine cervical cancers, but it will be effective in early stages and small tumor sizes. However,low dose rate brachytherapy, caesium-137 has the advantage of long half-life activity, about 30 years and cheaper

Table 3. Patient characteristics.1,2

Patient characteristics		
1. Geographic distribution		
Northeastern part		99.1%
Other parts		0.9%
2. Age		
The average age (youngest =16, oldest = 76)		48 yrs
3. Histopathology		
Squamous cell carcinoma	(no=359)	87.1%
Adenocarcinoma	(no=43)	10.4%
Adenosquamous cell CA.	(no=6)	1.5%
Others	(no=4)	1.0%
4. Staging		
Stage IB	(no=13)	3.2%
Stage IIA	(no=5)	1.2%
Stage IIB	(no=176)	42.7%
Stage IIIA	(no=5)	1.2%
Stage IIIB	(no=164)	44.7%
Stage IVA	(no=14)	3.4%
Stage IVB	(no=15)	3.6%
5. Tumor Size (Mean tumor size = 4.6 cm)		
< 2 cm		8.8%
> 2 cm		91.2%
6. Gross appearance		
Exophytic		83.8%
Infiltrative		3.6%
Ulcerative		12.6%
7. Brachytherapy Insertion		
No brachytherapy	(no=23)	5.6%
During teletherapy	(no=30)	7.3%
After teletherapy 1-2 wk	(no=77)	18.7%
After teletherapy >2 wk	(no=282)	66.4%

The acturial survival rate was analysed as followed. (Table 4, 5, 6, 7).

in the cost than high dose rate brachytherapy. So it may be suitable for developing countries in the beginning of setting up the radiotherapy unit. But one disadvantage of low dose rate brachytherapy is that patients must be treated in hospital beds for 48-72 hours, so it needs many beds for servicing many patients. When hospital beds are available, low dose rate brachytherapy with mechanical remote after-loading offers the best effective value in quality of therapeutic results and economical reasons.[20]

ACKNOWLEDGEMENT

We would like to express our appreciation and thank to assistant professor Jitijaroen Chaiyakhum (Head of Department of Radiology), assistant professor Nopadol Asavametha, assistant professor Varodom Boonvisuth, Dr. Charoonsak Somboonporn, Mrs.Prapatsorn Sri-Esan, staffs in Department of Obstetrics and Gynecology, staffs in Division of Radiotherapy and Cancer Unit for helping hands and encouragement to make this paper possible.

REFERENCES

1. Pesee M, Tangvoraphonkchai V, Boonvisuth V, etal. Radiotherapy alone in the Treatment of carcinoma of Uterine Cervix in Srinagarind Hospital. Analysis of treatment Failure. The Thai Journal of Radiology 1989; 26 : 67-70.

Table 4 : Acturial survival rate due to tumor size in all stages.

Tumor size	Acturial survival rate	
	3 yrs (%)	5 yrs (%)
< 2 cm	74	74
> 2 cm	64	56

Table 5 : Acturial survival rate due to staging.

Stage	Acturial survival rate	
	3 yrs (%)	5 yrs (%)
IB	89	-
IIA	100	-
IIB	70	63
IIIA	60	-
IIIB	56	39
IVA	28	-
IVB	29	-

References: (Con't)

2. Boonvisuth V, Pesee M, Tangvoraphonkchai V, et al. Radiotherapy alone in the treatment of carcinoma of Uterine Cervix in Srinagarind Hospital : Analysis of complication. The Thai Journal of Radiology 1989; 26 ; 139-146.
3. Tumor Registry (Statistical Report), Cancer Unit, Srinagarind Hospital, Faculty of Medicine, Khon Kaen University, 1988.
4. Tumor Registry (Statistical Report), Cancer Unit, Srinagarind Hospital, Faculty of Medicine, Khon Kaen University, 1989.
5. Tumor Registry (Statistical Report), Cancer Unit, Srinagarind Hospital, Faculty of Medicine, Khon Kaen University, 1990.
6. Tumor Registry (Statistical Report), Cancer Unit, Srinagarind Hospital, Faculty of Medicine, Khon Kaen University, 1991.
7. Tumor Registry (Statistical Report), Cancer Unit, Srinagarind Hospital, Faculty of Medicine, Khon Kaen University, 1992.
8. Tumor Registry (Statistical Report), Cancer Unit, Srinagarind Hospital, Faculty of Medicine, Khon Kaen University, 1993.
9. Kottmeier HL (ed). Annual report on the results of treatment in carcinoma of the uterus, vagina and ovary, vol. 15 Stockholm : International Federation of Gynecology and Obstetrics, 1973.
10. Cutler SJ,Ederer F. Maximum utilization of the life table method in analyzing survival. J. chronic Dis 1958 ; 8 : 699-712.
11. Rotman M, John M, Boyce J : Prognostic Factors in Cervical Carcinoma : Implications in Staging and Management. Cancer 1981 ; 48 : 560-7.

Table 6 : Acturial survival rate due to gross appearance in all stages.

Gross appearance	Acturial survival rate		
	3 yrs (%)	4 yrs (%)	5 yrs (%)
Exophytic	63.7	56.6	50.3
Infiltrative	67.1	-	-
Ulcerative	58.2	58.2	58.2

Table 7 : Acturial survival rate due to pathology in all stages.

Pathology	Acturial survival rate		
	2 yrs (%)	3 yrs (%)	5 yrs (%)
Squamous cell CA.	70	63	51
Adenocarcinoma	70	64	58
Adenosquamous cell CA.	60	-	-

References: (Con't)

12. Perez CA, Grigsby PW, Nene SM, et al. Effect on tumor size on the prognosis of carcinoma of the uterine cervix treated with irradiation alone. Cancer 1992 ; 69 : 2796-806.
13. Attia AB, Mourali N, Maalej M, etal. Brachytherapy Technique and Results for Early cancer of the Cervix. In : Mould RF, Tungsubutra, K, eds. Diagnosis and Treatment of Carcinoma of the Cervix in Developing Areas. Bristol and Boston : Adam Hilger Ltd, 1985 : 251-3.
14. Tepmongkol P.Radiation Therapy for Carcinoma of Cervix Uteri, 1968-73: A Clinical Study in Siriraj Hospital. In : Mould RF, Tungsubutra K, eds. Diagnosis and Treatment of carcinoma of the Cervix in Developing Areas. Bristol and Boston : Adam Hilger Ltd, 1985 : 227-30.
15. Banerjee SK, Mukherji DP. Results of Radiotherapy in Early Cases of cancerCervix.In : Mould RF, Tungsubutra K, eds. Diagnosis and Treatment of carcinoma of the Cervix in Developing Areas. Bristol and Boston : Adam Hilger Ltd, 1985 : 99 -101.
16. Jampolis S, Andras EJ, Fletcher GH. Analysis of Sites and Causes of Failures of Irradiation in Invasive Squamous Cell Carcinoma of the Intact Uterine Cervix. Radiology 1975 ; 115 : 681-5.
17. Perez CA, Camel HM, Kuske RR, et al. Radiation Therapy Alone in the Treatment of Carcinoma of the Uterine Cervix : A 20-year Experience. Gynecologic Oncology 1986 ; 23 : 127-140.
18. Horiot JC, Achille E, Combes PF, etal. Results of Radiotherapy Alone in the Treatment of 1485 Cases of Cancer of the Cervix. In : Mould RF, Tungsubutra K, eds. Diagnosis and Treatment of Carcinoma of the cervix in Developing Areas. Bristol and Boston : Adam Hilger Ltd, 1985 : 33-5.
19. Masubuchi K. Comparison of Treatment Results by Method of RadiationTherapy for Cancer of the Uterine Cervix at Japan Cancer Institute Hospital, Tokyo. In : Mold RF, Tungsubutra K, eds. Diagnosis and Treatment of Carcinoma ofthe Cervix in Developing Areas. Bristol and Boston : Adam Hilger Ltd, 1985 : 129-132.
20. Horiot JC. Is Sophistication Really Necessary in the Design of Remote Loading Systems in Gynaecological Curietherapy.? In : Mould RF, Tungsubutra K, eds. Diagnosis and Treatment of Carcinoma of the cervix in Developing Areas. Bristol and Boston : Adam Hilger Ltd, 1985 : 31-2.

INTEGRIS V3000
a new vision on integration

X-ray system for vascular and non-vascular diagnostic and interventional procedures

Philips Medical Systems

For more Information please contact
Philips Electronics (Thailand) Ltd.
tel. 745-4090

PHILIPS...MOVING AHEAD IN ELECTRONICS.

PHILIPS

Vidar VXR–12™

Film Digitizer

12–bit Performance at an Affordable Price

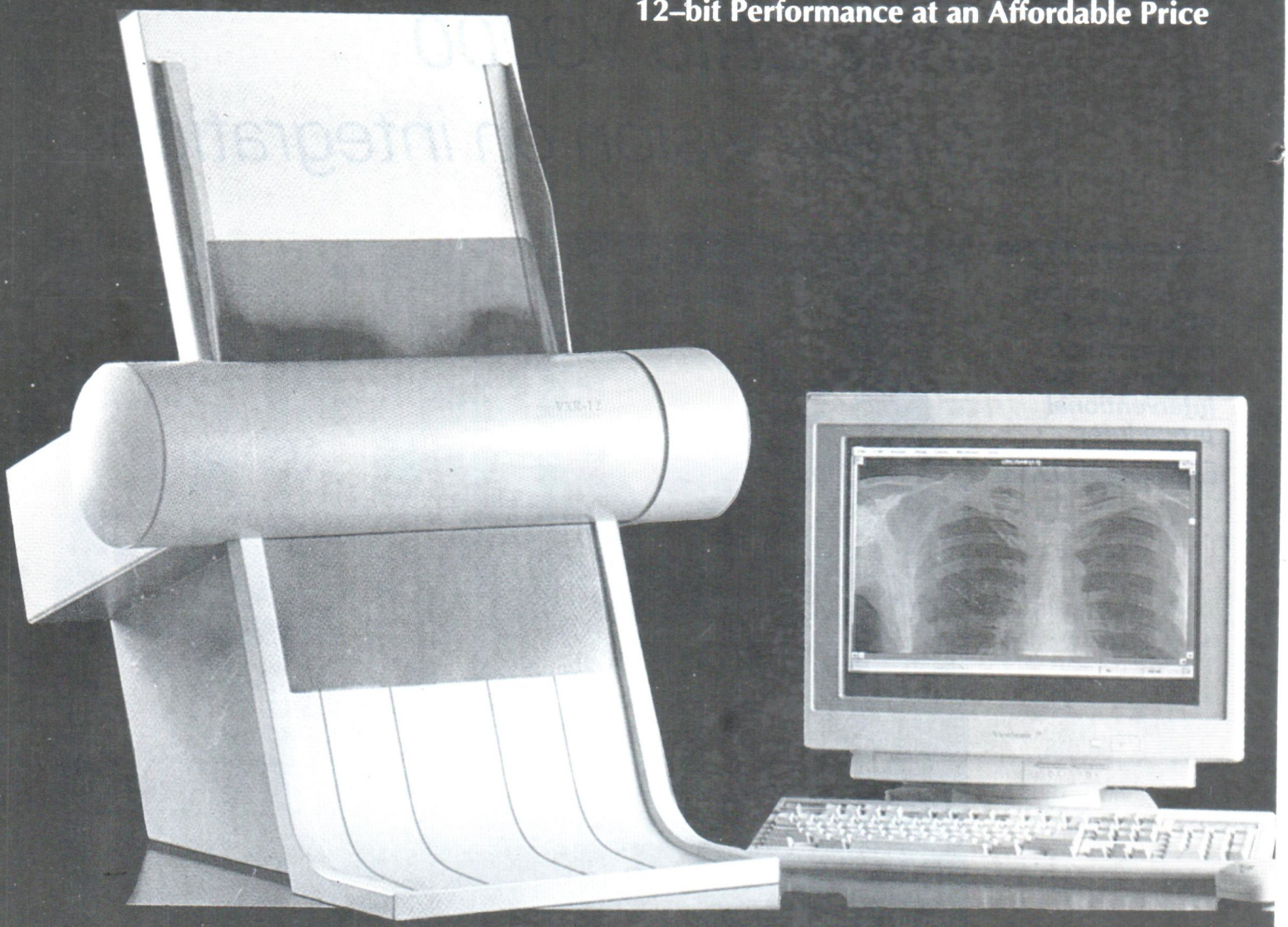

- **12–bit grayscale imaging provides a large dynamic range to handle dark and low contrast films.**
- **Built-in grayscale translation tables provide powerful viewing options.**
- **Resolution choices from 1k x 1k to 4k x 4k accommodate all scanning applications.**
- **Excellent geometric accuracy allows precise measurements.**
- **Fast scan times increase productivity.**

HATEC

THE VISION OF YOUR SUCCESS

Hatta Technology Co.,Ltd. (HATEC)

ชั้น 19 อาคารสีลมคอมเพล็กซ์ 191 ถนนสีลม แขวงสีลม เขตบางรัก กรุงเทพฯ 10500

โทรศัพท์ 231-3373-6 โทรสาร 231-3377

PC Teleradilogy, iNET a reader of Teleradiology of Thailand

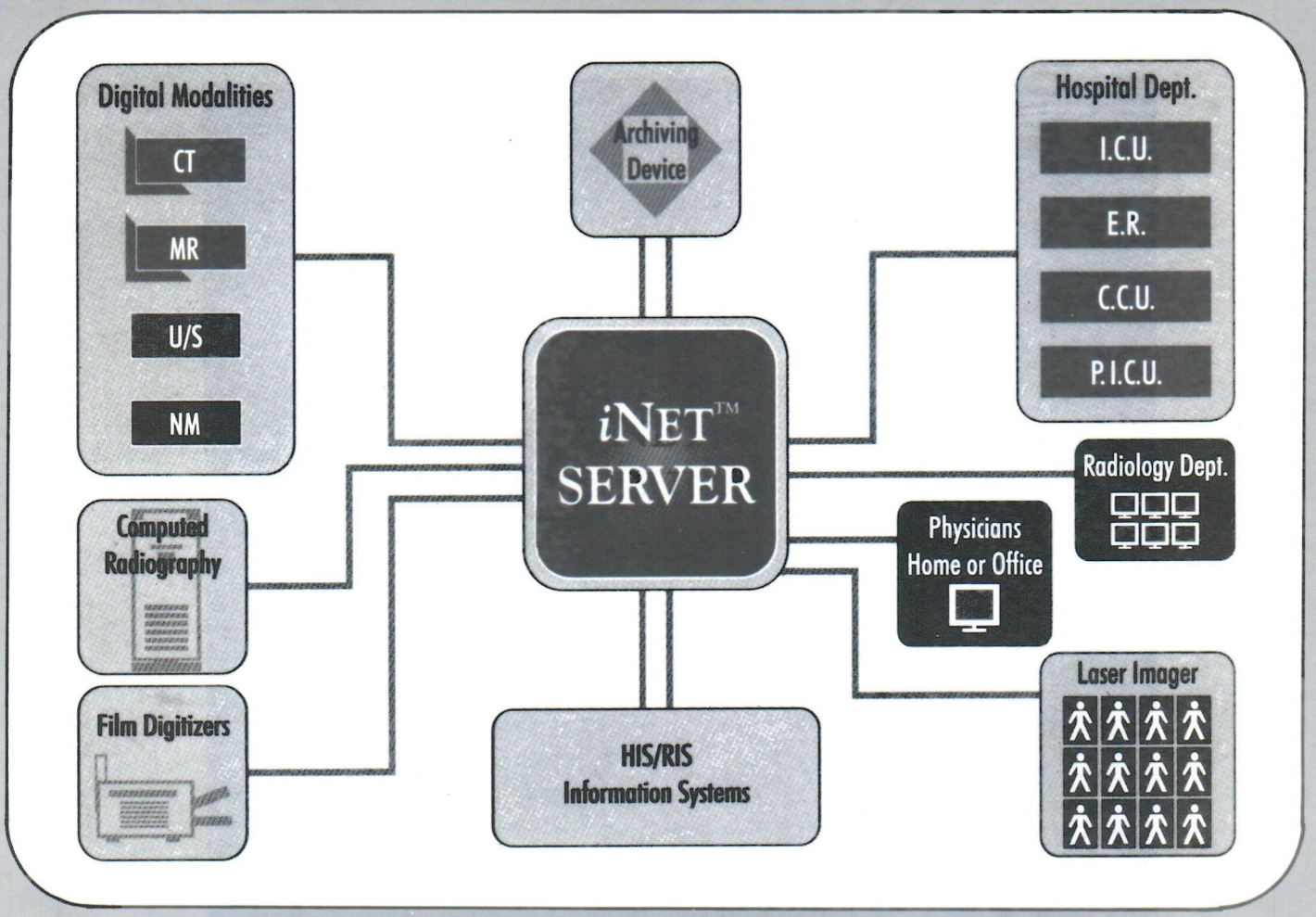

iNET™

The Image Networking and Management Solution

iNET™ is a Windows-based client/server software package that manages the distribution of images and data throughout a hospital or medical facility. In its simplest form, iNET can be used to send images from the radiology department to other hospital departments (ICU, ER, etc.). When its full line of features are utilized, iNET provides the platform from which to implement a complete PACs system. Either way, iNET's comprehensive array of features lets physicians and staff make the most of valuable patient and image information, empowering them to make better decisions and improve patient care.

PC Teleradiology™

The On-call Teleradiology Solution

PC Teleradiology™ encompasses a group of comprehensive—yet simple-to-use—software packages that let you capture, transmit, receive and view radiological images with speed and proficiency.

CompuMed
The Momentum Is Growing

HATEC

Hatta Technology Co.,Ltd. (HATEC)

19th Floor, Silom Complex Building 191 Silom Road, Bangrak, Bangkok 10500, Thailand.

THE VISION OF YOUR SUCCESS Tel: 231-3373-6 Fax: 231-3377

In Touch with Tomorrow

TOSHIBA

OBAL IMAGING ■ MEDICAL SYSTEMS

Helical Scanner

Xvision

XVISION: IT'S POWERFUL. IT'S FLEXIBLE. IT'S SMALL. IT'S THE CT OF THE FUTURE.

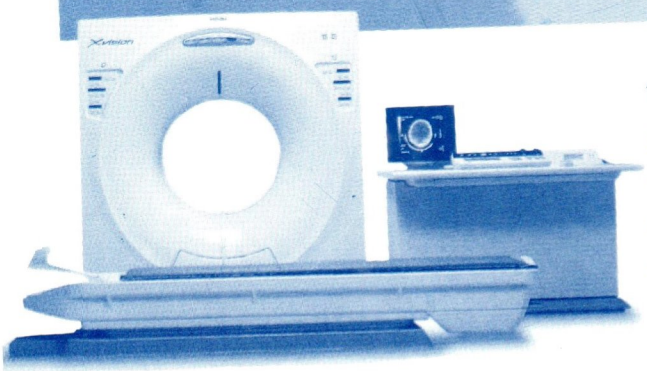

Toshiba introduces the Xvision, a highly compact, flexible, fast and efficient CT scanner that employs the unique Helical Scan™ system. This system makes it possible to complete a scan in a mere 1.5 seconds in routine examinations. Image quality is excellent, and speed, flexibility and efficiency are outstanding features of this scanner, so that high patient throughput can be achieved over a wide range of examinations.

CMC BIOTECH

CMC BIOTECH CO.,LTD.

1433 Soi 3/3 Muban Town-in-Town Ladphrao 94 Road, Bangkapi Bangkok 10310 Tel. 530-4995-6, 559-3261-2 Fax: (662) 539-6903

Southern Branch

306 Prachayindee Road, Khorhong Haadyai Songkhla 90110 Tel. (074) 356259, Handphone 01-9359703 Pagephone 151, 152 call 341790

North Eastern Branch

301/155 Muban Khon Kaen Villa, Mittrapab Road, Amphur Muang, Khon Kaen 40000 Tel. (043) 246210, 244729, Handphone 01-9283082 Pagephone 151, 152 call 341787